BULLETIN

OF THE AMERICAN PHYSICAL SOCIETY

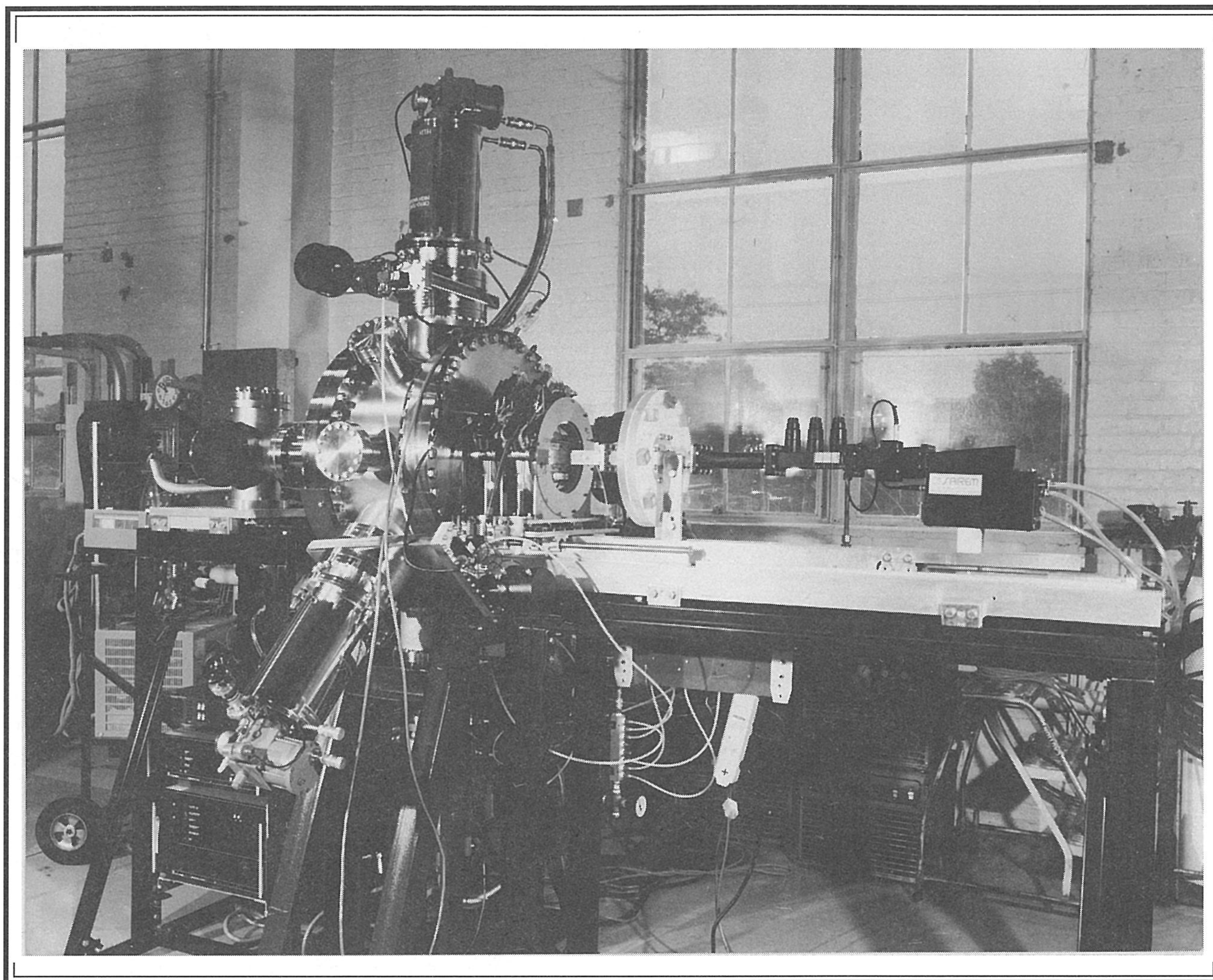

Program of the 49th Annual Gaseous Electronics Conference
20–24 October 1996
Argonne, Illinois

October 1996
Volume 41, No. 6

BULLETIN OF THE AMERICAN PHYSICAL SOCIETY
Coden BAPSA6 ISSN: 0003-0503
Series II, Vol. 41, No. 6 October 1996

APS COUNCIL 1996

President
Robert Schrieffer, *Florida State University*

President-Elect
D. Allan Bromley, *Yale University*

Vice-President
Andrew M. Sessler, *Lawrence Berkeley Laboratory*

Executive Officer
Judy R. Franz, *University of Alabama, Huntsville*

Treasurer
Harry Lustig, *City College of the City University of New York*

Editor-in-Chief
Benjamin Bederson, *New York University*

Past-President
C. Kumar N. Patel, *University of California-Los Angeles*

General Councillors
Daniel Auerbach, Kevin Aylesworth, Arthur Bienenstock, Virginia R. Brown, Jolie A. Cizewski, Jennifer Cohen, Charles Duke, Elsa Garmire, Laura H. Greene, Donald Hamann, William Happer, Anthony M. Johnson, Miles V. Klein, Zachary Levine, Susan Seestrom, Ronald Walsworth

Chair, Nominating Committee
Martin Blume

Chair, Panel on Public Affairs
David Hafemeister

Division and Forum Councillors
Frank C. Jones *(Astrophysics)*, Joseph Dehmer, Gordon Dunn *(Atomic, Molecular, and Optical)*, "TBA" *(Biological)*, Stephen Leone *(Chemical)*, Joe D. Thompson, David Aspnes, Lu J. Sham, Allen Goldman *(Condensed Matter)*, David Anderson *(Computational)*, Guenter Ahlers *(Fluid Dynamics)*, James J. Wynne *(Forum on Education)*, Albert Wattenberg *(Forum on History of Physics)*, Ernest Henley *(Forum on Interational Physics)*, Dietrich Schroeer, *(Forum on Physics and Society)*, Andrew Lovinger *(High Polymer)*, Daniel Grischkowsky *(Laser Science)*, Howard Birnbaum *(Materials)*, John Schiffer, Peter Paul *(Nuclear)*, Henry Frisch, George Trilling *(Particles and Fields)*, Hermann Grunder *(Physics of Beams)*, Roy Gould, William Kruer *(Plasma)*

COUNCIL ADVISORS

Sectional Representatives
John Pribram, *New England;* Peter Lesser, *New York;* Perry P. Yaney, *Ohio;* Joseph Hamilton, *Southeastern;* Stephen Baker, *Texas*

Representatives from Other Societies
Howard Voss, *AAPT;* Marc Brodsky, *AIP*

Editor: Barrett H. Ripin
Meeting Publications Coordinator: Danita Boonchaisri

APS MEETINGS DEPARTMENT
One Physics Ellipse
College Park, MD 20740-3844
Telephone: (301) 209-3200
FAX: (301) 209-0866
Michael Scanlan, *CMP, Meetings Manager*
Tammany Buckwalter, *Assistant Meetings Manager*
Joanne Fincham, *Publications Specialist*
Desiree Atherly, *Assistant to the Meetings Manager*

Staff Representatives
Barrett Ripin, *Associate Executive Officer*; Irving Lerch, *Director of International Affairs*; Robert L. Park, *Director, Public Information*; Michael Lubell, *Director, Public Affairs*; Stanley Brown, *Administrative Editor*; Reid Terwilliger, *Director of Editorial Office Services*; Michael Stephens, *Controller and Assistant Treasurer*

The *Bulletin of The American Physical Society* is published 10X in 1996: March, April, May, June, October (2X), November (3X), and December, by The American Physical Society, through the American Institute of Physics. It contains advance information about meetings of the Society, including abstracts of papers to be presented, as well as transactions of past meetings. Reprints of papers can only be obtained by writing directly to the authors.

The *Bulletin* is delivered, on subscription, by Periodicals mail. Complete volumes are also available on microfilm. **APS Members** may subscribe to individual issues, or for the entire year. **Nonmembers** may subscribe to the Bulletin at the following rates: Domestic $380; Foreign Surface $400; Air Freight $425. Information on prices, as well as subscription orders, renewals, and address changes, should be addressed as follows: **For APS Members**—Membership Department, The American Physical Society, One Physics Ellipse, College Park, MD 20740-3844. **For Nonmembers**—Circulation and Fulfillment Division, The American Institute of Physics, 500 Sunnyside Blvd., Woodbury, NY 11797. Allow at least 6 weeks advance notice. For address changes, please send both the old and new addresses, and, if possible, include a mailing label from a recent issue. Requests from subscribers for missing issues will be honored without charge only if received within 6 months of the issue's actual date of publication.

Periodicals postage paid at Woodbury, NY 11797, and additional mailing offices. Postmaster: Send address changes to *Bulletin of The American Physical Society*, Membership Department, The American Physical Society, One Physics Ellipse, College Park, MD 20740-3844.

On the Cover: Microwave-driven ECR source for producing high-current high-purity H^+, D^+, H^-, and D^- cw beams. The large UHV chamber houses beam and source diagnostics. *Photocourtesy of Ion Source Development Group, Technology Development Division, ANL.*

BULLETIN
OF THE AMERICAN PHYSICAL SOCIETY

Vol. 41, No. 6, October 1996

TABLE OF CONTENTS

GEC '96 Executive Committee i
For Further Inquiries i
General Information i
Conference Headquarters, Registration ii
Presentations ii
Will Allis Lecture ii
Travel Information ii
Hotel ii
Program Information iii
Location of Sessions iii
Banquet iii
Oak Brook Area Restaurants iii
Registration Form iv
Maps v
Epitome vii
Main Text 1283
Index 1346

49TH ANNUAL GASEOUS ELECTRONICS CONFERENCE
20–24 October 1996; Argonne, Illinois

GEC '96 EXECUTIVE COMMITTEE

J. Norman Bardsley, Chairman,
Lawrence Livermore National Lab;
Michael A. Dillon, Secretary,
Argonne National Lab;
Harold M. Anderson, Treasurer,
University of New Mexico;
Mark J. Kushner, Chairman-Elect,
University of Illinois;
Thad G. Walker, Secretary-Elect,
University of Wisconsin;
David B. Graves, Past Secretary,
University of California;
Michael Barnes
Lam Research Corporation;
J. William McConkey,
University of Windsor, Windsor, Canada;
Robert Piejak
OSRAM Sylvania;
Seiji Samukawa
NEC Corporation.

FOR FURTHER INQUIRIES

Michael A. Dillon, Secretary,
49th Annual Gaseous Electronics
Conference Bldg. 212,
Argonne National Laboratory, Argonne, IL 60439
(708) 252 4193,
FAX (708) 252 4798,
email mdillon.@anl.gov

GENERAL INFORMATION

The Forty-Ninth Annual Gaseous Electronics Conference will be held Oct. 20-24, 1996 in the conference facilities of the Advanced Photon Source (APS) at Argonne National Laboratory. The meeting is a topical conference of the American Physical Society and this year it will be hosted by Argonne National Laboratory. For further information you are welcome to visit the GEC web site at: http://www.gec.org/gec/

Each year the GEC selects topics for special emphasis in arranged sessions or workshops. The arranged sessions will include both invited and contributed papers. Topics selected for arranged sessions at the 1996 meeting include:

Plasma and Surface Chemistry in Semiconductor Processing.

Optical Diagnostics for Analysis and Control.

Electromagnetic Coupling and Probes in Discharges.

Advances in Electron Scattering Techniques.

Applications of Electron Scattering to Critical Processes.

Heavy Particle Collisions in Ionized Gases and Cold Traps.

Radiation Transport and Photon Absorption Processes.

Ion-Surface Interactions in Materials Processing.

Deposition of Diamond and Diamond-like Films.

Dielectric Etch Techniques and Mechanisms.

Laser Ablation for Processing and Spectroscopy.

Magnetron Sputtering and Physical Vapor Deposition.

Plasma Sprays and Plasma Torches.

Plasma Processing outside the Electronics Industry.

Discharges in Air and Atmospheric Processes.

Plasmas in Displays.

CONFERENCE HEADQUARTERS, REGISTRATION

Headquarters for the conference will be the Hyatt Regency Oakbrook. Registration and opening reception will be held there from 19:00 PM to 21:00 PM, Sunday, October 20, 1996. Registration will also be open at the Advanced Photon Source (APS) each day of the conference.

Fees for regular members are $210, $105 for retirees and students, with $30 added for all registrations after September 30th.

Sign-up for the APS tours will also take place at registration. All participants are required to register and wear their name tags to all scientific sessions and social events.

PRESENTATIONS

Papers that have been accepted for presentation are indicated in the enclosed Technical Program. The abstracts will be published in the Bulletin of the American Physical Society (BAPS), which will be printed prior to the meeting and distributed at registration. Post deadline abstracts will also be distributed.

Lecture papers have been allocated 12 minutes plus 3 minutes for discussion. Invited papers have been allocated 25 minutes for presentation plus 5 minutes for discussion. Projection equipment available will consist of standard 35 mm slide and vugraph overhead projectors.

Posters employ Velcro attachments (supplied). The poster dimensions are height - 6 1/2 ft(4 ft useful), width - 5 ft. with an interior angle of 160 degrees.

WILL ALLIS LECTURE

The Will Allis Prize Lecture entitled: *Electron-Atom Collisions: An Evergreen in Physics and Technology*, will be delivered by Prof. Chun C. Lin at 10:30 Tuesday morning, October 22.

TRAVEL INFORMATION: DIRECTIONS FROM O'HARE TO THE HYATT REGENCY

Take 294 South, Exit Interstate 88 (East-West Tollway to Aurora). Exit Cermak Road(after paying the toll). As you come off the exit ramp you will come to an intersection, proceed straight through the intersection, the hotel is located 3 blocks on the right side of the street.

DIRECTIONS FROM MIDWAY TO THE HYATT REGENCY

Take 55 South, Exit 294 North, Exit Interstate 88 (East-West Tollway). Exit Cermak Road (after paying the toll). Proceed through the intersection, the hotel is located 3 blocks on the right side of the street.

GROUND TRANSPORTATION:

Argonne Conference Services recommends:

American Limousine - (708) 920-8888

United Limousine - (708) 969-3865 or Out of State (800) 826-0341

Oak Brook Limousine - (800) 654-1442 or (708) 495-1212

HOTEL

Hyatt Regency Oakbrook
1909 Spring Road
Oakbrook, Illinois 60521
Phone (630) 573-1234
Fax (630) 573-1909

ROOM RATE

Single/Double-Quad $89 + tax

CUT-OFF DATE

Sept. 29 1996

Program Information

LOCATION OF SESSIONS

All lecture technical sessions will be held Oct. 21-24, 1996 in the main Auditorium and lecture hall of the APS conference center at Argonne National Laboratory. The poster technical sessions will be held in Alcoves A and B located off the main wing. These are clearly indicated in the enclosed map. Lunch (included in the registration fee) will be provided in the cafeteria beneath the main conference auditorium.

BANQUET

The conference Banquet will be held Tuesday, October 22, from 19:00 PM to 21:00 PM at the Hyatt Regency Oakbrook and will be preceded by a social hour beginning at 18:00 PM. The after dinner speaker will be Prof. Michael Turner who will give a talk entitled *The Age of the Universe and Other Large Questions.*

For technical information contact the Secretary at the address given on page i. For registration information contact Joan Brumsvold of Conference services at the address given on the registration form.

1996 Gaseous Electronics Conference

October 21-24, 1996

Argonne National Laboratory

Argonne, Illinois U.S.A.

Oak Brook Area Restaurants

CASUAL

Bennigan's, 17W460 22nd Street, Oak Brook Terrace 832-5611.

Claim Company, 232 Oak Brook Center Mall, Oak Brook 574-3077.

Horseradish Cafe, Hyatt Regency Oak Brook, 1909 Spring Rd. 573-1234.

Houlihan's Old Place, 56 Oak Brook Center Mall, Oak Brook 573-0220.

Copperfield's, 1341 Butterfield Road, Downers Grove 852-2424.

CONTINENTAL

Andy's Steak & Seafood, 2205 W. 22nd Street, Oak Brook 574-2210.

Bully's 1, S130 Summit, Oak Brook Terrace 833-1310.

The Club 2100, Stouffer Hotel, 2100 Spring Rd. Oak Brook 573-2800.

Morton's of Chicago, One Westbrook Corp. Center, Westchester 562-7000.

FRENCH

Fond de la Tour, 40 North Tower, Oak Brook 620-1500.

GREEK

Greek Islands, 300 East 22nd Street, Lombard 932-4545.

ITALIAN

Giordano's, 18W048 22nd Street, Oak Brook Terrace 620-7979.

Maggiano's Little Italy, 240 Oak Brook Center Mall, Oak Brook 368-0300.

Sylviano's, 2809 Butterfield, Oak Brook 571-3600.

MEXICAN

El Torito, 270 Oak Brook Center Mall, Oak Brook 574-3340.

Chi Chi's, 17W744 22nd Street, Oak Brook Terrace 629-5830

ORIENTAL

China Terrace, 1S616 Summit, Oak Brook Terrace 620-6700

Benihana of Tokyo, 747 Butterfield Road, Lombard 571-4440.

RIBS

Carson's for Ribs, 400 East Roosevelt, Lombard 627-4300.

SEAFOOD

Braxton Seafood & Grill, 3 Oak Brook Center Mall, Oak Brook 574-2155.

Rusty Pelican, 777 East Butterfield, Lombard 573-0400.

REGISTRATION FORM

(Please Print or Type)

Name

____

(First) (Middle) (Last)

Organization____________________ Department ____________________

Business Address

____

(Street)

____

(City) (State) (Zip Code) (Country)

Business Phone ______________________________ Fax No:______________

(Area Code) (Number) (Extension)

Email: ________________________ Citizenship ____________________

THE FOLLOWING APPLIES TO NON-U.S. CITIZENS ONLY:

Place of Birth ______________________________ Date of Birth ____________________

(City) (Country) (Mo/Day/Yr)

Immigrant Alien (Y/N)_____________ Gender: (M/F) _______

Title ____

Position or Description of Duties:____

REGISTRATION FEES

______Early Registration (before September 30, 1996) - $210

______Late Registration (after September 30, 1996) - $240

______Banquet - $ 25 (partly subsidized)

______Please make check payable to: ARGONNE NATIONAL LABORATORY.

(Credit cards not accepted)

CONFERENCE EVENTS (included in Registration Fee) - I will attend:

______Reception at The Hyatt Regency, Sunday, October 20 (7:00 p.m. - 9:00 p.m.).

______Banquet at The Hyatt Regency, Tuesday, October 22 (6:00 p.m. - 9:00 p.m.).

Map to Argonne National Lab

MAIN ENTRANCE

ENTRANCE GATE

VISITOR RECEPTION

ENTRANCE GATE

(TO I-55 INTERCHANGE VIA LEMONT RD.)

Advanced Photon Source (400 Area)

NORTH

0 1 km 2 km

WATER

ROADS & PARKING

BUILDINGS

Argonne National Laboratory is located 25 miles southwest of Chicago. Take the southbound Cass Ave. exit from I-55 (the Stevenson Expressway), then turn right on Northgate Road to the ANL main (north) gate and Visitor's Reception Center (VRC). For those without an ANL ID card, a gate pass, arranged for by an ANL contact, is issued at the VRC. For after-hours access, an ANL contact must leave the visitor's name on the access list at the main gate.

Access hours: Main gate — 24 hrs./day
West gate — 6:00 a.m.-7:00 p.m.

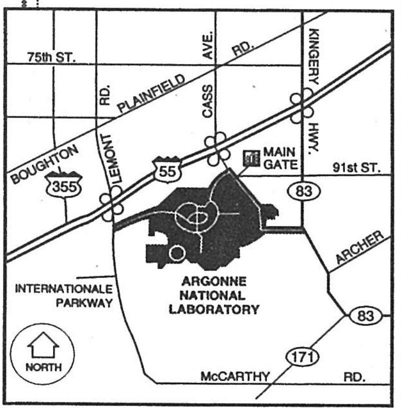

ANL Buildings

004	Property/Records/Materials; EMW Program
005	Shipping/Receiving/Central Mail Room
046	Transportation & Grounds
091	Guard Post
108	Central Boiler House
145	Fuel Facility
146	Fuel Control Office
200	Chemistry
201	DOE-CH; ANL Administration; University of Chicag
202	Center for Mechanistic & Biotechnology
203	Physics & Environmental Research;TIS
205	Chemical Technology
206	Engineering Development Laboratory
207	Engineering Physics
208	Engineering Research
211	Low Energy Accelerator Facility
212	Energy Technology; Materials Science Division
213	Cafeteria
214	Plant Facilities & Services; EMW Program
221	ECT Division; Mathematics & Computer Science; IPI
222	Electronics Technologies; Film & Video; Media Servic
223	Materials Science; Educational Programs
224	Visitors Reception Center
233	Credit Union
291	Guard Post
301	Hot Laboratory; Storage; Office
302	Security
306	Environment & Waste Management Program
308	Energy Technology Division
309	Energy Technology Division
310	Experimental Breeder Reactor II
314	Fast Neutron Generator
315	Technical Development; Special Projects Office
316	Technical Development; IPD -TIS
331	Reactor Engineering
333	Central Fire Station
335	Energy Technology Division
340	Environment & Waste Management Program
350	New Brunswick Laboratory
360	Intense Pulsed Neutron Source
361	Intense Pulsed Neutron Source
362	Auditorium; ES; HEP
363	Central Shops
372	RREGES Div.
375	Intense Pulsed Neutron Source
400-450	**Advanced Photon Source**
600	Lodging Facility Office
603	Swimming Pool
617	Exchange Club
891	Guard Post
900	EAISs;IPD; Technology Transfer Center
950	Restrooms – Recreation Area
951	Argonne Recreation Center
952	Child Care Center

EPITOME OF THE 1996 FALL MEETING OF THE 49TH ANNUAL GASEOUS ELECTRONICS CONFERENCE

MONDAY MORNING 21 OCTOBER 1996

8:00

Session M1A. **Dielectric Plasma Etching.**
Arnold, Goto.
Auditorium.

Session M1B. **Advances in Electron Scattering Techniques.**
Bartschat, James, Trajmar, Kim.
Lecture Hall.

MONDAY MORNING 21 OCTOBER 1996

10:30

Session M2A. **Laser and Optical Diagnostics for Analysis and Control.**
Anderson.
Auditorium.

Session M2B. **Plasma Sprays.**
Girshick, Fincke, Chang, Bernecki.
Lecture Hall.

MONDAY AFTERNOON 21 OCTOBER 1996

13:30

Session M3A. **Critical Electron Scattering Processes.**
Becker, Sugai, Orel.
Auditorium.

Session M3B. **Heavy Particle Collisions and Effects.**
Holland, Adams.
Lecture Hall.

MONDAY AFTERNOON 21 OCTOBER 1996

15:45

Session MPA. **Inductively Coupled Plasmas Poster Session.**
Alcove A.

Session MPB. **Discharge Modeling Poster Session.**
Alcove A.

Session MPC. **Electron Interactions I Poster Session.**
Alcove B.

Session MPD. **Discharge Experiments Poster Session.**
Alcove B.

TUESDAY MORNING 22 OCTOBER 1996

8:00

Session TU1A. **Electromagnetic Coupling Effects in Discharges.**
Ellingboe.
Auditorium.

Session TU1B. **Radiation Transport and Photon Processes.**
Lister, Orlando, Tolk.
Lecture Hall.

TUESDAY MORNING 22 OCTOBER 1996

10:30

Session TU2A. **Will Allis Prize Lecture.**
Lin.
Auditorium.

TUESDAY AFTERNOON 22 OCTOBER 1996

13:30

Session TU3A. **Modeling and Diagnostics in High Density Plasmas.**
Nakano.
Auditorium.

Session TU3B. **Plasma in Display.**
Weber, Punset, Parker.
Lecture Hall.

Meeting Site
Advanced Photon Source

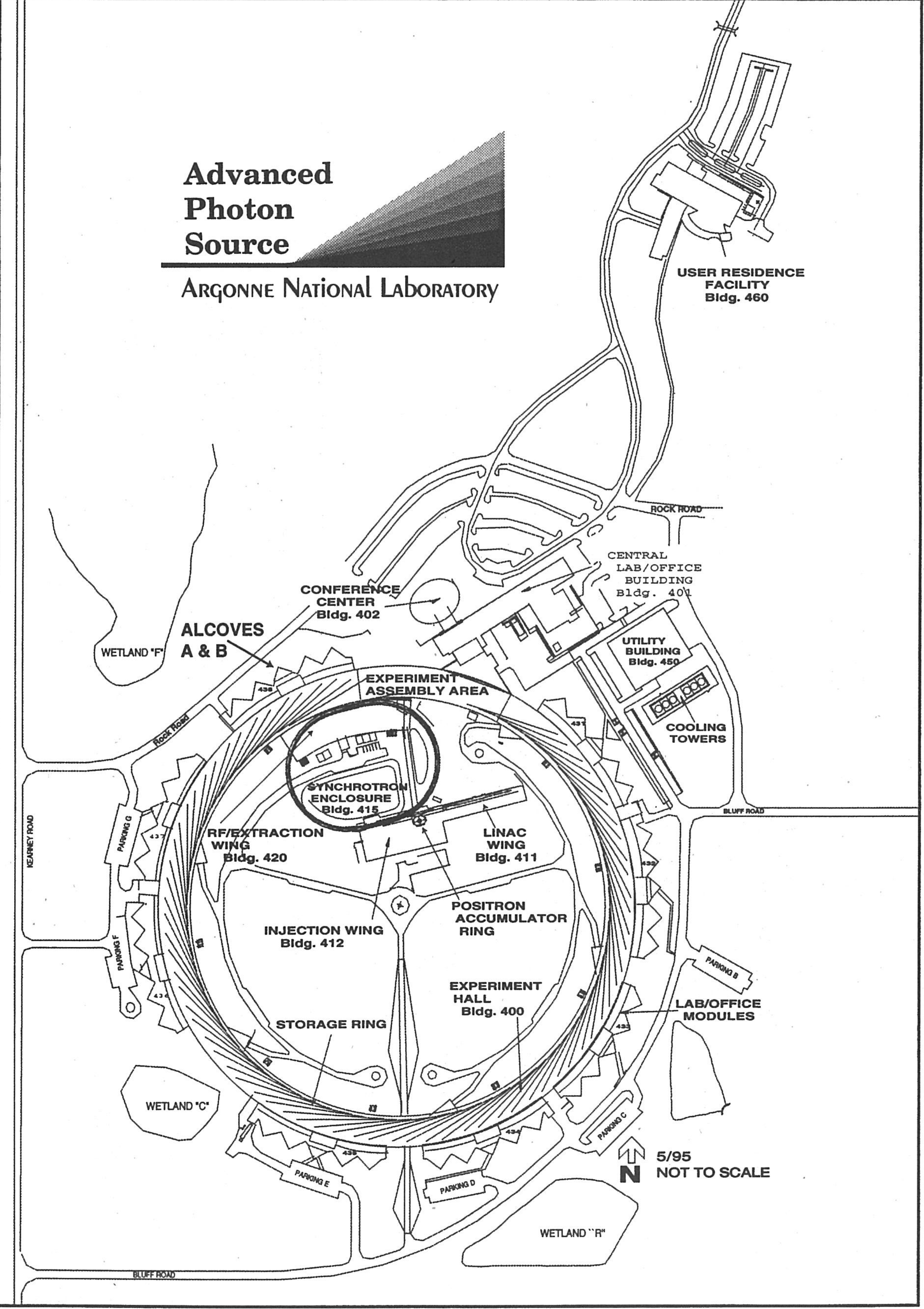

TUESDAY AFTERNOON 22 OCTOBER 1996

15:45

Session TUPA. **ECR and Microwave Discharges, Ablation and Dusty Plasmas Poster Session.**
Alcove A.

Session TUPB. **Electron Interactions II Poster Session.**
Alcove B.

Session TUPC. **Discharge Theory and Simulation Poster Session.**
Alcove B.

WEDNESDAY MORNING 23 OCTOBER 1996

8:00

Session W1A. **Ion Surface Interactions.**
Rabalais, Hanley, Ruzic.
Auditorium.

Session W1B. **Diamond and Diamond-like Carbon Deposition.**
Gruen, Curtiss, Angus.
Lecture Hall.

WEDNESDAY MORNING 23 OCTOBER 1996

10:30

Session W2A. **Plasma and Surface Chemistry in Materials Processing.**
Meeks, Langan, Doughty.
Auditorium.

Session W2B. **Electron Scattering.**
Lecture Hall.

WEDNESDAY AFTERNOON 23 OCTOBER 1996

13:30

Session W3A. **Inductive Coupling and Heating in Low Pressure Plasmas.**
Keller.
Auditorium.

Session W3B. **Laser Discharges and Ablation.**
Raizer, Gilgenbach, Geohegan.
Lecture Hall.

WEDNESDAY AFTERNOON 23 OCTOBER 1996

15:45

Session WPA. **Discharge Phenomena Poster Session.**
Alcove A.

Session WPB. **Heavy Particles and Electron Interactions Poster Session.**
Alcove B.

Session WPC. **Sheaths and Electrode Effects Poster Session.**
Alcove B, .

Session WPD. **Environmental Applications Poster Session.**
Alcove B.

THURSDAY MORNING 24 OCTOBER 1996

8:00

Session H1A. **Phenomena in Glow Discharge Plasmas.**
Auditorium.

Session H1B. **Environmental Applications.**
Van Brunt, Chang, Giuliani.
Lecture Hall.

THURSDAY MORNING 24 OCTOBER 1996

10:30

Session H2A. **Plasma and Surface Chemistry in Semiconductor Processing.**
Ono, Wendt.
Auditorium.

Session H2B. **Discharge Models.**
Lecture Hall.

THURSDAY AFTERNOON 24 OCTOBER 1996

13:30

Session H3A. **Discharge Experiments.**
Auditorium.

Session H3B. **Models of Glow Discharges and Positive Columns.**
Lecture Hall.

MAIN TEXT

SESSION M1A: DIELECTRIC PLASMA ETCHING
Monday morning, 21 October 1996; Auditorium at 8:00; Mike Hartig, Motorola, presiding

Invited Paper

8:00
M1A 1 Diagnostic Investigation of Oxide Etching in a Commercial High-Density Plasma Etcher.
JOHN ARNOLD, *Motorola, Advanced Products Research and Development Laboratory*

As device geometries shrink and cost and performance demands increase, the semiconductor industry must find ways to etch dielectric materials with unprecedented levels of feature aspect ratio, mask and underlying film selectivity, and system throughput. High density plasma (HDP) etch tools have demonstrated great promise for meeting present and future needs, but the simultaneous deployment of this new technology and migration to unfamiliar and more complex etchant chemistries has left a growing chasm between industrial practice and theoretical understanding of process mechanisms. In an attempt to address this problem, a series of diagnostic tools were applied to a commercial HDP etcher in a semi-production environment. Combination of data from different sensors allowed development of a qualitative but coherent model of the etching process, and highlighted the importance of thermal transients, polymer deposition and removal, and chamber wall interactions in controlling etch behavior. In addition to these phenomena, the presentation will cover implementation of diagnostic instruments, major process trends, and suggestions for future sensor development.

Contributed Papers

8:30
M1A 2 rf sensors for plasma process monitoring MAHESWARAN SURENDRA, C. RICHARD GUARNIERI, *IBM Res. Ctr. Yorktown Hts. NY* MARIANO ANDERLE, *CMBM, Instituto Trentino di Cultura, Trento, Italy* Sensors are becoming increasingly important in plasma processing as a result of increasingly stringent process tolerances. Diagnostics of capacitive/inductive rf current and voltage signals are gaining popularity, partly due to their simplicity and robustness. In this work we report measurements of rf signals in SiO_2 etching with CF_4/Ar capacitively coupled rf discharges. Results indicate that certain rf voltage harmonics are good indicators of endpoint at the SiO_2/Si interface. In addition, we show that the time-dependent signal trace is related to the spatial uniformity of the etch, which we vary by changing electrode assembly geometry. The data are also in good agreement with mass-spectra traces. We also discuss methods through which spatial uniformity information can be extracted from these and other related time-varying sensor traces.

8:45
M1A 3 Absolute Densities of CF_4 Discharge Products in an MCICP by FTIR ION C. ABRAHAM, ROBERT A. BREUN, R. CLAUDE WOODS, *ERC for Plasma-Aided Manufacturing, Univ. of Wisconsin-Madison* Absolute densities of CF_4 discharge products were measured in a magnetically confined inductively coupled plasma (MCICP) etching tool. Input power levels of 800, 1000, and1200 W were used at 4 mTorr and 25 sccm of CF_4 flow rate, and also at 10 mTorr and 3 sccm. The observed products are present in the discharge under steady state conditions, resulting from etching of the quartz window in the ICP source. The only detectable species in the plasma were CF_4 and the stable neutral etch products CO, CO_2, COF_2, and SiF_4. About one third of the total neutral pressure was accounted for by the identified species. The largest product fractions were $SiF_4$and COF_2. The rotational temperature of CO was 350-450 K, slightly increasing with power. The CO vibrational temperature was estimated to be close to the rotational temperature, after careful exclusion of the infrared emission from the plasma, as confirmed by the complete removal of the intense atomic emission lines observed in the spectrum of the Cl_2 discharge. This work was supported by NSF Grant No. ECD-8721545.

9:00
M1A 4 Mechanism study of highly selective SiO_2 etching to Si_3N_4 HISATAKA HAYASHI, MAKOTO SEKINE, *Toshiba Corporation* Selectivity in SiO_2 etching is crucial to realize high-performance, reliable and low-cost semiconductor devices. For high selectivity, it is necessary to control reactive species that are applied to the bottom of the holes where the etch reaction proceeds. We examined which fluorocarbon species were effective and how they were transported through deep holes. Based on the results, we established a reliable highly selective SiO_2 etch process over Si_3N_4 with C_4F_8 + CO gas chemistry, where a large amount of CO addition produced favorable species such as CF_2 and C_2F_4.[1] With a view to achieving further improvement necessary for 1G-bit devices and beyond, we investigated the origin of the selectivity with CO addition, because the role of CO was not understood in detail. First, CO decreased $CF_3{}^+$ ion that was an etchant of Si_3N_4. Second, C^+ ion in the plasma increased drastically, according to the CO addition amount. Also, C-implanted Si_3N_4 showed lower etch rate. We speculate that C on Si_3N_4 surface enhanced fluorocarbon deposition that reduced the etch rate. Further investigation of carbon's role in the surface reaction is necessary to control and improve the selectivity.

[1]T.Sakai *et al.*; Proc. Dry Process Symp. 1993 (The Institute of Electrical Engineers of Japan) p.193.

9:15
M1A 5 Vacuum Ultraviolet Absorption Spectroscopy for Absolute Density Measurements of Fluorine Atoms in Fluorocarbon Plasmas K. SASAKI, Y. KAWAI, K. KADOTA, *Department of Electronics, Nagoya University, Nagoya 464-01, Japan* A key parameter for obtaining the high etching selectivity of SiO_2

over Si is considered to be the density ratio of CF_x/F in fluorocarbon plasmas. This paper describes vacuum ultraviolet (VUV) absorption spectroscopy for the absolute density measurements of ground-state F atoms. The measurements were carried out in high-density CF_4 plasmas excited by helicon-wave discharges. By employing an ECR CF_4 plasma device as a light source in the VUV wavelength range, an absorption spectroscopy system with no vacuum windows was constructed. The vacuum tube connecting the helicon plasma to the ECR plasma was differentially evacuated to prevent neutral radicals from passing through each other. Electron densities higher than 10^{12} cm^{-3} were obtained by the helicon-wave discharges. The F atom density was also on the order of 10^{12} cm^{-3}, which was one-order smaller than the density of the parent gas and was one-order higher than the CF radical density measured by LIF. The F atom density increased monotonically with the rf power of 0.2–1 kW, and had a similar trend with the electron density. The present results of the absolute F atom density were compared with those by the conventional actinometry technique.

Invited Paper

9:30
M1A 6 Behaviors of CF_x Radicals in ECR Fluorocarbon Plasmas and Control of SiO_2 Etching by Radical Injection.
TOSHIO GOTO, MASARU HORI, *Dept. of Quantum Engineering, Nagoya University, Nagoya, JAPAN*

In SiO_2/Si selective etching processes using fluorocarbon plasmas, the etching selectivity is affected by the surface reactions of CF_x radicals. Therefore, it is necessary to obtain information on the behaviors of the CF_x radicals in fluorocarbon plasmas and their surface reactions.

We developed the in-situ measurement method of radicals in plasma by infrared diode laser absorption spectroscopy (IRLAS) and could be measured the CF_x (x=1-3) radicals in the on-off modulated ECR plasmas using CHF_3, CF_4, C_2F_6 and C_4F_8 for the first time. It was shown from those measurements that the CF_x radical densities, the deposition rate of the fluorocarbon film on the substrate and also the SiO_2/Si etching selectivity could be controlled with changing the duty ratio of the on-off modulated ECR CHF_3 plasma and that the CF_2 radical was an important precursor of the fluorocarbon film formation.

Moreover, we have recently developed radical injection techniques into plasma (RIT) to know the important radical for the plasma etching process. The heated HFPO gas was flown into the process chamber and the CF_2 radical density of about 1×10^{13} cm^{-3} (at 900 K) was obtained in t he present experiment. In the Ar and H_2/Ar ECR downstream plasmas with CF_2 radical injection, the deposition rates of fluorocarbon films formed on Si surfaces and the etching rates of Si and SiO_2 were measured. It was shown that the fluorocarbon film was formed from the CF_2 radical under the assist of the ion flux, and in the ECR H_2/Ar plasma where the carbon-rich (F/C=0.4) fluorocarbon film was formed, the high SiO_2/Si etching selectivity was obtained. These results will be useful for the developments of ultrafine plasma process technology.

In this review, the results on the behaviors of the CF_x radicals in the on-off modulated ECR CHF_3 plasma and the highly selective etching of SiO_2/Si in the ECR H_2/Ar downstream plasma with CF_2 radical injection are described.

SESSION M1B: ADVANCES IN ELECTRON SCATTERING TECHNIQUES
Monday morning, 21 October 1996; Lecture Hall at 8:00; Mitio Inokuti, ANL, presiding

8:00
M1B 1 Recent progress in the theory of electron–atom collisions.
KLAUS BARTSCHAT, *Drake University*

The rapid growth in the performance of computer hardware has allowed for the development of new numerical models to describe electron collisions. In addition to methods that attempt to solve the Schrödinger equation directly, i.e., without the use of basis function expansions, standard close-coupling-type approaches such as, among others, the "Convergent Close-Coupling" (CCC) [1], the "Intermediate Energy R-Matrix" (IERM) [2], or the "R-Matrix with Pseudo-States" (RMPS) [3] methods, have been extremely successful. The key advantage of those methods, when compared to perturbative approaches such as first- and higher-order plane- or distorted-wave approximations, lies in the fact that they are able to account for the effect of the target continuum states in the close-coupling expansion but still keep the full coupling between all the physical discrete as well as the bound and continuum pseudo-channels. The importance of such sophis-

ticated treatments will be demonstrated with some key examples, followed by a critical assessment of the reliability of current theoretical models.

[1]I. Bray and A.T. Stelbovics (1995), *Adv. Atom. Mol. Phys.* **35**, 209
[2]P.G. Burke, C.J. Noble and M.P. Scott (1987), *Proc. Roy. Soc.* **A 410**, 289
[3]K. Bartschat, E.T. Hudson, M.P. Scott, P.G. Burke and V.M. Burke (1996), *J. Phys. B* **29**, 115

8:30

M1B 2 Measurement of the Total Cross Section for Excitation of the 2p State of Atomic Hydrogen by Electron Impact.

GEOFFREY JAMES, *Jet Propulsion Laboratory, California Institute of Technology*

The excitation function of prompt Lyman-α radiation, produced by electron impact excitation of atomic hydrogen in the energy range from threshold to 1.8keV, has been measured in a crossed-beam experiment [1]. Measurements were carried out using both magnetically confined and electrostatically focused electron beams in collision with atomic hydrogen produced by an intense discharge source. A vacuum ultraviolet monochromator was used to measure the emitted Lyman-α radiation. The absolute H (1s - 2p) cross section was obtained from the experimental excitation function by normalization to the known oscillator strength, with appropriate corrections for polarization and cascade. The present data are significantly different from earlier experimental results [2] [3] and are in good agreement with recent theoretical convergent close coupling calculations [4] over a two order of magnitude range in impact energy. Multistate coupling affecting the excitation function to 1keV is apparent in both the present experimental and recent theoretical results.

[1]This work was performed in collaboration with J.A.Slevin, D.E.Shemansky, J.W.McConkey, D.Dziczek, I.Kanik and J.M.Ajello

[2]R.L.Long, D.M.Cox and S.J.Smith, J.Res.Nat.Bur.Stand.Sect.A:Phys. Chem. **72A**, 521 (1968)
[3]J.F.Williams, J.Phys.B.:At.Mol.Opt.Phys. **14**, 1197 (1981)
[4]I.Bray, private communication (1996)

9:00

M1B 3 Electron Collisions with Coherently Excited Atoms. Alignment Creation and Transfer Cross Sections and their Role in Plasma Polarization Spectroscopy.

SANDOR TRAJMAR, *Jet Propulsion Laboratory, California Institute of Technology, Pasadena, CA, 91109*

In "conventional" electron-atom collision experiments, one measures differential (integral) cross sections associated with initially ground state species representing averages over initial and final magnetic sublevels. In "conventional" plasma diagnostic spectroscopy, one measures the intensity of emission lines to deduce information about the plasma conditions. A deeper understanding of electron-atom collision physics requires cross sections for magnetic to magnetic sublevel transitions as well as consideration of the coherence effects in this excitation. To achieve this, one needs to design new, more sophisticated experimental techniques and evaluation schemes. The results of such experiments are magnetic sublevel cross sections, information on alignment (and orientation) creation (destruction) in the electron collision process as well as on coherences among magnetic sublevel transition amplitudes. Experiments will be described concerning, elastic, superelastic, and inelastic electron scattering by coherently prepared Ba $(\ldots 6s6p\ ^1P_1)$ atoms to demonstrate these techniques and the extraction of alignment creation and destruction cross sections from the measurements. Similarly, a deeper understanding of plasma characteristics, requires the measurement not only the intensity of emission lines but also their polarization. We will show how this polarization of radiation is connected to the polarization of the atomic ensemble responsible for this radiation and to the local properties of the plasma.

9:30

M1B 4 New Theory for Electron-Impact Ionization Cross Sections of Atoms and Molecules* .

YONG-KI KIM, *NIST, Gaithersburg, MD 20899*

A versatile theory has been developed to calculate electron-impact ionization cross sections of atoms and molecules.[1] The theory combines the Mott cross section for low incident energies, T, and the Bethe theory for high T. Two versions of the theory exist. The first version requires continuum dipole oscillator strengths (df/dE) per atomic/molecular orbital, and leads to singly differential ionization cross sections (dσ/dW), while the second version does not require df/dE and leads to total ionization cross section (σ_i) only. To obtain good agreement with available experiments on atoms, we found that the use of reliable df/dE was essential. However, the simpler second version was found to produce accurate σ_i from threshold to several keV in T for a variety of neutral molecules and radicals, including O_3, CF_4, and SF_6, in a compact analytic form. The second version[2] requires only three parameters per orbital in the ground state—electron occupation number, binding energy, and average kinetic energy—which are readily available from public domain computer codes for

atoms and molecules. The theoretical cross sections agree with experiments in most cases to 10–15% at the cross section peak, and closely follow the experimental shape between the threshold and the peak.

*Work supported in part by the Office of Fusion Energy, USDOE.

[1]Y.-K. Kim and M.E. Rudd, Phys. Rev. A **50**, 3954 (1994).
[2]W. Hwang, Y.-K. Kim, and M.E. Rudd, J. Chem. Phys. **104**, 2956 (1996).

SESSION M2A: LASER AND OPTICAL DIAGNOSTICS FOR ANALYSIS AND CONTROL

Monday morning, 21 October 1996; Auditorium at 10:30; Tom Ni, Lam Research Corporation, presiding

Invited Paper

10:30

M2A 1 Diode Laser Absorption Measurements of Species Concentrations.
HAROLD ANDERSON, *University of New Mexico*

Characterization of gas phase species densities is critically important to the understanding of complex plasma chemistry and the mechanistic development of plasma processes. Infrared diode laser absorption provides a relatively simple and cost effective means of gaining access to species concentrations for a large number radicals important to plasma etching. It is particularly well suited for aiding it process development in new high density plasma etch tools where the combination of low pressure and high dissociation means the plasma chemistry component is largely comprised of atomic or two- and three-body molecular fragment species at low partial pressures. This paper describes how single-pass, FM diode laser absorption spectroscopy has been used to measure chlorine and fluorocarbon dissociation in inductively coupled discharges in a variety of both laboratory and commercial plasma etchers. The detection of atomic chlorine by measurement of the spin orbit transition around 882 cm^{-1} in a GEC/ICP Reference Cell plasma is discussed. Both bulk and spatially resolved diode laser measurements were performed. The results are used to show chlorine is largely dissociated throughout the chamber at almost power in the inductive mode and that a large fraction of the atomic chlorine is in the long lived ${}^2P_{1/2}$ spin orbit level due to increased electron collisions at high power. Measurements of CF_x radicals made in both the Reference Cell and in commercial ICP plasma etchers are also discussed. A relatively small, portable version of the diode laser system is described which has actually been transported and used on site at semiconductor fab facilities for etch tool process characterization. The utility of this information in defining critical reaction pathways in complex fluorocarbon oxide etch chemistries is described. [1]

[1]This work has been supported by grants from both SEMATECH and Sandia National Labortories

Contributed Papers

11:00

M2A 2 Sensitive Diode Laser Based Diagnostics for Gaseous Species WILLIAM KESSLER, MARK ALLEN, DAVID SONNENFROH, STEVEN DAVIS, *Physical Sciences Inc., Andover, MA* Room Temperature Diode Laser Gas Sensors We have developed sensors for several gases based on ultra-sensitive absorption spectroscopy with tunable visible to near IR diode lasers. Gases that we have detected include: HF, H2O, IF, I2, I, O2, CO2, and NO2. The diode laser sensors make extensive use of optical fibers to deliver and capture the probe optical radiation, and are therefore relatively easy to couple to test facilities. We have also used these sensors in flowing afterglows where to detect species that were generated in microwave discharges. In this presentation we will describe some of these sensors and experimental results and indicate how they can be applied to a variety of problems such as the manufacture of advanced conposite materials using feedback control.

11:15

M2A 3 Relative atomic chlorine density in inductively coupled chlorine plasmas GREGORY A. HEBNER, *Sandia National Laboratories, Albuquerque NM, 87185* Two photon laser induced fluorescence (LIF) has been used to measure the relative atomic chlorine density in an inductively driven radio frequency discharge in chlorine gas. Relative density of the chlorine ground state was monitored by exciting the $3p^2P^0_{3/2}-4p^4S^0_{3/2}$ transition at 233.3 nm while the relative density of the upper spin orbit ground state (882 cm^{-1}) was monitored by exciting the $3p^2P^0_{1/2}-4p^4S^0_{3/2}$ transition at 235.7 nm. In both cases, LIF was observed from the $4p^4S^0_{3/2}-4s^4P_{5/2,3/2,1/2}$ transitions at 725.6, 754.7, and 774.5 nm, respectively. The measured Cl density in the center of the discharge was constant with changes in rf power and increased a factor of two when the pressure was increased from 11 to 50 mTorr. LIF measurements performed on both levels of the chlorine spin-split ground state indicate similar trends for both energy levels in the inductive plasma mode. The implications of these measurements on chlorine discharge chemistry and gas temperature will be discussed. This work was supported by the United States Department of Energy (DE-AC04-94AL85000) and SEMATECH.

11:30

M2A 4 Argon Metastable Densities in a High Density Plasma Processing Reactor D. LEONHARDT, C.R. EDDY, V.A. SHAMAMIAN, J.E. BUTLER, *U.S. Naval Research Laboratory* In support of a NRL plasma processing research initiative, argon metastable state densities are measured in an ECR plasma processing reactor. Metastable states are probed using low power laser diodes in the optically thin ECR environment of pure argon and etching gas mixtures. On resonance absorptions of various near infrared lines (from the $1s \rightarrow 2p$ manifold) give absolute densities

of metastable and resonant states. Metastable densities remain fairly constant over the chamber length (>50cm) and are much lower than electron densities. Measurements were made at the ECR zone and at two typical downstream etching regions. Microwave power, pressure and rf bias effects were investigated in real etching environments and dependences on microwave power and pressure were found to be the strongest. Clearly resolved Zeeman splittings of the metastable components also permits accurate measurements of the Doppler widths and therefore the temperature of the neutral species in the high magnetic field region of the ECR.

11:45

M2A 5 Three dimensional optical emission tomography of inductively coupled plasma in Ar A. OKIGAWA, M. TADOKORO, N. NAKANO, T. MAKABE, *Keio University, Yokohama* We have developed a robot assisted optical emission tomography system[1] to measure a 3-D profile of the production rate in an inductively coupled plasma (ICP) reactor. In this work, a typical ICP is maintained in a coaxial quartz cylinder 10 cm in diameter and 20 cm in height by a one-turn current coil driven at 13.56 MHz in Ar. Short lived-excited states $Ar(3p_5)$ with radiative lifetime, 90 ns, is used as the probe of electrons with energy greater than 14.57 eV. The profile of excitation rate to $Ar(3p_5)$ is reconstructed from a series of measurements of line integrals of emission by utilizing the algebraic reconstruction techniques. An azimuthal asymmetry of the net excitation is found from the present sliced-images. The result is caused by the lack of the azimuthal field between the current feed terminals. In addition we have performed measurements of the electron density by Langmuir probe. The radial distribution of electron density follows closely the production profile.

[1]A.Okigawa, T.Makabe, T.Shibagaki, N.Nakano, Z.Lj.Petrović, T.Kogawa, A.Itoh, Jpn.J.Appl.Phys. **35**,1890 (1996).

12:00

M2A 6 Electric Field Measurements in an Argon Glow Discharge M.D. BOWDEN, Y.W. CHOI, S. TAGUCHI, K. MURAOKA, *Kyushu University, Japan* The electric field in an argon glow discharge was determined by measurement of the Stark shift of transition wavelengths in argon atoms in the discharge. Measurements were made in the sheath region of a parallel-plate dc plasma. Both laser optogalvanic spectroscopy and laser induced fluorescence spectroscopy were used to detect the Stark shift of the wavelength of transitions from the metastable 4s(J=2) level to 6f, 7f and 8f levels. An experimental calibration of the wavelength shift against electric field was made using laser optogalvanic spectra from argon and helium atoms in an Ar/He discharge, and using the helium spectra to determine the electric field [1]. Using this calibration, measurements were made in pure argon discharges.

[1]D.K. Doughty and J.E. Lawler, Appl. Phys. Lett. Vol. 45, 611 (1984)

12:15

M2A 7 Radical production mechanisms in a CF_4 RIE plasma J.P. BOOTH, G. CUNGE, P. CHABERT, F. NEUILLY, N. SADEGHI, J. DEROUARD, *Lab. de Spectrométrie Physique, Université de Grenoble, France* Laser induced fluorescence was used to measure the spatial concentration profiles of CF and CF_2 radicals in a pure CF_4 13.56MHz RIE reactor. The concentrations were put on an absolute scale by comparison with NO LIF or by UV absorption with a Xe lamp, respectively. The profiles show that these radicals are produced predominantly at the powered electrode surface, and not by gas phase feedstock dissociation. The absolute magnitudes of the incident ion and backscattered neutral fluxes are compared. We propose that the mechanism responsible is neutralisation, fragmentation and backscattering of the CF_x^+ ions incident at high energy on this surface, and in some circumstances sputtering of polymer layers formed from heavier precursors. The strongest production of these radicals was observed with an Si substrate, which removes atomic fluorine and increases the concentration of heavier species (eg C_2F_5) which may be the polymer precursor. Both CF and CF_2 radicals are lost predominantly by reaction at the chamber walls. However, polymer deposition is poorly correlated with the net flux of these species to the wall, suggesting that they are not direct polymer precursors.

SESSION M2B: PLASMA SPRAYS

Monday morning, 21 October 1996; Lecture Hall at 10:30; C. B. Fleddermann, Univ. of New Mexico, presiding

10:30

M2B 1 Nanostructured Materials Synthesis Using Hypersonic Plasma Particle Deposition.

STEVEN L. GIRSHICK, *Department of Mechanical Engineering, University of Minnesota, Minneapolis, MN 55455, USA*

We [1] report a new deposition process in which ultrafine particles nucleate in a thermal plasma undergoing a supersonic expansion and are deposited on a substrate by hypersonic impaction. The objective of this process is to produce nanostructured material at high rates without having to collect and process a loose powder. Preliminary experiments in which silicon was synthesized by injecting vapor-phase silicon tetrachloride into an argon-hydrogen plasma produced in 20 minutes a deposit measuring approximately 1.3 mm thick and 5 mm in diameter, for a linear growth rate of about 1 um/s. In these experiments the plasma was generated by a DC torch operating at 200 A and 40 V. Flow rates were: argon, 35 slm; hydrogen, 4 slm; and $SiCl_4$, 0.2 slm. In previous experiments with similar operating conditions [2], the expansion of this mixture through a converging nozzle produced a silicon aerosol with a number-mean particle diameter of about

10 nm. In the present experiments the boron nitride nozzle was lengthened from 5 mm to 10 mm. The pressure was 66 kPa (500 torr) upstream of the nozzle and 0.3 kPa (2.5 torr) in the deposition chamber, driving a hypersonic flow which is capable of depositing particles down to about 3 nm in diameter by inertial impaction. The particle deposition process was recorded by a telemicroscope video camera, and deposits were characterized by scanning electron microscopy, x-ray diffraction, atomic force microscopy, and energy-dispersive x-ray analysis. The grain size of the deposit is expected to depend on substrate temperature, an effect which we are presently studying.

[1]Work performed with P. H. McMurry, J. V. R. Heberlein, N. Rao and H. J. Lee

[2]N Rao, B. Micheel, D. Hansen, C. Fandrey, M. Bench, S. Girshick, J. Heberlein and P. McMurry, J. Mater. Res. 10, 2973 (1995); N. Rao, S. Girshick, J. Heberlein, P. McMurry, S. Jones, D. Hansen and B. Micheel, Plasma Chem. Plasma Process. 15, 581 (1995)

11:00

M2B 2 Measurement and Control of Thermal Plasma Jets and Sprays.

JIM R. FINCKE, *Physics and Mathematics Group, Idaho National Engineering Laboratory, Idaho Falls, ID 83415, USA*

Recent developments in the diagnostics of thermal plasma flow fields and injected particles in the thermal plasma spray process are reviewed. The plasma diagnostics techniques discussed are Rayleigh and coherent Thomson scattering, laser schlieren, Coherent-Anti-Stokes-Raman Spectroscopy (CARS) and enthalpy probes. The quantities measured are heavy species and electron temperature, ionized fraction, plasma composition, and velocity. Examples of results from both subsonic and supersonic jets are presented and the diffusive demixing of atomic species in Ar/He thermal plasmas is described. Injected particle size, velocity, temperature and number density are simultaneously measured by laser velocimetry, laser scattering, and high speed pyrometry. Measured particle parameters are compared to plasma results and control applications are described.

11:30

M2B 3 Modeling of Plasma Spray Processes.

CHONG H. CHANG, *Idaho National Engineering Laboratory, Idaho Falls, ID*

A comprehensive computational model for thermal plasma processes is being developed with sufficient generality and flexibility to apply to a wide variety of present and proposed plasma processing concepts and devices. In our model for gas-particle flows, the gas is represented as a continuous multicomponent chemically reacting gas with temperature-dependent thermodynamic and transport properties. Ions and electrons are considered as separate components or species of the mixture, while ionization and dissociation reactions are treated as chemical reactions. Entrained particles interacting with the plasma are represented by a stochastic particle model in which the velocities, temperatures, sizes, and other characteristics of typical particles are computed simultaneously with the plasma flow. The model in its present form can simulate particle injection, heating, and melting, but not evaporation and condensation. This model is embodied in the LAVA computer code, which has previously been applied to simulate plasma spraying, mixing and demixing of plasma gases, and departures from chemical (ionization/dissociation), thermal, and excitation equilibrium in plasmas. A transient simulation has been performed of stainless steel particles injected into a swirling high-velocity nitrogen-hydrogen plasma jet in air under typical operating conditions for a newly developed high-velocity high-power (HVHP) torch, which produces plasma jets with peak velocities in excess of 3000 m/s. The calculational results show that strong departures from ionization and dissociation equilibrium develop in the downstream region as the chemical reactions freeze out at lower temperatures. The calculational results also show good agreement with experimental data on particle temperature, velocity, and spray pattern, together with important statistical effects associated with distributions in particle properties and injection conditions. This work was performed under the auspices of the U. S. Department of Energy under DOE Field Office, Idaho, Contract DE-AC07-94ID13223, supported by the U. S. Department of Energy, Office of Energy Research, Office of Basic Energy Sciences, Division of Engineering and Geosciences.

12:00

M2B 4 Small Particle Plasma Spray Technology.

THOMAS BERNECKI, *Northwestern University*

This abstract was not submitted electronically.

SESSION M3A: CRITICAL ELECTRON SCATTERING PROCESSES
Monday afternoon, 21 October 1996; Auditorium at 13:30; Steve Buckman, Australian National Univ., presiding

Invited Papers

13:30
M3A 1 Electron-Impact Ionization and Dissociative Ionization of Species Relevant to Plasma Processing.

K. BECKER, V. TARNOVSKY, *City College of CUNY, USA*
R. BASNER, M. SCHMIDT, *INP Greifswald, Germany*
H. DEUTSCH, *Universitaet Greifswald, Germany*

Electron-impact ionization and dissociative ionization of the various constituents in a processing plasma is not only the dominant process for the formation of the charge carriers in the plasma, it is also the crucial step that initiates the multitude of plasma chemical reactions through the formation of reactive ionic and neutral radicals. This talk will summarize recent progress in the experimental determination of absolute electron-impact ionization and dissociative ionization cross sections for a variety of molecules and free radicals relevant to plasma processing such as CH_x and SiH_x (x=1-4), NH_x (x=1-3), SO and SO_2, and the Si-organic molecules TMS, HMDSO, and TEOS.[1]

[1]This work has been supported in part by the US Department of Energy (DOE), the US National Science Foundation (NSF), the US National Aeronautics and Space Administration (NASA), and by a NATO Collaborative Research Grant.

14:00
M3A 2 Measurements of Cross Sections for Electron-Impact Dissociation of Molecules into Neutral Radicals.

HIDEO SUGAI, *Department of Electrical Engineering, Nagoya University, Nagoya 464-01, Japan*

Neutral radicals have been considered to play key roles in plasma CVD and etching. In order to model and control such plasma processing, there has been a great need to obtain cross section data for electron-impact dissociation of molecules into neutral radicals. Earlier electron impact studies have given the extensive data of ionization cross sections. However, little is known about dissociation into neutral fragments since detection of neutral radicals is extremely difficult. Recently, we[1] have developed a highly sensitive technique for radical detection, appearance mass spectrometry (AMS), and succeeded in measuring cross sections for neutral radical yield from several species of molecules important for CVD and etching.[2,3] Firstly, we present an experimental method for measuring an electron impact energy dependence of cross sections. The experiment was performed in a dual electron beam device where a primary electron beam dissociates molecules into neutral radicals which are selectively ionized by a probing electron beam based on the AMS method. Although the relative cross sections are readily obtained in these procedures, determination of the absolute cross sections necessitates the ionization cross sections of radicals. At present, such data are available only for several restricted species of radicals . Secondly, the cross sections we could measure to date are briefly reviewed: dissociations from methane (CH_4) into CH_3 and CH_2 radicals; from carbon tetrafluoride (CF_4) into CF_3, CF_2 and CF; from trifluoromethane (CHF_3) into CF_x (x=1-3) and CHF_2 and CHF; from silicon tetrafluoride (SiF_4) into SiF_x (x=0-3); from sulfur hexafluoride (SF_6) into SF_x (x=1-3). Finally, we report extension of these works to a large molecule C_4F_8 and detection of fluorine atom dissociated from fluorocarbon molecules. Furthermore, a recent effort to overcome difficulties in measuring the cross sections for monosilane (SiH_4) dissociation will be described.

[1]Hideo Sugai, Makoto Iio, Hirotaka Toyoda
[2]H. Sugai, H. Toyoda, T. Nakano and M. Goto, *Contrib. Plasma Phys.* **35** (1995) 415.
[3]M. Iio, M. Goto, H. Toyoda and H. Sugai, *Contrib. Plasma Phys.* **35** (1995) 405 and references therein.

14:30
M3A 3 Electron Impact Dissociation of Molecules and Molecular Ions.

ANN E. OREL, *University of California, Davis, Department of Applied Science*

Substantial progress has been made in the study of electron collisions with molecules and molecular ions. Collisions that result in dissociation, such as dissociative recombination, dissociative attachment, and excitation into dissociative electronic states, play an important role in many plasma processes such as low-temperature plasma etching. Reliable theoretical methods are exceptionally important because of the extreme difficulty of experiments in this area. In many of these processes, resonances play a crucial role, and there is additional complexity due to the importance of both the nuclear as well as the electron scattering dynamics. I will describe our progress in this area with examples from the simplest system, H_2^+ to more complicated polyatomics, such as CH_3Cl . * Supported by the National Science Foundation. Work performed under the auspices of the US Department of Energy by the Lawrence Livermore National Laboratory under Contract No. W-7405-Eng-48.

Contributed Papers

15:00

M3A 4 Low-Energy Electron Interactions with CHF_3L. G. CHRISTOPHOROU*, J. K. OLTHOFF, M. V. V. S. RAO, YICHENG WANG*, *NIST, Gaithersburg, MD 20899* Trifluoromethane is a commonly used plasma processing gas. The available information on the cross sections and rate coefficients for collisional interactions of CHF_3 with electrons has been synthesized and assessed, and will be presented. Significant data exist on optical emission from CHF_3 under electron impact. The limited measurements on electron impact ionization and dissociation of CHF_3 vary considerably. A "recommended" set of electron impact cross sections is presented based upon the limited available data. No experimental values are currently available in the literature for any of the electron scattering cross sections, or the electron transport, attachment, and ionization coefficients. Progress on experimental efforts to determine these parameters will be discussed. Research sponsored in part by the U.S. Air Force Wright Laboratory under contract F33615-96-C-2600 with the University of Tennessee. *Also, Department of Physics, The University of Tennessee, Knoxville, TN.

15:15

M3A 5 Electron-Polyatomic Molecule Scattering: Experimental and Theoretical Studies for C2F6H. TANAKA, L. BOESTEN, *Sophia University, Tokyo, Japan*M. KIMURA, *Yamaguchi University*H. SATO, *Ochanomizu University Sophia University, Tokyo, Japan*M. DILLON, *Argonne National Lab, Argonne, IL* Elastic cross section measurements for electron scattering from C2F6 molecules was carried out earlier and details of the observation were reported [1]. Recently, we carried out a theoretical study on elastic processes of electron scattering based on the continuum multiple scattering method in the energy range from 1 eV to 100 eV. Present theoretical cross sections for scattering reproduce typical features in the cross sections seen experimentally, namely, a feature near 7 eV where the experimental result shows a broad peak due to a shape resonance.

[1]T. Takagi *et al.* J. Phys B27, 5389 (1994)

SESSION M3B: HEAVY PARTICLE COLLISIONS AND EFFECTS
Monday afternoon, 21 October 1996; Lecture Hall at 13:30; Richard Van Brunt, NIST, presiding

Invited Papers

13:30

M3B 1 Boltzmann equation approach to cold collisions.
MURRAY HOLLAND, *JILA and Department of Physics, University of Colorado, Boulder, CO 80309-0440*

The regime of macroscopic quantum effects demonstrated in the recent Bose-Einstein condensation experiments[1] was associated with cooling a trapped alkali vapor to nano-Kelvin scale temperatures. The key technique for achieving this was runaway evaporative cooling. This cooling process is described by the theory of non-equilibrium physical kinetics for a gas with low density as given by the Boltzmann transport equation. The evolution depends nonlinearly on the distribution function of the atoms which makes it difficult to model current experiments. An alternative linear theory of physical kinetics has now been formulated to describe the relaxation of atoms from a non-equilibrium distribution. The distribution function is decomposed into trajectories, each corresponding to a different realization of a sequence of collisions for a single particle. Accumulating all possible trajectories gives the usual kinetic dynamics. The significance of the method is that it overcomes the nonlinear scaling of the Boltzmann equation and the required computation time therefore scales linearly with the number of points used to sample the distribution function. This method is now being extended to include the quantum statistical effects and consequently it should be possible to simulate the condensation into the ground state.

[1]M. H. Anderson *et al.*, Science **269**, 198 (1995); K. B. Davis *et al.*, Phys. Rev. Lett. **75**, 3969 (1995).

14:00

M3B 2 Thermal Energy Ion-Neutral Reactions Relevant to the Interstellar Medium and Planetary Ionospheres* .
NIGEL G. ADAMS, *University of Georgia*

Ion-molecule and ion-atom reactions are important in many ionized media. They are implicated in the molecular formation that occurs in the extensive interstellar gas clouds that pervade galaxies and in which star formation is occurring. These clouds contain molecular species, ranging from H_2 to $HC_{11}N$, of which over 100 have been identified, 10% being ions. Ion-molecule reactions are also central to understanding the structure of planetary ionospheres and provide a means of detecting toxic trace impurities in the lower atmosphere of the Earth. The types of ion-neutral reactions important in these media will be discussed. These vary from conventional binary reactions, such as proton transfer and ligand switching, to association reactions and reactions with atomic hydrogen. Examples will be taken from recent experimental work in our laboratories using flow tube techniques. In these experiments, structures of ions are also being probed by their reactivity. The importance of this is becoming more evident as different isomeric forms are revealed. The final step of electron-ion recombination by which many of the ions in plasmas are neutralized will also be briefly mentioned.

*Work supported by NSF Grant No. AST-9415485.

14:30

M3B 3 Proton and electron transfer for low energy collisions of H_3^+ and D_3^+ with molecular hydrogen and deuterium. BRIAN L. PEKO, ROY L. CHAMPION, *Department of Physics, College of William and Mary, Williamsburg, Virginia 23187* Total cross sections for electron transfer, proton (deuteron) transfer, and proton (deuteron) transfer followed by dissociation have been measured for collisions of H_3^+ on H_2 and D_2 and D_3^+ on H_2 for impact energies ranging from 3 ot 300 eV. Electron transfer resulting in target ionization is dominant for projectile energies larger than 60 eV. At energies less than 40 eV proton (deuteron) transfer, H_3^+ (D_3^+) + $H_2 \rightarrow$ H_2H^+ (H_2D^+) + H_2 (D_2), often leads to an unstable H_3^+ (H_2D^+) product ion which subsequently decomposes primarily by ejecting a proton (deuteron, proton) and secondarily by decomposing into H_2^+ (HD^+, H_2^+). In both instances, proton (deuteron) transfer cross sections continue to increase as collision energy is decreased, while threshold collision energies are observed for product dissociation. The importance of these measurements for modeling hydrogen discharges will be discussed. This work was supported in part by the Division of Chemical Sciences, Office of Basic Energy Sciences of the U.S. Department of Energy.

14:45

M3B 4 Silicon atoms in ECR oxide deposition plasmas EDWARD AUGUSTYNIAK, KOK HENG CHEW, J. LEON SHOHET, R. CLAUDE WOODS, *ERC for Plasma-Aided Manufacturing, University of Wisconsin, Madison, WI 53706* Silicon atom concentrations were measured in silane/oxygen and tetraethoxysilane (TEOS)/oxygen plasmas created in a 2.45 GHz electron cyclotron resonance (ECR) reactor. Atomic absorption using a Si hollow-cathode lamp source was applied to measure attenuation of the six Si I resonance lines 4s $^3P^0$ - 3p^2 ^3P (250.69 - 252.85 nm) permitting independent determination of the populations of the three sublevels (J = 0, 1, 2) of the ground state. The relative populations followed a Boltzmann distribution, and the determined internal temperature varied from 380 K (200 W) to 720 K (650 W). Silicon atom concentration increased with power and silane or TEOS flow rate, reaching 10^{11} cm^{-3} at 650 W, 5 mTorr, 20 sccm of SiH_4, and 20 sccm of O_2. The Si concentration was strongly correlated with the deposition rate and quality of the silicon oxide films. Inferred Si atom fluxes were high enough to account for the observed silicon oxide deposition rates in silane/oxygen plasmas. This work was supported by the NSF under Grant No.EEC-8721545.

15:00

M3B 5 Contribution of ion species to thin film deposition of silicon dioxide in oxygen/silane helicon diffusion plasmas C. CHARLES, R.W. BOSWELL, *Space Plasma Group, RSPhysSe, The Australian National University, ACT, 0200* Energy selective mass spectrometer measurements of positive ions have been performed in a low pressure (a few mTorr) high density (1011 cm^{-3}) oxygen/silane helicon deposition reactor for 02/SiH4 flow rate ratios varying from 1 to 10. A simple model of the ion-induced deposition rate has been developed and the results have been compared to the measured deposition rate. It appears that 20 to 50 % of the silicon atoms in the near-stoichiometric deposited oxides could result from the flux of silicon-containing ions (essentially Si+ and SiOH+) to the substrate during deposition. An oxidation process via 02+ ions and an etching process via H3+ ions could possibly be involved in the ion-induced deposition mechanism.

➢➢➢➢➢➢➢➢➢➢➢➢

SESSION MPA: INDUCTIVELY COUPLED PLASMAS POSTER SESSION
Monday afternoon, 21 October 1996
Alcove A at 15:45
Dave Spence, ANL, presiding

MPA 1 The Spatial Distribution of the Electric Field in an Inductive Discharge ROBERT PIEJAK, VALERY GODYAK, BENJAMIN ALEXANDROVICH, *OSRAM SYLVANIA INC* The magnitude and relative phase of the electric field (E-field) has been determined from measurements of the time varying magnetic flux density (dB/dt) in inductively coupled argon discharges driven at 6.78 MHz. Two different probes were used to (independently) determine the E-field. One probe is a small wire loop (0.5cm OD) that measures the radial component of dB/dt; the integral of dB/dt over axial position is the electric field. The other probe is a large thin wire loop (8 cm OD) which measures the electric field directly (no integration). dB/dt was measured as a function of axial distance from a planar induction coil at a fixed radial distance from the center axis of the discharge chamber. Measurements were made over gas pressures ranging between 1 mT and 100 mT and at discharge powers ranging between 25W and 200W. The electric field found from the two probes is in very good agreement. At 100 mTorr the magnitude of the electric field decreased monotonically as its relative phase lag increased with increasing distance from the induction coil. At lower gas pressures, however, the E-field was observed in some cases to decrease non-monotonically with increasing distance from the coil. In addition, a remarkable variety of behavior was found in the relative phase of the E-field. The observed magnitude and phase behavior of the electric field will be discussed in terms of the components of the field due to induction coil current and discharge current.

MPA 2 Investigations of an Inductively Coupled GEC Reference Cell by means of Langmuir Probes AXEL SCHWABEDISSEN, ERIC C. BENCK, JAMES R. ROBERTS, *NIST, Gaithersburg, MD* Measurements of the plasma potential, electron density, mean electron temperature, and electron energy distribution function (EEDF) have been performed with cylindrical Langmuir probes in planar, electrostatically shielded, low pressure (3-50 mtorr) inductively coupled plasmas in pure Ar, Xe, Kr, Ne, O_2, N_2, and a He:Ar (96:4) gas mixture. The plasma source is a modification of the GEC reference cell with the upper electrode replaced by a five turn, pancake coil and a quartz vacuum interface. Observations show that with increasing ionization potential of the rare gas, the electron density decreases, while the mean electron temperature and plasma potential increase. Electron densities in oxygen and nitrogen are approximately a factor of ten below those of argon at the same power. The EEDF's are non-Maxwellian above the energy range for elastic collisions. Axially and radially resolved measurements confirmed that the EEDF's are determined only by spatially averaged quantities instead of the local electric field distribution.

MPA 3 Electron Properties of an Argon Inductively Coupled Plasma Measured using Laser Thomson Scattering T. HORI, M.D. BOWDEN, K. UCHINO, K. MURAOKA, *Kyushu University, Japan* Electron temperature, density and energy distribution functions (EEDF) in an argon, planar, radiofrequency inductively-coupled plasma (ICP) were measured using laser Thomson scattering. In dc plasmas, the EEDF in higher pressure discharges was Maxwellian but in low pressure discharges, a non-Maxwellian dis-

tribution was observed. The non-Maxwellian distribution in the low pressure discharge was attributed to local heating effects in the discharge. These effects were detectable in low electron density (N_e $10^{17} m^{-3}$) discharges but were not measurable in higher density discharges (N_e $10^{18} m^{-3}$) due to effects of electron-electron and electron-neutral collisions. Measurements of T_e, N_e and the EEDF were also made in pulsed discharges and temporal dependencies of these quantities will be presented. The mechanisms which determine these quantities, and particularly the EEDF, will be discussed.

MPA 4 Argon Ion Velocity Distribution in an ICP Reactor. N. SADEGHI, *Lab Spectrometrie Phys. Grenoble Univ, Grenoble, France* M. VAN DE GRIFT, D. VENDER, G.M.W. KROESEN, F.J. DE HOOG, *Eindhoven Univ. Technology, Phys. Dept., Eindhoven, The Netherlands* Doppler Shifted Laser Induced Fluorescence technique was used to determine the distribution functions of the radial and axial velocity components of the $Ar^{+*}(^2G_{9/2})$ metastable ions on the axis of an ICP reactor (ϕ=15 cm, h=4 cm; RF up to 500 W; p_{Ar}=2.5 to 80 mTorr). To avoid metal sputtering, the internal walls of the reactor are covered by a glass layer. The gas temperature, deduced from the Doppler width of the absorption profile of the 772.376 nm argon line on $Ar^*(^3P_2)$ metastable atoms, increases with p_{Ar} and the RF power (500 K at 2.5 mTorr, 200 W ;800 K at 80 mTorr, 500 W). In the center of the plasma volume, the ion velocity profiles are Gaussian shaped, corresponding to an isotropic ion temperature of around 0.12 eV. Under the influence of the E-field in the presheath, ions are accelerated toward the wall and gain up to 5 eV axial kinetic energy at 1 mm from the surface. At this point, the transverse ion temperature also rises to 0.2 eV at 40 mTorr. This is attributed to the elastic and charge exchange collisions of the ions. Results show that $Ar^{+*}(^2G_{9/2})$ metastable state is mainly populated by electron impact from the ground state argon ions. The velocity profile of ions in these states are therefore identical.

MPA 5 Mass Spectrometric Measurement of Molecular Dissociation in SF_6-Ar and O_2-Ar rf Discharges YICHENG WANG, JAMES K. OLTHOFF, RICHARD J. VAN BRUNT, *NIST, Gaithersburg, MD 20899* We report the measured dissociation fraction of molecules in radio-frequency (rf) SF_6-Ar and O_2-Ar discharges. A Gaseous Electronic Conference rf reference cell with an inductively-coupled plasma source is used to produce the discharges, with the gas pressures ranging from 1.3 to 5.3 Pa and applied rf powers from 100 to 300 W. Neutrals are sampled through a 0.2 mm diameter orifice in a grounded cone positioned on the side of the discharges and analyzed with a quadropole mass spectrometer. By cycling the rf power on and off, and measuring the percentage change of the ion intensity originating from the parent molecule, we determine the dissociation fraction under various discharge conditions. We find that the dissociation fraction in a mixture of 40% SF_6 with 60% Ar at 200 W is as high as 91%, while it is about 10% for an O_2-Ar mixture under similar conditions.

MPA 6 Etching Rate Characterization in a Magnetically Confined Inductive Plasma Tool MOSHE SARFATY, MIKE HARPER, NOAH HERSHKOWITZ, R.C. WOODS, *Engineering Research Center for Plasma-Aided Manufacturing, University of Wisconsin-Madison* Etch rates of SiO_2 and Poly-Si using fluorocarbon and chlorine gas discharges over a wide range of conditions are measured in a Magnetically Confined Inductively Coupled Plasma (MCICP) tool. The etch rates are determined simultaneously and in real time using an in-situ two color laser interferometer. The etch rate uniformity across the 100 mm wafer is measured in-situ using a full wafer interferometer. The effects of the etching species concentration, atomic fluorine and chlorine, and the ion energy flux to the wafer on the etch rate of these films are examined. The concentration of the atomic fluorine and chlorine in the gas phase is obtained by using argon actinometry. The spatial distribution of both the plasma density and the atomic etching species along the chamber axis, are determined. The measured etch rates of both films are compared to the results of a Langmuir kinetics model. This work is funded by NSF grant No. EEC-8721545.

MPA 7 Ion Flux and Ion Energy Distributions in an Inductively Coupled GEC Rf Refererence Cell in Chlorine SVETLANA RADOVANOV, RAY FORRISTER, HAROLD ANDERSON, *The University of New Mexico* Ion flux and energy distribution measurements in pure chlorine were performed in an inductively coupled Gaseous Electronics Reference Cell 13.56 MHz radiofrequency discharge . Measurements were made using miniaturized gridded energy analyzer. This detector was developed at the University of New Mexico, based on earlier design of the small size energy analyzers at MIT. The detector was mounted on a 12 inch water cooled carrier to suppress probe heating. The probe could be radially moved in the discharge cell to monitor the radial uniformity of the plasma. In addition, the detector was protected with a ceramic coating to supress for the electron saturation current of unshielded probe areas. The measurements were done in the "bright " mode dominated by inductive coupling at different pressures and powers. The radial variation of the ion flux in pure chlorine and argon show similar strongly nonuniform profile. As expected, absolute ion flux values in chlorine are substantially decreased compared to pure argon discharge. The spatial nonuniformity across the 16 cm diameter surface of the grounded electrode is in agreement with the Langmuir probe measurements done by Miller and MIT measurements in pure argon. The ion energy distribution functions (IEDs) measured exhibit a complex structure indicative of both light Cl^+ and heavier Cl_2^+ ions. The IEDs in chlorine are much broder than those measured in pure argon plasma. The radial profile of IEDs found in the GEC/ICP chlorine discharge indicate large changes are occuring in the nature of power coupling to the discharge moving center to edge.

MPA 8 Effect of Rf Ground Location in an Inductively Coupled Plasma Reactor on the Plasma Density and Ion Energy SVETLANA RADOVANOV, HAROLD ANDERSON, *The University of New Mexico* GARY BELL, HONG-MEI ZHANG, DAN HOFFMAN, *Oak Ridge National Laboratory* VICTORIA RESTA, DAVE RASMUSSEN, *Sematech* Measurements of the electromagnetic (EM) fields, plasma density and ion energy distribution (IED)were performed in a high density ICP etch tool.The obtained EM fields have shown that a virtual radio frequency (RF) ground exists on the current strap. A set of experiments were performed to investigate the impact of altering the location of this RF ground on the EM fields produced and on the uniformity of the plasma density and ion energy distribution. Vacuum RF field measurements for "virtual" and "imposed" ground configurations show a dramatic effect on the electric and magnetic fields. In the standard "virtual" ground case (ground located near the outer edge of the coil), the electric field magnitude is center peaked, while in the "imposed" ground mode (ground shifted toward the coil center), the electric field magnitude has an annular shape. A miniaturized retarding grid ion energy analyzer (mini-IEA) was used to determine radial profiles of the ion saturation current and ion energy distribution (IED)[1]. Radial profiles of the ion current

in the "virtual" ground mode are uniform and IEDs are sharp and narrow. In the "imposed" ground mode an annular shaped profile was obtained. The IEDs are significantly broadened, suggesting a larger electrostatic coupling component to the discharge. The changes in the IED are important owing to their impact on the isotropy of etching of microelectronic devices and uniformity of plasma generation. [1]

[1]G.W. Gibson, Jr, H.H. Sawin, I. Tepermeister, D.E.Ibbotson, and J.T.C. Lee, J. Vac. Sci. Technol. B, 12, 2333 (1994).

MPA 9 A Simple Analytic ICP Model and Comparison to Experiment DANIEL R. JULIANO, DOUGLAS B. HAYDEN, DAVID N. RUZIC, *University of Illinois–Urbana* An analytic model is developed for a cylindrically symmetric inductively coupled plasma system in order to find the electron temperature and density distribution. Boltzmann's equation is solved by a computer code using a 2-term spherical harmonic expansion. Analytic results are compared to experimental measurements made with a Langmuir probe. The apparatus is a magnetron system [1] with an RF coil or other ionization source inserted between the target and substrate. Far from the target, the resulting plasma is dominated by this ionization source, so the plasma at the magnetron target is not accounted for in the analytic model. In the model, electric and magnetic fields from the RF coil are found as a function of position and the power deposition profile is calculated. Insights gained from this model have been used to guide research efforts in ionizing the sputter flux in the magnetron.

[1]magnetron system donated by MRC

MPA 10 Carbon Radical Measurement In Inductively Coupled CO Plasma MASANOBU IKEDA, MASAFUMI ITO, MASARU HORI, TOSHIO GOTO, *Nagoya University, JAPAN* HARUHIKO ITO, *Nagoya Municipal Industrial Research Institute, JAPAN* Recently, the behavior of carbon radical is noticed in high-density plasma process such as diamond formation and SiO_2 etching. In this study, carbon radical in an inductively coupled RF (13.56 MHz) CO plasma was measured by using ultraviolet absorption spectroscopy with carbon hollow cathode lamp for the first time. Measured carbon line was at 296.7 nm ($2s^22p^2\ ^3P_2$-$2s2p^3\ ^5S_2$ transition). In order to measure the absorption signal attributed to carbon radical, RF power was modulated to a square-wave-amplitude pulse with on-period of 20 ms and off-period of 38 ms. The absorption ratio of carbon radical was measured as a function of RF power at a CO pressure of 4 Pa and a flow rate of 50 sccm. Below the RF power of 200 W, the signal of absorption attributed to carbon radical was not detected. At the region of the RF power above 300 W, the absorption ratio of carbon radical increased with increasing the RF power. The behavior of carbon radical in inductively coupled CO and CO/H_2 plasma will be discussed.

MPA 11 Langmuir Probe Diagnostics using a Reference Probe in Inductively Coupled Plasmas MICHAEL HOPKINS, DAVID VENDER, *Plasma Research Laboratory, Dublin City University, Glasnevin, Dublin 9, IRELAND* Langmuir probes are widely used as a diagnostic in capacitively and inductively coupled plasma devices. It is now generally accepted that a compensation technique is required to remove radio frequency fluctuations across the probe sheath which result in a distortion of the probe current voltage characteristic. In many plasmas of interest similar distortion of the probe current voltage characteristic is caused by shifts in the plasma potential at frequencies well below the fundamental driving frequency. Changes in plasma potential can result from current drawn through the measuring probe and shifts of 10V for probe currents of 10mA have been recorded. Such shifts are due to insulating reactor walls, or poorly conducting plasma-ground sheaths. Low frequency fluctuations in plasma potential can also originate from plasma instabilities and the power supply and matching network. To overcome such problems we are using a Langmuir probe system which has passive compensation at 13.56 MHz and active compensation, using a reference probe, at low frequency. We show that such a system measures electron temperatures which are up to a factor of two lower in both capacitively coupled and inductively discharges. We also show that the electron energy distribution function (eedf) in low pressure discharges are non-Maxwellian and accurate measurements require the use of a reference probe. Without a reference probe it is often impossible to resolve the low energy component of the eedf and interesting structure in the eedf is lost.

MPA 12 Measurement of Plasma Uniformity in an Inductively-Coupled Plasma Reactor A.H. SATO, V.N. TODOROV, X.Y. QIAN, *Applied Materials, Inc.* A simple linear four point ion current collector probe array, and a high-accuracy 20 point probe array are described. Such probe arrays are used for measuring ion current flux at the wafer position in prototype commercial polysilicon and tungsten silicide etch chambers. These measurements allow one to measure how the plasma uniformity at the wafer changes with discharge conditions; with the geometry of the inductively-coupled plasma (ICP) source antenna; and with chamber body geometry. The uniformity of the ion current flux at the wafer is influenced by both antenna construction as well as chamber body design. A simple method is described which allows one to measure (in part) how much of the plasma non-uniformity is due to the chamber, and how much is due to the ICP antenna.

MPA 13 Simulation of Inductively Coupled Plasma Reactors with a Fully-Implicit Fluid Transport Model* ROBERT B. CAMPBELL, *Sandia National Laboratories, Albuquerque, NM 87185* There is considerable incentive to develop a simulator for plasma processing reactors which is numerically efficient, robust, and flexible. Rather than construct a code which iterates between gas transport, plasma transport, and electromagnetics (perhaps even on several different grids), we are building a code which solves the three moment plasma-fluid transport and electromagnetic equations fully-coupled on a common grid using an implicit Newton's algorithm. The fully-implicit nature of the algorithm allows for the oscillatory steady state to be approached with timesteps much larger than the limiting Courant timescale. The structure of the new finite volume code, PLASFLO, is such that tracked species, gas phase and surfaces chemistries can be easily modified and be of arbitrary complexity. Storage for the Jacobian is minimized by using a preconditioned iterative solver for sparse linear equations. The always important initial guess for the 2-D axisymmetric problem is obtained by a simple point model computation preprocessing step. Results will be presented describing typical argon and reactive gas chemistries, with validation comparison to GEC experimental data.

*This work performed under the auspices of the U.S.D.O.E. under contract DE-AC04-94AL85000

MPA 14 Numerical Simulations of Low Pressure Inductively Coupled Plasmas in Geometrically Complex Reactors BEN YU, HANMING WU, ANANTHA KRISHNAN, *CFD Research Corporation* A two-dimensional fluid model has been developed for simulation of low pressure inductively coupled plasma (ICP)

reactors. The model obtains solutions for the plasma density, electron temperature, and electric field for the given operating conditions. The physical phenomena and processes such as ambipolar diffusion, thermal diffusion, quasi-neutrality, ionization, inductive Joule heating, and excitations are considered in the model. A significant feature of the model is its capability of handling complex geometries that are often encountered in industrial reactors. Complex reactor geometries are modeled by a body-fitted-coordinate (BFC) formulation. A series of numerical experiments have been conducted using the model to study effects of various parameters such as chamber pressure, size of the wafer, position of the inductive coil, and the power input into the plasma. Different reactor geometries such as the GEC ICP reference cell and the belljar reactor have been simulated. The results of the parametric experiments are presented to show certain systematic trends in performance parameters such as uniformity and processing rates. The ICP model has been coupled to a computational fluid dynamics (CFD) code (capable of 3D simulations) that obtains the flow and pressure distribution inside the chamber. The ICP model will use pressure predictions (from the CFD model) to compute the local ionization rates. Chemical source/sink terms from the plasma dissociation model will be used by the CFD code to account for local reactant depletion effects.

MPA 15 Helicon plasma sources: Differences between M=+1 and M=-1 power coupling[1] ALBERT R. ELLINGBOE, *Lawrence Livermore National Laboratory, Univ. of California* Measurement and modeling of plasma wave fields in the near and far field of a helicon plasma source will be presented. A phased pair of double-half-turn antennas are used to produce a *vacuum* power spectrum selectively devoid of either the M=+1 or M=-1 azimuthal modes. The resultant plasma wave fields give insights into power coupling and dispersion of the different azimuthal modes.

[1]This work performed for US DOE by LLNL under contract W-7405-ENG-48.

MPA 16 Helicon Wave and Ion Density Measurements in an RF Plasma Deposition Reactor JOSEPH KHACHAN, CHRIS CARTER, BRIAN JAMES, IAN FALCONER, *Plasma Physics Department, Sydney University* A series double loop m = 1 antenna is used to generate an Argon plasma and launch a helicon wave in a reactor used in thin film deposition. We have found that a collimated plasma is produced when the DC magnetic field in the diffusion region is higher than that in the plasma source. This has the advantage of minimising plasma wall interactions. Consequently, it has been found that under these conditions moderate RF powers (~400 W) produce ion densities of the order $\sim 10^{12}$ cm^{-3} near the substrate. The ion density profile is radially symmetric with excellent uniformity over a diameter of ≃10 cm. Interestingly, this optimal density plasma was found to contain two dominant azimuthal mode numbers, namely ~75% m=0, and ~25% m=1, that give rise to an asymmetric radial RF magnetic field profile. Moreover, prominant axial standing waves are observed under these conditions. These results will be compared to the same measurements on a plasma produced by a single loop m = 0 antenna in the same reactor.

MPA 17 A Comparison of Magnetic Probe Measurements in an Inductive Discharge ROBERT PIEJAK, VALERY GODYAK, BENJAMIN ALEXANDROVICH, *OSRAM SYLVANIA INC* The magnitude and relative phase of the time varying magnetic field (dB/dt) has been measured in argon inductive discharges driven by a planar induction coil at 6.78 MHz. Measurements were made at 1, 10 and 100 mT. dB/dt was measured with two types of probes under the same conditions. One probe was immersed directly into the plasma while the other was inserted into a glass tube in the discharge. Both probes were used to measure two components (radial and axial) of dB/dt resulting in the determination of dBr/dz and dBz/dr. Assuming azimuthal symmetry, the electric field and the current density were determined (from Maxwell's equations) along axial positions z at a fixed radial position r from the discharge center axis. As a check, the electric field was also measured directly with a large wire loop (third) probe . In vacuum, the electric field determined by all probes agreed very well, however with a discharge, the E-field determined from the probe in the glass tube compared poorly with the other two probes. Based on our measurements, the perturbation of the plasma and the rf current introduced by the glass tube and the validity of dB/dt probe measurements made in glass tubes will be discussed.

MPA 18 Electromagnetic Field Structure in a Weakly-Collisional Inductively Coupled Plasma VALERY GODYAK, ROBERT PIEJAK, *OSRAM SYLVANIA INC* Two-dimensional, phase resolved magnetic probe measurements have been performed in a cylindrical inductively coupled plasma source driven with a planar coil. The rf electric field and current density distributions determined from these measurements exhibit an abnormal non-monotonic spatial evolution in a weakly-collisional plasma. Formation of a second current layer, phase bifurcation, a reverse of the rf field phase velocity and negative rf power absorption found here are attributed to spatial dispersion of the plasma conductivity due to collisionless electron thermal motion.

SESSION MPB: DISCHARGE MODELING POSTER SESSION
Monday afternoon, 21 October 1996
Alcove A at 15:45
Dave Spence, ANL, presiding

MPB 1 Modeling of Cl_2/O_2 Etching Chemistry in High Density Plasma Reactors* JAI K. SHIN, *Samsung Advanced Institute of Technology* WHIKUN YI, *Samsung Electronics Company* MARK J. KUSHNER, *University of Illinois, Urbana-Champaign* Low pressure (<10s mTorr) High Density Plasma (HDP) reactors are rapidly becoming standard tools for anisotropic plasma etching during the fabrication of submicron semiconductor devices. There have been many 2-dimensinoal modeling studies to address the feasibility and scaling of HDP reactors for optimization of geometries and control parameters. Actual reactors usually have asymmetries which are difficult to capture in. A 3-dimensinoal model for HDP reactors has recently been developed to address these potential asymmetries.[1] In this study, 2-d and 3-d models have been applied to analysis of Cl_2/O_2 HDP reactors for metal and polysilicon etching. Comparisons will be made to experimental results for uniformity and rates of etching. The effect of plasma parameters on topographic defects in etching pattern will also be discussed. [1]M. J. Kushner, et. al, J. Appl. Phys, Aug. 1996. *Work partially supported by NSF.

MPB 2 Parametric Study of Localized Plasma Mechanisms in ICP reactors using HBr/Cl2 Gas Mixtures J. W. SHON, *Sandia National Laboratories* P. VITELLO, *Lawrence Livermore National Laboratory* HBr/Cl2 gas mixture is often used for etching poly-Si. As the dimensions of the transistors are reduced, profile control, high poly-Si etch rate, high selectivity over the gate oxide, low ion-induced damage become critical. We have investigated detailed plasma mechanism for HBr/Cl2 and applied to two dimensional plasma transport code in order to investigate localized behavior of HBr/Cl2 plasma chemistry. The initial mechanism for HBr/Cl2 is investigated using well mixed model. (1) For a HBr/Cl2 plasma, the nominal conditions are 1000 Watts of input power, 5 mTorr of pressure, and a gas mixture of HBr/Cl2 = 20/80%. The major ions are Cl+, Cl2+ and Br+. The well mixed computational results show that approximately HBr/Cl2 = 55/45% will produce the equal amount of Br+ and Cl+ ions. The generation of Br+ and Cl+ are almost exclusively from the ionization of ground states and excited states of Br and Cl, where Br and Cl is mostly formed from the electron dissociation of HBr and Cl2, respectively. Cl2+ is mostly from the ionization of ground state Cl2. For a two dimensional transport code, we have used latest version of INDUCT, (2) which solves a set of time dependent fluid equations for electron and ions self-consistently with Poisson's equation for the electric potential. The dominant plasma reactions are identified for several locations in the reactor chamber including the areas below the coils, close to the side wall, center of the reactor, and above the wafer. (1) E. Meeks and J. W. Shon, IEEE Trans. on Plasma Sci., 23, 539, 1995. (2) P. Vitello, J. N. Bardsley, G. Dipeso, and G. J. Parker, IEEE Trans. on Plasma Sci., 24, 123, 1996.

MPB 3 Reactor simulations of the GEC reference cell reactor with an ICP source for Ar/Cl2 and BCl3/Cl2 gas mixtures.* RAMANA VEERASINGAM, SEUNG J CHOI, MERLE RILEY, *Sandia National Laboratories,New Mexico* ROBERT HOEKSTRA, MARK KUSHNER, *U. Illinois, Urbana-Champaign,IL* The ICP (inductively coupled plasma) device is a widely researched plasma etching technology to meet the stringent requirements of dielectric and metal etch for the next generation semiconductor wafers. At Sandia, the GEC reference cell has been modified to include a planar coil geometry to couple the RF power to the plasma inductively. Measurements of densities of electrons, CL-, Ar+, and recently of ion current flux have been made. In this paper, we will present results of simulations modeling the GEC cell for Ar/CL2 and BCL3/Cl2 gas mixtures using the HPEM and GEMINI code packages. Results will be parametrized with power, pressure, and gas mixture. In addition, simulations of the ion current flux using a sheath model developed at Sandia and the HPEM will be performed and compared to data.

*This work performed under the auspices of the U.S. D.O.E. under contract DE-AC04-94AL85000

MPB 4 Simulation of Ar/CF_4 and Ar/O_2 Plasmas in the GEC Reference Cell* SHAHID RAUF, MARK J. KUSHNER, *University of Illinois, Urbana, IL 61801* A major goal for developing the Gaseous Electronics Conference reference cell (GECRC) was to provide reliable data for plasma model validation. In this regard, useful measurements have been recently made by McMillin & Zachariah.[1] Using laser induced florescence (LIF), they measured 2-d profiles of the $1s_4$ level of argon (Ar*) in Ar/CF_4 and Ar/O_2 plasmas for a range of gas pressures and applied rf voltages. In this paper, we report on results from computer modeling of the GECRC for these experimental conditions. The simulations were performed with the Hybrid Plasma Equipment Model (HPEM). The model consists of three coupled modules for electron Monte Carlo simulation, heavy particle fluid simulation and Poisson equation solution. These modules are iteratively solved until quasi-steady state conditions are achieved. The simulations were conducted in an Ar plasma with small amounts of CF_4 and O_2. In agreement with the experiments, these additions led to the quenching of Ar* and modification of the profile. Mechanisms for these trends will be discussed. [1]B. McMillin and M. Zachariah, J. Appl. Phys. **79**, 77 (1996). *Work supported by NIST, SNLA/Sematech, NSF and SRC.

MPB 5 Model for Passivation of Trench Sidewalls BARBARA ABRAHAM-SHRAUNER, * *Washington University* The passivation of sidewalls of rectangular trenches etched in integrated circuit fabrication is modeled. Deposition of a polymer layer in carbon containing feed gases or from etched materials from the photoresist mask produce the passivated sidewalls. The etch rate fora symmetric etching/deposition model [1] which was derived for a flat surface is extended to the trench profile. The model requires that the ratio of the deposited flux to the etchant flux be greater on on the sidewalls than on the trench bottom to shut off the sidewall etching but retain the etching of the trench bottom. Reemission of material from the trench bottom [2] is included and increases the deposited flux on the sidewalls. A simplified expression for the etch rate is derived for the trench sidewalls that are completely covered with the deposited polymer layer.

*Supported by the National Science Foundation under grant ECS-9310408

[1]J. Ding and N. Hershkowitz, Appl. Phys. Lett. 68,1619 (1996)
[2]H. Hubner, J. Electrochemical Soc, 139, 3302 (1992)

MPB 6 Effect of Helicon Distribution Functions on Etch Profiles WENJING CHEN, BARBARA ABRAHAM-SHRAUNER,* *Washington University* Measured ion energy distribution functions in a low pressure argon plasma produced by a Helicon source[1] are modeled by a set of drifted Maxwellians integrated over perpendicular velocities and expressed in energy variables. Simulated annealing produces the optimum fit to the data for a given number of drifted Maxwellians. Measurements with and without a multipolar cage are treated. We assume that an etching plasma has these ion energy distribution functions and that the etch rate is proportional to the ion energy flux in the ion flux-limited regime. Etch profiles are calculated for a trench where the etch rates for the ion distribution functions are given by the approximate expressions derived previously for drifted Maxwellians.[2]. The rounded etch profiles at low ion energies suggest that sidewall passivation may be required for straight trench sidewalls.

*Supported by the National Science Foundation under grant ECS-9310408

[1]C. Charles, J. Vac. Sci. Technol. A 11, 157 (1993)
[2]B. Abraham-Shrauner and C. D. Wang, J. Appl. Phys. 77, 3445, (1995)

MPB 7 Gas-Surface Dynamics and Profile Evolution during Etching of Silicon KONSTANTINOS P. GIAPIS, GYEONG HWANG, CHERYL ANDERSON, MICHAEL GORDON, TERESA MOORE, *Caltech, Pasadena, CA* TIMOTHY MINTON, *Montana State Univ., Bozeman, MO* Understanding the dynamics of gas-surface interactions during dry etching of silicon is a prerequisite to generating models of profile evolution with predictive capabilities. When neutral F atoms with translational energies in the 2-20 eV regime impinge on the SiF_x layer, known to exist during steady-state etching of Si, unreacted atoms and reaction products scatter via thermal and direct channels. The balance between the thermally-desorbing and inelastically-scattered fluorine atoms from the etched surface determines the shape of the sidewall profile. Direct reactions help overcome desorption limitations of the etch rate with a concomitant improvement in anisotropy. An empirical model, based on experimental trends in the interaction dynamics, is used in a Monte Carlo simulation of topography evolution during neutral beam etching of Si. Etching experiments with energetic fluorine atoms have verified model predictions of profile phenomena and of conditions for the anisotropic etching of Si at room temperature. Aspect ratio independent etching will be also demonstrated.

MPB 8 Reactor scaling for large area plasma processing M. MEYYAPPAN, *Scientific Research Associates, Glastonbury, CT* Migration to 300 mm wafer size is a topic of active research and development in semiconductor processing. Plasma process tool development for 300 mm wafers faces significant technical challanges, particularly from the point of view of process uniformity across the wafer. Process and reactor modeling can play a complementary role in tool design and development. Many of the models in the literature have focused thus far on discharge physics aspects of the modeling excercise. In this work, we also focus on gas flow and other reactor issues. The model involves two dimensional solution to compressible gas flow, energy and multispecies conservation equations. A simplified chemical scheme for the chlorine etching of silicon is considered. Simulation results are presented for various reactor geometrical parameters, pressures, and flow rates. Scaling to 300 mm wafer is discussed.

MPB 9 Volume of Fluids Methods Applied to Etching and Deposition JOHN J. HELMSEN, *Lawrence Berkeley National Laboratory, Center for Computational Sciences and Engineering, One Cyclotron Road, MS:50D-111, Berkeley CA 94720* The volume of fluids (VOF) method is applied to simulating etching and deposition processes employed in semiconductor wafer manufacturing. Some of these processes are: plasma etching, ion milling and chemical vapor deposition. The VOF method formulates surface motion as the movement of a front, where one fluid is moving into a regime occupied by another fluid. The fluids are represented as volume fractions in each cell and are expressed on a Euclidean grid. The interface that represents the boundary is then determined from the volume fractions contained in and surrounding each cell. Once the interface is determined, techniques from computational fluid dynamics can be used to simulate the advancement of the surface. Anisotropic etching is perfomed using the Hamaguchi method of determining surface characteristics. In this talk, the volume of fluids method is described and applied to advancement models that describe semiconductor manufacturing processes. Effects that are simulated include anisotropic etching and species flux dependent etching and deposition. Techniques for advancement and calculating the fluid interface are shown in two and three dimensions. Integration with surface chemistry solvers such as CHEMKIN is also demonstrated.

MPB 10 Comparison between RFEA and sector analysis of plasma ion energies R.W. BOSWELL, *Space Plasma Group, RSPhysSE, The Australian National University, ACT, 0200, Australia* A.J. PERRY, G.D. CONWAY, S. PAUTONIER, C. CHARLES, C.A. DAVIS, A. DURANDET, *Space Plama Group, RSPhysSE. The Australian National University, ACT, 0200,.Australia* In the measurement of the ion energy distribution exiting a plasma, care has to be taken with three main effects: bulk plasma ion acceleration and heating, sheath dynamics and distorsions caused by the analyser. We have made simultaneous measurements of ions in the diffusion region of a helicon source using a 4 grid miniature (1 cm^2) retarding field analyser and an energy selective ion mass analyser (HIDEN). The former is controlled by a Labview system and has an energy resolution of better than 0.3 eV. The latter has a possible resolution of the same order but is more complicated to set up. The similarities and differences between the two systems will be discussed, especially for rf modulated sheaths.

MPB 11 Molecular Rydberg States in HydrogenNegative Ion Discharges J. R. HISKES, *LLNL, Livermore, CA* There the suggestion that the presence of molecular Rydberg states in a hydrogen- negative-ion-discharge will enhance the negative ion population via dissociative attachment. Christophorou and Pinnaduwage [1 2]see evidence for large dissociative attachment rates, >10-6 cm3 sec-1 to molecular Rydberg states in laser driven high-pressure (5-50 Torr) discharges. The concentration of negative ions in low-pressure(5-10 mTorr) ion source discharges is calculated taking into account electron collisional excitation of the Rydberg spectrum followed by dissociative attachment at the postulated high rates. This concentration of Rydberg states will increase the concentration of negative ions on the order of one percent or less, compared to the concentration generated via dissociative attachment to ground state vibrationally-excited molecules. [3 4]

[1]L. A. Pinnaduwage and L. G. Christophorou, Phys. Rev. Lett. 70, 754 (1993)
[2]L. A. Pinnaduwage and L. G. Christophorou, J. Appl. Phys. 76 46 (1994)
[3]J. R. Hiskes, AIP Conf. Proc. No. 380 (1995)
[4]J. R. Hiskes, Appl. Phys. Lett. 69 (6), 755 (1996)

MPB 12 Excitation by Electrons and Fast Neutrals in N_2 Discharges at High E/n V.D. STOJANOVIC, B.M. JELENKOVIC, * Z.LJ. PETROVIC, *Institute of Physics, University of Belgrade, Belgrade, Yugoslavia* A Monte Carlo (MC) code was developed to simulate the behavior of electrons, ions and neutrals in gas discharges at high E/n (E - electric field, n - gas density), and uniform electric fileds. The results were compared with measurements of spatial excitation coefficients for 1^- in N_2^+ and 2^+ in N_2 at 6.3 kTd and 64 kTd (1 Td = 10^{21} Vm^2) [1]. The first transition is excited only by electrons [2], the second dominantly by energetic neutrals. The "next" collision event for every particle is determined from null collision technique with precalculated collision frequencies in a large number of energy bins. Electron anisotropic scattering was determined from precalculated differential cross sections in 70 energy ranges. Secondary electrons partition the available energy according to the published results. Ions (N^+, N_2^+) are followed from the point of ionization, neutrals (N, N_2) from the point of charge transfer. Fast atoms are followed till their energy drops below the threshold for excitation. The MC results of

MONDAY AFTERNOON \ MPB

the excitation by electrons and fast neutrals agree with experimental results and the proposed dominant fast neutral excitation near a cathode.

*NIST, Boulder, CO

[1]B.M.Jelenkovic and A.V. Phelps, Phys Rev. A 36, 5310 (1987)
[2]A.V.Phelps, B.M. Jelenkovic and L.C. Pitchford, Rev. A 36, 5327 (1997)

SESSION MPC: ELECTRON INTERACTIONS I
POSTER SESSION
Monday afternoon, 21 October 1996
Alcove B at 15:45
Dave Spence, ANL, presiding

MPC 1 Electron-Impact Total Ionization Cross Sections of Atmospheric Gases and Halogen Compounds Y.-K. KIM, W. HWANG, *NIST* M.A. ALI, *Howard Univ.* M.E. RUDD, *Univ. Nebraska, Lincoln* A versatile theoretical method[1] that combines the Mott cross section at low incident energies T and the Bethe cross section at high T was applied to atmospheric gases (O_3, H_2S, SO_2, NO_2, etc.) and halogen compounds (CF_x, HF, $HC\ell$, $C\ell_2$, etc.). The theory provides total ioniztion cross sections in compact analytic forms from the threshold to a few keV in T, thus making it convenient to use the theory for plasma chemistry modeling. Our theory is particularly effective for closed-shell molecules, such as CF_4. We found that the theory reproduces very well the shape of the relative cross section of O_3 measured by Newson *et al.*[2]

[1]W. Hwang, Y.-K. Kim, and M.E. Rudd, J. Chem. Phys. **104**, 2956 (1996).
[2]K.A. Newson, *et al.*, Int. J. Mass Spectrom. Ion Process. **148**, 203 (1995).

MPC 2 Electron-Impact Ionization and Fragmentation of Tetraethoxysilane (TEOS). K. BECKER, *City College of CUNY, USA* R. BASNER, R. FOEST, M. SCHMIDT, *INP Greifswald, Germany* The Si-organic compound TEOS is frequently used in plasma-assisted polymerization applications and for the deposition of thin SiO_2 films. We report measurements of absolute electron-impact ionization cross sections for the formation of the most abundant fragment ions from threshold to 100 eV[1]. The measurements were carried out in a modified double focussing mass spectrometer with sufficiently high resolution to distinguish between different fragment ions of nominally the same mass-to-charge ratio. These measurements were complemented by various mass spectrometric studies of the neutral and ionic components in a Ar/TEOS rf discharge. The mass spectra are interpreted using the previously measured ionization cross sections. We will also present calculated ionization frequencies for TEOS and Ar at different electron temperatures assuming a Maxwellian electron energy distribution function.

[1]This work is partially supported by the US National Science Foundation.

MPC 3 Excitation of unstable atomic species by controlled electron impact. W. KEDZIERSKI, J.W. MCCONKEY, *University of Windsor Ontario Canada N9B 3P4* This abstract was not submitted electronically.

MPC 4 Calculated And Measured Ratecoefficients For Electron Impact Excitation of Neutral And Singly Ionized Nitrogen ROBERT M. FROST, PETER AWAKOWICZ, *Lehrstuhl für Technische Elektrophysik, Technical University Munich, Munich, Germany* Collisional calculations for neutral and singly ionized nitrogen have been carried out with the R-Matrix method in the energy region below 50eV and 180eV respectivly. For both atomic systems collision strengths were calculated for optical allowed and forbidden transitions as well as for exchange transitions between all the levels with principal quantum numbers $n \leq 3$. Some of the ratecoefficients which result from these calculations were verified with experimental ones in the energy range near threshold. For this purpose four NI- and eleven NII-ratecoefficients were measured by means of a stationary low-pressure wall-stabilized arc discharge. Because of the low electron density, lying between 1.8 and $7.3 \cdot 10^{13} cm^{-3}$, the ratecoefficients could be obtained from absolute level densities applying the corona balance. The ground- and metastable state populations required therefor were determined by a collisional-radiative model. The electron temperature in the plasma ranged from 5.4eV to 8.8eV.

MPC 5 Vacuum Ultraviolet Emissions Produced by Controlled Electron Impact on Si-Organic Molecules. P. KURUNCZI, K. BECKER, *City College of CUNY* K. MARTUS, *William Paterson College, Wayne, NJ* The Si-organic molecules TMS, HMDSO, and TEOS are used as constituents of low-temperature processing plasmas in a variety of plasma deposition and plasma polymerization applications. Vacuum ultraviolet (VUV) photons resulting from the collisional interactions in the processing plasma have the potentirial to affect the processed materials adversely (or favorably). The present work reports results of the experimental determination of absolute photoemission cross sections and appearance energies for the hydrogen Lyman lines produced by electron impact on TMS, HMDSO, and TEOS, which were the only VUV emissions of significant intensity observed in our studies. The present studies[1] complement the recent analysis of near-ultraviolet and visible emissions produced by controlled electron impact on these three Si-organic molecules[2].

[1]This work has been supported by the US National Science Foundation (NSF).
[2]P. Kurunczi *et al.*, Contr. Plasma Phys. (1996), in press.

MPC 6 Characteristic Energy of Electrons in CO at High E/N JADWIGA MECHLINSKA-DREWKO, WŁADYSŁAW ROZNERSKI, *Faculty of Applied Physics and Mathematics, Technical University of Gdańsk, 80-952 Gdańsk, Poland* ZORAN PETROVIC, *Institute of Physics, 11001 Belgrade, Yugoslavia* Characteristic energy (D/μ) of electrons in carbon monoxide over the reduced electric field: $1250 \leq E/N \leq 2500$ Td at ambient temperature has been determined by means of experimental method and numerical procedure described earlier [1]. Our results lie at region of lower values than those of Lakshminarasimha *et al.* [2]

and difference increases from about 10% at 1250 Td up to 15% at 2500 Td and they are about 40% lower than results by Al–Amin *et al.* [3] for E/N=2000 Td. The estimated error of our results not exceed 5% for E/N≤ 1500 Td and 8% for E/N> 1500 Td.

[1]W. Roznerski *et al.*, J. Phys. D **27**, 2060 (1994)
[2]C.S. Lakshminarasimha *et al.*, J. Phys. D **7** (1974)
[3]S.A.J. Al–Amin *et al.*, J. Phys. D **18**, 2007, (1985)

MPC 7 Formula for the calculation of integral cross sections in a Fourier expansion method+ ZHIFAN CHEN, AND ALFRED Z. MSEZANE, *Clark Atlanta University* A method has been developed to calculate the integral cross sections from the measured generalized oscillator strengths that are fitted by a Fourier expansion. The method has been applied to the e-Xe and e-N_2 scattering problems. Excellent agreement has been obtained with existing measured values for the transitions to $5p^5(^2P_{\frac{3}{2}})6s$ and $5p^5(^2P_{\frac{1}{2}})6s$ of Xe at 100 and 500 eV. For the vibrational states, $v = 1-4$, of the $b^1\Pi_u$ electronic state of N_2 at 300 eV good agreement with the data calculated by the Lassettre expansion has also been achieved. + Supported in part by DoE Division of Chemical Sciences, Office of Basic Energy Sciences, Office of Energy Research and the Air Force Office of Scientific Research.

MPC 8 Absolute Total Cross Section Measurements for Electron Scattering on GeH_4 and SiH_4 Molecules PAWEŁ MOZEJKO, GRZEGORZ KASPERSKI, CZESŁAW SZMYTKOWSKI, * *Faculty of Applied Physics and Mathematics, Technical University of Gdańsk, 80-952 Gdańsk* We have measured absolute grand total electron–scattering cross section for GeH_4 and SiH_4 molecules in the energy range of 0.75–250 eV and 0.6–250 eV, respectively, using the linear transmission experimental setup[1]. The general character of both obtained total cross section (TCS) functions is similar. For germane TCS dramatically increases from 12×10^{-20} m^2 at 0.8 eV up to nearly 59×10^{-20} m^2 at the 3.8 eV maximum. For silane the maximum (57×10^{-20} m^2) is localized near 2.9 eV. These structures are partly attributable to the existence of short-lived negative-ion resonant states. From 10 eV to the highest applied energy TCS' decrease monotonically with increasing impact energy E, and above 50 eV the total cross sections change like $E^{-0.5}$. None low-energy e^--GeH_4 experiment is available for comparison. Above 75 eV our results are in good agreement with the recent intermediate-energy TCS measurements of Karwasz[2] and with calculations of Baluja *et al.*[3]. There is also reasonably agreement of present e^--SiH_4 data with available experimental results.

*This work was in part sponsored by Komitet Badań Naukowych

[1]A.M. Krzysztofowicz and Cz. Szmytkowski 1995 J. Phys. B **28** 1593
[2]G.P. Karwasz 1995 J. Phys. B **28** 1301
[3]K.L. Baluja *et al.* 1992 Europhys. Lett. **17** 139

MPC 9 OH Yields of the Dissociative Recombination of Polyatomic Ions THEODOSIA GOUGOUSI, MICHAEL F. GOLDE, RAINER JOHNSEN, *University of Pittsburgh* OH(v=0,1) yields for the dissociative recombination of H_3O^+, HN_2O^+, HCO_2^+ and HCO^+ ions have been determined at 300 K using a flowing afterglow apparatus. Spatially resolved Laser Induced Fluorescence (LIF) was utilized for the detection of the OH product. The OH(v=0) yield for the H_3O^+ recombination (0.50 ± 0.10) was determined by two independent methods: i) by comparing it to the OH produced by the ion-molecule reaction $Ar^+ + H_2O$ and ii) by comparing it to the known yield of the reaction of metastable Ar^* with H_2O. The yields for the other recombining species were determined relative to that from H_3O^+ recombination. Those measured for OH(v=0) are in good agreement with results obtained by Herd et al[1]. However, we find significantly lower OH(v=1) yields for the recombination of HN_2O^+ and HCO_2^+ ions. We ascribe this discrepancy to OH production by extraneous reactions that the above mentioned authors failed to consider. 0.1cm This work was supported by NASA.

[1]C. R. Herd, N. G. Adams, D. Smith, 1990, Ap. J., 349, 388

MPC 10 Spectroscopic Identification of Products of Electron-Ion Recombination and Internal Excitation* JEFFERY BUTLER, TED WILLIAMS, LUCIA BABCOCK, NIGEL ADAMS, *U. of Georgia, Athens, GA* Dissociative electron-ion recombination is a major process by which plasmas are deionized. Only recently has a concerted effort been made to identify the neutral products. This involved vuv, visible and laser fluorescence spectroscopies and revealed that molecular products are often vibrationally excited, prompting Bates[1] to develop theories to explain the excitation. Our experiments have determined the complete product distribution for recombination of H_3O^+ (OH + H_2 36%, OH + 2H 29%, O + H + H_2 30%, H + H_2O 5%), the first time for a polyatomic ion recombination with multiple products. Such recombination is critical in producing neutral species detected in interstellar gas clouds. It is also important in the Earth's D-region where H_3O^+ is one of the ionic species present and in plasmas with H_2O impurities. There are also data on vibrational and electronic excitation of CO and N_2 products of the HCO^+/DCO^+ and N_2H^+/N_2D^+ recombinations. This further tests Bates' theory and shows population enhancement of the N_2 B state vibrational level which is almost resonant in energy with the recombining ion. * Work supported by NSF Grant No. AST-9415485.

[1]D.R. Bates, MNRAS, 263, 369 (1993)

MPC 11 Recombination of Electrons with $NH_4^+(NH_3)_n$-Series Ions. MIROSLAW P. SKRZYPKOWSKI, RAINER JOHNSEN, *University of Pittsburgh, Pittsburgh, Pa* The dissociative recombination of $NH_4^+(NH_3)_n$-series ions with electrons for n=2 and n=3 has been studied in an afterglow experiment over the electron temperature range 300K$<T_e<$1000K . Electrons were heated by an rf field, while the gas and ions temperatures remained at 300K. A mass spectrometer was used to determine the relative abundance of n=2 and n=3 cluster ions in a potoionized helium plasma (p~300Torr), with ammonia as a minor (less than .01%) additive. The values of recombination coefficients $\alpha_2 \simeq \alpha_3 = 4.8\times10^{-6}$cm^3/sec are ~70% higher than previously [1,2] reported. The recombination coefficient for the n=2 cluster ion varies with the electron temperature as $T_e^{-0.7}$ in contrast with a very weak temperature dependance found by Huang *et al.*[1] This work was supported by NASA

[1]C.-M.Huang, M.A.Biondi, R.Johnsen, Phys.Rev.A 14, 984(1976)
[2]E.Alge, N.G.Adams, D.Smith, J.Phys.B 16, 1433(1983)

MPC 12 Small-Angle Electron Impact Excitation of Optically Allowed Transitions: Reliability of Theory* Z. FELFLI, A.Z. MSEZANE, *CTSPS, Clark Atlanta U.* A recent theory of generalized oscillator strengths (GOSs) for forward electron scattering for optically allowed transitions provides a stringent test of theory and experiment of small-angle electron scattering [1]. Results will be presented showing that the converged close-coupling calcula-

MONDAY AFTERNOON \ MPC

tion [2] has problems obtaining reliable DCSs for He $1^1S \rightarrow 2^1P$ near $\theta = 0^o$ at all their impact energies. Also, the distorted wave approximation experiences difficulties in calculating DCSs near $\theta = 0^o$ for the resonance transition in Cu [2] and Na. Other results will be presented, demonstrating the need for careful investigations of small-angle electron DCSs in general. *Research supported by the Air Force Office of Scientific Research and U.S. DoE Division of Chemical Sciences, Office of Basic Energy Sciences, Office of Energy Research. [1] Z. Felfli, N. Avdonina and A. Z. Msezane, Phys. Rev. A to appear (1996) [2] D. V. Fursa and I. Bray, Phys. Rev. A 52, 1279 (1995) [3] D. H. Madison *et. al.*, J. Phys. B 28, 4841 (1995)

MPC 13 Ion Chemistry in Trifluoromethane CHF_3 CHARLES Q. JIAO, RAJESH NAGPAL, PETER D. HAALAND, *Wright Laboratory, Wright-Patterson AFB, OH* The energy dependence of cross sections for dissociative ionization of trifluoromethane by electron impact has been measured using Fourier-transfrom mass spectrometry. The ionization is exclusively dissociative, yielding CHF_2^+ and CF_x^+ (x=1-3), with a toal cross section of $3.4 \pm 0.4 \times 10^{-16} cm^2$ at 60 eV. Combined with the results of Winters and Inokuti [1] these data imply cross sections for dissociation into neutral radicals of $1.6 \times 10^{-16} cm^2$ and $2.1 \times 10^{-16} cm^2$ at 22 and 72 eV, respectively. Double resonance experiments show that while CHF_2^+ is unreactive with CHF_3, CF_x^+ react readily with CHF_3 forming CHF_2^+ Reaction kinetics are studied under different experimental conditions including the primary electron energy and the reactant pressure. The negative ions, F^- and CF_3^-, are formed in non-resonant processes with cross sections that are less than $3 \times 10^{-20} cm^2$ between 30 and 60 eV.

[1]H. F. Winters and M. Inokuti, *Phys. Rev. A*, (1982), **25**, 1420.

SESSION MPD: DISCHARGE EXPERIMENTS POSTER SESSION
Monday afternoon, 21 October 1996
Alcove B at 15:45
Dave Spence, ANL, presiding

MPD 1 Electron Beam Modification of EEDFs in RF Plasmas* ALEC GOODYEAR, N.ST.J. BRAITHWAITE, *Open University, Oxford Research Unit, Oxford, UK* The efficiency and effectiveness of RF plasmas used for materials processing will benefit from a greater degree of control over the physical and chemical interactions in the plasma and these can in principle be manipulated through the electron energy distribution. This work investigates the electrical means of tailoring plasma properties so that more effective use can be made of particular plasma sources. This is achieved by controlled injection of electrons into the plasma. A robust, electron gun has been developed for use with a capacitively driven radio frequency (13.56MHz) discharge. Experiments and particle simulations are in progress. Early results show considerable scope for controlling plasma density, potential structure and electron energy. The location of the gun within the plasma system is found to be critical and the use of two guns at different locations to be advantageous.

*Work funded in the UK by EPSRC

MPD 2 Plasma Generation in High-Current Ion Sources A.B. FILUK, M.E. CUNEO, T.A. MEHLHORN, T.D. POINTON, R.A. VESEY, *Sandia National Laboratories* D. WELCH, *Mission Research Corporation* We are using kA/cm^2 ion sources to generate intense pulsed ion beams for driving Inertial Confinement Fusion targets. These sources are the anode of an ion diode that uses several-Tesla magnetic fields to restrict electron flow across the diode while permitting ion acceleration. Our 2 cm diode anode-cathode gaps have 10 MV applied in order to accelerate Li ions from 100-1000 cm^2 anode areas. During the 50 ns beam pulse, we observe a transition in beam content from Li ions to H,C,O impurity ions. As well, a significant fraction of the total diode current is in electrons leaking across the magnetic insulation to the anode. The several-GW/cm^2 leakage flux of MeV electrons deposits large amounts of energy into the anode surface, releasing physi- and chemi-sorbed impurities in the modest $10^{-5} - 10^{-6}$ Torr diode vacuum. These desorbed impurity neutrals can expand and rapidly ionize within about 200 μm of the anode during the beam pulse. We are modeling this process in a multi-dimensional hybrid fluid/PIC code and making spectroscopic measurements to quantify these mechanisms.

MPD 3 Investigations of the 147 nm radiative efficiency of Xe Surface Wave Discharges N. D. GIBSON*, U. KORTSHAGEN**, J. E. LAWLER, *Physics Department, University of Wisconsin, Madison, WI 53706* The radiative efficiency of the 147 nm resonance radiation of Xe excited in a low-pressure, high-frequency surface wave sustained plasma has been investigated. The radiative UV power has been obtained from optical absorption spectroscopic measurements of the Xe resonance level population and from Monte Carlo calculations of the effective decay rate of this level. Precise measurements of the RF power absorbed by the plasma enable the determination of the absolute UV discharge efficiency for the Xe surface wave discharge. Results show efficiencies as high as 0.80 (10).[1] *Dept. of Physics and Astronomy, Denison Univ., Granville, OH 43023. **Dept. of Mech. Eng., Univ. of Minnesota, Twin Cities, MN 55455

[1]Work supported by General Electric and the NIST under the ATP (# 70NANB3H1372).

MPD 4 Excimer Emission using 20keV Electron Beam Excitation J. WIESER, A. ULRICH, *TU München* D.E. MURNICK, *Rutgers University* A small, continuously emitting rare gas excimer light source has been developed. The gas is excited by a 20keV dc-electron beam. A 300nm thick, $1 \times 1 mm^2$ SiN_x foil sustaining a pressure difference up to 2bar, separates the target volume from the high vacuum part of the electron gun. Spectra of the rare gases Ar, Kr, and Xe have been studied. The monochromator detector system was intensity calibrated in the wavelength range from 115nm to 320nm. Electron beam currents of typically 1 μA were used for excitation. When used as a VUV lamp on the second excimer continua, energy conversion efficiencies of 30% were obtained. Emissions originating from the so called left turning points have been clearly observed at 155, 173, and 222nm in Ar_2^*, Kr_2^*, and Xe_2^*, respectively. The so called third continua between 185nm and 240nm (Ar), 220nm and 250nm (Kr), and at 270nm (Xe) have been studied. A new continuum in Xe at 280nm was found. [1]

[1]Funded by the A.v.Humboldt Foundation and NSF (CTS 94-19440). The authors acknowledge support by H. Huggins, A. Liddle and W.L. Brown (Bell Laboratories, Lucent Technologies)

MPD 5 Experimental and Theoretical Studies in the Pulsed Xenon Medium Pressure Discharge ECKHARD KINDEL, DETLEF LOFFHAGEN, CONRAD SCHIMKE, *Institut für Niedertemperatur-Plasmaphysik, 17489 Greifswald, Germany* In the positive column of a pulsed xenon glow discharge time-resolved measurements of the axial electric field strength, the absolute densities of the $1s_5$ (metastable) and the $1s_4$ (resonance) state, and the VUV radiation in the range of 140-180 nm have been performed. For gas pressures between 1 and 40 Torr, currents between 100 and 300 mA, and repetition frequencies of some kHz the densities of the excited states, measured by hook method, varied from 1×10^{11} to 5×10^{12} cm^{-3}. The experimental results are compared with results obtained by model calculations. In the frame of the model for the pulsed, constricted discharge plasma the time-dependent electron Boltzmann equation for the determination of the electron kinetics, the rate equation system for the relevant heavy particles occurring in the plasma, and an appropriate equation for the axial electric field are self-consistently solved. The time-dependent treatment of the electron kinetic equation (including electron-electron interaction) is based on the conventional two-term approximation and the quasi-steady-state description of the anisotropic part of the velocity distribution. The rate equation system describes the temporal evolution of three excited atomic states, two molecular levels, the atomic and the molecular ion. Based on the theoretical results the time-dependent behaviour of the electron and the heavy particle kinetics is analysed.

MPD 6 Quantitative Analysis of a Stabilized Discharge-Pumped XeCl* Laser SERGUEI GORTCHAKOV*, DETLEF LOFFHAGEN, ROLF WINKLER, *Institut für Niedertemperatur-Plasmaphysik, 17489 Greifswald, Germany, *Institute of High Current Electronics, Russian Academy of Sciences, 634055 Tomsk, Russia* Recently a new method for providing stable, homogeneous electrical discharges for pumping wide-aperture excimer lasers has been proposed [1]. The development of a homogeneous discharge plasma has been achieved by applying a special pumping technique using an additional stabilizing low-current preliminary discharge with a typical duration of 0.5 to 1 μs. For this excimer laser discharge a theoretical analysis of the kinetics of electrons, heavy particles, and laser photons is given and the impact of various parameters characterizing the discharge on the temporal behaviour of the discharge characteristics is discussed. To model the discharge plasma the equation system for the electrical circuit, the rate equation system for various heavy particles occurring in the plasma and for the laser photons in the optical cavity, and the time-dependent electron Boltzmann equation including the electron-electron interaction has self-consistently been solved. The contribution reports on a XeCl* laser with a calculated output energy of about 1.4 J with an efficiency of about 1% and a laser pulse duration of about 400 ns.

[1]Yu. Bychkov, I. Kostyrya, M. Makarov, A. Suslov, A. Yastremsky, Rev. Sci. Instrum. **65**, 793 (1994).

MPD 7 Abnormal beharviors of O_2^- mobility in O_2/O_3 mixtures. H. ITOH, K. NORIMOTO, T. HAYASHI, *Chiba Institute of Technology* Negative ion mobilities in O_2 have been investigated at atmospheric pressure [1]. The measured range of E/p_0 for our experiment is the lowest among in the reported ones. The zero field mobility of O_2^- is determined to 2.07 $\pm$ 0.02 cm^2/V$\cdot$s in 99.9995% O_2. This value agrees well with the value mesured by Sunggs *et al.* [2]. These experiment is expanded in O_2/O_3 mixtures. Ozone is produced by a silent discharge tube connected at the upstream side of gas inlet of the main chamber. The concentrations of ozone are maintained at 270 and 500 ppm during the experiment. Our value of mobility of O_2^- in O_2/O_3 mixtures becomes smaller than that in O_2. The dependence of E/p_0 of the mobility do not appeares. We assume the accumulative effect of any neutrals generated by silent discharge.

[1]H. Itoh, K. Norimoto and T. Hayashi, Proc. Korea-Japan Symp. on Electrical Discharge and High Voltage Engineering, 179 (1996)
[2]R.M. Sunggs *et al.*, Phys. Rev. A, 3, 477 (1971)

MPD 8 New Laser Induced Fluorescence Studies of Low Temperature Noble Gas Discharges A.M. PATERSON, I.S. BORTHWICK, R.S. STEWART, *University of Strathclyde,Glasgow,Scotland* Low temperature noble gas discharges have been investigated both experimentally and theoretically using laser induced fluorescence (LIF) in the pressure and current regimes of 1–10 torr and 1–10mA, respectively. Here we employ slowly chopped (90 Hz) CW laser radiation to perturb the excited-state populations of the noble gases and record the fluorescence as the system relaxes. We have developed a successful rate equation model for the LIF spectrum observed from the positive column of the neon normal glow discharge. We have also carried out experiments with helium and argon and are at present using our model to describe these observations. The model successfully describes the observed primary and secondary (i.e. collisionally coupled) LIF signals in neon and we are confident this will be the case for argon and helium. The theory used to describe the observed LIF complements our work on laser optogalvanic spectroscopy (LOGS),emission and absorption spectroscopy of these discharges. These diagnostics will be discussed along with our experimental and theoretical LIF results.

MPD 9 Diffusive Cooling of Ions in a Hollow Cathode Discharge K. L. MULLMAN, M. SAKAI, J. E. LAWLER, *Physics Department, University of Wisconsin, Madison, WI 53706* We present evidence of diffusive cooling of ions in the negative glow (NG) of a hollow cathode discharge (HCD). For typical radius-gas density products in a HCD, the ambipolar diffusion (ion loss) rate from the NG and the collisional thermalization rate are nearly same. Since collisional thermalization fills out the tail of the Maxwellian distribution, the competition results in a somewhat truncated ion velocity distribution. This effect is observed in our High Sensitivity Absorption experiment on iron ions. The curve-of-growth for the analysis of our absorption data uses a Voigt spectral lineshape. The most satisfactory "effective" ion temperature in the Voigt lineshape is unphysically low (below the water cooled cathode temperature) under low current conditions. Effective ion temperatures are determined by requiring that the curve-of-growth analysis of the absorption data accurately reproduce well known oscillator strength ratios for singly ionized iron. [1]

[1]Supported by the NASA and the NSF.

MPD 10 AES Temperature Diagnostics in an Inductively Coupled Plasma Torch for the Deposition of High Purity Fused Silica for Optical Waveguides. G. COCITO, L. COGNOLATO, C. PANCIATICHI, A. ZAZO, *CSELT-Italy* V. COLOMBO, *University of Bologna-Italy* Atomic Emission Spectroscopy has been used to investigate temperature fields in a supposed LTE, cylindrical symmetric and optically thin plasma generated in an inductively coupled plasma torch working at 13.56 MHz, with maximum power 5 kW at atmospheric pressure, with various $Ar+O_2$ mixtures. Emission spectra have been obtained guiding plasma radiances to a monochromator and then to a powermeter using a

single-mode optical fiber suitably set in front of the discharge region. Side-on experimental intensity profiles have been treated to obtain the radial distributions of the emissions through Abel inversion; Boltzmann plot method has then been used to evaluate the radial plasma temperature behavior at various axial levels. Partial validation of results has been performed adding a small amount of H_2 to the discharge for the determination of H_β line broadening. First results of deposition of high purity fused silica will be described together with torch operating conditions and reactive mixture characteristics (O_2+SiCl_4).

MPD 11 Pulsed Discharge Excited Argon Clusters Formed in a Supersonic Slit Expansion E. THORESON, M. TERRELL, M. DEEBEL, R.E. MIERS, M.F. MASTERS, *Indiana Purdue University Fort Wayne* The argon second continuum excimer emission is observed in a pulsed discharge excited pulsed supersonic jet. The expansion nozzle is a 15 cm long slit with a width which can be varied from 35 μm to 250 μm. The intensity of the argon excimer emission near 126nm is investigated as a function of the width of the expansion nozzle slit, position within the cathode-anode gap and electrode configuration. The pressure within the nozzle has been measured as 2–4 bar and the excitation consists of a 50 ns negative (or positive) current pulse of about 15kV and 700A. The observation of the emission depends directly on the size and quantity of clusters formed in the expansion.[12] To determine the dependence of the emission upon clusters and the cluster size distribution, the cluster size distribution is varied by varying the expansion nozzle slit width. The temporal evolution of the second continuum emission and the observed spectra are presented as a function of nozzle slit width. The observed behavior are modeled using a kinetics code.

[1]M.F. Masters et. al. J. Appl. Phys. 75 3777 (1994),
[2]K. Mitsuhashi *et al.* Opt. Lett. 20 2423 (1995)

MPD 12 Radical Density Measurements in an Oxyacetylene Torch Diamond Growth Flame M. D. WELTER, K. L. MENNINGEN, *University of Wisconsin - Whitewater* The densities of several molecular radicals are measured in an oxyacetylene torch flame during the growth of diamond films. The densities of radicals such as CH, C_2, CN, and OH are determined by high sensitivity absorption spectroscopy. The radical densities are measured as a function of position in the flame for different fuel/oxidant ratios. The growth of diamond is confirmed by scanning electron microscopy and Raman spectroscopy. The measured densities are compared with other theoretical and experimental values.

MPD 13 Contaminant Ion Effects on PSII Fabricated Diodes R.R. SPETH, J.L. SHOHET, J.H. BOOSKE, H. LIU, S.S. GEARHART, R. MAU, *Engineering Research Center for Plasma-Aided Manufacturing, University of Wisconsin-Madison* Plasma Source Ion Implantation[1] has long been regarded as an alternative to classical ion implantation. An open question concerns the effect of plasma- sputtered contaminant ions on device characteristics. A suite of experiments is currently underway which quantifies the allowable level of contamination in a diode array fabricated on 3 inch N type <100> silicon wafers. The processing of the wafers is standard except for the implantation step which introduces measured quantities of both boron and contaminant ion species. The energies of both ion species is the same to simulate conditions found in the PSII chamber. The first contaminant to be studied is aluminum since it represents the material of choice for constructing PSII chambers. Other contaminants will be investigated as well. Supported by NSF Grant EEC-8721545.

[1]J.R. Conrad, J.L. Radke, R.A. Dodd, F.J. Worzala and N.C. Tran, J. Appl. Phys. 62, 4591 (1987).

MPD 14 The Kinetics of processes in decaying plasma of a Jet Diaphragm-Type Discharge E.V. KALASHNIKOV, *Vavilov State Optical Institute St. Petersburg 199034 Russia* This abstract was not submitted electronically.

MPD 15 The Effect of Precursor Composition on 2-D CF_2 Concentration in $C_xH_yF_z$/Ar Plasmas in the GEC rf Reference Cell Measured by Planar Laser-Induced Fluorescence KRISTEN L. STEFFENS, MICHAEL R. ZACHARIAH, *National Institute of Standards and Technology, Gaithersburg, MD* Although low-pressure radiofrequency (rf) plasmas are extensively used during microelectronics device fabrication, the chemical processes occurring in these plasmas are not well-understood. Because a clear understanding of the chemistry of such plasmas would aid in ensuring reproducibility during plasma processing, both model development and experimental investigations concerning the chemistry of these plasmas are currently underway. Spatially-resolved, two-dimensional species concentrations in the plasmas measured in a standardized reactor add insight into the important chemistry occurring in the plasmas and also provide necessary experimental input and verification of the models. In this work, planar laser-induced fluorescence (PLIF) is used to determine the spatial distribution and relative density of CF_2 in low-pressure $C_xH_yF_z$/Ar plasmas generated in a 13.56 MHz parallel-plate Gaseous Electronics Conference (GEC) reference cell. By using various $C_xH_yF_z$ precursors including CF_4, CHF_3, CH_2F_2, CHF_3 and C_2F_6, the effects of precursor stoichiometry (C:H:F ratio) and precursor chemical form on the spatial distribution and density of gaseous CF_2 was investigated. These results provide insight into possible chemical mechanisms important in plasma chemistry.

MPD 16 Time-resolved negative ion flux from a pulsed inductive discharge BRIAN SMITH, LAWRENCE OVERZET, *University of Texas at Dallas, Richardson, TX* Pulsed rf discharges are gaining popularity in research into plasma processing because of the potential benefits of reduced particulate formation, lowered electron temperature, and the possibility of new surface reactions arising from the presence of negative ions at the substrate. The time-evolution of a pulsed inductive discharge is revealed by several diagnostics, including a mass spectrometer, ion energy analyzer, langmuir probe, B-dot probe, and microwave interferometer. We will present measurements of the negative ion flux from plasmas in common electronegative processing gases, including SF6, correlated with density, temperature, potential, and field measurements to present an overall picture of the properties of pulsed inductive discharges.

MPD 17 Compact slot antenna type plasma source: Improvement of performance by magnet confinement D. KORZEC, CH. SEIBERT, J. ENGEMANN, *University of Wuppertal, Microstructure Research Center* A new compact 2.45 GHz magnetically enhanced plasma source of slot antenna type is presented. Plasma is generated in a quartz tube with diameter of 40 mm and a length of 500 mm. The microwave power is supplied from an annualar cavity through four slot antennae positioned equidistantly around the inner wall of an application space. The application space is closed in axial direction by two permanent magnet holder. The plasma ignition/extinction performance of the source and plasma parameter for different atomic (Ar, He) and molecular (oxygen, nitrogen) gases were studied. Ion concentrations and electron temperatures

were measured by use of a double Langmuir probe technique in the pressure range from 0.0008 to 0.5 Pa. Typical ion concentration achieved for 600 W microwave power is 4×10^{11} cm^{-3} at a pressure of 0.0005 Pa for argon and 0.02 Pa for oxygen. Electrone temperatures in plasma confined between magnet holders are as high as 10 eV. Out of this region values from 1 to 4 eV are measured. The results for three different magnetic confinements: the axial, multi-cusp and the filter one were compared. The higher values of ion concentration are achieved for axial confinement with vector of magnetization azimuthally oriented accordingly to the slot antenna position. The ionization ratio of 55% for argon and 12% for oxygen are obtained. Axial distributions of plasma parameter were used to examine the influence of the application volume length on the plasma parameter distributions.

SESSION TU1A: ELECTROMAGNETIC COUPLING EFFECTS IN DISCHARGES

Tuesday morning, 22 October 1996; Auditorium at 8:00; Rusty Jewett, Lam Research Corporation, presiding

Invited Paper

8:00

TU1A 1 Heating mechanisms and mode changes in helicon plasmas.

ALBERT R. ELLINGBOE, *Lawrence Livermore National Laboratory* *

Measurements of plasma wave fields and time-dependent (within the rf cycle) warm electron density give insight into near-resonant transit time heating of electrons in a helicon plasma source. Experimentally, rf power and magnetic field are found to determine the mode of coupling (E, H, or Wave [1]) with significant warm electron density only in W mode. A second Wave mode which yields an order of magnitude increase in warm electron current is identified as the second *axial* eigenmode of the antenna. The turn-on of the second *axial* eigenmode prior to the second *radial* eigenmode is predicted by the ANTENA computer code[2]. Orbit code modeling of the wave-particle interaction finds that increased plasma and/or neutral density significantly degrades interaction because of collisions.

*This work performed for US DOE by LLNL under contract W-7405-ENG-48.

[1]A. R. Ellingboe and R. W. Boswell, Physics of Plasmas, July (1996).
[2]B. McVey, Plasma Fusion Center, Massachesetts Institute of Technology, Report No. PFC/RR-84-12.

Contributed Papers

8:30

TU1A 2 Simulating the effect of Helicon waves on the Ionisation Rate by Electron Trapping in the wave Electric Field A.W. DEGELING, R.W. BOSWELL, *Space Plasma Group, RSPhysSE, The Australian National University, ACT, 0200, Australia* The response of the electron distribution function to a travelling wave electric field is modelled for parameters relevant to a Helicon wave plasma source, and the resulting change in the ionisation rate calculated. This is done by calculating the trajectories of individual electrons in a given wave field and assuming no collisions to build up the distribution function as a function of distance from the antenna. The ionisation rate is calculated for Argon at 3 millitorr by considering the ionisation cross section and electron flux at a specified position and time. The simulation shows pulses in the ionisation rate which move away at the phase velocity of the wave, demonstrating the effect of resonant electrons trapped in the wave's frame of reference.We find that the ionisation rate is highest when the phase velocity of the wave is between 2 and 3 x106 m/s, where the electron's interacting strongly with the wave (i.e. electrons with velocities inside the wave's 'trapping width') have initial energies just below the ionisation threshold. We also find that the ionisation rate increases dramatically with the wave amplitude, due to an exponential increase in the number of resonant electrons with the increasing trapping width.

8:45

TU1A 3 Low-Field, Large-Area Helicon Sources F.F. CHEN, J.D. EVANS, X. JIANG, *UCLA* G. TYNAN, *PMT, Inc.* Previous experiments [1] with helicon discharges in both 1- and 2-inch diam tubes have shown a density peak at magnetic fields B between 10 and 40 G and that this peak appears only with RF powers >1kW. Theory indicates that the Trivelpiece-Gould branch of the dispersion relation is important at low B, but it is not clear whether the density rise is due to increased absorption or simply to impurities from the wall. Multiple discharges of this type can be used to create a large-area plasma source for industrial applications. Two devices have been constructed to test this idea. Device 1 has a 2-in diam tube, 6-in long, with a right-hand helical antenna and a 0-100 G field, injecting plasma into a large $B = 0$ region. RF power at 13.56 and 27.12 MHz is applied up to 600W. The plasma density falls off with increasing B-field and is highest at 0 G. With a 12-in long tube, this fall-off is eliminate d. Device 2 has 7 tubes of the same type arranged in a honeycomb pattern on the top plate of a large chamber with multi-dipole confinement. By careful matching, discharges can be struck in all 7 tubes simultaneously. Density uniformity data is not available at the time of this abstract. These devices unfortunately cannot be used to verify the theory, since the magnetic fields are nonuniform.

[1]F.F. Chen and G. Chevalier, J. Vac. Sci. Technol. A 10, 1389 (1992).

9:00

TU1A 4 Quasilinear theory of collisionless electron heating in rf gas discharges Y. M. ALIEV, *Lebedev Institute, Russia* I. D. KAGANOVICH, H. SCHLÜTER, *University Bochum, Germany* On the basis of quasilinear kinetic theory the rf electron heating is studied. The main attention is devoted to the case when electron heating is due to low frequency electromagnetic wave coupling as encountered in inductively coupled discharges. Expressions for the energy diffusion coefficients are obtained. Comparison with previously published results is given. The profile of the electric field under conditions of the anomalous skin effect is found in analytical form. It differs considerably from an exponential one. The integration of this electric field over the coordinate equals to zero. As a result the heating of fast electrons is much more suppressed than in the case of an exponential profile. The bearing of the model on the case of capacitively coupled and surface wave discharges is discussed qualitatively. The equivalence of the one particle and the quasilinear approach is pointed out. The general formula for the energy diffusion coefficient is derived for arbitrary rf and ambipolar electric fields.

9:15

TU1A 5 Simulation of plasma breakdown in a low pressure, rf plasma. H.B. SMITH, R.W. BOSWELL, *Space Plasma Group, RSPhysSE, The Australian National University, ACT, 0200, Australia* D. VENDER, *School of Physical Sciences, Dublin City University, Dublin, Ireland.* Despite extensive studies plasma breakdown and formation in low pressure rf systems is still only poorly understood. A ID particle-in-cell (PIC) simulation, with spherical electrodes has been used to study plasma breakdown

from a low starting density (10^3 cm$^-$3). The inner electrode is coupled through a capacitor to the rf generator, and the outer electrode is grounded. Initially densities are very low so the electric field strongly penetrates the plasma, producing very hot electrons. At breakdown there is an extremely rapid increase in the density and at a critical value the debye length becomes less than the system length, sheaths form and the electron temperature drops rapidly to 3eV. Concurrently the plasma potential develops a large positive dc offset, preventing electrons from leaving the plasma via the outer, grounded electrode. A net current flows, charging up the external circuit capacitor and producing a bias voltage on the powered electrode. As the bias voltage increases the plasma behaviour changes from that of a "symmetric" to that of an "asymmetric" system.

9:30

TU1A 6 Sheath dynamics in a high-density, inductively-coupled plasma MARK SOBOLEWSKI, *NIST, Gaithersburg, MD* In high-density plasma etchers, radio-frequency (rf) bias is usually applied to the wafer electrode to control ion bombardment energies, but the sheath dynamics that relate rf bias power to ion energy are not fully understood. Here, these dynamics were investigated for argon plasmas at pressures of 10-100 mTorr, in a GEC Reference Cell in which one electrode was replaced by a high-density, inductively-coupled plasma source. RF bias of 1-100 V at 1-50 MHz was applied to the other electrode. The current and voltage were measured on the biased electrode and on a capacitive probe inserted into the bulk plasma. At frequencies < 25 MHz the rf bias voltage was shared between a sheath at the biased electrode and an opposing sheath at grounded cell surfaces. (At higher frequencies, the voltage was dropped across the bulk plasma.) The electrical behavior of each sheath can be represented by a nonlinear resistor and a nonlinear capacitor, in parallel. Equivalent circuit models of the sheaths will be presented that allow the measured current and voltage waveforms to be related to the electron temperature, ion flux, and ion energy.

9:45

TU1A 7 The role of collisions and non-linear effects on collisionless heating in inductive and capacitive discharges U. BUDDEMEIER, I. D. KAGANOVICH, U. KORTSHAGEN, *University Bochum, Germany* In the traditional theory of anomalous skin-effect, which is applied without principal modifications to the theory of collisionless (stochastic) heating, the semi–infinite geometry is considered. It has been demonstrated that in bounded systems (in the sense that the discharge gap width is smaller than the mean free path), the situation is far more complicated. Two cases of velocity kicks along and normal to the plasma boundary have to be distinguished. For kicks along the plasma boundary the non–linear stochastization is absent and only the collisional stochastization of resonant particles remains. If the number of these particles is small the collisionless heating is strongly suppressed. For the case of kicks normal to the plasma boundary non–linear effects due to the dependence of the bounce frequency on the velocity and collisional stochastization are combined. A comparison of analytical results and Monte Carlo simulations is presented.

SESSION TU1B: RADIATION TRANSPORT AND PHOTON PROCESSES

Tuesday morning, 22 October 1996; Lecture Hall at 8:00; Russ Huebner, ANL, presiding

Invited Papers

8:00

TU1B 1 Radiation Transport and Optical Diagnostics in the Lighting Industry.
GRAEME LISTER, *OSRAM SYLVANIA INC., Beverly MA 01915*

This paper will review modeling and diagnostics of radiation processes in discharges used for lighting. Both low pressure and high pressure discharges will be discussed. Models depend on accurate measurements or calculations of transition probabilities and line broadening parameters, and not all of this data is available. In many cases, only approximations of line broadening parameters for particular limiting cases are currently possible, and this issue will be addressed. For high pressure discharges, such as in metal halide lamps, spectra are extremely complex and inclusion of radiation transport self consistently in multi-dimensional lamp models is highly computer intensive. A complementary approach using simpler models supported by optical diagnostic experiments can give valuable information on discharge behavior with considerably less computer resources. For low pressure discharges, simplified radiation models coupled to detailed non-LTE diffusion models have been successful in reproducing many aspects of discharge behavior.

8:30

TU1B 2 Photon And Electron-Stimulated Desorption From Surfaces.
THOMAS M. ORLANDO, *Environmental Molecular Sciences Laboratory, Pacific Northwest National Laboratory Richland, WA 99352* [1]

Irradiation of surfaces with electrons and photons produces electronic excitations which stimulate desorption. It is well known that electron- and photon-stimulated desorption (ESD and PSD) from wide band-gap materials can be initiated by Auger decay of deep valence, shallow core and/or deep core holes. This process, which was first postulated by Knotek and Feibelman, generally consists of hole production, Auger decay, reversal of the Madelung potential, and ion expulsion due to the Coulomb repulsion. The cation thresholds and yields from single crystals of $NaNO_3$, $ZrO_2(100)$ and soda-glass indicate that ESD and PSD from these complex materials also involves Auger stimulated events. However, the primary ESD and PSD products are neutral and are detected using sensitive and selective laser resonance-enhanced, multiphoton ionization techniques. The low-energy thresholds and high atomic oxygen (i.e. O (^3P_J,^1D) yields demonstrate the

importance of shallow valence excitations and exciton decay.

[1]PNNL is operated for the U.S. Department of Energy by Battelle Memorial Institute under contract DE-AC06-7RLO 1830.

9:00
TU1B 3 Free-electron laser wavelength-selective materials alteration and photoexcitation spectroscopy.
NORMAN TOLK, *Vanderbilt University*

This abstract was not submitted electronically.

Contributed Papers

9:30
TU1B 4 Femtosecond Laser Ionization with Applications to Surface*MICHAEL R. SAVINA, KEITH R. LYKKE, *Argonne National Lab, Argonne, IL*Atomic and molecular imaging of surfaces by mass spectrometry requires efficient postionization of desorbed neutral species. To obtain quantitative results, the relative sensitivity factors for atoms and molecules must be known, since some atoms are much easier to ionize than others and are thus selectively enhanced. To alleviate these difficulties, we use intense femtosecond laser pulses (800 nm, 100 fs pulses from a Ti:Sapphire chirped-pulse amplification system, focused to 10^{15} Wcm^{-2}) to photoionize laser-desorbed atoms and molecules. At these intensities, electrons from most elements can be "field stripped" (i.e., by barrier suppression ionization) and all atoms in the high-irradiance region of the femtosecond laser beam will be ionized with unit efficiency. This should help to quantify the amount of material removed and allow for high-quality imaging. We will present experimental and theoretical results detailing the sensitivity factors in our imaging mass spectrometer. *Work supported by the US Department of Energy, BES-Materials Sciences, under Contract W-31-109-ENG-38.

9:45
TU1B 5 Kinetics in Xe/I_2 Inductively Coupled RF Discharges at Low PressurePAUL BARNES, *Wright Laboratory, WPAFB, OH*MARK KUSHNER, *University of Illinois, Urbana, IL*In this paper, the experimental investigation of low pressure, inductively coupled plasmas sustained in Xe & I_2 mixtures is reported. Radio Frequency power at 11.5 MHz was supplied to a solenoid surrounding a cylindrical discharge cell. Xenon pressures of 0.25-5.0 Torr and iodine pressure of 0.3 Torr were used. The diagnostics applied include laser-induced fluorescence for the I_2 density, microwave interferometry for the electron density, optical absorption spectroscopy for the Xe*(6s metastable) density, and optical emission spectroscopy of a variety of species. Observations were made as a function of radius in the steady state discharge and as a function of time following the termination of the discharge. Results from this study indicate that ion-ion neutralization is the major contributing reaction for population of the $I^*(^2P_{3/2})$ state in the afterglow of a modulated discharge. I*(206 nm) emission has decay times of 100s μs in the afterglow. Experimental evidence indicates that excited states of various neutral species are populated largely by ion-ion neutralization in high power inductively coupled discharges.

SESSION TU2A: WILL ALLIS PRIZE LECTURE
Tuesday morning, 22 October 1996; Auditorium at 10:30; Wilmer Anderson, Univ. of Wisconsin, presiding

10:30
TU2A 1 Electron-Atom Collisions: An Evergreen in Physics and Technology.*
CHUN C. LIN, *University of Wisconsin-Madison*

The general principles of electron-impact excitation out of the ground levels of the rare-gas atoms are reviewed. This is followed by discussions of recent measurements of electron-impact cross sections for excitation out of the metastable levels of He. The metastable atom targets are produced by two different methods, i.e., hollow-cathode discharges and charge-exchange collisions of rare-gas ions with Cs atoms. The measured cross sections show features very different from those of excitation out of the ground levels. Another new development is the use of atom traps for measuring ionization cross sections. The experiment is conducted by passing an electron beam pulse through magneto-optically trapped Rb atoms while the trap is momentarily turned off. Turning the trap back on immediately after the electron beam pulse recaptures the unionized atoms allowing only the ions to escape. The ionization cross section is determined by measuring the electron beam current density at the trapped atom region and the fractional loss of trapped atoms due to the electron beam. This method avoids measurements of the absolute number of the target atoms and the overlap between the atomic and electron beams and therefore eliminates the major sources of uncertainty associated with the crossed-beam method for measuring ionization cross sections.

*Supported by the National Science Foundation and the Air Force Office of Scientific Research.

SESSION TU3A: MODELING AND DIAGNOSTICS IN HIGH DENSITY PLASMAS

Tuesday afternoon, 22 October 1996; Auditorium at 13:30; Peter Lowenhardt, Applied Materials, presiding

Invited Paper

13:30

TU3A 1 Comparison of Ion and Neutral Temperatures in Various High Density Plasma Sources.

TOSHIKI NAKANO, HIROTO OHTAKE*, SEIJI SAMUKAWA*, *National Defense Academy, *NEC Corporation*

High-density, low-pressure plasmas such as ultrahigh frequency discharge (UHF), electron cyclotron resonance (ECR) and inductively coupled (ICP) plasmas have been devised to meet severe requirements for the fine-line etching in fabrication of ultra-large-scale-integration devices. In this work, we measure metastable ion (Ar^+: $3p^4 3d\ ^2G_{9/2}$, Cl^+:$3p^3 3d\ ^5D°_4$) and neutral (Ne:$2p^5 3s\ ^3P°_2$) temperatures perpendicular to the surface normal of a substrate, $T_{i,n\perp}$,in these plasmas by Doppler-shifted laser-induced fluorescence (DSLIF). For the UHF plasma, metastable Ne $T_{n\perp}$ is found to be $0.033 \pm 0.004 eV$ ($380 \pm 50\ K$)in a plasma produced at 0.26 Pa through Ne with a power of 1 kW. The obtained $T_{n\perp}$ is a half of 0.068 eV (800 K), the reported $T_{n\perp}$ of metastable Ne for the ECR plasma source.[1] Metastable Ar^+ $T_{i\perp}$ is estimated to be $\approx 0.066 eV$ ($\approx 770\ K$) in an Ar plasma produced under the same conditions as used for the Ne plasma. The $T_{i\perp}$ in the UHF plasma is also low compared with $T_{i\perp}$'s in the conventional ECR ($\approx 0.5 eV$ in the source and $\approx 0.25 eV$ downstream)[1] and helicon wave (0.15-0.33 eV) plasmas,[2] measured under similar plasma conditions to those for this work. We extend the DSLIF measurement to Cl_2 plasmas. The plasmas are produced at 0.39 Pa with a power of 1 kW. The metastable Cl^+ $T_{i\perp}$'s for the UHF, compact ECR and ICP plasmas are estimated to be $\approx 0.17 eV$, $\approx 0.99 eV$ and $\approx 0.19 eV$, respectively. Probably, the low $T_{i\perp}$ for the UHF plasma results from the excellent plasma uniformity. Since neutrals are heated through collisions with ions, the low $T_{i\perp}$ results in the low $T_{n\perp}$ in the UHF plasma. The low $T_{i\perp}$ enhances the normal incidence to a substrate of ions and the low $T_{i\perp}$ reduces the isotropic etching by neutrals. Thus, the smaller loss in critical dimension is expected for fine-line etching using the UHF plasma.

[1]T. Nakano, N. Sadeghi and R. A. Gottscho, Appl. Phys. Lett. 58, 458 (1991).
[2]T. Nakano, K. P. Giapis, R. A. Gottscho, T. C. Lee, and N. Sadeghi, J. Vac. Sci. Technol. B11, 2046 (1993).

Contributed Papers

14:00

TU3A 2 Modeling and Measurements of Plasma Properties in a 300mm Inductively-Coupled Plasma Etching System WENLI Z. COLLISON, TOM Q. NI, MICHAEL S. BARNES, This abstract was not submitted electronically.

14:15

TU3A 3 Two Dimensional Flux Non-Uniformities in High Density Plasma Reactors Using BCl3/Cl2 Gas Mixtures S. J. CHOI, *Sandia National Laboratories* J. W. SHON, *Sandia National Laboratories* The distribution of fluxes for various neutral and ion species to the substrate are parametrically studied in HDP reactors using BCl3/Cl2 gas mixtures. The initial plasma mechanism for BCl3/Cl2 is investigated using well mixed model. (1) For a BCl3/Cl2 plasma, the nominal conditions are 1000 Watts of input power, 5 mTorr of pressure, and a gas mixture of BCl3/Cl2 = 50/50%. The major ions are Cl+, Cl2+ and BCl3+. The dissociation of BCl3 to BCl2 is relatively small compared to that of Cl2 to Cl. Thus, the addition of BCl3 tends to decrease the production of Cl. The reactor conditions are varied for gas mixtures, pressure, and input power. The nonuniformities of fluxes show the effects of pump port location, pressure, plasma nonuniiformity. (1) E. Meeks and J. W. Shon, IEEE Trans. on Plasma Sci., 23, 539, 1995.

14:30

TU3A 4 Development and Optimization of the Decoupled Plasma Source for Metal Etch Using Wafer-based Probes PETER K. LOEWENHARDT, HIROJI HANAWA, DIANA X. MA, PHILLIP SALZMAN, KIEN CHUC, ARTHUR SATO, VALENTIN TODOROV, GERALD Z. YIN, *Applied Materials, Santa Clara, CA 95054* Plasma uniformity impacts metal etch reactors via charging device damage. New etching reactors must therefore provide excellent plasma uniformity over a large process parameter window. Critical dimension control is also influenced by plasma uniformity and ion energy. The Decoupled Plasma Source (DPS) has been developed and optimized using wafer mounted flux and energy probes. Experimental measurements of the source design will be presented. Effects of chamber design, gas chemistry and source configuration on the ion current flux reaching a wafer will be discussed along with the decoupling of the ion current flux from ion energy.

14:45

TU3A 5 Ion Distribution Functions in an ECR Discharge Plasma GLENN JOYCE, MARTIN LAMPE, W. M. MANHEIMER, STEVE SLINKER, *Naval Research Laboratory, Washington, DC* We have recently developed an axisymmetric quasineutral particle simulation code to study heating and transport of plasma in an ECR reactor configuration. All species are treated as particles with the electrons always strongly magnetized, and the degree of magnetization of the ions varying spatially. For an argon plasma with pressures on the order of a few milliTorr, the plasma has high density and is weakly collisional, with mean free paths on the order of a few centimeters. Particles may collide with the neutral gas. The neutral collisions include momentum transfer and charge exchange. Electron-electron collisions are also included.

The ion velocity distribution is primarily determined from the particle dynamics in the quasi-neutral fields and sheaths, and by collisions with the neutral gas. Ion collisions in the pre-sheath are particularly important, since they may determine the anisotropy of the ions after they traverse the sheath. We present details of the ion distribution function at various locations in the plasma, both inside the pre-sheath, and at the walls, and analyze their energy and anisotropy properties.

15:00
TU3A 6 Pulse-Power Modulated High Density Electronegative Discharges for Plasma Processing MICHAEL LIEBERMAN, SUMIO ASHIDA, VENKATESH P. GOPINATH, *EECS Dept., U. C. Berkeley, Berkeley, CA 94720-1770* Pulse-power modulated high density discharges are under active consideration for materials processing applications. It has been claimed that such discharges can increase SiO_2/Si etch selectivity, reduce aspect ratio dependent etch effects, eliminate notching and charge build-up damage of gate oxide, increase etch uniformity, increase etch and deposition rates, reduce the heat flux to the substrate, extend discharge pressure and power operating regimes, and reduce particulate formation. Global (volume-averaged) models of high density, low pressure discharges can provide considerable insight into the dynamics for both continuous wave (cw) and pulsed-power excitation. Chlorine and oxygen discharges are treated as benchmark examples of electronegative process gases. The particle and energy balance equations are applied to determine the charged particle and neutral dynamics. The time-average n_e can be considerably higher than that for cw discharges for the same time-average power. For chlorine, a cw discharge is highly dissociated and the negative ion density n_{Cl^-} is lower than n_e. A pulsed discharge can have the same neutral radical (Cl) flux to the walls for a reduced average power. Similar phenomenon are observed for oxygen. The analytical models are compared to more complete global model simulations and to experimental observations.

SESSION TU3B: PLASMA IN DISPLAY

Tuesday afternoon, 22 October 1996; Lecture Hall at 13:30; Robert McGrath, Sandia National Lab, presiding

Invited Papers

13:30
TU3B 1 Recent developments in plasma display technology.
LARRY WEBER, *Plasmaco*

This abstract was not submitted electronically.

14:00
TU3B 2 AC Plasma Display Panel Cells: Overview and Modeling.
C. PUNSET, J.P. BOEUF, L.C. PITCHFORD, *CPAT, 118 route de Narbonne, 31062 Toulouse Cedex France*

Plasma display panels (PDP's) are arrays of individually addressable microdischarges which produce uv radiation which is, in turn, converted to visible radiation by a phosphor. In ac plasma display panels the electrodes are coated with dielectrics, and discharges are initiated and extinguished on each half cycle as the dielectric surfaces become charged. Typical discharge conditions are 50 kHz, 500 torr, 9010a 100 micron gap spacing, and the microdischarges in PDP's are thus transient glow discharges (pd (5 torr cm). We have developed models (Refs. 1,2) to study the effects of changing discharge conditions on the characteristics of individual discharges and the effects of the geometry on the electrical and optical cross talk between discharges in neighboring cells2. An overview of the principles of ac PDP's will be presented with particular emphasis on the trade-offs which must be made in order to optimize several parameters at once. Results from the 2-D model calculations will be presented to show the characteristics of PDP cells in complex geometries. 1. J. Meunier, P. Belenguer and J.P. Boeuf, J Appl Phys 78 731 (1995). 2. J.P. Boeuf and L.C. Pitchford, IEEE Trans Plasma Sci 24 95 (1996).

14:30
TU3B 3 2-D models of plasma switches for display addressing.
G. J. PARKER, *Lawrence Livermore National Laboratory*

Plasma switches have been introduced as replacements for thin-film transistors in the addressing mechanism for liquid crystal displays, facilitating the manufacture of large-area devices suitable for TV and high-resolution computer terminals. A 2-D fluid/kinetic hybrid model of a plasma switch has been developed for arbitary Cartesian and cylindrical geometries. A fluid equation description is used for particle transport and is augmented by a kinetic treatment of electrons via the Monte Carlo (MC) technique. In the fluid equation routines, the electron and ion continuity equations, the ion momentum equation and the neutral particle diffusion equation are solved in conjunction with Poisson's equation. The drift/diffusion approximation is assumed to be valid for electrons. The Monte Carlo routine provides the electron energy distribution function (EEDF) in terms of 'groups' of electrons. These groups include electrons emitted off surfaces, electrons trapped in the electrostatic potential and electrons generated via heavy particle ionizing collisions. This computed EEDF is then used to specify the appropriate terms in the fluid equations. The model is used to predict the active

(on) state of the plasma switch as well as the inactive (off) decay of the plasma. Numerous geometries and physical parameters have been modeled for a pure Helium gas. Results are compared to experiment where available.

Contributed Papers

14:45

TU3B 4 Two dimensional simulations of pixel cross-talk in plasma displays.* RAMANA VEERASINGAM, ROBERT B. CAMPBELL, ROBERT T. MCGRATH, *Sandia National Labs, New Mexico* Plasma displays are on the verge of rapid and extensive introduction to the market place for large area information video displays. In the effort to obtain high resolution ac color plasma displays, pixel to pixel cross-talk is an issue that needs to be addressed. To this end we have developed two dimensional fluid models to simulate pixel to pixel cross-talk. We will present simulations of several different pixel heights in a two pixel geometry to demonstrate plasma overflow and cross-talk. The effect of the pixel width on the ON voltage will also be shown. Finally, using a single pixel geometry, we will present results from two dimensional simulations showing the transport of excited states including the radiative atomic xenon [6s,j=1] state and the xenon dimer.

*This work performed under the auspices of the U.S. D.O.E. under contract DE-AC04-94AL85000

15:00

TU3B 5 High Pressure Hollow Cathode Discharges KARL H. SCHOENBACH, THOMAS TESSNOW, AHMED ELHABACHI, *Physical Electronics Research Institute, Old Dominion University, Norfolk, VA* The sustaining voltage of hollow cathode discharges is dependent on the product of pressure and cathode hole diameter. By reducing the dimension of the cathode hole to 0.2 mm we were able to operate micro-hollow cathode discharges at pressures up to 750 Torr in argon in a direct current mode. The current-voltage characteristics of the 0.2 mm cathode hole discharges was found to have a positive slope at currents below 0.25 mA. Up to this current level hollow cathode discharges can be operated in parallel without ballast. The negative slope observed above the threshold current seems to be due to the onset of thermionic electron emission caused by Joule heating of the cathode. This assumption is supported by the experimental observation that multi-hole operation without ballast even at currents far above the dc-threshold current was possible when the discharge was operated in a pulsed mode. The possibility of generating large arrays of ballast-free, pulsed micro-hollow cathode discharges suggests their use as flat panel light sources or electron sources.

SESSION TUPA: ECR AND MICROWAVE DISCHARGES, ABLATION AND DUSTY PLASMAS POSTER SESSION
Tuesday afternoon, 22 October 1996
Alcove A at 15:45
Keith Lykke, ANL, presiding

TUPA 1 Behaviors Of Si Atom And SiH_x^+ (x=0-3) Ions In ECR SiH_4 Plasma YASUO YAMAMOTO, SHINJI SUGANUMA, MASAFUMI ITO, MASARU HORI, TOSHIO GOTO, *Nagoya University, Nagoya, Japan* MINEO HIRAMATSU, *Meijo University, Nagoya, Japan* Recently, ECR SiH_4 plasma CVD has been applied to the preparation of hydrogenated amorphous silicon thin films in a high deposition rate. In order to understand the mechanism of thin film formation, it is necessary to know behaviors of radicals in the ECR SiH_4 plasma. At low operating pressure region as the ECR plasma, it is expected that fluxes of ions incident on the film become large and the effect of ions on film formation becomes important. In this work, ions incident on the substrate were measured by quadrupole mass spectrometer in ECR SiH_4 plasmas. Si atom was also measured using ultraviolet absorption spectroscopy. At a total pressure of 0.4 Pa, both Si atom and SiH_x^+ (x=0-3) ions increase in ECR SiH_4 plasmas with an increase in microwave power from 100 to 800 W. SiH_3^+ ion is larger by about one order of magnitude than SiH_x^+ (x=0-2) ions. At 300 W, Si atom increases with an increase in total pressure from 0.16 to 0.8 Pa. On the other hand, SiH_x^+ (x=0-2) ions decrease and SiH_3^+ ion slightly decreases with an increase in total pressure. On the basis of these measured results, the effect of Si atom and ions to the film formation is discussed.

TUPA 2 Dissociation Processes of Fluorocarbons in ECR Etching Plasmas KOJI MIYATA, HIROYOSHI ARAI, MASARU HORI, TOSHIO GOTO, *School of Engineering, Nagoya University* Fluorocarbon high-density plasmas have been widely used for etching process in ULSI devices. To meet requirements of precise etching, it is indispensable to understand the chemistry in the high-density plasma. The basic chemistry in the high-density plasmas is associated with electron-collisional dissociations of feed molecules and other products, some rapid gas-phase reactions, and wall-diffusional disappearances of chemically-activated species. In this study, we have studied the dissociation processes in ECR-CF_4 and C_4F_8 plasmas. We first measured the initial rising phase of CF and CF_2 radical densities at the plasma ignition. Infrared diode laser absorption spectroscopy was used for measuring the CF and CF_2 radical densities. It was found that CF and CF_2 radical densities transiently became larger at the rising phase than those in the stationary phase in the C_4F_8 plasma. The finding shows CF_2 is abundantly generated through the rapid dissociation of C_4F_8. CF and CF_2 radicals monotonically rose and were saturated after the plasma ignition in the CF_4 plasma. Second, the measured risings were demonstrated using computer calculation involved more than forty reactions, resulting rate constants for the reactions were fixed. Based on these results, the chemistry of CF_4 and C_4F_8 plasmas will be presented in this session.

TUPA 3 A Comparison of Thomson Scattering and Langmuir Probe Measurements of Electron Temperature and Density in High Density Plasma Sources. M.D. BOWDEN, T. HORI, K. UCHINO, K. MURAOKA, *Kyushu University, Japan* M.B. HOPKINS, *Dublin City University, Ireland* C. O'MORAIN, *Scientific Systems Ltd., Ireland* Electron temperature T_e and density N_e were measured in argon plasmas using two different methods: incoherent Thomson scattering of a Nd:YAG laser [1] and a Langmuir probe [2]. Measurements were made in an (unmagnetized) inductively coupled rf discharge and in a (magnetized) electron cyclotron resonance discharge. For most conditions measured, the value of T_e determined by the probe was slightly higher than that determined by the laser method. N_e values determined by the probe were consistently lower than those determined by Thomson scattering, but generally differed by less than a factor of two.

Measurements made for varying power and pressures will be discussed and examples of EEDFs measured by both methods will also be presented.

[1]T. Hori *et al.*, J. Vac. Sci. Technol. A Vol. 14, 144 (1995)
[2]C. O'Morain *et al.*, 48th GEC, Berkeley, Paper NC5 (1995)

TUPA 4 Ion & Electron Energy Analysis of Pulsed and CW Helicon Plasmas. G.D. CONWAY, A.J. PERRY, R.W. BOSWELL, *Plasma Research Lab., Australian Natl. Univ.* Using a water cooled, 4-grid, planar, variable geometry retarding field energy analyser (RFEA) with a 0.3eV energy resolution, temporal and spatial profiles of ion and electron energy distributions of argon plasmas have been measured for pulsed and CW RF power in a helicon reactor. Time resolved measurements show three distinct phases during high ($\approx$ 1kW) pulsed power operation: (i) Breakdown (first 300μs) - characterised by high electron temperatures (T_e) and ion energies $<$30eV (= plasma potential V_p), (ii) Mid-pulse - identical to CW regime, $T_e \approx 3.5$eV, ion energy peak $\approx$10eV, (iii) Pulse tail - displays collapsing V_p, ion energy peak splitting, and a transient hot electron component. Breakdown and tail phase believed to be predominantly capacitive antenna coupling. Mid-pulse/CW phase is entirely inductive/helicon wave coupling. Reactor radial profiles show uniform plasma density, V_p and T_e across wafer in helicon mode, but with two axial columns of energetic ions and fast electrons (correlate with "burn" patterns on wafer) corresponding to an m=1 mode structure in the helicon plasma source. Column locations show broadening of ion energy distribution (under certain conditions two clear peaks observed) due to modulation of plasma potential - also confirmed with an emissive probe.

TUPA 5 Time-Dependent Kinetics of the Nitrogen Afterglow in N_2 and N_2-Ar Microwave Discharges J. LOUREIRO, *CEL-IST, Lisbon Tech.Univ.,Portugal* P. A. SÁ, *DEEC-FEUP, Oporto Univ.,Portugal* We present a theoretical analysis of the N_2 afterglow induced by a microwave discharge in N_2 and N_2-Ar. The initial conditions at the beginning of the afterglow were obtained by solving the electron Boltzmann equation coupled to the rate balance equations for the $N_2(X\ ^1\Sigma_g^+\ v)$ levels, the electronic states of N_2 and the $N(^4S)$ atoms. The relaxation of this system is investigated in the afterglow. It is shown that as a result of the mechanisms leading to associative ionization by collisions between the electronic metastables $N_2(A\ ^3\Sigma_u^+)+N_2(a'\ ^1\Sigma_u^-)$ and $N_2(a'\ ^1\Sigma_u^-)+N_2(a'\ ^1\Sigma_u^-)$, the so-called pink afterglow (emission of the 1^- system bands of N_2^+) appears after a time $t \simeq 10^{-3}$s in pure N_2 at p=2 Torr, while for N_2-Ar mixtures this emission occurs for higher pressures and longer residence times (e.g., $t \simeq 10^{-2}$s in a N_2-50%Ar mixture at p=10 Torr). This emission prevails upon the usual Lewis-Rayleigh afterglow in agreement with the experiment[1].

[1]C.Normand-Chave, PhD Thesis, Université Paris-Sud, France (1991)

TUPA 6 Neutral Chemistry in CF_4/O_2 Microwave Downstream Plasmas M. TUDA, T. NAKAHATA, K. ONO, *Mitsubishi Electric Corp., Amagasaki 661, Japan* The downstream plasma processing is strongly dependent on chamber geometry, wall material, wall passivation, and distance between the discharge region and the wafer to be processed. This paper presents optical and mass spectroscopic diagnostics of CF_4/O_2 microwave downstream plasmas, in combination with etch rate measurements of Si and SiO_2 and also several surface analyses. The discharge was established in a 2.45-GHz microwave cavity equipped with a 3-cm-i.d. quartz tube, and the substrate was placed 40 cm downstream from the discharge. Experiments were performed by varying the O_2/CF_4 mixture ratio at a total gas pressure of 0.5 Torr and a microwave power of 300 W, when the plasma densities at the substrate position were measured to be more than five orders of magnitude lower than those in the discharge region. The etch rate of Si peaked at about 20% O_2, corresponding to the maximum F concentration probed by argon actinometry; however, the Si etch rate decreased substantially at higher O_2/CF_4 ratios, being ascribed to the formation of a SiO_xF_y layer on Si surfaces evidenced by XPS, FTIR, and AFM analyses. The optical and mass spectroscopic measurements implied that the SiO_xF_y arose primarily from gas-phase reaction between SiF_x coming from etching of the quartz tube walls and feedstock oxygen.

TUPA 7 Selective Etching of Silicon Nitride using a Remote Microwave Plasma C.B. BROOKS, WALTER MERRY, *Applied Materials; Dielectric Etch Division; Santa Clara, CA* Semiconductor manufacturing has been moving from wet etching and stripping to dry processing. The removal of the silicon nitride LOCOS structure has been traditionally done by hot phosphoric acid bath. The removal of this silicon nitride layer must be highly selective to silicon oxide to prevent loss in the field oxide and pad oxide underlayer. Etching of silicon nitride is achieved chemically with a remote microwave plasma of CF4 and the addition of other gases to enhance selectivity to silicon oxide. Silicon nitride dry strip process results will be presented along with selectivity enhancing schemes. This process will be compared to the hot phosphoric bath alternative.

TUPA 8 The Roles of Plasma Species on Polycrystalline Silicon Film Formation by ECR SiH_4/H_2 Plasma MASAFUMI ITO, RYOUICHI NOZAWA, KAZUYA MURATA, MASARU HORI, TOSHIO GOTO, *Quantum Engineering, Nagoya University, JAPAN* We investigated the roles of species in electron cyclotron resonance (ECR) SiH_4/H_2 plasma for the poly-Si formation at substrate temperature of 300degC using permanent magnets. Plasma condition was as follows; The substrate bias, total pressure, hydrogen dilution rate, microwave power and the distance from ECR point to the substrate were +50V, 0.5Pa, 90.9%, 300W and 35cm respectively, which was the best condition for the crystallinty under our experimental apparatus. The permanent magnets were set so that the only charged species incident on the substrate might be pushed away. They enable us to deposit the film by only neutral species with the light radiation of plasma. These films deposited with the permanent magnets showed polycrystalline structures. Moreover, we scanned the distance from ECR point to the substrate. The X-ray diffraction intensity at the distance of 35cm was around two times as much as that at 40cm. From these results, we found that neutral species with high energy and the light radiation of plasma play very important roles in the poly-Si formation at 300degC in ECR plasma CVD.

TUPA 9 Ionized Magnetron Sputtering with a Coupled DC and Microwave Plasma D. B. HAYDEN, K. M. GREEN, D. R. JULIANO, D. N. RUZIC, *University of Illinois* C. A. WEISS, A. LANTSMAN, J. ISHII, *Materials Research Corperation* A DC magnetron sputtering system is enhanced via an antenna microwave source. The ability of the microwaves to ionize the metal atoms from the aluminum target though electron impact and Penning ionization is studied as a function of microwave power, magnetron power, and pressure. A bias in the tens of volts (negative) is applied to the substrate and sample. This creates an electric field

between the plasma and the substrate which is designed to draw the metal ions into the sample orthogonally for filling increased aspect ratio trenches. A quartz crystal oscillator is placed behind a gridded energy analyzer and embedded in the substrate. It determines the ion-to-neutral ratio and the deposition rate, and the gridded energy analyzer determines the energy spectrum of the ions, the ion current density, and the uniformity. These quantities are compared to the results of a computer simulation.

TUPA 10 Antenna coupling to helicon waves in a radially non-uniform plasma.* D. ARNUSH, F.F. CHEN, *UCLA* Coupling of a coaxial, thin-shell antenna to an enclosed cylindrical plasma in a conducting cavity is calculated. Above about 100G, a weakly damped helicon (H) wave is excited in the plasma bulk and a strongly damped Trivelpiece-Gould (TG) wave is excited on its surface. Shamrai and Taranov [1] have shown that mode conversion from H to TG waves accounts for anomalously high absorption of the RF energy. They assume a constant plasma density, whereas plasma gradients play an important role in mode conversion. McVey [2] and others model radial density variations using layers of constant density cylindrical shells, thereby neglecting important density gradient terms in the exact equations for the fields. Using a PC, we solve the exact equation for the H and TG fields, neglecting the displacement current and ion motions for convenience. Antenna coupling and impedance, as well as the role of the two waves are discussed.

*Supported by the LLNL, NSF, and SRC.

[1]ISSN 0346-8887, TENIKUM Institute of Technology, Uppsala University, 1996.
[2]PFC/RR-84-13, Plasma Fusion Center, MIT, 1984.

TUPA 11 2-D Optical Imaging of Permanent Magnet ECR Source AARON R. WILSON, STEVE S. SHANNON, MARY L. BRAKE, WARD D. GETTY, *Center for Display Technology and Manufacturing, University of Michigan* Optical images of a permanent magnet ECR source were collected with a CCD camera [1] The plasma images were focused directly on the CCD. The images indicate field patterns for various pressures, flowrates, and power. A 1-kW, 2.45 GHz microwave source is connected through a circulator and a three-stub tuner to a horn which expands the microwave aperture to a 15 cm x 20 cm rectangle. The horn is attached to the top plate of the vacuum chamber which holds a 15 cm x 20 cm aluminum 6 slot grill containing 5 rows of permanent magnets. The ECR surface of 875 G is approximately 1 cm from the grill. The plasma expands to fill the 28-cm diameter chamber. Depending upon the magnetic configuration and the input conditions, the mode of the plasma changes. This is noted in the two dimensional optical images observed by the CCD. These results will be compared to Langmuir probe data, microwave interferometry, and optical emission spectroscopy. Etch results of oxide patterned silicon wafers will also be discussed. The results of these diagnostics indicate the uniformity of this new plasma source in different modes of operation.

[1]W. Getty and J. Geddes, J. Vac. Sci. Technol. B 12(1), pp. 408-415 (Jan/Feb 1994)

TUPA 12 Determination of the negative ion concentration in an SF_6/Ar magnetoplasma created by an electromagnetic surface-wave under ECR conditions. L. ST-ONGE, *Dept de Physique, Universite de Montreal, Canada* M. CHAKER, *INRS-Energie et Materiaux, Varennes, Canada* J. MARGOT, *Dept de Physique, Universite de Montreal, Canada* The negative ion concentration in an SF_6/Ar high density, large volume plasma reactor sustained by the propagation of a surface-wave under ECR conditions was studied using a laser photodetachment/electrostatic probe technique. The negative ions in such a plasma are observed to constitute up to 90% of the negative charge carriers even in the low pressure regime investigated ($p < 5$mTorr). In addition, it is found that even low percentages of SF_6 introduced in an argon plasma generate large concentrations of negative ions. The results of the laser photodetachment measurements are also compared with those determined from ion acoustic wave propagation. It is found that both techniques provide similar results concerning the negative ion fraction for gas pressures higher than about 1 mTorr.

TUPA 13 Positive ion and electron characteristics in an SF_6/Ar magnetoplasma created by an electromagnetic surface-wave under ECR conditions. L. ST-ONGE, J. MARGOT, *Dept de Physique, Universite de Montreal, Canada* M. CHAKER, *INRS-Energie et Materiaux, Varennes, Canada* Over the last few years, a high density, large volume plasma reactor was designed and implemented at Universite de Montreal in order to fulfill the requirements of submicron etching of materials. The plasma is generated at 2.45 GHz by an electromagnetic surface wave and is confined by a static magnetic field under conditions close to ECR. The plasma is operated either in pure Ar or pure SF_6 as well as in SF_6/Ar gas mixtures at very low pressure ($p < 5$ mTorr). In this presentation, we report on the basic characteristics of the pure SF_6 plasma. In particular, we examine the spatial and pressure dependence of the positive ion density and electron temperature. We also examine the evolution of these characteristics in an SF_6/Ar gas mixture as a function of the SF_6 concentration.

TUPA 14 Etching Characterization of a Cusped-Field Helicon Plasma Etcher ANTHONY QUICK, MOSHE SARFATY, NOAH HERSHKOWITZ, *Engineering Research Center for Plasma-Aided Manufacturing, University of Wisconsin-Madison* Recent experiments on the UW Cusped-Field Helicon Plasma Etcher (CFHPE) have concentrated on characterizing the SiO_2 and polycrystalline Si (p-Si) etching performance in fluorocarbon-based etching chemistries. In the cusped field arrangement, the usual magnetic field coils for the helicon plasma source are augmented by a set of opposing field coils on the downstream side of the substrate to give a net field of zero Gauss at the substrate location. The substrate can then be located at various axial positions near the zero-field point to optimize radial plasma etching uniformity. Issues to be covered in this paper are radial etching uniformity for different substrate positions, etching selectivity of SiO_2 over p-Si in CHF_3/H_2 gas chemistries, and etching anisotropy of large aspect ratio, sub-micron features. At the edge of a 100 mm diameter substrate in the CFHPE the radial magnetic field can be as high as 20 Gauss so there is a concern about etching anisotropy at the edge of the substrate. The effects of the radial magnetic field variations on etching anisotropy will be presented. This work is supported by National Science Foundation grant #EEC-8721545.

TUPA 15 Relationship Between Plasma Emission Intensity and Film Properties for ECR Silicon Oxide Deposition KOK HENG CHEW, EDWARD AUGUSTYNIAK, R. CLAUDE WOODS, J. LEON SHOHET, *ERC for Plasma-Aided Manufacturing, University of Wisconsin, Madison, WI 53706* A 2.45 GHz electron cyclotron resonance (ECR) reactor, using both silane + O_2 and tetraethoxysilane (TEOS) + O_2, was employed to deposit

TUESDAY AFTERNOON \ TUPA

silicon oxide films, which were characterized using IR absorption, multicolor ellipsometry, and ESCA. Optical emission spectrometer was used to monitor Si, O, H, OH, and SiH in SiH_4 plasma and Si, O, H, C, CO, CH, C_2, OH, and H_2 in TEOS plasma. In SiH_4 based deposition the silicon oxide film quality approaches that of thermal oxide for films deposited using O_2/SiH_4 ratios higher than 1.0 at 500 W and 5.0 mTorr. Under these conditions no OH emission was detected for O_2/SiH_4 ratios lower than 1.0, while no SiH emission was observed for ratios higher than 1.0. In TEOS based deposition the carbon content in the film is less than 1.0 atomic Strong O emission intensity correlated with high film quality for both chemistries. This work was supported by the National Science Foundation under Grant No. EEC-8721545.

TUPA 16 In-Situ Surface Diagnostics of a-Si:H Films during ECR-H_2 Plasma Annealing MASARU HORI, RYOUICHI NOZAWA, HIROHISA TAKEDA, MASAYUKI NAKAMURA, MASAFUMI ITO, TOSHIO GOTO, *Quantum Engineering, Nagoya University, JAPAN* The surface reaction of amorphous silicon films during ECR-H_2 plasma annealing has been investigated by using in-situ Fourier transform infrared reflection absorption spectroscopy (FTIR-RAS). First, amorphous silicon films were formed on Al film/Si substrate by ECR-SiH_4/H_2 plasma at 0.53 Pa, 300W, flow rate of SiH_4/H_2:10/100sccm and room temperature. It was observed that these films contained SiHx(x=1-3) bonds by using FTIR-RAS. Next, the films were exposed by ECR-D_2 plasma at 0.53 Pa, 300W, 100sccm and room temperature with varying the substrate DC bias from -50V to 50V. It was found that at -50V, the only SiH_3 bond on the film decreased with D_2 plasma duration while at 50V, the SiH, SiH_2 and SiH_3 bonds decreased. The bonds generated by D_2 plasma duration were mainly SiD and SiD_2. These bonds increased with increasing ion energy. On the basis of these results, the mechanism of surface reactions through H ions and/or H radicals in ECR-H_2 plasma annealing will be discussed.

TUPA 17 Mass spectrometric detection of F atoms and CF_x radicals and their kinetics in CF_4 plasmas. A. TSEREPI, J. DEROUARD, W. SCHWARZENBACH, N. SADEGHI, *Lab Spectrometrie Phys. Grenoble Univ, Grenoble, France* Detection of atomic fluorine and determination of its kinetics in a discharge environment is essential for understanding the F atom loss mechanisms by surface and/or gas-phase reactions. In this work, threshold-ionization mass spectrometric methods are employed for the detection of F atoms and CF_x (x=1-3) radicals present downstream a CF_4 microwave plasma (p=15 to 50 mTorr), with emphasis on atomic fluorine detection. Actinometry, on F atoms, and LIF, on CF_2 radicals, have also been employed. In addition to the estimation of the fluorine concentration in a continuous discharge, time-resolved measurements allow us to investigate the kinetics of fluorine atoms in the afterglow of a pulsed plasma. The influence of the discharge parameters such as power, pressure, and gas flow, on F atom concentrations and kinetics has been investigated. Important modification of the loss rates of F atoms is observed, under certain conditions, with introduction into the reactor of fluorine-consuming materials, such as a Si or a polymer (Hexatriacontane) surface. All of our observations are consistent with a predominant surface loss of atomic fluorine on the reactor walls and the exposed surfaces.

TUPA 18 Energy selective compact electron cyclotron resonance plasma-induced nitridation processes on sapphire substrates PATRICK O'KEEFFE, HARUNOBU MUTOH, SHOJI DEN, YUZO HAYASHI, *Irie Koken Co., Ltd. Japan* SHUJI KOMURO, TAKITARO MORIKAWA, *Toyo University, Japan* Control of the ion energy distribution by movement of the discharge magnetic field is demonstrated for the first time in a compact ECR plasma source. The ion energy can be tuned from 10eV to 30eV. An explanation based on different ambipolar diffusion coefficients in the downstream region due to different magnetic fields is outlined. Nitrogen plasma induced surface reaction processes on sapphire substrates with a view to achieving growth of a thin AlN buffer layer prior to group III nitride growth was investigated using this novel energy selective ECR plasma source. Nitrogen radical species were identified as the reaction-inducing agent and it is demonstrated that by control of the ion energy distribution function independent of plasma flux, the surface morphology could be altered while maintaining a high rate of nitridation.

TUPA 19 Measurements of Molecular Densities in Low Pressure Discharge Plasmas Using Laser Raman Scattering K. MURAOKA, Y.B. SONG, K. UCHINO, *Kyushu University, Japan* T. SAKODA, *Kitakyushu National College of Technology, Japan* K. YANAGISHITA, S. NAKAMURA, *ULVAC Japan Ltd.* The possibility of using Raman scattering as a method to measure molecular in low pressure discharge plasmas has been investigated. This technique was applied to detect methane and its reaction products in an ECR plasma operated at a pressure of 50 Pa and microwave power of 100 W. Raman signals from CH_4, C_2H_2, C_2H_6, and H_2 were clearly detected and the densities of these species were absolutely determined using a calibration of the optical system [1]. Similar measurements were performed for different gas flow rates in the range of 10 - 75 sccm. The initial methane gas pressure was kept constant at 50 Pa and the microwave input power was fixed at 100 W. The results clearly indicated that the gas flow rate has a strong influence on the reaction processes in the discharge These experimental results showed the usefulness of the method for quantitative measurements of molecular! densities in processing plasmas.

[1]Y. B. Song *et al.*, Proc. 7th LAPD Symposium, Fukuoka, 1995

TUPA 20 Ionization waves in a dusty plasma. D. SAMSONOV, J. GOREE, *The University of Iowa* Previously Praburam[1] showed the presence of a periodically rotating structure or "great void mode" in a particulate cloud grown in a parallel plate RF sputtering discharge. Here we show that there is a disturbance of electon temperature and density rotating at the same frequency which can be interpreted as an ionization wave. The discharge glow was seen rotating with a phase lag of 0° to 90° after the void in the particulates. The rotational frequency slowed down gradually from a few Hz until the mode stopped, facing the gas inlet. The experiment was performed using two video cameras fitted with different bandpass filters to select the glow and laser light scattering from dust. Work is supported by NSF and NASA.

[1]G. Praburam and J. Goree, Phys. Plasmas 3, 1212 (1996).

TUPA 21 Observation of Individual Particles in a Flowing Silane rf Discharge by Laser Light Scattering M. A. CHILDS, ALAN GALLAGHER, *JILA, University of Colorado - Boulder, Boulder, CO* Particle contamination of hydrogenated amorphous silicon films grown in a silane rf discharge is suspected of degrading the films' electronic properties. We detect individual particles

in a flowing pure silane discharge using a novel laser-light scattering technique. In this technique a frequency-doubled YAG laser beam is formed into a thin sheet which is sent through the plasma parallel to the rf electrodes. Light scattered perpendicular to the beam is imaged onto a CCD. Provided that the plasma volume imaged onto a pixel contains, on average, less than one particle, each particle is detected separately. This is an important advantage since it allows the detection of small particles which might otherwise be overwhelmed by scattering off large particles. Particle density is calculated by dividing the number of observed particles by the imaged volume. The intensity of the scattered light yields particle size since the scattering cross section is proportional to the sixth power of the radius. This system is capable of detecting a particle with a radius of less than 20 nm. The change in the spatial configuration over a few minutes as most of the particles collect at the downstream edge of the plasma is monitored. Shorter time period dynamics are also observed as the particles escape from the plasma downstream. It is hoped that by understanding particle dynamics, the particles' impact on film quality may be controlled.

TUPA 22 Electron Beam Ablation of Metals* S.D. KOVALESKI, R.M. GILGENBACH, J.I. RINTAMAKI, L.K. ANG, H.L. SPINDLER, † W.E. COHEN, Y.Y. LAU, *University of Michigan, Ann Arbor, MI* J.S. LASH, *Sandia National Lab, Albuquerque, NM* An experiment has recently been devised for material ablation using a channelspark electron beam. The ultimate goal of this experiment is to deposit thin films by electron beam ablation. The channelspark is a pseudospark device developed by Forschungszentrum Karlsruhe [1] for production of high current, low energy electron beams. The channelspark has the following operating parameters: a 15-20kV accelerating potential and measured source current of <2000A. Initial experiments have concentrated on characterizing ion-focused electron beam current transport through the necessary background fill gas (typically 5-50 mTorr of Argon). Ablation of Al, Fe, and Ti is being studied with spectroscopy and electron beam current diagnostics. Physical beam target damage is also being investigated and compared to laser ablated targets. Simulations of electron transport and energy deposition are being conducted via the ITS-TIGER code [2] developed at Sandia National Laboratory.

*Supported by the National Science Foundation
†NSF Fellowship support

[1]G. Muller, C. Schultheiss, Proc. of Beams, 2, 833(1994)
[2]Sandia Report No. SAND 91-1634

TUPA 23 XeCl Excimer Laser Ablation of ZnO for Preparation of Transparent Conducting Thin Films KOUICHI IMAEDA, MINEO HIRAMATSU, MASAHITO NAWATA, *Meijo University, Nagoya, JAPAN* Aluminum-doped zinc oxide (AZO) thin films have attracted considerable attention for transparent conducting films in place of indium tin oxide. Transparent conducting AZO thin films have been prepared using pulsed laser ablation method. A XeCl excimer laser (308 nm) was used for ablation of AZO bulk target. The energy density of XeCl laser beam at the target surface was maintained at 1.5 J/cm^2. Substrate heating was carried out using CO_2 laser irradiation. The c-axis oriented AZO films were successfully grown at substrate temperatures ranging from 100 to 300 C in an oxygen atmosphere. Optical transmittance above 80 % was observed in the visible region of the spectrum for the 450 nm-thick film deposited from the ZnO target doped with 1 $wt\%$ Al_2O_3. Resistivity of 1.34×10^{-4} Ωcm was obtained at a low substrate temperature of 200 C. Furthermore, effects of hydrogen addition to the oxygen atmosphere on the film properties have been investigated.

TUPA 24 Oxygen Radical Assisted Laser Evaporation of Polysiloxane for Preparation of Insulating Films with Low Dielectric Constant TOSHIAKI FUJII, TSUNEKI YOKOI, MINEO HIRAMATSU, MASAHITO NAWATA, *Meijo University, Nagoya, Japan* MASARU HORI, TOSHIO GOTO, *Nagoya University, Nagoya, Japan* SHUZO HATTORI, *Nagoya Industrial Science Research Institute, Nagoya, Japan* Fabrication of insulating thin films with dielectric constants lower than that of SiO_2 is required to realize high-performance ultralarge scale integration circuits (ULSI) devices. In this work, we proposed laser evaporated polysiloxane films modified by oxygen radical injection as low dielectric constant interlayer dielectrics. Film formation system was simply composed of a vacuum chamber including a polysiloxane bulk target and a halogen lamp for substrate heating, a continuous wave (cw) CO_2 laser for vaporizing the target, and a remote microwave O_2 plasma as an oxygen radical source for surface modification of polysiloxane films. From XPS analysis the carbon content of the films decreased with the increase of microwave power and substrate temperature. Polysiloxane thin films with low dielectric constant as low as 2.0 were successfully prepared by using this system. The film thickness did not decrease after annealing at 300 C in N_2 atmosphere.

SESSION TUPB: ELECTRON INTERACTIONS II POSTER SESSION
Tuesday afternoon, 22 October 1996
Alcove B at 15:45
Keith Lykke, ANL, presiding

TUPB 1 Enhanced Electron Attachment to Highly-Excited Molecules Using a Plasma Mixing *Scheme** DENNIS MCCORKLE, LAL PINNADUWAGE, *ORNL and Univ. Tenn., Knoxville* We report preliminary results on enhanced electron attachment to molecules excited to highly-excited states via excitation transfer from rare-gas metastable states; a rare-gas plasma from a hollow-cathode discharge was extracted to an adjoining region and was mixed with the molecular gas under study. These studies confirm the mechanism proposed [1] to explain the observation [2] of efficient H^- formation from methane in a similar discharge source. 1. L. A. Pinnaduwage, Appl. Phys. Lett. 67, 1034 (1995). 2. S. Iizuka *et al.*, Appl. Phys. Lett. 63, 1619 (1993). * Work supported by the LDRD Program of the Oak Ridge National Laboratory, managed by Lockheed Martin Energy Research Corp. for the US Department of Energy under contract number DE-AC05-96OR22464, and by the National Science Foundation under contracts ECS-9626217 and CHE-93113949 with the Univ. of Tenn., Knoxville.

TUPB 2 Ionization and Electron Attachment in Methane J. DE URQUIJO, C. A. ARRIAGA, I. DOMíNGUEZ, C. CISNEROS, I. ALVAREZ, *Instituto de Física, UNAM, México.* There has been a number of swarm experiments dealing with ionization in methane, but only one of them has dealt with electron attachment in this gas [1]. We have observed and interpreted direct, well diferentiated ionic avalanches in methane gas obtained from the pulsed Townsend method. The E/N range covered was 130 – 950Td, at pressures from 80 to 530Pa. From the pulse current shapes, values

of the density–normalized effective ionization coefficient have been derived, and are in good agreement with existing ones. Also, the average positive ion drift velocities agree well with those measured mass spectrometrically [2]. The ability of the present method to differentiate between positive and negative ion components from the pulsed signal shape enabled us to obtain values of the attachment coefficient which are in fair agreement with those of Hunter *et al* [1] in the overlapping range. [1] S. R. Hunter, J. G. Carter and L. G. Christophorou, J. Appl. Phys., **60** 24 (1986) [2] J. de Urquijo, C. Cisneros, H. Martínez and I. Alvarez, Gaseous Dielectrics VII, L. G. Christophorou, Ed. Plenum Press, 1994, pp. 55–62 Work supported by DGAPA, Project IN104795

TUPB 3 Temperature Dependence of Dissociative Electron Attachment to Halogenated Hydrocarbons YICHENG WANG*, LOUCAS G. CHRISTOPHOROU*, *NIST, Gaithersburg, MD 20899* Most of the gas mixtures currently in use for plasma processing of semiconductors involve halogenated hydrocarbons such as the strongly electronegative gases CCl_4 and $CFCl_3$, the weakly electronegative gas CF_2Cl_2 and the very weakly electronegative gases CHF_3 and CF_4. Many dissociation processes are known to occur for these molecules. One of these dissociation reactions which is particularly effective for the strongly electronegative hydrocarbons is dissociative electron attachment. Even for weakly electron attaching gases, molecular dissociation via dissociative electron attachment at low energies can be an efficient dissociation process if the gas temperature is higher than ambient. Dissociative electron attachment is known to increase with increasing temperature above room temperature for many such compounds. In this paper, we report our measurements on the increases of the total electron attachment rate constant for CF_2Cl_2 with increasing gas temperature from room temperature to about 600 K. -Research sponsored in part by the U.S. Air Force Wright Laboratory under contract F33615-96-C-2600 with the University of Tennessee. *Also, Department of Physics, The University of Tennessee, Knoxville, TN.

TUPB 4 Low-Energy Electron Impact Excitation of the (010) Bending Mode of CO_2 WINIFRED M. HUO, *NASA Ames Research Center* Low-energy electron impact excitation of the fundamental modes of CO_2 has been extensively studied, both experimentally and theoretically. Much attention has been paid to the virtual state feature in the the (100) mode excitation and the $^2\Pi_u$ resonance feature around 3.8 eV, which is observable in all three fundamental modes. For the excitation of the (010) mode away from the resonance region, the Born dipole approximation was generally considered adequate. The present study employs the Born dipole approximation to treat the long range interaction and the Schwinger multichannel method for the short range interaction. The roles of the two interaction potentials will be compared.

TUPB 5 Small Angle Elastic Electron Scattering by Polarized 3P Sodium H. WEI, Z. SHI, Y. WANG, L. VUSKOVIC, *Old Dominion University, Norfolk, VA* Experiment is being performed with low energy electrons scattered by laser-excited sodium atoms prepared in the $3^2P_{3/2}$ F=3 (M_F=+3 or M_F=-3) polarized states. Differential cross setions for $3^2P_{3/2}$ $M_L=\pm1$ states at polar angle 45° are being determined as a function of energy. Absolute scale is calibrated in respect with ground-state cross section by measuring fraction of excited atoms in the interaction region. Azimuthal asymmetry[1] as an orbital effect due to M_L state perpendicular to the scattering plane is being investigated. Preliminary results and theoretical predictions[2,3] will be discussed at the conference. [1 2 3]

[1]Z. Shi, C. H. Ying, and L. Vušković, Phys. Rev. A **54**, No 1 (1996).
[2]I. Bray, D. V. Fursa, and I. E. McCarthy, Phys. Rev. A **49**, 2667 (1994); I. Bray (private communication).
[3]B. L. Whitten, W. K. Trail, H. L. Zhuo, M. Morison, K. Bartschat, and D. W. Norcross, Bull. Am. Phys. Soc. **39**, 1073 (1994); B. L. Whitten and W. K. Trail (private communication).

TUPB 6 Atomic Rearrangements in Electron Attachment to Laser-Excited *Molecules** LAL PINNADUWAGE, DENNIS MCCORKLE, *ORNL and Univ. Tenn., Knoxville* We report the observation of extensive atomic rearrangements in dissociative electron attachment to triethylamine "[1]" and benzene laser excited to energies above their ionization thresholds. Large signal of "rearranged" negative ions, such as C_3^- (which is observed in both cases), were observed. This is in contrast to negative-ion formation via electron attachment to molecules in their ground states, where "rearranged" negative ions are comparatively weak and have been observed only occasionally. However, formation of "rearranged" positive ions is of common occurrence in the ionization of polyatomic molecules; it is possible that the formation of "rearranged" positive ions in the ionization processes, and the formation of such negative ions via electron attachment to excited states located close to the ionization threshold, are related. * Work supported by the LDRD Program of the Oak Ridge National Laboratory, managed by Lockheed Martin Energy Research Corp. for the US Department of Energy under contract number DE-AC05-96OR22464, and by the National Science Foundation under contract CHE-93113949 with the Univ. of Tenn., Knoxville.

[1]Pinnaduwage and McCorkle, Chem.Phys. Lett. (in press, 1996)

TUPB 7 Photophysical and Electron Attachment Properties of ArF-Excimer-Laser Irradiated Molecular *Hydrogen** PANOS DATSKOS, LAL PINNADUWAGE, *Oak Ridge National Laboratory and University of Tennessee, Knoxville* We report on new experimental observations of electron attachment to H_2 molecules irradiated by an ArF (=193 nm) excimer-laser. These studies indicate that the electron attachment is to the $E,F\,^1\Sigma_g^+$ state; the respective electron attachment rate constants for the E and F wells are $10^{-4}\ cm^3\ s^{-1}$ and $10^{-5}\ cm^3\ s^{-1}$. We also provide evidence that the previously reported quenching of the v=6 level of E well with increasing H_2 number density is mainly due to collisional excitation transfer to the v=4 level of F well. The ionization cross section from the $E,F\,^1\Sigma_g^+$ state was found to be smaller than what was previously reported. *Work supported by the LDRD Program of ORNL, managed by Lockheed Martin Energy Research Corp. for the U. S. DOE under contract number DE-AC05-96OR22464, and by the NSF under contracts ECS-9626217 and CHE-9313949 with the Univ. of Tenn.

TUPB 8 LTE Deviations as Function of radial position in Hg High-Pressure Discharge Lamps GEORGES ZISSIS, *CPAT, Toulouse, France* KAMEL CHARRADA, *ESSETT, Tunis, Tunisia* In the electric discharge plasma the electrons pick up energy from the electric field and partially transfer it to the heavy particles by collisions. Due to the relatively large difference between electron and heavy species mass, the energy exchange between them is rather inefficient. Thus, even in atmospheric pressure Hg discharges, the electron temperature may be substantially higher than the heavy particle temperature. We developed a model based on hydrodynamic conservation equations for electrons and gas particles. This equation set is solved by using a 2-D semi-implicit

finite element scheme. Our results confirm quantitatively the existence of thermal equilibrium deviations in a such type of discharges. Furthermore, we show that, in a such type of discharges, the hot core is anyway closer to thermal equilibrium than the outer discharge jacket. As example, when pressure is relatively high (3 atm) the relative deviation on the axis is less than 0.5% however the same value becomes higher than 5% in the outer discharge regions. A similar behaviour is detected in the case of high arc currents.

TUPB 9 Electron and Positron Polyatomic Molecule Scattering: Experimental and Theoretical Studies for Benzene R. HAMADA, O. SUEOKA, M. KIMURA, *Yamaguchi Univ., Japan* H. SATO, *Ochanomizzu Univ., Japan* Total cross section measurement for electron and positron scattering from benzene molecules was carried out experimentally earlier and details of the observation was reported [1]. Recently we carried out a theoretical study on elastic processes of electron and positron scattering based on the continuum multiple scattering method in the energy range from rev to 100 eve. Present theoretical cross sections for electron and positron scattering reproduce typical features in the cross sections seen experimentally, namely, 1) a slightly smaller cross section for the positron case at the highest energy studied and 2) This energy difference decreases with decreasing electron energy. For electron scattering our result also reproduces a resonance like structure near 7 eV.

[1]O. Sueoka, J. Phys. B21, L631 (1988)

TUESDAY AFTERNOON \ TUPB

TUPB 10 Low-Energy Electron Interactions with CF_4 LOUCAS G. CHRISTOPHOROU*, JAMES K. OLTHOFF, M. V. V. S. RAO, *NIST, Gaithersburg, MD 20899* Carbon tetrafluoride is one of the most widely used components of feed gas mixtures employed for a variety of plasma assisted materials processing applications. In this presentation, we synthesize and assess the available information on the cross sections and rate coefficients of collisional interations of CF_4 with electrons.[1] A "recommended" data set is presented, based upon available data for: (i) cross sections for electron scattering (total, elastic, momentum, differential, inelastic), electron impact ionization (total and partial), electron impact dissociation, and electron attachment; and (ii) coefficients for electron transport, electron attachment, and electron impact ionization. -Research sponsored in part by the U.S. Air Force Wright Laboratory under contract F33615-96-C-2600 with the University of Tennessee. *Also, Department of Physics, The University of Tennessee, Knoxville, TN.

[1]L. G. Christophorou, J. K. Olthoff, and M.V. V. S. Rao, J. Phys. Chem. Ref. Data, submitted (May 1996)

TUPB 11 Boltzmann Calculations of Electron Transport in CF_4 and CF_4/Ar YICHENG WANG*, R. J. VAN BRUNT, *NIST, Gaithersburg, MD 20899* A new set of electron collisional cross sections[1] for CF_4 has been proposed, based primarily upon available experimental measurements. In this paper we present the results of calculations of the drift velocity, ionization coefficient, and attachment coefficient for electrons in CF_4 based upon the new cross section set, using a two-term Boltzmann calculation. Comparison of results with experimental determinations of the transport parameters, such as drift velocity, are presented, along with comparison of results obtained using two previously pubished[2] electron impact cross section sets for CF_4. Additions and adjustments to the cross section sets required for the model to achieve consitency with transport data are discussed. - Research sponsored in part by the U.S. Air Force Wright Laboratory under contract F33615-96-C-2600 with the University of Tennessee. *Also, Department of Physics, The University of Tennessee, Knoxville, TN.

[1]L. G. Christophorou, J. K. Olthoff, and M. V. V. S. Rao, J. Phys. Chem. Ref. Data, submitted (May 1996)
[2]M. Hyashi, in *Swarm Studies and Elastic Electron-Molecule Collisions* (1987); and Y. Nakamura in *Gaseous Electronics and Their Applications* (1991)

TUPB 12 Production of metastable atoms following dissociative excitation of oxygen containing molecules.* J.M. DERBYSHIRE, W. KEDZIERSKI, J.W. MCCONKEY, *University of Windsor* A novel detector [1] has been used to investigate the production of metastable $O(^1S)$ atoms following electron impact on oxygen containing molecules in the energy range from threshold to 500 eV. By pulsing the electron beam and using time-of-flight (TOF) techniques it is possible to distinguish between prompt photons, produced by excitation of the target, and the oxygen atoms released in the dissociative excitation process. The TOF data are readily transformed to obtain the kinetic energy released in the dissociative process, often enabling parent repulsive potential curves to be identified. Data will be presented for different targets particularly H_2O and D_2O. * Research supported by the Natural Sciences and Engineering Research Council of Canada.

[1]L.R. LeClair and J.W. McConkey, J. Chem. Phys. **99**, 4566 (1993).

TUPB 13 The Cross Section for the Formation of $N_2^+(X)$ Ions Produced by Electron Impact on N_2. R. SIEGEL, N. ABRAMZON, K. BECKER, *City College of CUNY, USA* We report measurements of the absolute cross section for the formation of $N_2^+(X)$ ground state ions produced by electron impact ionization of N_2 under single collision conditions. The measurements were carried out in a new "triple beam" apparatus utilizing an effusive gas beam and an electron beam that can be operated continuously or pulsed to produce electron-impact fragments in conjunction with a tunable pulsed dye laser system to pump ground state species into excited states whose spontaneous emission is then detected (LIF). Therefore, the method is applicable to a variety of electron-impact processes which produce ground state species with a bound electronically excited state, which is accessible by laser pumping using available tunable dye lasers. The ionization of N_2 was studied as a test case to demonstrate the viability of the method.[1]

[1]This work has been supported by the US National Science Foundation (NSF).

TUPB 14 LIF detection of unexcited fragments following electron impact dissociation of molecules.* T. HARB, W. KEDZIERSKI, L.R. LECLAIR, J.W. MCCONKEY, *University of Windsor* A supersonically-cooled target gas beam is crossed by a pulsed electron beam and the resultant fragments are interrogated by a pulsed YAG dye laser system.[1] A magnetically collimated electron gun has been added to the previous experimental arrangement to obtain higher currents at lower energy and thus enable the important near threshold region to be probed. Full details of the various experimental procedures will be presented at the Conference together with our preliminary data on near threshold OH production following electron impact on H_2O. * Research sup-

ported by the Natural Sciences and Engineering Research Council of Canada.

[1]M. Darrach and J.W. McConkey, J. Chem. Phys. **95**, 754 (1991).

TUPB 15 Neutral Dissociation Plus Excitation Cross Section in N_2. L. MI, R. A. BONHAM, *Dept. of Chemistry, Illinois Institute of Technology , Chicago, IL 60616* Pulsed electron beam time-of-flight measurements of the electron energy loss spectrum at scattering angles of 28, 45, 71,112 and 135° were made at impact energies of 24.5, 33.1 and 33.6 eV in coincidence with positive ions. The angular dependent elastic, total inelastic, ionization, and neutral dissociation plus excitation cross sections were measured. The data were integrated over electron energy loss for each scattering angle, fitted with smooth analytical functions, and integrated over angle to obtain individual total cross sections. Cross section data were placed on an absolute scale by matching to total cross section measurements. The angular dependent elastic cross section and the integrated cross sections for elastic and total inelastic scattering were in good agreement with literature values. The neutral dissociation plus excitation cross section agrees with the sum of separate measurements of these quantities. Total ionization cross sections are in fair agreement with literature values.

SESSION TUPC: DISCHARGE THEORY AND SIMULATION POSTER SESSION
Tuesday afternoon, 22 October 1996
Alcove B at 15:45
Keith Lykke, ANL, presiding

TUPC 1 Simulations of the ionization growth in a plasma display cell. RAMANA VEERASINGAM, ROBERT B CAMPBELL, ROBERT T MCGRATH, *Sandia National Labs,New Mexico* It is well known that for ac color plasma displays, using a mixture of helium-xenon or neon-xenon provides a better switching characteristic and bistable margin than pure helium or neon. The synergistic effect in the gas mixture modifies the electron energy distribution function (EEDF) so that the ground state ionization rate coefficient of xenon increases by up to 500 times compared to pure xenon. The enhanced ionization rate results in the growth of volumetric charge which collects on the wall leading to a growth in wall voltage to satisfy the requirement for the bistable margin, i.e., the slope in the wall voltage transfer characteristic becomes 2 or larger. From fluid simulations, we conclude that the bistable margin depends strongly on the volumetric ionization rate coefficient, which is dependent upon the EEDF and the ionization energy and cross sections of the minority gas species; while the value of the secondary electron emission coefficient serves to raise or lower the voltage at which the margin manifests.

TUPC 2 Simulations of the ionization growth in a plasma display cell.* RAMANA VEERASINGAM, ROBERT B. CAMPBELL, ROBERT T. MCGRATH, *Sandia National Labs,New Mexico* It is well known that for ac color plasma displays, using a mixture of helium-xenon or neon-xenon provides a better switching characteristic and bistable margin than pure helium or neon. The synergistic effect in the gas mixture modifies the electron energy distribution function (EEDF) so that the ground state ionization rate coefficient of xenon increases by up to 500 times compared to pure xenon. The enhanced ionization rate results in the growth of volumetric charge which collects on the wall leading to a growth in wall voltage to satisfy the requirement for the bistable margin, i.e., the slope in the wall voltage transfer characteristic becomes 2 or larger. From fluid simulations, we conclude that the bistable margin depends strongly on the volumetric ionization rate coefficient, which is dependent upon the EEDF and the ionization energy and cross sections of the minority gas species; while the value of the secondary electron emission coefficient serves to raise or lower the voltage at which the margin manifests.

*This work performed under the auspices of the U.S. D.O.E. under contract DE-AC04-94AL85000

TUPC 3 Cascade Model of Ionization Multiplication of Electrons in Glow Discharge Plasma V.A. ROMANENKO, S.A. SOLODKY, *S.I.Vavilov State Optical Institute, Sosnovy Bor, St.Petersburg, Russia* A.A. KUDRYAVTSEV, I.A. SULEYMANOV, *St.Petersburg University, Russia* For determination of EDF in non-uniform fields a Monte-Carlo simulation[1,2] is applied. As alternative multi-beam cascade model[3] is offered. Our model eliminates defects of that model and enables to determine EDF of low pressure plasma in non-uniform fields. A cascade model (with EDF dividing in monoenergetic electron groups) for arbitrary electric potential profile was used. Modeling was carried out for electron forward scattering only, constant electron mean free path; ionization was considered only. The equation system was solved for the region with kinetic energies more than ionization energy. The boundary conditions (on ionization energy curve) take into account electron transitions from higher-lying level in the less than ionization energy region and secondary electron production. The problem solution in analytical functions was obtained. The insertion of additional processes does not make significant difficulties. EDF and electrokinetical parameters in helium from numerical calculations are well agreed with above-mentioned authors. Work was carried out under RFFI (project N 96-02-18417) support.

[1]Tran Ngoc An *et al.*, J.Phys.D: Appl. Phys. 10, 2317 (1977)
[2]J.P. Boeuf *et al.*, Phys.D: Appl.Phys. 15, 2169 (1982)
[3]H.B. Valentini, Contrib.Plasma Phys. 27, 331 (1987)

TUPC 4 New Convected Scheme simulations of positive column discharges G. J. PARKER, *Lawrence Livermore National Laboratory* W.N.G. HITCHON, E.R. KEITER, *Univ. of Wisconsin–Madison* An efficient scheme for description of long mean-free path particle transport at a kinetic level has been extended to a case where particle distributions are highly anisotropic- implantation of ions into a solid. The method calculates the scattering rate of particles throughout a region and obtains the particle distribution from the scattering rate. The scattering rate is found using a numerical form of a propagator to solve an integral equation. The propagator is the probability that a particle which scattered in a cell has its next scatter in any other cell of the mesh. The main focus of this work is the way this propagator can be computed efficiently and accurately as compared to other computer models for an arbitrary angular distribution of scattered particles. The method is illustrated in application to implantation of boron into silicon.

TUPC 5 Neutral Gas Dynamic Transport in a Model GEC Cell DEAN C. WADSWORTH, *Hughes STX* ANDREW D. KETSDEVER, DAVID P. WEAVER, *Propulsion Directorate, Phillips Lab, Edwards AFB, CA* Experimental and numerical studies have been made of cold neutral rarefied gas dynamic flow in a model GEC RF cell. The cell uses the standard showerhead inlet in the upper electrode. Exhaust pumping is done through a side-mounted port, leading to the potential for (undesirable) highly non-uniform gas flow near the substrate. In addition, low pressure operating conditions lead to rarefied gas dynamic phenomena such as species separation and slip layers near the substrate surface. In the initial studies, experimental measurements of gas density profiles above the substrate have been obtained with the electron beam technique for a range of operating pressures and gases. Matching 2-d and 3-d direct simulation Monte Carlo (DSMC) calculations have been made for quantitative comparison. Additional parametric calculations have been done to quantify the influence of operating conditions on transport through the cell, and ultimately on deposition characteristics on the substrate for this model problem. The present results are used to guide future experimental studies, with the ultimate objective of obtaining sufficient data to validate computational models required for increasingly accurate simulations of the complex ionized, chemically reacting, non-equilibrium flows present in realistic reactors.

TUPC 6 Time-Dependent Multi-Term Treatment of the Velocity Distribution of Plasma Electrons Acted upon by RF Fields DETLEF LOFFHAGEN, ROLF WINKLER, *Institut für Niedertemperatur-Plasmaphysik, 17489 Greifswald, Germany* Recent investigations of the temporal behaviour of electrons in spatially homogeneous, weakly ionized, collision-dominated plasmas have led to the development of a new technique [1] for solving the time-dependent electron Boltzmann equation in higher order accuracy. This solution technique is based on a multi-term approximation of the expansion of the electron velocity distribution function in Legendre polynomials. Conventionally this expansion is restricted to the first two terms and the time-dependence of the remaining distribution anisotropy is described in a quasi-steady-state approximation. As former electron kinetics studies have shown this conventional two-term approximation can fail e.g. in CO plasmas acted upon by rf fields [2]. In the present contribution results for the established periodic behaviour of the electron velocity distribution in inert and molecular gases subjected to rf fields are reported. The impact of higher (than two) order terms in the Legendre polynomial expansion is studied and that approximation order has been analysed by which the converged solution of the electron Boltzmann equation and the related macroscopic quantities is obtained.

[1]D. Loffhagen and R. Winkler, J. Phys. D: Appl. Phys. **29**, 618 (1996).

[2]G. L. Braglia *et al.*, Il Nuovo Cimento **13D**, 1235 (1991).

TUPC 7 Plasma instabilities due to ponderomotive forces of low pressure RF discharges containing negative ions I. D. KAGANOVICH, *University Bochum, Germany* V. A. SCHWEIGERT, *Novosibirsk Institute of Theoretical and Applied Mechanics, Russia, 630090* In the presence of rf fields ponderomotive forces arise, which result in additional ion fluxes. For some plasma parameters these forces lead to anti-diffusion and can cause instabilities: the plasma stratification. The instability increment was calculated analytically and numerically. Another possible instability is the parametric one. For typical ion densities in rf discharges the value of the ion plasma frequency can be close to the discharge frequency, and ion plasma waves can be excited. Intense ion oscillations were observed near the plasma-sheath boundary in numerical modelling. They correspond to the generation of two plasmons. The increment of this parametric instability in a uniform plasma has been derived. The influence of the plasma inhomogeneity on the instability has also been analyzed.

TUPC 8 Modeling Low Pressure Plasmas with Fluid Models: Comparison to Monte Carlo and Nonlocal Electron Kinetic Treatments D.B. GRAVES, H. DATE, M. LI, J. BUKOWSKI, *University of California, Berkeley, CA* In this paper we compare various model predictions for low pressure inductively coupled plasmas in chlorine with each other. A self-consistent fluid model is solved to obtain the electrostatic and electromagnetic fields, as well as the neutral density profiles. This information is used for an electron Monte Carlo model and a nonlocal electron kinetics model. Cases were run at 5 and 20 mtorr in an axisymmetric, cylindrical geometry with purely inductive power coupled into electrons. A comparison is made between the predicted electron-neutral inelastic rate coefficients from each model. At 5 mtorr, the agreement between the three model was good, but at 20 mtorr the models predict significantly different rate coefficients, the reasons for the disagreement are discussed and possible stategies to improve the fluid model accuracy are suggested.

TUPC 9 PIC-MCC Simulation of Discharges with Secondary Emission M. M. TURNER, *Dublin City University, Ireland* The Particle in Cell procedure with Monte Carlo collisions (PIC-MCC) is useful for simulating many types of discharge when kinetic behavior of electrons or ions is important, but simulation of discharges such as direct current discharges and some radio frequency discharges has been found difficult because in these cases a statistically small group of electrons emitted from the electrodes are dominant sources of ionization. These electrons tend not to be adequately represented in simulations containing a manageable number of particles. In this paper we will discuss the use of particle simulation with variable particle weights to avoid this difficulty. We will describe the variable weight technique and give examples of results.

TUPC 10 Numerical Solution of the Multiboundary Problem for Multicomponent Plasmas with Respect to Ion Temperature FRANZ-BURKHARD ANSCHÜTZ, PETER AWAKOWICZ, *Physics of Electrotechnology, Technical University Munich, Germany* HANS-BURKHARD VALENTINI, *Institut für Physikalische Hochtechnologie, Jena, Germany* The hydrodynamic modeling of multicomponent plasmas at low pressures with respect to ion inertia and ion partial pressure leads to a multiboundary problem with one unkown boundary (point of sound speed) per ion species. A finite volume based method for solving this task is used. A plasma model containing three ion species in a cylindrical discharge is presented. The ion and electron motion is described by particle and momentum balance. Space charge, inertia, gradient of partial pressure, elastic and charge transfer collisions of carriers

with neutral gas are taken into account. The radial distributions of densities are compared with measurements. The experimental setup is a *ash7*mm cascade arc containing helium and small admixtures of nitrogen and hydrogen at low pressures in the range of 1 mbar. Spectroscopic measurements are made for the radial distributions of electron density, electron temperature and for the nitrogen ion density on the axis.

TUPC 11 Two Dimensional Fluid Simulation of Glow Discharges in Arbitrary Cartesian Geometry JAE J. OH, *Samsung Advanced Institute of Technology, Korea* Glow discharge is used as a source of reactive species for microelectronics fabrication. To satisfy the need of the industrial applications, more effective and generalized scheme is demanded to save efforts on numerical simulation and pay more attention to physical modeling itself. We develope 2D multicomponent fluid model simulation of rf glow discharges in nonorthogonal body-fitted coordinate system. The model with self-consistent power deposition includes the continuity equations of electrons, ions, and neutral species, the momentum equations of ions and neutral species, the electron energy balance equation, and Poisson equaton. In case neglecting convective flow, the drift-diffusion approximation is used in place of the full momentum equations. The spacial distributions of charged particle densities, electric field, electron temperature, and ionization rate are calculated for the inductively coupled plasma source. The effects of applied power and gas pressure on the radial profiles of the plasma parameters are presented in detail.

TUPC 12 Experimental studies of kinetic energy release distribution of argon atoms from homogeneous and heterogeneous rare gas clusters using covariance mapping mass spectroscopy DAVID KHATCHATRIAN, CHARLES RHODES, *University of Illinois at Chicago Physics Department Laboratory for Atomic, Molecular and Radiation Physics* Homogeneous and heterogeneous argon - rare gas clusters are photoionized with a KrF, 248 nm wavelength and 20 nanosecond FWHM laser focused to $I = 10^{12}$ W/cm^2 intensity. The Kinetic Energy Release (KER) of argon atoms from the clusters of differnt consistencies and sizes (from 10 to 10^4) are obtained by means of Time of Flight Mass Spectrometer and processed using covariance mapping mass spectroscopy. Argon, having essentially no isotopes, is an ideal gas for kinetic energy measurements.These experiments reveal new insights in the cluster fragmentation dynamics.

➢➢➢➢➢➢➢➢➢➢➢

SESSION W1A: ION SURFACE INTERACTIONS

Wednesday morning, 23 October 1996; Auditorium at 8:00; Wally Calaway, ANL, presiding

Invited Papers

8:00

W1A 1 Recent Developments in Silicon Ion Beam Epitaxy.

J. WAYNE RABALAIS, *Department of Chemistry, University of Houston, Houston, TX 77204-5641*

fast atoms and molecules, with surfaces spans a copious panorama of fundamental chemical and physical phenomena which are presently incompletely understood and which have important potential, as well as current, practical applications. The phenomena spanned by these interactions include stimulation of surface chemical reactions, reactive and nonreactive scattering, nonthermal desorption and decomposition processes, film growth from energetic species, surface photochemistry, electronic charge exchange processes, etc. This talk will discuss the parallelism of these sseemingly disparate topics and then will focus on the mechanism of film growth from energetic species, with examples of low temperature silicon ion beam epitaxy and silicon oxidation. Direct ion beam deposition of Si+ ions for homepitaxial film growth on Si100 has been studied over the ion energy range of 8 - 80 eV in the low temperature range of 50=B0 - 500=B0C. Deposition was performed by means= of a mass-selected, low-energy, ultra-high vacuum ion beam system. The films were analyzed in situ by reflection high energy electron diffraction (RHEED) and Auger electron spectroscopy (AES) and ex situ by cross section high-resolution transmission electron microscopy (TEM), Rutherford backscattering spectrometry (RBS), and secondary ion mass spectrometry (SIMS). The growth mode, crystalline quality, and number of defects in the films are found to be extremely sensitive to both substrate temperature (at low temperature) and ion energy (at low energy). An optimum ion energy window for achieving layer-by-layer epitaxial growth and high crystalline quality films has been observed at 15 - 25 eV at 200=B0C. This behavior is discussed in terms of the changes in the phenomena which dominate the growth process as a function of ion energy and temperature.

8:30

W1A 2 Surface Modification with Low Energy Polyatomic Ions.

LUKE HANLEY, *University of Illinois at Chicago*

Low energy polyatomic ions can be used either directly or in plasmas to modify surfaces. Mass selected beams of positively charged polyatomic ions, mass spectrometry, x-ray photoelectron spectroscopy, ultrahigh vacuum methods and trajectory calculations are used to probe energy transfer, sputtering, and deposition processes which occur during polyatomic ion-surface collisions. Trimethyl silyl ions are scattered at $<$90 eV off clean and hexanethiolate covered Au(111) and the mass and energy distribution of the scattered ions are measured experimentally. This data is analyzed in conjunction with classical trajectory calculations to determine the energy transfer function between the ion and the surface. $>$90 eV pentafluoro sulfur ions are used to bombard an ammonia/carbon monoxide multilayer adsorbed on Ni(111). Comparision with xenon atomic ion bombardment shows that the pentafluoro sulfur ions not only sputter the adsorbate more efficiently, but also result in complex chemical modifation of the surface. The implications of these results for ion beam and plasma processing of materials will be discussed.

9:00

W1A 3 Measurements and Modelling of Sputtering Rates with Low Energy Ions.

DAVID N. RUZIC, PRESTON C. SMITH, ROBERT B. TURKOT JR., *University of Illinois*

The angular-resolved sputtering yield of Be by D+, and Al by Ar+ was predicted and then measured. A 50 to 1000 eV ion beam from a Colutron was focused on to commercial grade and magnetron target grade samples. The S-65 C grade beryllium samples were supplied by Brush Wellman and the Al samples from TOSOH SMD. In our vacuum chamber the samples can be exposed to a dc D or Ar plasma to remove oxide, load the surface and more-nearly simulate steady state operating conditions in the plasma device. The angular distribution of the sputtered atoms was measured by collection on a single crystal graphite witness plate. The areal density of Be or Al (and BeO2 or Al2O3, after exposure to air) was then measured using a Scanning Auger Spectrometer. Total yield was also measured by deposition onto a quartz crystal oscillator simultaneously to deposition onto the witness plate. A three dimensional version of vectorized fractal TRIM (VFTRIM3D), a Monte-Carlo computer code which includes surface roughness characterized by fractal geometry, was used to predict the angular distribution of the sputtered particles and a global sputtering coefficient. Over a million trajectories were simulated for each incident angle to determine the azimuthal and polar angle distributions of the sputtered atoms. The experimental results match closely with the simulations for total yield, while the measured angular distributions depart somewhat from the predicted cosine curve.

9:30

W1A 4 Secondary Electron and Negative Ion Emission from Oxidized Aluminum* JOHN C. TUCEK, ROY L. CHAMPION, *Department of Physics, College of William and Mary, Williamsburg, VA 23187* Absolute yields and kinetic energy distributions for secondary electrons and negative ions due to collisions of positive alakli ions with an aluminum surface with controlled exposures to oxygen and sodium have been measured for impact energies, E < 500 eV. The electron and negative ion yields, Y_e(E) and Y_i(E), behave similarly as the oxygen coverage is varied. [1] However, lowering of the surface work function due to exposure to sodium increases the negative ion emission considerably and that of the electrons only slightly. The kinetic energy distribution of O^-, the dominant negative ion observed, is used to model the negative ion yield accurately. It is suggested that the adsorbed oxygen, and subsequent sputtering of O^-, serves as a precursor to surface generated secondary electrons.

*Supported in part by the U. S. DOE, Division of Chemical Sciences, Office of Basic Energy Sciences.

[1]J.C. Tucek, S.G. Walton and R.L. Champion, Phys. Rev. B, 53, 14127 (1996).

W1A 5 Energy and Angle Distributions of Ions Reflected from Chlorinated Silicon Surfaces BRYAN HELMER, DAVID GRAVES, *University of California, Berkeley, CA* Ion reflection from sidewalls can lead to microtrench formation on the bottom of an etched feature. Data on the energies and angles of ions reflected from surfaces exposed to plasmas are sparse, however, and profile evolution simulation studies often rely on simple models of ion reflection. In the present study, we describe the distributions of reflected ion energies E_r and angles (polar θ_r and azimuthal ϕ_r) obtained from molecular dynamics simulations of Ar^+, Cl^+, and Cl_2^+ impacts onto chlorinated silicon surfaces with incident energies E_i from 20 to 100 eV and angles θ_i from 0° to 85° from the surface normal. Use of these distributions in profile simulations provides a more accurate treatment of reflected ions. For impacts at glancing angles ($\geqslant$75°), we found that the distribution of reflected energies was quite broad; ions retained <10% up to >90% of E_i. Ions with the highest reflected energies scattered from the surface with super-specular polar angles ($\theta_r > \theta_i$) in the forward direction (ϕ_r near 0). We also compare these distributions with those predicted by binary collision models of the scattering process.

SESSION W1B: DIAMOND AND DIAMOND-LIKE CARBON DEPOSITION

Wednesday morning, 23 October 1996; Lecture Hall at 8:00; Ben Yu, CFD Research Corporation, presiding

Invited Papers

8:00

W1B 1 Microwave Plasma Enhanced Synthesis of Nanocrystalline Diamond Films*.

DIETER GRUEN, *Argonne National Laboratory, Argonne, IL 60439*

Synthesis of diamond films using fullerene (C_{60}) precursors in an argon (Ar) microwave plasma without the addition of hydrogen has now been accomplished and strongly suggests that the diamond phase grows by a new and hitherto unexplored mechanism. Diamond films produced in this way are nanocrystalline, smooth (20-30 nm rms surface roughness) and highly reflective. They maintain their nanocrystallinity to thicknesses of more than 20 μm. More recently is has been found by us that films with similar properties can also be grown from argon microwave plasmas containing 1% CH_4. Conditions using both C_{60}/Ar and CH_4/Ar mixtures are comparable to "standard" CH_4/H_2 plasma parameters: 1% carbon content, 100 sccm, 100 Torr, 1 KW microwave power, 700-800 °C substrate temperatures. Growth rates of 0.5-1 μm/hr have been measured laser interferometrically on Si, Si_3N_4, SiC, W and WC substrates, which had been prepared by treatment with 0.1 μm diamond powder or by using bias enhanced nucleation. Emission spectra from CH4/H2 microwave plasmas show the presence of $CH_3^{\cdot}$ and CH molecules, as well as atomic H. By contrast, spectra from C_{60}/Ar and CH_4/Ar discharges are dominated by the well-known Swan bands of carbon dimer, C_2. Fragmentation of C_{60} by intense laser irradiation as well as collisionally induced and surface-induced dissociation has for a long time been known to proceed by sequential loss of C_2 molecules at least until cage sizes of C_{28} are reached. We now have found that fragmentation of C_{60} in an argon microwave discharge also occurs via the C_2 pathway. Fragmentation in the plasma appears to be very efficient as a result of a number of different and competing processes, including collisionally induced dissociation by metastable argon atoms. The experimental work has recently been suplemented by quantum chemical calculation, which strongly supports the idea that the chemically highly energetic C_2 molecule with an adsorption energy of 8 eV can grow diamond without the intervention of atomic hydrogen, while hydrocarbon precursors ($CH_3^{\cdot}$ or C_2H_2) with adsorption energies of 1 ev require the intervention of atomic hydrogen. Very high nucleation rates (10^{10},cm^{-2},sec^{-1} are responsible for the microstructure of the films (average crystallite size of 15 μm) grown from argon discharges. Arguments will be advanced to show that diamond nucleation occurs in preference to graphite nucleation as a result of the thermodynamic stability of nanocrystalline diamond. Once established at the level of supercritical or embryonic nuclear size, growth continues even in the absence or virtual absence of hydrogen because of the large energy barrier for the solid-state nucleation of the stable bulk graphite phase. *Work supported by the U.S. Department of Energy, BES-Materials Sciences, under Contract W-31-109-ENG-38.

8:30

W1B 2 Reaction Mechanisms for Growth of Diamond Thin-Films from Buckyball Precursors.

LARRY CURTISS, *Argonne National Lab, Argonne, IL*

Rapid growth of thin-films of diamond has been observed recently in experiments involving chemical vapor deposition following fragmentation of C_{60} in a microwave discharge [1]. The C_2 molecule has been proposed as the principal growth species, with diamond growth occurring by insertion of C_2 into the C-H bonds of a hydrogen terminated diamond surface. Mechanisms for growth on the diamond surface, with dicarbon (C_2) as the growth species, have been examined using using ab initio and semi-empirical quantum mechanical methods. These calculations have provided information on the intermediates, reaction energies and activation energies of various possible reaction pathways for addition of C_2 to a diamond surface. Clusters of 18 and 48 carbon atoms terminated by hydrogen atoms are used to model the diamond surface in these calculations.

[1]D. M. Gruen, S. Liu, A. R. Krauss, and X. Pan, J. Appl. Phys. 75, 1758 (1994)

Invited Papers

9:00

W1B 3 Diamond Nucleation and Growth by Chemical Vapor Deposition.

JOHN ANGUS, *Chemical Engineering Department, Case Western Reserve University Case Western Reserve University, Cleveland, OH 44106-7217*

The growth of diamond thin films at low pressures, where diamond is metastable, is one of the most exciting developments in materials science of the last two decades. However, low growth rates and poor quality currently limit applications. Diamond growth is achieved by a variety of processes using very different means of gas activation and transport. Generalized models, coupled with experiments, show how process variables, especially pressure, gas activation temperature, characteristic diffusion length, and source gas composition, influence diamond growth rates and diamond quality. The modeling is sufficiently general to permit comparison between growth methods. The models indicate that typical processes, e.g., hot-filament, microwave and thermal plasma reactors, operate at pressures where concentrations of atomic hydrogen, [H], and methyl radicals, [CH3], reach maxima. The results strongly suggest that the growth rate maxima with pressure arise from changes in the gas phase concentrations rather than changes in substrate temperature. The results also suggest that, at one atmosphere pressure using only hydrocarbon chemistry, growth rates saturate at gas activation temperatures above 5000 K. Models of defect incorporation indicate that the amount of sp2, non-diamond material incorporated in the diamond is proportional to [CH3]/[H] and therefore can be correlated with the controllable process parameters. The unusual and interesting connection between diamond nucleation and growth with graphitic, sp2, precursors will be explored.

Contributed Papers

9:30

W1B 4 Deposition of Diamond-Like Carbon Film Using RF Plasma Enhanced CVD foran Anti-Reflection Layer on Polarizers in TFT LCD Display Y.K. LEE, K.C. PARK, K.W. LEE, Y.K. LEE, J.W. LEE, H.B. LEE, K.B. KIM, *Image and Media Lab. LG Electronics Inc., Woomyeon-Dong 16, Seocho-Gu, Seoul, Korea* This paper describes the deposition of diamond-like carbon (DLC) film using RF plasma enhanced CVD for an anti-reflection layer on polarizers in TFT LCD display. The materials of polarizers in TFT LCD display are polymers, which are easily scratched. They need anti- reflection coating for using the LCD outside under sunlight. The DLC film has following properties : mechanically hard, chemically inert and optically transparent over visible light range. DLC film was deposited on some sublayers on polarizer by using RF plasma enhanced CVD method considering the trade-off between low optical absorption and hardness of DLC film with increasing the quantity of hydrogen. The RF plasma enhanced CVD method is suitable for larger substrates and economical to deposit DLC film. We got good results on them by measuring the optical properties from spectroscope and mechanical properties from scotch tape test : 0.4 absorption over visible light range, chemical inert and scratch resistant.

9:45

W1B 5 Heavy-Ion Radiation-Induced Diamond Formation in Carbonaceous Materials T. L. DAULTON, *Argonne National Lab., Argonne IL* M. OZIMA, *U. of Tokyo, Bunkyo-Ku, Tokyo 113, JAPAN* The feasibility of a radiation-induced diamond formation (RIDF) mechanism is demonstrated by the observation of nanodiamonds in carburanium, a U-rich fine-grained, coal-like assemblage containing amorphous carbonaceous material of Precambrian age from North Karelia, Russia. This mineral deposit represents an ideal natural environment for RIDF because the carbonaceous grains present have received a high fluence of energetic particles over a geological time scale. Fragments of carburanium were subjected to acid dissolution treatments to isolate any diamond present. Transmission electron microscopy on these acid residues identified 500 nm polycrystalline diamond aggregates. This observation and estimates of formation efficiencies supports the hypothesis that diamond can form in carbonaceous material irradiated by U decay fragments. Diamond concentration in bulk carburanium is #197# 30 ppm indicating that the RIDF efficiencies might be relatively low as compared to the competing formation of graphite; the acid treatment was an essential key in the recovery of diamond in carburanium. This fact could contribute to the lack of observation of diamond in well- studied ion-implanted carbons. Experiments to synthesize nano-diamonds by heavy-ion irradiation are scheduled for late 1996 at ANL's accelerator ATLAS.

SESSION W2A: PLASMA AND SURFACE CHEMISTRY IN MATERIALS PROCESSING

Wednesday morning, 23 October 1996; Auditorium at 10:30; Kostas Giapis, Cal. Inst. of Technology, presiding

Invited Papers

10:30

W2A 1 Models of Gas-phase and Surface Chemistry for Plasma Enhanced Chemical Vapor Deposition.

ELLEN MEEKS, *Sandia National Laboratories*

Plasma enhanced chemical vapor deposition for inter-metal-layer gap-fill processes are increasingly important in semiconductor device manufacture, as the devices include increasing numbers of metal layers with decreasing linewidth and spacing. Optimization of these processes requires knowledge of the microscopic consequences of variations in reactor operating conditions. Topographical simulation can address the gap-fill performance of a depositing film, but the predictive capabiliities are limited by the ability of the model user to accurately supply ion and radical fluxes at a gas/surface interface. Critical to determining this information are the chemical kinetics between gas-phase species and the deposition surfaces. Recent improvements and extensions to the CHEMKIN and Surface CHEMKIN software allow general inclusion of detailed chemical mechanisms in plasma simulations and in models of plasma-surface interactions. In the results presented here [1], we have used a CHEMKIN-based well mixed reactor model of a high-density $SiH_4/O_2/Ar$ plasma to predict and characterize species fluxes, oxide-deposition rates, and ion-milling rates on a flat surface. These calculated rates can be used as direct input to a topographical simulator. The gas-phase chemistry in the plasma reactor model is comprised of electron impact reactions with silane, oxygen, hydrogen, and argon, as well as neutral radical recombination, abstraction, and oxidation reactions. The surface reaction mechanism contains four classes of reactions: silicon-containing radical deposition, radical abstraction, ion-induced desorption, and physical ion sputtering. We include relative thermochemistry of the surface and gas species to allow reversible reaction dynamics. The plasma model results show good agreement with measured ion densities, as well as with measured net deposition rates.

[1]This work represents a collaboration with R. Larson and P. Ho at Sandia, J. Rey and J. Li at TMA, S. M. Han and E. Aydil of UCSB, and S. Huang at Lam Research Corporation

11:00

W2A 2 Optimization of PECVD Chamber Cleans Through Fundamental Studies of Electronegative Fluorinated Gas Discharges..

JOHN LANGAN, *Air Products and Chemicals, Inc., Allentown, PA.*

The predominance of multi-level metalization schemes in advanced integrated circuit manufacturing has greatly increased the importance of plasma enhanced chemical vapor deposition (PECVD) and in turn in-situ plasma chamber cleaning. In order to maintain the highest throughput for these processes the clean step must be as short as possible. In addition, there is an increasing desire to minimize the fluorinated gas usage during the clean, while maximizing its efficiency, not only to achieve lower costs, but also because many of the gases used in this process are global warming compounds. We have studied the fundamental properties of discharges of NF_3, CF_4, and C_2F_6 under conditions relevant to chamber cleaning in the GEC rf reference cell. Using electrical impedance analysis and optical emission spectroscopy we have determined that the electronegative nature of these discharges defines the optimal processing conditions by controlling the power coupling efficiency and mechanisms of power dissipation in the discharge. Examples will be presented where strategies identified by these studies have been used to optimize actual manufacturing chamber clean processes. [1]

[1]This work was performed in collaboration with Mark Sobolewski, National Institute of Standards and Technology, and Brian Felker, Air Products and Chemicals, Inc.

11:30

W2A 3 Deposition of ultrahard coatings in a plasma environment.

C. DOUGHTY, *Oak Ridge National Laboratory, Oak Ridge TN, 37831*

Hard materials are an area of great technological interest, and deposition in a plasma environment offers enhanced control over a variety of process aspects. These might include the chemical nature and excitation of the depositing species as well as effects due to energetic particle bombardment during nucleation and growth. Non-equilibrium and metastable structures can be realized, including phases impossible to synthesize in the bulk. Key issues relevant to the use of plasmas for the synthesis of thin, hard layers will be reviewed and discussed with examples from several material systems of current interest, including diamond, carbon nitride, and boron-based hard materials. Oak Ridge National Laboratory, managed by Lockheed Martin Energy Research Corp. for the U.S. Department of Energy under contract number DE-AC05-96OR22464.

12:00

W2A 4 Simulation of Ionized Copper Deposition in a Magnetron Sputter-Inductively Coupled Plasma Reactor* MICHAEL J. GRAPPERHAUS, MARK J. KUSHNER, *University of Illinois, Urbana, IL* Post ionization of magnetron sputtered metals by an inductively coupled plasma provides a method to voidlessly fill high aspect ratio features for microelectronics fabrication. These devices are typically powered by three sources: an rf generator for the coils, a dc supply for the sputter source and either an rf or dc power supply to accelerate ions into the substrate. A high fraction of ionized metal atoms (as compared to neutral metal atoms) in the deposition flux has been demonstrated for rf powers of 100s W to kW and sputter powers of 100s W. To investigate the synergism between these power sources on the flux of metal ions to the substrate, A 2-d hybrid model has been developed. The base model consists of an electromagnetics module, an electron Monte Carlo simulation, and a fluid kinetics module. Algorithms for long mean free path transport of sputtered metal atoms, ballistic secondary electron emission, and guiding center kinetic electron transport in the high magnetic fields of the magnetron have additionally been developed. Typical results for copper deposition in Ar/Cu plasmas will be presented. *Work supported by SRC, NSF and the U of Wisconsin ERC.

12:15

W2A 5 Design of a Sputtering Cathode for Binary Alloys Deposition in Plasma Source Ion Implantation SHAMIM MALIK, ROBERT BREUN, PAUL FETHERSTON, KUMAR SRIDHARAN, JOHN CONRAD, *University of Wisconsin-Madison* In Plasma Source Ion Implantation (PSII)1,2 a target is immersed in a plasma and pulse biased to a high negative voltage (50kV). Ions are injected into the near surface of target material under the influence of the electric field. In order to produce Ion Assisted Deposition (IAD) films in PSII, materials of interest are sputtered using DC or RF bias and up to 20 kV negative bias pulses are applied while depositing films. We have performed deposition of titanium aluminum nitride (TiAlN) films using a perforated aluminum cathode stacked on a planar titanium cathode. Design characteristics of the sputtering cathodes as a function of the ratio of material area, plasma parameters, and stoichiometric deposition rates have been evaluated. Analysis of these results will be presented. * This work was supported by NSF. No DMI-9528746, US-Army No. DAALH 03-94-G-0283 1 J. R. Conrad, *et al.* J. Appl. Phys.62, 4951 (1987). 2 M.M. Shamim *et al.*, J. Vac. Sci. Technol. 12(2), 843 (1994).

SESSION W2B: ELECTRON SCATTERING
Wednesday morning, 23 October 1996
Lecture Hall at 10:30
Russell Bonham, Illinois Inst. of Tech., presiding

10:30

W2B 1 Cross Section Results for Electron Excitation out of the 2^3S Level of Helium*GARRETT A. PIECH, JOHN B. BOFFARD, MARK E. LAGUS, L. W. ANDERSON, CHUN C. LIN, *University of Wisconsin, Madison*We have used two independent experiments to measure cross sections for electron excitation out of the 2^3S level of He into the n = 2, 3, 4, and 5 triplet levels. The first experiment uses a hollow cathode as its source of metastable He, and produces a metastable target density of 10^8cm^{-3}. However, due to ground state He contamination of the beam, it is limited in energies to below 20 eV. The second experiment uses charge exchange of a fast He^+ beam with cesium to produce a metastable target density of 10^6cm^{-3}. This target is relatively free of ground state contamination, and thus with this experiment we can extend our measurements to up to 1 keV. The two experiments are indpendently calibrated, and they agree quite well in both the absolute magnitude of the cross sections and in the shapes of the excitation functions that they observe. The trends and patterns of the results will be discussed and comparison with theoretical calculations will be made.

*Work supported by the National Science Foundation.

10:45

W2B 2 Measurement of Electron Impact Excitation Cross Sections out of the metastable levels of Argon* JOHN B. BOFFARD, GARRETT A. PIECH, MARK F. GEHRKE, MARK E. LAGUS, L. W. ANDERSON, CHUN C. LIN, *University of Wisconsin-Madison*Electron-impact cross sections for excitation out of the argon metastable levels ($3p^54s$ J=0 and J=2) into levels of the $3p^54p$ configuration have been measured using the optical method. We use two different metastable sources. A hollow cathode discharge is used for high signal to noise relative measurements at energies less than the onset for excitation from the ground state. A second apparatus uses charge exchange of 2.1 keV Ar^+ with cesium to produce a primarily Ar* beam with a relatively low metastable number density of 10^5 atoms/cm^3. The fast beam is used for high energy absolute measurements for selected levels. In general, the excitation process is characterized by very large cross sections having broad shapes as a function of electron energy (similar to the $2^3S \rightarrow 2^3P$ cross section for He*). The cross section for excitation into the $3p^54p$ J=3 level ($2p_9$ in Paschen's notation) is 35×10^{-16} cm^2 at 10 eV. The exceptions to this general behavior are the two J=0 levels ($2p_1$ and $2p_5$) which have sharply peaked excitation functions.

*Work supported by the National Science Foundation

11:00

W2B 3 Measurement of Cross Sections for Electron-Impact Excitation of Argon by Fourier Transform Spectroscopy*J. ETHAN CHILTON, JOHN B. BOFFARD, CHUN C. LIN, *University of Wisconsin, Madison*We report absolute measurements of electron-impact excitation cross sections from the ground level to the ten levels of the $3p^54p$ configuration of argon, between 0 and 200 eV incident electron energy. We determine apparent excitation cross sections by measuring the optical cross sections for the $3p^54p \rightarrow 3p^54s$ emission lines. The cascade corrections are found by measuring the optical cross sections for the $3p^55s \rightarrow 3p^54p$ and $3p^53d \rightarrow 3p^54p$ infrared lines in the range of 0.9 to 1.7 μm with a Fourier transform weak emission spectrometer. This cascade correction is then subtracted from the apparent excitation cross sections to yield direct excitation cross sections. While the measured optical cross sections are found to vary with pressure in the regime of 0.1 to 4 mTorr, the direct excitation cross sections

resulting from cascade subtraction are not pressure dependent. These pressure effects are understood within the framework of a radiation reabsorption model. The excitation functions for the different transitions show considerable variation in shape.

*Supported by the Air Force Office of Scientific Research.

11:15

W2B 4 Superelastic Scattering from Metastable State-Selected Rare-Gas Atoms B.G. BIRDSEY, H. BATELAAN, M.E. JOHNSTON, T.J. GAY, *University of Nebraska, Lincoln, NE 68588-0111*Superelastic scattering is the time reversal of any inelastic scattering process where the excitation and photon emission can be treated as discrete events. Therefore, superelastic scattering can be used to probe excitations from the ground state to metastable states. Ultimately, we will use polarized electrons and prepared metastable states to determine parameters related to coherence and correlation such as <Lperp>, which cannot be determined using electron-photon coincidence experiments because of the extremly long lifetimes of the excited state. The present apparatus is in a colliding beam configuration, which consists of a high flux (5.4 x 10^{14} Kr^* /s-sr) metastable rare-gas source and an unpolarized electron gun, which will soon be replaced with a GaAs polarized electron gun. We have recently made much progress in increasing the signal to noise ratio by using apertures to reduce the volume which can directly produce counts to the interaction region. Recent results will be discussed. This work is supported by the NSF Grant PHY-9201289.

11:30

W2B 5 Measurement of Electron Impact Excitation Cross Sections of the Xenon Atom at Various Pressures*JOHN T. FONS, J. ETHAN CHILTON, SUNGGI CHUNG, CHUN C. LIN, *University of Wisconsin, Madison*In an electron-beam experiment at low gas densities, the optical emission cross sections obtained by dividing the measured intensity of the resultant emission by the target gas pressure and electron beam current are expected to be independent of gas pressures as is usually the case when the measurements are conducted at pressures below a few mTorr and no significant secondary processes are present. Many of the xenon emission cross sections exhibit pressure dependence at much lower pressures. Our measured cross sections for emissions from the $5p^5 6p$ configuration show pressure dependence down to pressures as low as 0.05 mTorr. Measurements of the optical emission cross sections for transitions of the types $5p^5 ns \rightarrow 5p^5 6p$ and $5p^5 nd \rightarrow 5p^5 6p$ and their pressure dependence have been made. The results indicate that much of the observed pressure dependence of the optical cross sections for emission from the $5p^5 6p$ configuration is due to cascade.

*Work done under the support of the U.S. Department of Commerce, National Institute of Standards and Technology.

11:45

W2B 6 Electron Impact Excitation of the $3d^9 4s^2\ ^2D$ State in Copper V SUVAROV, P.J.O. TEUBNER, *Dept. of Physics, The Flinders University of South Australia, GPO Box 2100, Adelaide, Australia, 5001*A stepwise laser excitation technique has been used to probe the excitation of the $D_{3/2}$ state in copper by electrons over the energy range from 1.6eV to 5eV. A broad resonance is observed at about 3eV. This resonance had been predicted by the close coupling calculation of Scheibner *et al.* [1] but at a different energy. The observed cross section at the peak of the resonance is significantly larger than that predicted by the theory.

[1]K.F. Scheibner, A.V. Hazi and R.J.W. Henry, Phys. Rev. A 35, 4869 (1987)

12:00

W2B 7 Studies of Dissociative Recombination Final Product States in a Argon Glow Discharge CARLOS AVILA, GESSLER HERNANDEZ, J.W. SHELDON, K.A. HARDY, *Physics Department, Florida International University*J.R. PETERSON, *SRI International*We measured the yield the of 4s final product state atoms from the dissociative recombination (DR) reaction as a function of applied magnetic field in a argon glow discharge. The DR reaction takes place in a low voltage, low pressure hot cathode discharge. The final product states are identified by time of flight (TOF) spectroscopy. The glow discharge is in a axial magnetic field that was maintained between 0 and 400 Gauss. The yield of metastable atoms and 4s final product state atoms was measured as a function of applied magnetic field. The yield of metastable atoms exhibits saturation effects. Preliminary results indicate that the yield of 4s final product state atoms does not exibit saturation similar to the metastable states at magnetic fields of up to 400 Gauss.

12:15

W2B 8 Absolute differential and integral cross sections for electron impact excitation of the $A^2\Sigma^+$, $b^4\Sigma^-$, $C^2\Pi$ and D $^2\Sigma^+$ electronic states of NO M.J. BRUNGER, P.J.O. TEUBNER, B. MOJARRABI, L. CAMPBELL, M. A. GREEN, *Dept. of Physics, The Flinders University of South Australia, GPO Box 2100, Adelaide, Australia, 5001*D.C CARTWRIGHTJ, *Theoretical Divisions, Los Alamos National Labs, Los Alamos, New Mexico, USA, 87545*We present new DCS and ICS results for low energy (E <= 50eV) electron inpact excitation of some of the lower lying electronic states of NO. These results are discussed and compared, where possible, with those of other experimental measurements and theoretical calculations.

12:30

W2B 9 Future opportunities for experimental and theoretical studies into low energy electron-molecule scattering processes S. J. BUCKMAN, *MElectron Physics Group, Australian National University, Canberra, ACT, Australia, 0200*M. J. BRUNGER, *Physics Dept., Flinders University of SA, GPO Box 2100, Adelaide, SA, Australia, 5001*In the course of up-dating the seminal review of Trajmar and colleagues [1] for low energy electron-molecule collision cross sections, we have chanced upon several scattering systems for which further experimental (beam and swarm) and theoretical investigations are urgently required. The available absolute cross section data for these targets, including CH4, N2O and CO2, will be examined in detail, specific experiments and calculations proposed and a rationale for these experiments and calculations given.

[1]S. Trajmar, D.F. Register and A. Chutjian, Phys. Rep. 97 (1983), 219.

➢➢➢➢➢➢➢➢➢➢➢➢➢

SESSION W3A: INDUCTIVE COUPLING AND HEATING IN LOW PRESSURE PLASMAS

Wednesday afternoon, 23 October 1996; Auditorium at 13:30; Greg Hebner, Sandia National Laboratory, presiding

Invited Paper

13:30

W3A 1 The Physics and Potential Development of Inductively Coupled Reactors.
JOHN H. KELLER, *IBM, Bldg. 630-EL1, Hopewell Jct., NY 12533*

Inductively Coupled Plasmas have become one of the dominant high density plasma sources for etching. More varied etch sources are presently being developed and inductive systems for high density plasma deposition are also being developed. In addition helicon inductive sources are being developed in single loop and spiral configurations. In the future these two fields may merge to combine the optimum features of both systems. This paper will discuss the physics of this new trend and possible configurations of future etching systems aimed at higher aspect ratios, selectivity and rate.

Contributed Papers

14:00

W3A 2 Investigation of Asymmetries in Inductively Coupled Plasma Etching Reactors Using a 3-Dimensional Hybrid Model* MARK J. KUSHNER, MICHAEL J. GRAPPERHAUS, *University of Illinois, Urbana, IL 61801* Inductively Coupled Plasma (ICP) reactors have the potential for scaling to large area substrates while maintaining azimuthal symmetry or side-to-side uniformity across the wafer. Asymmetric etch properties in these devices have been attributed to transmission line properties of the coil, internal structures (such as wafer clamps) and non-uniform gas injection or pumping. To investigate the origins of asymmetric etch properties, a 3-dimensional hybrid model has been developed. The hybrid model contains electromagnetic, electric circuit, electron energy equation, and fluid modules. Continuity and momentum equations are solved in the fluid module along with Poisson's equation. We will discuss results for ion and radical flux uniformity to the substrate while varying the transmission line characteristics of the coil, symmetry of gas inlets/pumping, and internal structures. Comparisons will be made to expermental measurements of etch rates. *Work supported by SRC, NSF, ARPA/AFOSR and LAM Research.

14:15

W3A 3 Capacitive Effects in Inductively Coupled Plasma Reactors PETER VITELLO, NICHOLAS TISHCHENKO, GERGORY PARKER, *LLNL, Livermore, CA* MICHAEL BRANCH, *Applied Materials, Santa Clara, CA* The physics of industrial plasma reactors operating with highly reactive gases is poorly understood. For optimum operation of such systems a more thorough understanding of the discharge physics and plasma chemistry must be achieved. With this goal in mind we have developed the two-dimensional time-dependent computer simulation code, INDUCT95. INDUCT95 has the ability to accurately and efficiently treat a wide range of plasma discharges including glow discharges, rf inductively coupled discharges, and rf capacitively coupled discharges. Comparison between simulations and experimental discharges in argon, chlorine, nitrogen, and other gases has shown excellent agreement. With current computer technology two-dimensional simulations are now beginning to be practical. We present results based upon the LLNL large area inductively coupled discharge experiment. The effects of rf coil capacitively coupling and rf substrate biasing are shown for argon and chlorine plasmas. Capacitive coupling leads to modifications in the time averaged plasma potential and enhanced ion energy losses. This results in significant variations in plasma spatial density profile, and in the ion flux and energy profiles at the substrate. Strong capacitive coupling may also generate a transition between the inductive mode and the capacitive mode of operation.

14:30

W3A 4 Simulations of Feedback Control Schemes for Inductively Coupled Plasma Sources NAOKI YAMADA, PETER L.G. VENTZEK, Y. SAKAI, *Hokkaido University, Dept. of Elect. Eng., Sapporo 060 Japan* H. DATE, *Hokkaido University, College of Med. Tech., Sapporo 060 Japan* H. TAGASHIRA, K. KITAMORI, *Hokkaido Institute of Technology, Sapporo 065 Japan* Real-time control of etch uniformity, selectivity, and rate are becoming necessary as feature sizes decrease and wafer sizes increase. Results from a computer model of a feedback control scheme for a planar coil inductively coupled plasma source will be presented. The simulation is a hybrid arrangement of a plasma dynamics model, a well-stirred chemistry model, a circuit model and an etch rate model. Results will be presented for multi-coil, multi-frequency, and pulsed mode operation in chlorine plasmas. Multi-coil, multi-frequency operation may allow control of plasma uniformity and composition whereas pulse-mode operation is used to enhance selectivity and reduce charge damage. The observability of control variables will be addressed as will the limitations of the model and the control concept.

14:45

W3A 5 Inductive Electron Heating Revisited MICHEL TUSZEWSKI, *Los Alamos National Laboratory, Los Alamos, NM 87544* The induced radio frequency (rf) magnetic fields of a low-frequency inductively coupled plasma (ICP) are measured and modeled. The fields penetrate deep into the discharges (argon and oxygen, 5 - 50 mTorr, 0.46 MHz, 0.5 - 1.5 kW), in contrast with existing predictions of field decay within a thin skin layer. Stochastic (anomalous) effects are unimportant for these data. Fluid calculations show that the enhanced rf field penetration is due to a substantial reduction of the plasma conductivity by the induced rf magnetic fields whenever the electron cyclotron frequency exceeds the rf frequency and the electron-neutral collision frequency. This condition is satisfied for many low-pressure ICPs. Hence, the induced rf magnetic fields must be included in ICP models to predict electron heating and the resulting plasma transport.

15:00

W3A 6 Influence of magnetic field on the structure in ICP (Modeling and CT measurement-) T. MAKABE, K. IYANAGI, A. OKIGAWA, N. NAKANO, *Keio University, Yokohama* The sustaining mechanism of ICP is of great interest to us from the physical viewpoint of the electron transport in both electric and

magnetic fields in gases/plasmas. Various kinds of modelings have been successful in developing an ICP reactor. However, there is no consideration of the effect of magnetic field on the electron transport except Refs.[1 2] Recently, we have developed a robot assisted optical emission tomography.[3] The sliced-2D image of the net excitation rate at any plane in ICP exhibits its ability to investigate the detailed plasma structure. In this work, we have investigated the effect of reduced **E**-drift, appearance of **E**× **B**-drift and the change of ionization rate etc., even under a weak **B**-field on the ICP structure by both the RCT model and CT measurement. Also the influence of metastable molecules on the ICP structure is discussed.

[1]K.Kondo, H.Kuroda and T.Makabe,Appl.Phys.Lett.65,31 (1994).
[2]K.Kamimura, T.Makabe, K.Iyanagi and N.Nakano, J.Phys.D (submitted).
[3]A. Okigawa, T. Makabe, Z. Lj. Petrovic, etal, Jpn. J. Appl. Phys. 35, 1890 (1996).

15:15

W3A 7 A Comparative Study of Models for Non-Collisional Heating in Inductively Coupled Plasmas* SHAHID RAUF, MARK J. KUSHNER, *University of Illinois, Urbana, IL 61801* It has been acknowledged that non-collisional heating plays an important role in low pressure high plasma density inductively coupled plasma (ICP) reactors for etching and deposition. A number of computational techniques have been developed to address this phenomena. We have recently introduced a self-consistent method to couple plasma dynamics with the electromagnetic fields by directly computing electron current using a Monte Carlo scheme in a hybrid model.[1] It takes into account all pertinent heating and can, in principle, be used with arbitrary plasma chemistries and geometries. Other techniques use an effective collision frequency (computed using a phenomenological model),[2] an effective conductivity (computed using a simplified kinetic model), or correct collisionally derived power deposition. In this paper, we present a comparative study of these methods and discuss their relative advantages and disadvantages. This comparison is conducted using simulations of Ar and Ar/O_2 plasmas in several reactor configurations for a range of gas pressures and powers. [1]S. Rauf and M. J. Kushner, submitted to J Appl. Phys. [2]V. Vahedi *et al.*, J. Appl. Phys. **79**, 1446 (1995). *Work supported by NIST, SNLA/Sematech, NSF, SRC and UW-ERC.

15:30

W3A 8 "Politically-Incorrect" Electron Behavior in Low Pressure RF Discharges VALERY GODYAK, *OSRAM SYLVANIA INC* VLADIMIR KOLOBOV, *Univ. of Houston, Houston TX* The main interaction of plasma electrons with electromagnetic fields for bounded plasma of an rf discharge occurs in the vicinity of its boundaries (in the rf sheath of a capacitive rf discharge and in the skin layer of an inductive one). On the other hand, due to plasma inhomogeneity, a dc ambipolar field is always present in the bounded plasma. in low pressure discharges the ambipolar potential well captures low energy electrons within the discharge center while high energy electrons freely overcome the ambipolar potential and reach the plasma boundaries where heating takes place. Being segregated in space, low energy electrons are discriminated from participation in the heating process. When Coulomb interaction between low and high energy electron groups is weak, their temperatures appear to be essentially different (a low energy peak on the EEDF). In this presentation we present theoretical and experimental evidence of such an apartheid in the low and high energy electron populations of the EEDF in rf discharge and we outline discharge conditions where such abnormal EEDF behavior is possible.

SESSION W3B: LASER DISCHARGES AND ABLATION
Wednesday afternoon, 23 October 1996; Lecture Hall at 13:30; Ken Stabler, SRI, presiding

Invited Papers

13:30

W3B 1 Radio-Frequency Discharges at Moderate Pressures and CO2-Lasers with RF Excitation.
YURI RAIZER, *Dept Physical Gasdynamics of The Institute for Problems in Mechanics Russian Acad.Sci*

Lasers with rf excitation belong to the newest generation of technological CO2-lasers.They have a number of advantages as compared with dc current lasers. But rf glow discharge is more complicate phenomenon than the dc one.The understanding of rf discharge physics is a necessary step for it successful application.The important for laser physical points,choice of discharge mode,frequency dependence of parameters are treated.The effect of normal current density for rf alfa mode that determines the frequency dependence of power is considered. Its physical nature, results of experiments,theory and modeling are given. The reason and conditions of the transition to gamma rf mode unsuitable for slit and waveguide lasers are discussed as well as effect of dielectric cover of electrodes. Various types of rf lasers are considered

14:00

W3B 2 Plasma Ionization Dynamics of Energy Beam Ablation of Materials.
R.M. GILGENBACH, *Intense Energy Beam Interaction Laboratory, Nuclear Engineering and Radiological Sciences Dept., University of Michigan, Ann Arbor, MI 48109-2104*

Species-resolving diagnostic experiments have been performed on plasmas generated by three energy sources: 1) KrF laser ablation, 2) Laser ablation-assisted-plasma-discharges (LAAPD), and 3) electron beam ablation. Dye-laser-resonance diagnostics (ultraviolet-resonant-interferometry and resonance-absorption-photography) and emission spec-

troscopy have been employed to study the ionization dynamics of ablated metals for KrF laser (248nm, < 1 J, 40 ns) ablation versus LAAPD. Plume ion versus neutral line densities, expansion velocities, and temperatures have been characterized. Results demonstrate that the ionization ratio (ni/nn) of a laser-ablated Fe plume can be increased by up to a factor of 5 by applying a discharge of 3,600 V and 680A. More recent experiments have been conducted on electron beam ablation of metal (Fe) utilizing optical spectroscopy diagnostics. The electron beam is generated by a channelspark at parameters: 20 kV, 1.5 kA, 200 ns. Plasma plume characteristics and energy absorption mechanisms in metals are being compared between lasers and electron beams [1 2].

[1]In collaboration with J.S. Lash, S.D. Kovaleski, H.L. Spindler, W.E. Cohen, J.I. Rintamaki, L.K. Ang, and Y.Y. Lau
[2]Research supported by National Science Foundation grants CTS–9108971 and CTS-9522282

14:30

W3B 3 Dynamics of Laser Ablation Plasmas in Vacuum and Background Gases: Effects of Scattering and Interplume Collisions on Velocity Distributions used for PLD Film Growth.
DAVID GEOHEGAN, *Solid State Division, Oak Ridge National Laboratory*

Pulsed laser deposition (PLD) uses laser ablation of a solid target to accelerate atoms and ions in a high-density plasma to superthermal kinetic energies (typically 10-100 eV). These high kinetic energies have proven essential for the non-equilibrium formation of thin films of new ultrahard metastable phases, such as the synthesis of amorphous diamond (ta-C, tetrahedrally-coordinated, amorphous carbon) from the laser ablation of pyrolytic graphite in vacuum. However in low-pressure background gases (< 200 mTorr, often employed during PLD), the kinetic energy of the plume atoms is moderated by collisions with the background gas. In this talk, fundamental collisional phenomena relevant to PLD film growth in vacuum and background gases will be described using a combination of fast plasma diagnostics. Optical emission spectroscopy, optical absorption spectroscopy, fast Langmuir probe analysis, and species-resolved gated-ICCD fast photography are combined to permit an understanding of the importance of gas dynamic effects on the time-of-flight distributions of species arriving during the deposition of thin films in both vacuum and background gases. Comparative diagnostics of the ArF- and KrF-laser ablation of pyrolytic graphite will be presented to illustrate the role of laser wavelength and intensity on the species and kinetic energies responsible for optimized ultrahard amorphous diamond thin films. Evidence for interplume collisions and clustering during propagation of the graphite plume in vacuum will be shown. When penetrating a background gas, diagnostics indicate that the plume flux arriving for film growth divides into distinct "fast" and "slow" velocity distributions at certain distances. The fast component is target material which penetrates the background gas in accordance with a scattering model, while the slow component is material which has undergone momentum-changing collisions with the background gas, or with other plume atoms. This 'plume-splitting' effect will be described for several materials along with the results of several computer simulations. An understanding of this effect is highly relevant to understanding cluster formation and aggregation by ablation into background gases, a topic of current practical importance for the current synthesis of nanocrystalline and composite materials. Imaging of cluster formation during graphite ablation into inert gases will be presented.

Contributed Paper

15:00

W3B 4 A Simulation of Laser Ablation During the Laser Pulse MOTOYUKI SUZUKI, PETER L.G. VENTZEK, Y. SAKAI, *Hokkaido University, Dept. of Elect. Eng., Sapporo 060 Japan* H. DATE, *Hokkaido University, College of Med. Tech., Sapporo 060 Japan* H. TAGASHIRA, K. KITAMORI, *Hokkaido Institute of Technology, Sapporo 065 Japan* Charge damage considerations in plasma assisted etching are prompting the development of neutral beam sources. Already, anisotropic etching of has been demonstrated by neutral beams generated by exhausting heated ecthing gases into vacuum via a nozzle. Laser ablation of condensed etching gases may also be an attractive alternative means of generating neutral beams. Laser ablation coupled with electrical breakdown of the ablation plume may afford some degree of control over a neutral beam's dissociation fraction and ion content. Results from a Monte Carlo simulation of the laser ablation plume as it expands into vacuum at time-scales during the laser pulse will be presented. The model includes both heavy particle interactions and photochemistry. In particular, the influence of the initial particle angular distribution on the beam spread will be demonstrated as will the relationship between laser beam energy and initial ionization and dissociation fraction.

SESSION WPA: DISCHARGE PHENOMENA POSTER SESSION
Wednesday afternoon, 23 October 1996
Alcove A at 15:45
Steve Pratt, ANL, presiding

WPA 1 Collisional radiative model for surface-wave helium discharges at atmospheric pressure. I. PERES, J. MARGOT, *Dept de Physique, Universite de Montreal, Canada* L.L. ALVES, C.M. FERREIRA, *IST, Lisbon Tech. U., Portugal* J. HUBERT, *Dept de Chimie, Universite de Montreal, Canada* Atmospheric pressure helium discharges present a major interest as atomization, excitation and ionization sources in atomic spectrochemical analysis of trace elements and have been widely investigated experimentally. Very few theoretical studies have been reported so far. In the present study, the characteristics of discharges sustained at 2.45 GHz in capillary tubes are obtained from a collisional-radiative model. This model was adapted from the model previously presented by Alves *et al.* [1],which involves a detailed description of the electron kinetics. Typically, bulk electron energy distribution functions are shown to be Maxwellian functions with temperature around 1.75 eV. Other discharge characteristics (excited states and ion populations, power balance, etc), which help

gain insight into the mechanisms governing power losses in such discharges, are also shown to be in good agreement with experimental data.

[1]L.L. Alves, G. Gousset, C.M. Ferreira, J. Phys. D 25, 1713 (1992)

WPA 2 A Plasma Purification Method for Plasma Source Ion Implantation Doping of Semiconductors THOMAS SNODGRASS, DINA ARNOTT, MAURA JENKINS, LEON SHOHET, JOHN BOOSKE, *Engineering Research Center for Plasma-Aided Manufacturing, University of Wisconsin Madison* MARK KUSHNER, *Engineering Research Center for Plasma-Aided Manufacturing, University of Illinois Urbana* Using Plasma Source Ion Implantation (PSII) to create the shallow source and drain structures required for next generation devices may be a necessity [1]. For example, future devices are predicted to require heavy metal doses be kept less than 3×10^9 atoms per square centimeter[2]. Plasma purification is done using ion cyclotron resonance to selectively expel unwanted ions from the plasma where they are neutralized upon collision with the chamber wall and no longer an implantation hazard[3]. With a computer simulation we determine the necessary field strengths and uniformity for plasma purification, cleaning efficiency and frequency/mass resolution of the method. Initial results to evaluate the theory using mass spectrometry will also be shown. Work supported by the National Science Foundation under Grant EEC-8721545.

[1]Semiconductor Industry Association, The National Technology Roadmap for Semiconductors, (1994).
[2]N. Natsuaki, T. Kamata, K. Kondo, Y. Kureishi (1995), Nucl. Inst. Meth. Phys. B, 96, 62.
[3]J. L. Shohet, E. B. Wickesberg, M. J. Kushner (1994), J. Vac. Sci. Technol. A, 12(4), 1380

WPA 3 Detection of Atomic Hydrogen in Processing Plasmas using Multi-Photon Laser-Induced Fluorescence K. MURAOKA, K. MIYAZAKI, T. KAJIWARA, K. UCHINO, T. OKADA, M. MAEDA, *Kyushu University, Japan* Although an attempt has been made previously to measure the atomic hydrogen density in a silane plasma, using Lyman-beta two-photon (2 x 205 nm) laser-induced fluorescence, this measurement was impossible due to the generation of hydrogen atoms by laser-induced dissociation of Si_2H_6 molecules the discharge [1]. This paper describes a successful measurement of the hydrogen density, using two-photon excitation from the ground state to the n=2 state at 243 nm, simultaneous excitation from the n=2 state to the n=3 state at 656 nm and then observation of fluorescence at 656 nm. Initially, the influence of laser-induced dissociation of molecules and radicals in the silane plasma on the measurement of hydrogen atoms was investigated. It was found that a fraction of the measured atomic hydrogen density came from the laser-induced dissociation of SiH_3 radicals. Then, taking into account the ef! fect of the laser-induced dissociation of SiH_3 radicals, we determined the absolute density of hydrogen atoms in the silane plasma.

[1]K. Miyazaki *et al.*, J. Vac. Sci. Technol. A Vol. 14, 125 (1996)

WPA 4 Electron Density and Temperature in a Neutral Loop Discharge Plasma T. SAKODA, M.D. BOWDEN, K. UCHINO, K. MURAOKA, *Kyushu University, Japan* M. ITOH, T. UCHIDA, *ULVAC Japan Ltd.* The neutral loop discharge (NLD) plasma has been proposed as a new plasma source. This source is expected to realize very uniform processing plasma with a large area because the diameter and position of the neutral loop can be actively controlled. This study aims to reveal electron behavior around the neutral loop based on unambiguous measurements of electron density and temperature made using laser Thomson scattering. Measurements were made in an argon plasma at pressures of several mTorr. Radial profile measurements indicated that the electron temperature had a peak on the neutral loop and, in contrast, the electron density had a peak at a position radially inward from the neutral loop. These facts suggest that charged particles are produced by electron impact ionization of argon atoms on the neutral loop and then flow radially inward.

WPA 5 Measurement of plasma velocity using UV spectrometer* M.K. VIJAYA SANKAR, E. EISNER, A. GAROFALO, T.H. IVERS, R. KOMBARGI, M.E. MAUEL, D. MAURER, D. NADLE, G.A. NAVRATIL, M. SU, E. TAYLOR, Q. XIAO, *Columbia University* A scanning monochromator has been installed to measure the rotation induced doppler shift at the CV emission line (2271 Å) in HBT-EP tokamak. Wavelength scanning is accomplished by oscillating a mirror in the light path at about 1 kHz to scan 2 Å from the center line. Two quartz-enveloped photomultiplier tubes will simultaneously measure the doppler shifts along and opposite to the direction of the toroidal plasma current. The estimated system resolution of the toroidal rotation velocity is 1 km/s in 1 ms intervals. Measurement of the radial profile of the toroidal velocity is also possible by linearly translating the associated focussing optics. Results from the initial measurements will be presented.

*Work supported by US DoE Grant: DE-FG02-86ER-53222

WPA 6 Application of Degenerate Four Wave Mixing as a Diagnostic Method for Processing Plasmas M.D. BOWDEN, H. TAGAWA, S. TOKONAMI, K. MURAOKA, *Kyushu University, Japan* Degenerate four wave mixing (DFWM) is a non-linear optical technique in which three laser beams of the same frequency are mixed in a medium to produce a fourth beam. The frequency at which the signal beam is generated and its intensity provide information about the medium [1]. In this paper, we report measurements made with DFWM in medium pressure discharges with the aim of determining the feasibility of using DFWM as a diagnostic for processing discharges. The Doppler-free nature of the DFWM signal beam means that it is possible to measure frequency very accurately using this method. We used DFWM to make measurements in a helium discharge, using transitions from both singlet and triplet metastable levels. The frequency of some of these transitions is affected by the electric field in the discharge and accurate measurement of this resonant frequency allows the electric field to be determined. The effect of atomic diffusion on the DFWM signal strength for these transitions has been studied and the feasibility of using DFWM as an electric field diagnostic will be discussed.

[1]Y.R. Shen, IEEE J. Quant. Electron. Vol. QE-22, p1196 (1986)

WPA 7 C_2 Swan Band Absorption in a Microwave Plasma A. N. GOYETTE, Y. MATSUDA*, L. W. ANDERSON, J. E. LAWLER, *Physics Department, University of Wisconsin, Madison, WI 53706* We report the observation of the $d\ ^3\Pi_g \rightarrow a\ ^3\Pi_u$ (0,0) vibrational band of the C_2 molecule in absorption and in emission in a microwave discharge. Input gases for the plasma consist of argon, hydrogen, and methane. The mole fraction of methane was varied as a parameter, from 33% to 1 %. The absorption is detected using high sensitivity white-light absorption spectroscopy and column densities of C_2 in the gas phase are calculated. This technique is useful in understanding the contribu-

WEDNESDAY AFTERNOON \ WPA

tion of the C_2 molecule in the gas phase chemistry of a microwave plasma-assisted chemical vapor deposition of diamond, both in the conventional diamond deposition process and in diamond deposition from C_{60} clusters. *Dept. of Electrical Engineering and Computer Science, Nagasaki University, Japan

[1]Supported by the Army Research Office.

WPA 8 Rotational Temperature in a N_2 Positive Column Discharge J. R. PECK, A. N. GOYETTE, Y. MATSUDA*, L. W. ANDERSON, J. E. LAWLER, *Physics Department, University of Wisconsin, Madison, WI 53706* We are conducting an experimental comparison of rotational temperature and gas kinetic temperature of N_2 and N_2^+ in a positive column discharge. The discharge is situated inside a high temperature oven. The oven temperature, determined with a thermocouple, provides a lower bound for the gas kinetic temperature. An upper bound for the gas kinetic temperature is determined using a calculation of the maximum temperature increase due to the energy deposited in the gas by the discharge. Complete conversion of input power into gas heating is assumed for this calculation, and thermal gradients in the gas and across the wall of the discharge tube are taken into consideration. We are comparing the experimental spectra with simulated spectra generated under the assumption that the rotational temperature is equal to the minimum and maximum gas kinetic temperature described above. The simulated and experimental spectra are compared to determine the usefulness of the rotational temperature as a diagnostic of the gas kinetic temperature. [1]*Dept. of Electrical Engineering and Computer Science, Nagasaki University, Japan

[1]Supported by the Army Research Office.

WPA 9 LIF measurements of CH, H and CH2 species in a H2-CH4 dc discharge G. SULTAN, G. BARAVIAN, *LPGP, CNRS, U. of Paris-Sud, F-91405 Orsay* C. HAYAUD, *Innovatique, F-69386 Chassieu* J. AMORIM, *ITA, Sao Jose dos Campos, Brazil* LIF measurements were used to determine the relative populations of CH, H and CH2 species in the cathode sheath of a H2-CH4 mixture dc discharge for 1-5 Torr and 2-5 mA ranges of pressure and current respectively. The CH radical is detected by fluorescence of the B-X system after excitation by one laser photon (around 387 nm). Each individual R1 and R2 transition presents a fine structure constituted by six lines. The rotational temperature is equal to room temperature. The H atom is detected by two-photon absorption LIF (around 205 nm). From the analysis of the resulting fluorescence profile at 656 nm we deduce that there are two bodies of H atoms. One is due to the dissociation of H2 in the plasma by electronic collisions and the other is due to the photolysis of CH2 which seems to be the major hydrocarbon species present in the discharge. [1]

[1]work supported in part by an EDF contract

WPA 10 IR Laser Diagnostics of Mixed Methane, Hydrogen and Oxygen Plasmas WAI Y. FAN, PAUL B. DAVIES, *Chemistry Dept., Cambridge University* JUERGEN ROEPCKE, *INP, Germany* Tunable infrared diode laser absorption spectroscopy has been used to investigate the gas species present in methane, hydrogen and oxygen discharge mixtures in a 10 kHz parallel plate carbon film reactor. The concentration of the methyl radical increased sharply when trace amounts of oxygen were added to the methane- hydrogen plasmas. In contrast, no significant change was observed in the acetylene concentration in the presence of oxygen. Many other gas phase species including ethane, ethylene, methanol, formaldehyde and formic acid were also detected using diode laser spectroscopy. Formaldehyde appears to be the main discharge product in the presence of oxygen and its concentration is not very sensitive to the fraction of oxygen present. The concentrations of ethylene, ethane or acetylene in methane-hydrogen-oxygen plasmas are about an order of magnitude lower than in pure methane plasmas.

WPA 11 Proton Donor Production and Transport M. HING, G. BROOKE, S. POPOVIC, L. VUŠKOVIC, *Old Dominion University, Norfolk, VA* We will present an experimental study of production and transport of polyatomic molecular ions to be used as proton donors in charge transfer reactions with organic molecules. The experimental set-up [1] consists of a discharge chamber as an ion source, and reaction and detection chambers. Ions are generated in the negative glow of a hollow cathode discharge. A model was developed to optimize the discharge and to maximize ion production on the axis. The model is being verified using emission and mass spectroscopy techniques. Preliminary tests are made with water-based ions. Preparations are under way to generate ions based on molecules with a higher proton affinity, suitable for study of reactions with organic molecules possessing an equivalent proton affinity. Design of primary ion extraction and transport section was completed using a combination of free molecular flow and SIMION codes [2] and estimating space charge effects. Results of preliminary experiments with pre-selected molecules will be discussed at the conference.

[1]D. Smith and N. G. Adams, Adv. At. Mol. Phys. **24**, 1 (1987).
[2]D. A. Dhal and J. E. Delmore, Idaho National Engineering Laboratory, Internal Publication EEG-CS-7233 (1988).

WPA 12 Experimental Studies of DC-excited Plasma Discharges in HMDSN-SF_6 Mixtures ROGERIO PINTO MOTA, REGIANE GODOY DE SANTANA, MAURICIO ANTONIO ALGATTI, ROBERTO YZUMI HONDA, MILTON EIJI KAYAMA, *FE-DFQ-UNESP, 12500-000 Guaratinguetá, SP, Brazil* The study of the structure of thin films from glow discharges and their correlation with discharge parameters is very important for choosing a pre- determined physical property. In this work, we performed measurements of electron temperature using a cylindrical Langmuir probe in DC discharges of HMDSN/SF_6 for several mixtures with the proportion of SF_6 varying from 0 to 50%, at a total pressure of 0.6 mbar. The voltage applied across the discharge was kept constant at 800V. The electron temperature varied from 0.6 to 2.0 eV, presenting a parabolic profile decreasing from the middle towards the edge of the electrode. The same behavior was also observed for the film thickness profile. The film growth rate varied from 12 to 155 Å/min, presenting a maximum at 20% SF_6. The FTIR spectra of the polymeric films showed the disappearance of the chemical bonds C-H, Si-H, and Si-CH_3 for SF_6 percentages above 30%, and the appearance C-F and Si-F chemical bonds.

WPA 13 Loading and Flow Rate Effects in an RIE Scale-up M.J. BUIE, *Applied Materials; Dielectric Etch Division; Santa Clara, CA* P.L.G. VENTZEK, *Hokkaido University, Sapporo, Japan* Differences in process control parameters (gas flows, pressure, etc.) trends have been noted as processes are scaled up from 150 to 200 mm in the new dielectric MxP+ magnetically enhanced reactive ion etch (MERIE) chambers. Both chamber are identical except for the size of the cathode and the respective process kit. In this paper, we illustrate the scale-up effects with reactive ion etching of silicon dioxide in the MxP+ chamber; however, the principles and method discussed are generally appli-

WEDNESDAY AFTERNOON \ WPA

cable. We attempt to describe these effects phenomenologically and computationally either as a simple loading effect or a simple flow rate effect.

WPA 14 Enhanced RF Sputtering of Dielectrics Using an Inductively Coupled Plasma PATRICK F. GONZALEZ, *Symbios Logic, Ft. Collins CO* DENIS SHAW, *Colorado State University* GEORGE J. COLLINS, *Colorado State University* The sputtering rate of Aluminum oxide with Ar on a capacitive plasma has been enhanced by a novel configuration where we increase the plasma density through inductive means. The inductive coil configuation to the chamber was used to achieve a very dense plasma, while the capacitive portion was used to enhance the ion energy for improved deposition rate. Preliminary tests indicate very promising results for deposition of thick layers in a short amount of time.

WPA 15 Detection of SiF_2 as a primary product of Si and SiO_2 reactive ion etching with CF_4 gas JEAN-PAUL BOOTH, GILLES CUNGE, PASCAL CHABERT, *Lab. de Spectrométrie Physique, Université de Grenoble, France* We have detected the SiF_2 radical in the gas phase by Laser Induced Fluorescence during the etching of both Si and SiO_2 substrates under Reactive Ion Etching conditions in a pure CF_4 plasma. The spatially and temporally resolved method shows unambigously that the predominant source for SiF_2 is the etched surface rather than the gas phase, and that SiF_2 appears to be a primary etch product of Si, both in presence of ion bombardment and by pure chemical etching by F atoms in the afterglow of a pulsed discharge. By contrast, with an SiO_2 subtrate, a significant concentration of SiF_2 is also detected, but only during ion bombardment. Absolute SiF_2 concentration measurements are underway to determine if it is the major etch product.

WPA 16 Probe Measurements of Negative Ions Densities in Electronegative Gas Plasmas N.A. KHROMOV, S.N. LAZARYUK, V.A. ROMANENKO, *S.I. Vavilov State Optical Institute, Sosnovy Bor, St. Petersburg, Russia* A.A. KUDRYAVTSEV, *St. Petersburg University, Russia* The method of Langmuir's probe measurements of negative ion concentration in plasmas of electronegative gases at low pressure employed for RF and DC discharges is presented. This method provides for discharge interruption for a time of ambipolar diffusion time (τ_{ap}) order and probe characteristics measuring at the plasma decay stage. If $N_-/N_e>1$ in discharge and, when it switching off, diffusion mechanism of deionization is predominated then in a time $t_0<\tau_{ap}$ after discharge switching off plasma becomes ion-ion one and positive part of probe characteristic corresponds to negative ion current[1]. During $t<t_0$ negative ions are locked in ambipolar potential well and its concentration changing can take place only at the expense of detachment and ion-ion recombination, which are easy to take into account. We have applied this method to experimental investigation of DC discharge (2...10 mA) in oxygen at 0,01...0,1 Torr in quartz tube of 6 cm diameter. Discharge repeatedly was switched off for the time of 0,6...1 ms; t_0 was 0,6...0,9 ms. O^- concentrations had been measured in negative glow and they were $5.10^8...2.10^9$ cm^{-3}. Work was supported by INTAS (project N 740) and RFFI (projects NN 96-02-8417 and 95-02-05064).

[1]N.A. Khromov *et al.*, Proc. GEC-95, Bull. Amer. Phys. Soc., 40, 1570 (1995)

WPA 17 Reaction Mechanisms in Glow Discharges of Tetramethylsilane- Nitrogen-Helium Mixtures MARIO BICA DE MORAES, ELIDIANE RANGEL, STEVEN DURRANT, *University of Campinas, SP, Brazil* Using actinometric optical emission spectroscopy, the species H, CH and CN were studied in film-forming discharges (40 MHz) of tetramethylsilane (TMS)-nitrogen-helium mixtures as a function of the proportions of nitrogen, R, and TMS in the gas feed. Sharp rises in [H], [CH] and [CN] are observed as R is increased, which are attributed to reactions involving nitrogen atoms and TMS molecules. While gas-phase reactions between atomic nitrogen and TMS undoubtedly contribute to CN formation, a relatively high CN concentration was detected in the discharge even in the absence of TMS in the gas feed, as long as a nitrogen-containing polymer was previously deposited on the inner walls of the chamber. This proves that plasma-film surface interactions also generate CN species. On the other hand, the CH concentration is negligible if TMS is not present in the discharge. Thus gas-phase reactions are responsible for the generation of CH. Additional measurements indicate that metastable He atoms may release their energy to the film surface, causing desorption of CN particles.

WPA 18 Optical Diagnostics of Electrical Effects of Ion Bombardment of Semiconductor Surfaces. ALI BADAKHSHAN,, JEFF L ENGLAND, *University of Northern Iowa* P THOMPSON, *Minnesota Supercomputer Institute* P. CHEUNG, *Dept. of Computer Engineering, University of Minnesota-Duluth.* We discuss the application of the noncontact electric field modulation technique of photoreflectance to study the effect of ion bombardment of semiconductors as it occurs during metalization by RF sputtering. A semi-transparent gold layer was grown on low doped n-GaAs using metalization by evaporation and by sputtering. Our experimental results indicate that the photoreflectance lineshape depends on the ionization process in a characteristic way. We employed simulation of photoreflectance lineshape based on a multilayer model to reproduce characteristic features of experimental lineshapes. For sputtered Au/GaAs samples the best simulated lineshape was obtained through an unusual modulation, which is based on a strongly pinned surface electric filed. The argon ions are expected to be responsible for a particular modification of the surface, which is not related to metal atoms. We believe the change in the lineshape is correlated with the density of interface states as it influences the extent of Fermi- level pinning.

WPA 19 Experimental investigation of capacitively coupled RF discharge in oxygen U. BUDDEMEIER, M. HARMS, H. SCHLÜTER, *Institute for Experimental Physics II, University of Bochum, Germany* Spatially resolved electron and negative ion densities as well as electron distribution functions are measured in a parallel plate CCRF discharge in oxygen. Measurements are performed using passively RF-compensated probes. The second derivative of the probe characteristic reveals a narrow peak due to negative ions as well as a broader structure related to the EDF. The negative ion (n_-) density is found to be axially uniform in the plasma bulk. Radial n_- profiles are homogeneous at larger pressures but an off-center maximum develops at reduced pressures. A steep n_- gradient is found at the edge of the discharge. The EDF is uniform over most of the discharge radius. The negative ion density is also determined by means of a laser photodetachement setup using a probe to detect the detached electrons. The application of the basic and 1st harmonic frequency of a YAG-Laser enables the distinction between O^- and O_2^- ions, which is not possible with probe techniques. Discharge parameters are: diam-

eter 30 cm, gap width 2-10 cm, discharge current 1-10 mA/cm^2, O_2 pressure 2-50 Pa. [1]

[1]Work supported by the Deutsche Forschungsgemeinschaft (SFB 191)

WPA 20 Measurement of Negative Ions in a RF NF_3/Ar Plasma A. KONO, T. HAYASHI, S. HIROSE, T. GOTO, *Nagoya University, Nagoya, Japan* Negative-ion and electron densities were measured in a low-power RF (13.56 MHz) NF_3/Ar plasma as a function of NF_3 mixing ratio at a total pressure of 100 mTorr. The plasma was produced in a microwave cavity for measuring electron density and negative ions were detected by laser photodetachment effect. The electron density decreased largely when 1% of NF_3 was added to Ar and it continued to decrease with increasing NF_3 mixing ratio (R), while the negative-ion density was relatively insensitive to R ($>10\%$). The negative-ion density was larger than the electron density by a factor of ~ 10 already at $R = 1\%$ and by a factor of ~ 100 at large R. The decay rate of the electron density in the afterglow increased with increasing R ($>1\%$), indicating that the major electron loss process was attachment to NF_3. The decay of the excess electron density produced by laser photodetachment showed similar behavior, but the decay rate was somewhat larger than that for the electron density in the afterglow.

WPA 21 Plasma Impedance Monitor for Characterising Capacitive and Inductive Discharges KIERAN DOBBYN, CIARAN O'MORAIN, MICHAEL HOPKINS, *Scientific Systems Ltd., Dublin City University, Glasnevin, Dublin 9, IRELAND* It has been established that accurate measurement of the current and voltage at the electrode of a process chamber provide a reliable method of monitoring and characterising process reactors. An effective diagnostic needs to measure accurately the amplitude and phase of the voltage and current at the plasma electrode. Because of the non-linear impedance that the plasma presents to the power supply circuitry, the current and voltage have an extremely wideband frequency content which is often added to by power supply instabilities. We present measurement of current-voltage characteristics of 13.56 MHz radio frequency driven discharges using a wide band current voltage sensor and high resolution data acquisition system. The high resolution (24 bit) measurement allows the plasma impedance to be established by subtracting the impedance associated with the chamber which is often the dominant impedance. The impedance of the plasma is presented as a function of both external parameters, power, gas pressure and internal plasma parameters measured by Langmuir probe.

WPA 22 Breakdown and afterglow physics of pulsed 13.56MHz capacitive discharges in Ar J.P. BOOTH, G. CUNGE, N. SADEGHI, *Lab. de Spectrométrie Physique, Université de Grenoble, France* R. BOSWELL, *PRL, Australian National University, ACT, Australia* N. ST J. BRAITHWAITE, *The Open University, Milton Keynes, UK* The breakdown and afterglow phases of rapidly modulated 13.56MHz parallel plate discharges in 50mTorr Ar were studied, using powered electrode voltage probe, planar ion flux probe, microwave interferometer and optical emission techniques. The RF risetime is determined by the generator and match box. At low repetition rates this is often faster than the time taken to establish the DC bias, leading to a symmetric discharge localised between the powered electrode and the nearest wall. For several μs the plasma is weakly ionised but highly energetic. As the plasma increases in density and fills more of the reactor, the blocking capacitor charges (rate determined by the Bohm-limited ion flux to the grounded reactor walls) and the plasma becomes asymmetric, approaching the steady state in 10's of μs. On plasma extinction, the electrons cool rapidly (3μs timescale), as seen by the rapid drop in optical emission intensity and ion flux, in excellent agreement with a simple diffusional cooling model. The DC bias is mostly discharged within 10μs. At longer times (100μs) the plasma density drops due to ambipolar diffusion.

WPA 23 A quasi-optical 1 mm heterodyne interferometer and its application for determination of the electron density in an RF plasma source V. SCHULZ-VON DER GATHEN, N. NIEMÖLLER, A. STAMPA, H.F. DÖBELE, *Universität Essen; Inst. f. Laser- und Plasmaphysik; 45117 Essen; Germany* A quasi-optical interferometer working at a frequency of 305 GHz is presented. The interferometer was used to detect the electron density in a capacitively-coupled 13.56 MHz Argon RF discharge at input powers of about 100 W and at pressures of some 10 Pa. A reasonable transverse resolution can be realized with this instrument even in the here used typical discharge geometry of diameter $R \approx 100$ mm and electrode distance $d \approx 40$ mm. The microwave source is a frequency tripled Gunn oscillator with an output power of app. 5 mW. Two Schottky mixers are used as detectors in the measuring and reference arm. The imaging is done by elliptical aluminum mirrors. The frequency shift for setting up a heterodyne interferometer is introduced by a rotating grating. The phase differences between the beat signals of measuring and reference arm are measured with a digital storage oscilloscope. The lower detection limit is at some 10^{-4} rad under the present conditions. The measured electron densities are in the order of 10^{10} cm^{-3}. [1]

[1]Supported by the DFG in the frame of the SFB 191

WPA 24 Comparison of Determination of Dissociation by emission spectroscopy and a two-photon LIF scheme U. CZARNETZKI, V. SCHULZ-VON DER GATHEN, H.F. DÖBELE, *Universität Essen; Inst. f. Laser- und Plasmaphysik; 45117 Essen; Germany* L. CHERIGIER, *CEA/ Cadarache; DRFC; 13108 Saint Paul lez Durance; France* In a capacitively coupled parallel plate RF discharge in pure Hydrogen at a frequency of 13.56 MHz the degree of dissociation is measured by emssion spectroscopy on Hydrogen atomic and molecular lines. The degree of dissociation is determined at different input powers (between 20 and 100 Watts), different positions between the electrodes of the device (maximum distance 40 mm) and also for different filling pressures. In parallel a two-photon LIF scheme at 205 nm with excitation to n= 3 in atomic hydrogen is applied. The exciting radiation is generated by Nd:YAG pumped dye-laser with subsequent frequency doubling and mixing with 532 nm radiation. Fluorescence at 656 nm is detected under 90°. Absolute calibration was obtained by titration with NO_2 in a flow tube reactor. Both schemes show comparable results regarding the absolute degree of dissociation of the order of 1 % as well as the qualitative dependences on the discharge parameters. [1]

[1]Supported by the DFG in the frame of the SFB 191 and by a stipendiate of the Humboldt-Foundation

WPA 25 Affects of rf platten biasing phase on inductive coupling in a planar spiral inductive coil[1] ALBERT R. ELLINGBOE, R. D. BENJAMIN, *Lawrence Livermore National Laboratory, Univ. of California* Transformer coupled plasma sources are widely used in semiconductor manufacturing. They offer greater efficiency in plasma production than traditional capacitively

coupled plasmas. More importantly, when used in conjunction with capacitive coupled power at the wafer, they are thought to offer "independent control of ion flux and ion energy." We will report on the affect rf bias phase has on TCP power coupling. By changing the phase between TCP coil and rf bias power we measure a 25% modulation in TCP magnetic field penetration, 25% modulation in ion density, 5 Volt modulation in plasma and floating potential, and significant changes in the electron energy distribution function. We conclude that ion flux and ion energy are *not* independent, and that subtle details in rf power design will affect the ultimate density and the gas-phase chemistry.

[1]This work performed for US DOE by LLNL under contract W-7405-ENG-48.

SESSION WPB: HEAVY PARTICLES AND ELECTRON INTERACTIONS POSTER SESSION
Wednesday afternoon, 23 October 1996
Alcove B at 15:45
Steve Pratt, ANL, presiding

WPB 1 The Hook Method for the Determination of Ground State and Metastable Density in a High-Pressure Mercury Discharge MANFRED KETTLITZ, ECKHARD KINDEL, CONRAD SCHIMKE, HEINZ SCHOPP, *Institut für Niedertemperatur-Plasmaphysik, 17489 Greifswald, Germany* The knowledge of plasma parameters in high-pressure discharges is important for the interpretation of the radiation output. The use of independent methods is advisable to get more information about temperature and particle density distributions in this type of discharges. Often the measurement of the emissivity is used for determining plasma parameters. Frequently the temperature distribution is determined from the absolute line intensities of optically thin lines. In this case the knowledge of the pressure is necessary. Statements about the pressure are possible for a given particle density distribution. In a high-pressure mercury ac discharge the hook method is chosen to determine population densities in the metastable state 6^3P_2 and ground state 6^1S_0. For this purpose the transitions 7^3S_1-6^3P_2 at 546.1 nm and 6^3P_1-6^1S_0 at 254 nm are used. The experimental set-up consists of a Mach-Zehnder interferometer with a dye laser as background light source. For measurements of the 6^1S_0 density a BBO I crystal for the generation of UV radiation is used. The interference figure is detected with a UV sensitive camera. For measuring the hooks the laser wavelength is scanned over the self-absorbed region of the broadened line. Details of the experiment and first results are presented.

WPB 2 Radiative Lifetimes of Odd-Parity Levels in Cr I J. C. COOPER, N. D. GIBSON*, J. E. LAWLER, *Physics Department, University of Wisconsin, Madison, WI 53706* Comprehensive sets of accurate atomic transition probabilities for iron-group elements are increasingly valuable for spectral synthesis and astrophysical data analysis. Time-resolved laser induced fluorescence (LIF) on a slow atomic or ionic beam is recognized as a broadly applicable and accurate method for measuring radiative lifetimes. We report the measurement of over 100 lifetimes in Cr I. Representative measurements and efforts to reduce systematic error will be discussed. These lifetimes will be combined with branching fractions from spectra recorded using the 1.0m Fourier transform spectrometer at the National Solar Observatory to determine a comprehensive set of accurate absolute atomic transition probabilities for Cr I.[1] *Dept. of Physics and Astronomy, Denison Univ., Granville, OH 43023

[1]Work supported by N.S.F..

WPB 3 Atomic Transition Probabilities for Rare Earths J. J. CURRY, HEIDI M. ANDERSON, E. A. DEN HARTOG, M. E. WICKLIFFE, J. E. LAWLER, *Physics Department, University of Wisconsin, Madison, WI 53706* Accurate absolute atomic transition probabilities for selected neutral and singly ionized rare earth elements including Tm, Dy, and Ho are being measured. The increasing use of rare earths in high intensity discharge lamps provides motivation; the data are needed for diagnosing and modeling the lamps. Radiative lifetimes, measured using time resolved laser induced fluorescence (LIF), are combined with branching fractions, measured using a large Fourier transform spectrometer (FTS), to determine accurate absolute atomic transition probabilities. More than 15,000 LIF decay curves from Tm and Dy atoms and ions in slow beams have been recorded and analyzed. Radiative lifetimes for 298 levels of TmI and TmII and for 450 levels of DyI and DyII are determined. Branching fractions are extracted from spectra recorded using the 1.0 m FTS at the National Solar Observatory. Branching fractions and absolute transition probabilities for 500 of the strongest TmI and TmII lines are complete. Representative lifetime and branching fraction data will be presented and discussed. [1]

[1]Supported by Osram Sylvania Inc. and the NSF.

WPB 4 Gas-Phase Reactions of $H_3O^+.(H_2O)_{0,1}$ with a Series of Sulfides and Thiols* TED WILLIAMS, LUCIA BABCOCK, NIGEL ADAMS, *U. of Georgia, Athens, GA* The reactions of $H_3O^+.(H_2O)_{0,1}$ have been investigated in a Selected Ion Flow Tube at 300K with $H_2S, CH_3SH, C_2H_5SH, (CH_3)_2S$, n- and $iso-C_3H_7SH, CH_3SC_2H_5$, and C_4H_4S. These compounds are major pollutants from the paper and pulp industry, fish processing, animal and human waste and are likely to be significant in interstellar chemistry. H_3O^+ is one of the most widely detected ions in the galaxy and is an impurity in many laboratory plasmas. Where there is significant H_2O, water cluster ions are often observed, e.g., in the stratosphere. H_3O^+ reacts with all these compounds by exothermic proton transfer at the collision rate. For $H_3O^+.H_2O$, proton transfer often occurs where it is "apparently" endothermic. A common competitive channel is rapid association followed by ligand switching. The rates (except for H_2S) are also collisional. Reasons for the "apparent" endothermicities are discussed and application to interstellar clouds is given. Use of these data for determining the concentration of sulfur compounds in the atmosphere by in-situ monitoring products of this type of reaction is discussed.

*Work supported by NSF Grant No. AST-9415485.

WPB 5 N^*+ Production from N_2^*+ Dissociation in Nitrogen at Elevated E/N J. DE URQUIJO, E. BASURTO, I. DOMÍNGUEZ, I. ALVAREZ, C. CISNEROS, *Instituto de Física, UNAM, México.* A drift tube–mass spectrometer has been used to measure the relative concentrations of N^*+ and N_2^*+ drifting and reacting in N_2 gas over the pressure range 0.84–6.66Pa, and drift distances between 4.72 and 38.82cm. Our measurements indicate that the concentration of N^*+ relative to that of N_2^*+ increases steadily from a value of 0.2% at 1.8kTd to 15% at 8.5kTd. The variation of measured mean energies of N_2^*+ in N_2 between approximately 8 and 30eV [1] for the above E/N range, together with the fairly high cross section for the same

energy range [2] for N^*+ formation from collisional dissociation of N_2^*+ in N_2, strongly suggest that this process is operative in our experimental conditions. [1] S. B. Radovanov, R. J. Van Brunt, J. K. Olthoff and J. M. Jelenkovic, Phys. Rev. E, **51**, 6036 (1995) [2] W. B. Maier, J. Chem. Phys. **55**, 2699 (1971) Work supported by DGAPA, Project IN104795

WPB 6 Kinetic Energy Distributions of N^+, N_2^+, and N_3^+ at High E/N. M. V. V. S. RAO, R. J. VAN BRUNT, J. K. OLTHOFF, *NIST, Gaithersburg, MD 20899* T. ŠIMKO, J. BRETAGNE, G. GOUSSET, *LPGP, Universitsé Paris-Sud 91405 Cedex, France* The kinetic energy distributions and total relaive fluxes of the ions N^+, N_2^+, and N_3^+ have been measured for electric field-to-gas density ratios (E/N) in the range of 1.0×10^{-18} to 30.0×10^{-18} Vm^2 (1 to 30 kTd) in diffuse Townsend discharges. The results are compared with predictions based on a simple charge-transfer model (for N_2^+) and with a Monte Carlo simulation that uses a recommended cross-section set[1] for N^+/N_2 and N_2^+/N_2 collisions. The energy distributions obtained for N_2^+ from both the experiments and Monte Carlo simulation deviate from Maxwellian form, thus indicating the inadequacy of the charge-transfer model and explaining the descrepancy between the predictions of this model and the results of previous measurements.[2] The results for N^+ from both the measurements and simulations show indications of "runaway" behavior at the highest E/N where the maximum observable ion energy is limited by the applied discharge gap voltage.

[1]A. V. Phelps, J. Phys. Chem. Ref. Data **20**, 557 (1991).
[2]S. B. Radovanov, R. J. Van Brunt, J. K. Olthoff, and B. M. Jelenkovic, Phys. Rev. E **51**, 6036 (1995).

WPB 7 Transport of H^+, H_2^+, and H_3^+ at High E/N and Relevant Ion-Molecule Collision Cross Sections. T. ŠIMKO, J. BRETAGNE, G. GOUSSET, *LPGP, Universitsé Paris-Sud 91405 Cedex, France* M. V. V. S. RAO, R. J. VAN BRUNT, J. K. OLTHOFF, YICHENG WANG, *NIST, Gaithersburg, MD 20899* B. L. PEKO, R. L. CHAMPION, *College of William and Mary, Williamsburg, VA 23187* The results from experimental and theoretical investigations of H^+, H_2^+, and H_3^+ transport in diffuse Townsend discharges for high electric field-to-gas density ratios (E/N) in the range of 0.5×10^{-18} to 20.0×10^{-18} Vm^2 (0.5 to 20 kTd) are reported. The measurements were performed using a parallel-plate discharge cell in which ions that pass through a small hole in the cathode were selected according to their mass and kinetic energy using an electrostatic ion-energy analyzer-mass spectrometer system. The calculations were performed using both a convective scheme model and a Monte Carlo simulation with ion-molecule collision cross sections based on reasonable adjustments to cross sections measured in recent beam experiments.[1] Satisfactory agreement is obtained between the predicted and measured ion kinetic energy distributions and the relative total fluxes of the three ions. The model results indicate a strong coupling among the three ions due ion-conversion processes.

[1]B. L. Peko, R. L. Champion, and Y. Wang, J. Chem. Phys. **104**, 6149 (1996).

WPB 8 Kinetic Energy Distributions of O_2^+ and O^+ from DC Townsend Discharge of O_2. M.V.V.S. RAO, R. J. VAN BRUNT, J. K. OLTHOFF, *NIST, Gaithersburg, MD 20899* Measurements of the kinetic energy distributions (KEDs) for O_2^+ and O^+ were made in an O_2 Townsend discharge at E/N from 2×10^{-18} to 40×10^{-18} Vm^2 (2 to 40 kTd). A detailed description of the apparatus and experimental procedure have been given elsewhere.[1] The measured KEDs for O_2^+ are Maxwellian up to 20 kTd consistent with predictions based on the assumption that resonant symmetric charge transfer is the dominant ion-neutral collision process using the cross sections derived from direct measurements[2]. Above 20 kTd, the results deviate from the simple charge-transfer model predictions. Unlike O_2^+, the KEDs for O^+ exhibit a non-Maxwellian, two temperature characteristic with the high-energy tail extending up to the maximum allowed by the applied electrode-gap voltage for $E/N>10$ kTd. The ratio of O^+/O_2^+ increases with increasing E/N, and the mean energies of these two ions become comparable at $E/N\geqslant20$ kTd.

[1]M. V. V. S. Rao, R. J. Van Brunt, and J. K. Olthoff, Phys. Rev. E (in press).
[2]R. F. Stebbings, B. R. Turner, and A. C. H. Smith, J. Chem. Phys. **38**, 2277 (1963).

WPB 9 Heterogeneous Deactivation Studies of N_2 at 17 Torr on Gold and Nitrided Pyrex* JOHN PARISH, PERRY YANEY, *University of Dayton* Deactivation of vibrational states v=1 through 5 of the $X^1\Sigma_g^+$ neutral electronic ground state in flowing N_2 afterglow from a dc discharge were measured on gold and "nitrided" pyrex using coherent anti-Stokes Raman spectroscopy (CARS). Our studies of deactivation on metals show up to an order of magnitude increase in deactivation probability γ compared to "neat" pyrex. Moreover, the magnitude of the vibrational populations on metals such as aluminum and stainless steel show growth during early (<6 ms) residence times which may be due to a "catalytic-type" reaction. It was expected that this reaction would be much weaker or absent at a gold surface. The gold data appears to confirm this expectation. Also, we have found that γ increases after extended exposure of pyrex to the afterglow which we tenatively attribute to nitriding of the pyrex surface. The nitriding was confirmed by XPS measurements. All CARS measurements were corrected for saturation due to stimulated Raman scattering.[1]

*Supported by USAF F33615-93-C-2303

[1]P. P. Yaney and J. W. Parish, Appl. Opt. 15, 2659 (1996)

WPB 10 Elastic, Vibrational and Integrated for e-Scattering Metyl Acetylene and Allene LUDWIG BOESTEN, HIROSHI TANAKA, *Sophia University, Tokyo, Japan* MICHAEL DILLON, *Argonne National Lab, Argonne, IL* We have measured the elastic cross sections of the two isomers of C3H4 over the range from 1.5 to 100 eV impact energy and scattering angles from (15) 20 deg to 130 deg. A modified phase shift program was used to estimate the integrated cross sections together with the momentum transfer cross sections. We have obtained the lowest virtual orbitals from a Gaussian-92 calculation and determined the fundamental vibrational modes that could be enhanced by a trapping of the incoming electron in these orbitals. Resolution of the observed vibrational loss spectra into fundamental modes and harmonics demonstrates that the LUMO, in either case irreducible species "e," is the origin of the observed resonances. The low energy resonances at 2 eV (allene) and 3 eV (methyl acetylene) are connected with the double carbon bonds. Supported by the U.S. Dpt. of Energy, Office of Energy Research, Office of Health and Environmental Research, under Contract W-31-Eng-38, and by Grant in Aid from the Ministry of Education, Science, and Culture, Japan.

WPB 11 Elastic Scattering From CO2 Molecules: Experimental and Theoretical Results T. MASAI, H. TANAKA, L. BOESTEN, *Sophia, Univ., Tokyo, Japan* M. TAKEKAWA, Y. ITIKAWA, *Inst. Sp. Astro. Sci., Japan* M. KIMURA, *Yamaguchi Univ., Japan* Elastic cross section measurements for electron scattering from CO2 molecules was made experimentally earlier [1], but the results obtained were limited in energies and scattering angles. We have recently carried out combined efforts for experimental and experimental studies on elastic electron scattering from CO2. The experimental study covered the energy range from 1.5 eV to 100 eV [2], while the theoretical study was performed below 50 eV employing a closed coupling approach [3,4]. The present results from experimental and theoretical studies are found to be in good accord in all studies . In particular, the present theoretical results at 10 eV and 4 eV reproduce present experimental results but are found to be in disagreement withe arlier measurements by Register et al.

[1]D. F. Register, H. Nishimura and S. Trajmar , J. Phys. B13, 1651 (1980)
[2]T. Masai, H. Tanaka,and L. Boesten, unpublished
[3]M. Takekawa, M.Sc. thesis at Univ. of Tokyo (1096)
[4]M. Kimura, unpublished

WPB 12 Electron and Positron Polyatomic Molecule Scattering: Experimental and Theoretical Studies for Acetic Acid and Formic Acid M. KIMURA, R. HAMADA, O. SUEOKA, *Yamaguchi Univ., Japan* H. SATO, *Ochanomizzu Univ., Japan* A combined effort of experimental and theoretical was carried out for the determination of total cross sections on electron and positron scattering from acetic acid and formic acid molecules with electron energies of 1 eV to 100 eV. The continuum multiple scattering method was employed theoretically[1]. The general trends seen in measured cross sections for both electron and positron scattering are similar to other molecular cases seen earlier, namely, 1) slightly smaller cross sections for the positron case about 30-40 eV and 2) this difference between the two cross sections increases with decreasing energies. The present experimental and theoretical elastic cross sections for electron and positron scattering are found to be in reasonable accord. For electron scattering, our theoretical result shows some structures identified as resonances.

[1]M. Kimura and H. Sato, Comment At. Mol. Phys.26, 333(1991)

WPB 13 Electron-Impact Excitation Cross Sections of H_2 Using the Method of Continued Fractions MU-TAO LEE, MILTON MASSUMI FUJIMOTO, IONE IGA, *Departamento de Química, UFSCar, CP676, 13565-905 São Carlos, SP, Brazil* TEODOSIO KROIN, *Departamento de Física, UFSC, 88049, Florianópolis, SC, Brazil* In this work, we applied by the first time the method of continued fractions(MCF) [1, 2] for studies of electronic excitation of molecules by electron impact in the two-state close-coupling level. Specifically we have calculated differential and integral cross sections for the excitation of the first 3 triplet excited states of hydrogen in the 10.5 to 40 eV impact energy range. Different from the early two-state studies of Chung and Lin[3] , in this work no orthogonality constraint between the bound and continuum orbitals is imposed and the one-electron exchange terms are explicitly considered. Comparison with available experimental and theoretical data shows good agreement. Results and discussions will be presented in the conference. This work is partially supported by Brazilian agencies: CNPq, FAPESP, CAPES-PADCT and FINEP-PADCT.

[1]J. Horáček and T. Sasakawa, P.R.A. 28,2151(1983)
[2]M.-T. Lee *et al.*, J.P.B. 28, 3325(1995)
[3]S. Chung and C.C. Lin, P.R.A. 17,1874(1978)

➢➢➢➢➢➢➢➢➢➢➢➢

SESSION WPC: SHEATHS AND ELECTRODE EFFECTS POSTER SESSION
Wednesday afternoon, 23 October 1996
Alcove B at 15:45
Steve Pratt, ANL, presiding

WPC 1 Optical Emission Measurements Adjacent to a rf Biased Electrode in an Inductively Coupled Plasma ERIC BENCK, AMELIA GATES, [1] JIM ROBERTS, *NIST* Time-resolved optical emission spectroscopy has been applied to the study of the sheath and nearby bulk plasma adjacent to an rf biased electrode in an argon inductively coupled plasma. The plasma source is a modified GEC reference source with an electrostatic shielded 5 turn pancake coil operated at 13.56 MHz. With the lower electrode grounded, no modulation of the optical emission at a wavelength of 750.4 nm is observed. With an applied rf bias to the lower electrode, modulation of the optical emission is observed close to the electrode and throughout the discharge at high rf bias frequencies (>20MHz). The behavior of the time-resolved optical emissions is investigated as a function of distance from the electrode, rf bias frequency, plasma density, and electrode composition.

[1]Summer Undergraduate Research Fellow, Miami University, Oxford, OH

WPC 2 Fast Time Resolved Measurements in the UK GEC Reference Reactor. C.M.O. MAHONY, W.G. GRAHAM, *Physics Dept.The Queen's University of Belfast, Northern Ireland* R. AL-WAZZAN, *Andor Technology, Malone Rd, Belfast, Northern Ireland* Measurements of time resolved plasma and electrode potentials along with spatially and temporally resolved optical emission spectroscopy (STROES) have been made in the UK GEC reference reactor. Plasma and electrode potentials were determined using electrical probes and standard IV measurement techniques. Emission data was acquired using a novel ICCD technique, which allowed fast (~ 2 minutes) STROES. In hydrogen, 656 nm emission shows the well known double layer over a wide range of rf driving powers and gas pressures. Electrical measurements show that during each rf cycle the powered electrode potential approaches the plasma potential and may well become positive with respect to it for a few nanoseconds. This allows electrons to leave the plasma. Near-electrode emission is observed at this time. Measurements in argon also show the powered electrode potential to approximate the plasma potential for short periods during each rf cycle but only for rf driving powers greater than ~ 50 W. Fast STROES at 750 nm in argon for these powers show near-electrode emission, believed to be the first observation of a double layer in an rf driven argon plasma. A model of the electron, ion and displacement currents to the electrodes in these plasmas is under development. Supported by UK EPSRC

WPC 3 RF Penetration of a DC Sheath HUSAIN KAMAL, NOAH HERSHKOWITZ, *University of Wisconsin, Madison* Sheath characteristics near a dc negatively biased planar cathode (diameter = 10 cm) in an inductively-capacitively coupled plasma are experimentally examined using an emissive probe. The Ar

plasma was sustained by 13.56 MHz rf applied to a single turn (insulated) antenna mounted inside the chamber and operated at a pressure of 1 Torr. The bias voltage was varied from -170 to 30 V. Using the emissive probe inflection-point-method, it was possible to measure the sheath potential versus position. It was found that the effects of the rf penetrate the sheath only up to the point where the reduction in the dc potential is the order of the amplitude of the fluctuating rf potential. A comparison is made between the measured and predicted sheath potential versus distance.

WPC 4 On the mechanism of the transition from bulk to sheath heating mode in CCRF discharges U. BUDDEMEIER, M. HARMS, I.D. KAGANOVICH, U. KORTSHAGEN, *University Bochum, Germany* L.D. TSENDIN, *St.Petersburg Technical State University, Russia* The transition between different heating modes of low-pressure CCRF α-discharges was observed in [1]. The sheath heating mode is characterised by an electron distribution function (EDF) with a pronounced peak of cold electrons, which is absent in the bulk heating mode. It is shown experimentally that the transition to the sheath heating mode can be obtained not only by a reduction of the pressure (as observed in [1]), but also by a rise of the RF current density or a decrease of the gap width. The peak arises from the fact that the low energy electrons are confined to the bulk by the ambipolar electric field and do not participate in the heating (collisional or stochastic) located in the sheath region. In the present communication the physical mechanism of this transition is discussed. The basic idea is to compare the power deposition to the electrons in the sheath and in the bulk plasma. A set of relations is derived to obtain an estimate of this ratio from basic discharge parameters. Results are compared to experimental data. 1. V.A. Godyak and R.B. Piejak, Phys.Rev.Lett. 65,996, (1990)

WPC 5 Relationship between ion flux and sheath impedance for low-density rf plasma sheaths MARK SOBOLEWSKI, *NIST, Gaithersburg, MD* The ion flux at the rf-powered electrode of the GEC RF Reference Cell was determined using a method [1] in which a large negative dc bias is simultaneously applied to the electrode and the resulting dc current is measured. For argon discharges at 10-1000 mTorr, the ion flux obeyed a power-law dependence on the fundamental amplitude of the sheath current, independent of pressure. The observed power law is in rough agreement with a simple calculation that equates approximate rates of ion generation and loss in the discharge. Simultaneous measurements of the sheath impedance, sheath voltage, and ion flux provide sufficient information to rigorously test electrical models of rf plasma sheaths. Except for a constant multiplicative factor, the results were in agreement with the model of Lieberman[2], even though several assumptions of that model do not apply to the asymmetric discharges studied here. Comparison with models of rf sheaths in asymmetric discharges yielded better agreement.

[1]V. A. Godyak, R. B. Piejak, and B.M. Alexandrovich, J. Appl. Phys. 69, 3455 (1991)
[2]M.A.Lieberman, IEEE Trans. Plasma Sci., 17, 338 (1989)

WPC 6 A Consistent Step Model for the Capacitive RF Sheath JOACHIM GIERLING, KARL-ULRICH RIEMANN, *Ruhr-Universität Bochum, D-44780 Bochum, Germany* In order to find analytically tractable models for the electrode sheath of a capacitively coupled RF discharge step models are used in the literature[1,2]. In these models the electron density is modeled by a step function oscillating with the radio frequency ($\omega_{pi} \ll \omega_{RF} \ll \omega_{pe}$). Comparison of the results of these step models with the results of our own numerical calculations shows similar current–voltage characteristics for symmetric discharges. On the other hand clear differences in the spatial behavior of field and potential for a single sheath are observed. We discuss the deviations of the step models and show them to arise from systematic errors in the boundary conditions which are due to misinterpretations of the asymptotic two scale formalism [3, 4]. On the background of a systematic two scale theory, we develop an improved step model with correct boundary conditions.

[1]M. Lieberman, IEEE Trans. Plasma Sci., **16**, 638 (1988)
[2]V. Godyak u. N. Sternberg, Phys. Rev. A, **42**, 2299 (1990)
[3]K.–U. Riemann, J. Phys. D: Appl. Phys., **24**, 493–518 (1991)
[4]K.–U. Riemann, Phy. Fluids B, **4**(9), 2693–2695 (1992)

WPC 7 Studies on the Transient Presheath PETER MEYER, KARL-ULRICH RIEMANN, *Theor. Physik I, Ruhr-Universität Bochum, Germany* In the past the mechanisms of *stationary* presheaths were studied and discussed in great detail [1]. Technical devices use so called pulsed modes in which during a short period a large negative voltage is applied to the electrode. In these processes the presheath develops from one stationary solution to another. We investigate this relaxation due to a damped attenuation wave by an analytical treatment, by a numerical solution of the continuum equations and by selfconsistent kinetic particle simulations. We compare the presheath relaxation for different presheath mechanisms: charge exchange collisions of the ions, geometrical concentration of ion flow and collisional ionization by electrons. The system we chosed for these investigations is an isolated electrode with a plasma in front of it. First, we look for the stationary solution with the floating potential, then, we apply a voltage with defined negative value. This leads to a motion of the sheath edge and results in altered boundary conditions for the presheath.

[1]K.-U. Riemann, J. Phys. D: Appl. Phys. **24**, 493 (1991)

WPC 8 Quasi-Steady-State Connection Formula for Sheaths,* MERLE RILEY, *Sandia National Labs, Alb., NM* The sheath transition from the bulk plasma to a boundary wall has been investigated for some time. I present a simple asymptotic analysis of the problem relevant to high density, low pressure, and low temperature plasmas. I derive an improved connection formula for the electric field on the wall side of the Bohm transition region. The basic analysis follows that of Godyak and Sternberg [1] and others. The field correction is higher order in the ratio of Debye to ion collision lengths. The correction is derived empirically by examination of numerical solutions to the 1D equations comprised of the sourceless ion continuity and ion momentum equations, combined with the electron description given by the Poisson and electron Boltzmann distribution. *Work performed at Sandia National Labs and supported by US DoE under contract DE-AC04-94AL85000.

[1]Valery A. Godyak and Natalia Sternberg, IEEE Trans. Plasma Sci. 18, 159-168 (1990).

WPC 9 Unified Model of the rf Plasma Sheath, Part II* MERLE RILEY, *Sandia National Labs, Alb., NM* By developing an approximation to the first integral of the Poisson equation, one can obtain solutions for the current-voltage characteristics of an rf plasma sheath that are valid over the whole range of inertial response of the ions to an imposed rf voltage or current. [1] The theory has been shown to adequately reproduce current-voltage characteristics of two extreme cases [2] of ion response. In this work I

show the effect of different conventions for connecting the sheath model to the bulk plasma. Modifications of the Mach number and a finite electric field at the Bohm point are natural choices. The differences are examined for a sheath in a high density Ar plasma and are found to be insignificant. A theoretical argument favors the electric field modification. *Work performed at Sandia National Labs and supported by US DoE under contract DE-AC04-94AL85000.

[1]M.E.Riley, 1995 GEC, abstract QA5, published in Bull. Am. Phys. Soc., 40, 1587 (1995).
[2]M.A. Lieberman, IEEE Trans. Plasma Sci. 16, 638 (1988). A. Metze, D.W. Ernie, and H.J.Oskam, J.Appl.Phys., 60, 3081 (1986).

WPC 10 Formation of a High Conducting Plasma in Front of a Cold Cathode JOCHEN SCHEIN, MICHAEL SCHUMANN, JUERGEN MENTEL, *Ruhr–University Bochum, Germany* The ignition of arc discharges does not proceed straight forward in many cases. The discharge very often remains in the stage of a glow discharge since the formation of an arc spot at the cold cathode does not take place. For investigation of this phenomena an experimental setup has been developed providing a plasma in front of a negatively biased electrode. The current transfer from the plasma to the electrode is recorded by electrical and optical means. The investigation revealed two different kinds of ignition. A diffuse and a constricted ignition. During the diffuse ignition a small precurrent can be noticed in combination with a luminous layer visible on the electrode surface whereas during the constricted ignition no precurrent is measured and only a plasma ball on the electrode surface can be noticed. It will be shown that these two cases are independent of the bulk properties of the electrode material but do depend in high degree on the properties of the electrode surface. A model will be presented pointing out that arc spot ignition is determined by the distribution of submicrometer structures which by acting as field–emitters are responsible for the different kinds of arc spot ignition.

WPC 11 Electron Yields per Ion, Resonant Photon, and Metastable at Ar Discharge Cathodes from DC and Transient Voltage and Current A.V. PHELPS, *JILA, U. of Colorado and NIST* We determine electron yields for ions, resonance photons, and metastables reaching the cathode from non-invasive measurements of dc and transient voltage and current at low currents. Models[1] of the individual contributions to the current-growth rates and the negative-differential, voltage-current ratio for parallel-plane electrodes have been extended to include all contributions. We use and test the sensitivity to previously measured or calculated excitation and ionization coefficients, ion mobilities, resonance-state radiative properties, metastable diffusion coefficients, and fractional electron backscattering. The yields for ions include any fast atom contributions. Measurements[2] for pd from 0.1 to 2000 Torr-cm (E/n from 15 Td to 100 kTd) are utilized. Typical yields per ion at moderate pd are much lower than for clean metals, but are similar to values[3] obtained using pulsed, UV-initiated discharges.

[1]A.V. Phelps, Phys. Rev. **117**, 619 (1960); A.V. Phelps, Z.Lj. Petrović and B.M. Jelenković, Phys. Rev. E **47**, 2825 (1993).
[2]Z.Lj. Petrović and A.V. Phelps, Bull. Am. Phys. Soc. **39**, 1490 (1994); M. Menes, Phys. Rev. **116**, 481 (1959).
[3]J.P. Molnar, Phys. Rev. **83**, 940 (1951).

WPC 12 DC sheath resistance of capacitively coupled discharges in the GEC reactor. L. J. OVERZET, B. E. CHERRINGTON, J. KLEBER, K. YI, *University of Texas at Dallas* M. B. HOPKINS, *Dublin City University* The dc sheath resistance (or the plasma to ground resistance) of RF capacitively or inductively coupled discharges can cause the plasma potential to rise significantly when a Langmuir probe is biased above floating potential.[1] This resistance is part of the Langmuir probe circuit and if it is not included in the analysis of single probe results, it can lead to significant errors in the estimation of plasma parameters (under extreme circumstances) or dramatically alter the shape of the EEDF at low energies. We have measured the sheath resistance in the GEC reactor for capacitively coupled discharges through argon, helium and nitrogen at pressures of 100, 250 and 500 mTorr. We will also make these measurements for the same gases using the inductive coupled source. There is at least one interesting development from the measurements at 250 mTorr. The sheath resistance as a function of the RF current, voltage or power does not sit on a single curve for the three gases investigated; however, it does sit on a single curve for all three gases when plotted as a function of the electron density. At 250 mTorr the sheath resistance can be fitted as $R_{sh} = 10^{28/3} * N_e^{-2/3}$ where R_{sh} is the sheath resistance in Ohms and N_e is the electron density per cubic cm.

[1]M. B. Hopkins, J. Res. NIST 100, 415-425 (1995)

SESSION WPD: ENVIRONMENTAL APPLICATIONS POSTER SESSION
Wednesday afternoon, 23 October 1996
Alcove B at 15:45
Steve Pratt, ANL, presiding

WPD 1 Evaluation of Ash Toxicity Generated From the Thermal Plasma Pyrolysis of Used Automobile Tires J.S. CHANG, D.R. NOVOG, S. JAMAL, *Dept. of Eng. Phys., McMaster University, Hamilton, Ontario, Canada, L8S 4M1* The disposal of used tires represents a severe environmental problem. As the heat content of the rubber tires is even higher than that of coal it should be considered as a future source of alternate fuel for power generation. There have been attempts to burn old tires directly in cofired boilers for production of electricity. However, there are several environmental concerns since the combustion flue gas may contain a significant concentration heavy metals (Fe, Zn, Cd, As, etc.). One technique currently being developed is the pyrolyzation of rubber tires by a thermal plasma to produce combustible gases. In this work, ashes generated during the plasma pyrolysis of used automobile tires using a DC Argon thermal plasma were analyzed using Neutron Activation Analysis (NAA) and produced syngas composition was analyzed by FT-IR.. The gas analysis indicates a significant quantity of combustible gases (CH4, C2H2, C2H4, CO, H2 etc..) was produced from the thermal plasma pyrolysis of used tires. The results also indicate that a majority of the heavy metals present in used tires were concentrated in the ashes deposited in reaction chamber wall and in the two-stage filtering system. Furthermore the heavy metal concentration decreases significantly with increasing distance from the plasma torch. Toxic components such as Zn, As and Cl were also collected in the filtering process.

WPD 2 RF Glow-discharge Enhanced Production of Oxygen from Carbon Dioxide * ZHONG SHI, ROBERT L. ASH, *Old Dominion University, Norfolk, VA* An experimental study of energy-efficient, RF glow-discharge enhanced production of oxygen from carbon dioxide is conducted. This effort has important applications for advanced life support system at space station to recover oxygen from waste carbon dioxide and *in situ* resource utilization for round trip planetary missions.[1] The system consists of a glow-discharge chamber and a silver permeation membrane used to separate oxygen from other species. The behavior of RF glow-discharge and the oxygen production rate was investigated as functions of discharge power, eletrodes geometry, membrane operating temperature, gas pressure, and RF frequency. Description of the experimental set up and the measured results compared with previous DC glow-discharge data [2] will be presented at the conference.

*Supported by NASA under Grant NAG-1-1140.

[1]R. L. Ash, W. L. Dowler, and G. Varsi, Acta Astronautica, **5**, 705, (1978).
[2]D. Wu, R. A. Outlaw, and R. L. Ash, J. Applied Phys., **74**, 4990, (1993).

WPD 3 Destruction of Hazardous Industrial Chemicals Using an Arcjet Plasma Torch* C. B. FLEDDERMANN, H. R. SNYDER, J. M. GAHL, *Department of Electrical and Computer Engineering, University of New Mexico, Albuquerque, NM 87131* A small-scale thermal plasma torch has been used for the disposal of hazardous industrial chemicals including alcohols, ketones, and chlorinated hydrocarbons. The plasma jet is operated at currents up to 200 Amperes and waste flow rates up to 600 ml/hr. Argon is used as the plasma gas with oxygen added to the reactor to alter the reaction chemistry. Destruction of the waste and by-product formation are monitored using a residual gas analyzer, and the temperature of the plasma plume is measured using an enthalpy probe. The by-products of the destruction of acetone are primarily carbon dioxide, carbon monoxide, and small amounts of hydrocarbons. Adding oxygen to the reactor increases the production of carbon dioxide and significantly decreases the amount of acetone in the exhaust gases. This reactor has achieved greater than 99 percent destruction efficiency for acetone when oxygen is added to the reaction mixture at an arcjet current of 75 Amperes, with similar destruction efficiencies observed for ethanol and trichloroethylene. *Supported by the U.S. DOE through the WERC program administered by New Mexico State University.

WPD 4 Correlation Between Spectral Intensities of Coal and Coal Ash Using Emission Spectroscopy W.L. COLLETT, B. BELL, S.M. MAHAJAN, S.S. MUNUKUTLA, *Tennessee Technological University* Leaching of trace metals such as arsenic, cadmium, lead, mercury, thallium, antimony, and selenium from coal ash into groundwater is a serious environmental concern. In an effort to develop an on-line technique to monitor these elements, a glow discharge based emission spectroscopy technique has been developed at Tennessee Tech University. A glow discharge at 1.25 torr of argon generates a plume near the base of a cooled hollow cathode with a compacted coal or coal ash sample as the base of the cathode. Five different samples of mineral coal and the corresponding samples of coal ash were obtained from a power plant. Spectral intensities were recorded for all seven trace metals with three discs of each sample and four scans of each disc. A correlation between coal and coal ash for each trace metal is currently being established. Such a correlation will help power plants to determine the toxicity level as a result of coal ash disposal prior to burning a particular batch of mineral coal.

WPD 5 Simulation of Microdischarges in a Dielectric-barrier SHIRSHAK DHALI, JING LI, *Southern Illinois University, Carbondale, Illinois 62901* Dielectric-barrier discharges have become a primary source of non-thermal plasma at atmospheric pressures for pollution control. We present the simulation results of streamer like microdischarges in air and oxygen. Fully two-dimensional simulations have been done for parallel plate geometry with a dielectric-barrier. An adaptive grid is used where the transport part is solved using Flux Corrected Transport (FCT) and the Poisson's equation is solved by Successive Over Relaxation (SOR). The development of electron density and current of the propagating microdischarge will be discussed. Also, the oxygen atom production efficiency for varying discharge parameter will be discussed.

SESSION H1A: PHENOMENA IN GLOW DISCHARGE PLASMAS

Thursday morning, 24 October 1996
Auditorium at 8:00
Uwl Kortshagen, Univ. of Minnesota, presiding

8:00

H1A 1 Flowing Microwave H atom source A. ROUSSEAU, P. CHABERT, G. GOUSSET, P. LEPRINCE, *LPGP, UPS-Orsay, France* The influence of the gas flow rate, on the dissociation degree, of a pulsed microwave (2.45 GHz) discharge in H_2, is investigated. The plasma column is created in a quartz tube (0.8cm, 1 Torr). The pulse duration is 20 ms, the cycle period is 100ms, the pulsed power up to 1500W. $1\% O_2$ is added in order to reduce the H atom wall recombination, so that H_2 dissociation degree as high as 80 % can be reached[a] [1]Rousseau A, Tomasini L, Gousset G, Boisse-Laporte C, Leprince P, J. Phys D: Appl. Phys 27, 2439, (1994).. The gas flow rate ranges from 25 sccm to 445 sccm corresponding to a gas velocity of 0.15 to 3 cm/ms at 300 K). Time and spatially resolved measurements of the H_2 dissociation degree, of the H atom temperature, and of the electron density are performed. The H atom temperature ranges from 1500 K to 2000 K, and appears not directly depending on the gas velocity. The H_2 dissociation degree, determined by actinometry along the plasma column, mainly depends on the time residence of the molecules in the plasma: 5ms are required to achieve dissociation of the H_2 molecules[b] [2]Tomasini L, Rousseau A, Baravian G, Gousset G, Leprince P Appl. Phys. Lett (1996) accepted.. For high gas velocities, the 450W plasma column is too short (15cm) to get high dissociation degree. A modelling of the discharge, taking into account the effect of the gas flow, is in progress to understand the induced power balance modification.

8:15

H1A 2 Effects of Minority Species on Plasma Composition in Microwave -Driven Ion Sources* DAVID SPENCE, KEITH R. LYKKE, *Argonne National Lab, Argonne, IL* It has long been known that the addition of certain minority species (1%) to microwave-driven discharges can greatly modify the equilibrium dissociation fraction in the plasma.[1] For example,[2] we have recently increased the proton fraction (H^+) of a beam consisting of H^+, H_2^+, and H_3^+ extracted from a magnetically-confined microwave-driven plasma from 80% to more than 95% when operating under non-resonant (non-ECR) conditions by the addition of about 1% H_2O. Similar results are achieved in deuterium. This enhancement is achieved by increasing the neutral atomic species in the plasma by blocking atomic recombination on the walls, as we demonstrated by the wall temperature dependence of the dissociation fraction. Modification of neutral and ionic fractions in a variety of plasmas by several environmentally benign additives will be discussed. *Work supported by US DOE via ANL LDRD Funds.

[1]F. Kaufman, Advances Chem. 80, 29 (1969)
[2]D. Spence and K. R. Lykke, Proc. 1995 Part. Accel. Conf., Dallas, TX. IEEE Vol. 2, 1019 (1996)

8:30

H1A 3 A Self-Consistent Zero-Dimensional Numerical Description of a Nonequilibrium Hydrogen Plasma U.M. KELKAR, M.H. GORDON, L.A. ROE, *High Density Electronics Center, University of Arkansas, Fayetteville, AR 72701* We have developed a zero-dimensional model to determine gas temperature and composition, electron density and temperature for a microwave generated hydrogen plasma. Low pressure microwave discharges are characterized as two-temperature plasmas with non-Maxwellian electron energy distribution functions (EEDFs). A self-consistent analysis is performed through simultaneous numerical solutions of the Boltzmann equation, electron energy equation, and the rate equations for various ionic (H^+, H_2^+, H_3^+) and neutral particle (H, H_2, $H^{\prime *}$, $H_2^{\prime *}$) densities. The ground and excited state densities of H predicted by this comprehensive model are in good agreement with our previous [1] predictions which relied on only an atomic hydrogen model. For a 1.6 kW, 40 Torr hydrogen plasma, the numerical results are validated by the optical emission spectroscopic measurements of H excited state and electron number densities.

[1]M.H. Gordon and U.M. Kelkar, Phy. Plasmas, Vol. 3, 1 (1996)

8:45

H1A 4 Growth of Particles in Plasmas of Tetraethoxytitanium-Oxygen- Helium-Mixtures MARIO BICA DE MORAES, NILSON DA CRUZ, STEVEN DURRANT, *University of Campinas, SP, Brazil* Particle formation was observed in rf (40 MHz) plasmas of tetraethoxytitanium (TEOT)-oxygen-helium mixtures. A lens system of variable magnification (1 to 10X) provided optical observation of the particles through a glass viewport and a video camera was used for image recording. Light scattering from a He-Ne laser beam traversing the chamber was also used for particle observation. The particles were seen to levitate in the discharge, forming a cloud near the plasma sheath interface. Particles were roughly spherical, with sizes ranging from 0.020 to 300 microns as determined by combined optical and electron microscopy (scanning and transmission). High resolution Auger electron spectroscopy analysis of particles larger than 10 microns revealed the presence of C, Ti and O. This finding, together with the strong reduction in the average particle size and number density when TEOT was absent from the gas mixture, shows that gas-phase recombination of the TEOT molecular fragments is the dominant mechanism of particle formation.

9:00

H1A 5 Particle dynamics in a strongly-coupled dusty plasma R. A. QUINN, J. GOREE, J. B. PIEPER, *The University of Iowa* We have used video imaging to study the dynamics of 9 μm plastic spheres in low-power Krypton discharges. The spheres, which are highly charged and levitated by the electrode sheath, form a strongly-coupled system. Using a digitized series of images, we tracked individual particles and measured collective and random particle motions.[1] Dust acoustic waves were excited at $\leqslant$ 10 Hz and their dispersion relation verified. The temperature of random particle motion in the horizontal plane (parallel to the electrode) was measured to be 2-10 times room temperature and

about 2 times the temperature in the vertical plane. It is proposed that the particles are heated by low-frequency (kHz) electrostatic plasma fluctuations.

[1]Pieper and Goree, submitted to PRL

9:15

H1A 6 A Study of Neutral Behaviour in an ECR Discharge M.D. BOWDEN, W. CRONRATH, K. UCHINO, K. MURAOKA, *Kyushu University, Japan* N. SADEGHI, *Laboratouire de Spectrometrie Physique, France* Most experimental studies of high density plasma sources such as ECR and ICP discharges concentrate on charged particle behaviour. It is also important to understand the factors determining the behaviour of neutral species in these discharge but this is difficult due to the relative lack of appropriate diagnostic techniques. In this paper, measurements of the neutral density and temperature are reported for an argon ECR plasma. Rayleigh scattering was used to measure the neutral density and laser absorption spectroscopy was used to measure the neutral temperature and the dependence of these quantities on input power and gas pressure was measured. The results showed that in high electron density discharges, the neutral density in the plasma was depleted by up to 50% and that in high pressure discharges, the neutral temperature increased significantly. The experimental results were consistent with those from a simple analytical model of neutral behaviour and also with those from a hybrid fluid/PIC simulation of the discharge. These comparisons indicated that ion-neutral charge exchange collisions were the most significant factor in determining the neutral atom temperature and density.

9:30

H1A 7 Transport phenomenon in a Helicon Activated Reactive Evaporation system C.A. DAVIS, A. DURANDET, R.W. BOSWELL, *Space Plasma Group, R.S.Phys.S.E., The Australian National University, Camberra, ACT, 0200, Australia* The Helicon Activated Reactive Evaporation is a deposition system that combines an electron beam evaporation source and a high density helicon plasma source in a configuration where the evaporant is transported through the helicon source. Previously, we have reported that the scattering of the evaporant by the gas has a major effect on the deposition rate at the substrate. In this study, we present the investigation of the effect of the plasma on the transport of the evaporant. By evaporating silicon in an oxygen plasma, and by looking at deposition rate of silicon dioxide on the substrate, we show that the plasma strongly affects the transport of the silicon from the evaporation source to the substrate. Furtherrmore, when argon is introduced in the discharge, the transport of the silicon clearly differs from that observed without a plasma. Optical emission and energy selective mass spectrometry are used to further investigate these phenomenon.

9:45

H1A 8 The Effect of Bumps and Probes on the Ion Distribution Functions in High Density Discharges Containing Ar and Ar/Cl Mixtures J. R. WOODWORTH, B. P. ARAGON, *Sandia National Laboratories* T. W. HAMILTON, *Applied Physics International* The presence of obstructions (i.e. wafer clamps, langmuir probes) in plasma processing reactors can significantly affect plasma parameters. We are using a gridded energy analyzer to measure ion fluxes, energy distributions, and angular distributions in the presence of bumps on the wafer and probes in the plasma. Our measurements are being performed on an inductively coupled GEC reference cell. Bump heights varied from 1.5 to 6 mm with both metallic and ceramic bumps being tested. The probe consisted of a 1.2 cm-diameter ceramic pipe covering a grounded metal rod whose end was flush with the end of the ceramic pipe. We find that these two disturbances affect the ion energy distributions only slightly, lower the ion fluxes by a factor of two, and dramatically alter the ion angular distributions. Details of the apparatus and results will be discussed.

➢ ➢ ➢ ➢ ➢ ➢ ➢ ➢ ➢ ➢ ➢ ➢

SESSION H1B: ENVIRONMENTAL APPLICATIONS

Thursday morning, 24 October 1996; Lecture Hall at 8:00; S. Dhali, Southern Illinois University, presiding

Invited Papers

8:00

H1B 1 Global Warming Potenials of SF_6 and CF_4 and Implications Concerning Future Use of These Gases in Processing and Power Systems.

R. J. VAN BRUNT, *NIST, Gaithersburg, MD 20899*

The anthropogenic gases SF_6 and CF_4 have been discovered recently to be accumulating at rapid rates in the earth's atmosphere (8.4% per growth rate for SF_6). Although these gases presently make an insignificant contribution to the atmospheric green-house effect, they have estimated global warming potentials that are many thousands of times greater than that of CO_2. The high global warming potentials are consequences of: 1) their relatively long atmospheric lifetimes that exceed 10^3 years due to their chemical inertness, and 2) their high efficiency as absorbers of reflected solar infrared radiation. Of greatest immediate concern is SF_6 which is now widely used as a gaseous dielectric and arc interrupting-medium in high-voltage electric-power transmission systems. The processes that are believed to destroy these compounds, including lightning discharges and incineration in the troposphere and low-energy electron attachment initiated chemistry in the mesosphere, are examined. The problems of controlling the release of these gases and the issues and controversies surrounding attempts to find suitable replacements for SF_6 in switching and other power-system applications are examined.

8:30

H1B 2 Pilot Plant Tests of Gas Cleaning by Electron Beam and Corona Discharge Techniques
JEN-SHIH CHANG, *McMaster University, Dept.of Eng.Phys., Hamilton, Ontario, Canada*

Current on - going pilot plant studies of the gaseous pollutant emission control by an energetic electron induced plasma process are critically reviewed. The gaseous pollutants considered are :1)Acid gases such as SOx, NOx, NOy, HCl, H2S etc. in combustion and incenelator flue gases or tunnel air circulation system flue gases; 2) Greenhouse gases such as CO2, CxHy, NxOy, CFCs, SF6, NF4 etc. in combustion, semiconductor or chemical plant process flue gases; 3) Toxic gases such as dioxin, mercury, C2F6 etc. in municipal waste incenelation and semiconductor process flue gases; 4) Ozone depletion gases such as CFCs, Halon, CCl4, TCE, TCA etc. in refrigerant and chemical industrial flue gases; 5) Volatile organic compounds such as Xylene, Toluene, EGM etc. in painting and chemical industrial flue gases. An energetic electron induced plasma process considered are electron beam, pulse corona, barrier discharge, flow stabilized corona and their superimposed or hybrid systems. Fundamental principles, mechanisms, economy, reactors and pilot plant performances will be discussed in detail.

Contributed Papers

9:00

H1B 3 Effect of Closely Interacting Microstreamers on Energy Efficiency XUDONG "PETER" XU, MARK J. KUSHNER, *University of Illinois, Urbana, IL 61801* Dielectric Barrier Discharges (DBDs) are attractive plasma sources for remediation of toxic gases, and N_xO_y in particular, due to their ability to operate at atmospheric pressure with moderate applied voltages. The filametary plasma in DBDs is sustained in a narrow gap (2-5 mm) and is extinguished by charging of the dielectric covered electrodes. The efficiency of remediation is largely determined by the transient E/N in the gap, the radial expansion of the filaments and the interaction of closely spaced filaments. A 2-dimensional plasma chemistry model has been developed to investigate the hydrodynamics and plasma chemical processes in the DBD remediation of N_xO_y. In this talk, we will discuss the results from the model for efficiency of generating N, O and OH radicals from humid air as a function of voltage pulse shape, dielectric properties and microstreamer spacing. *Work supported by NSF and Office of Naval Research.

9:15

H1B 4 Removal of Tricholoethylene from Air Streams by a Superimposed Barrier Discharge Plasma Reactor KUNIKO URASHIMA, *McMaster University, Dept.of Eng.Phys., Hamilton, Ontario, Canada* TAIRO ITO, *Musashi Insititute of Technology, Dept.of E&E Eng., Tokyo, Japan* JEN-SHIH CHANG, *McMaster University, Dept.of Eng.Phys., Hamilton, Ontario, Canada* In this work, superimposed barrier discharge - activated carbon filter hybrid systems are used to remove TCE from air streams, and the mechanism of TCE decomposition is investigated. The superimposed barrier discharge consisted of silent and a surface discharges. Experiments are conducted for the gas flow rate from 0.1 to 10 L/min, applied power from 0 to 7 W and TCE initial concentration from 0 to 2,000 ppm for 60 Hz ac applied voltage conditions. Discharge by-products are measured by FTIR, GC and TLV VOC detector. The results shows that; 1) TCE decomposition rate nonmonotonically increases with increasing applied power up to discharge power around 4 W and decreases with increasing applied power; 2) Approximately 50% of TCE is removed by plasma reactors and the other 50% is removed by activated carbon filters; 3) TCE is decomposition to form CO, CO2, H2O, HCl and Cl2, and HCl and Cl2 are adsorbed in activated carbon filters; 4) No COCl2 is observed in a discharge by-products for the present range of experiments; 5) Aerosol particles are also observed as a discharge by-products.

Invited Paper

9:30

H1B 5 Application of Plasma Arcs to the to the Remediation of Shipboard Waste[1].
JOHN L. GIULIANI, *Naval Research Laboratory*

The Naval Research Laboratory [2] (NRL) is investigating the application of plasma arc technology for the on-board remediation of waste material generated by sea faring ships. A 150kW DC arc torch within a 1 meter diameter chamber has been used for the pyrolysis of liquid and solid material which simulate the waste stream from a naval ship. A general discussion of the materials treated and the associated problems arising from their pyrolysis in a plasma torch will be presented. The greatest challenge for a shipboard plasma remediation, including any exhaust gas treatment, is the overall size of the system imposed by the limited confines of a ship. Connected with this issue are choices of the arc configuration: transfered vs non-transfered; and the feed stock gas: reducing vs oxidizing. The research component of NRL's program is to characterize the gaseous by-products, the remnant slag, and the plasma arc through systematic experiments, as well as to model the plasma dynamics and chemistry within the chamber. The environment within the chamber is primarily defined by several temperature measurements. Two color pyrometry is used to determine the molten slag temperature (~2200degK) and a suite of thermocouples within the chamber indicate a slighter cooler gas phase temperature. Synthetic spectra were generated from radiation transport calculations and compared with optical emission spectroscopy to map the gas temperature around the plasma arc itself (~5000degK). Spectroscopy offers the potential of a non-invasive diagnostic to eventually be used for on-line process control, a necessary feature for an operating system due to the heterogeneous waste stream. Other studies will be described including the addition of O_2 through a ring to achieve combustion of hydrocarbon wastes, residual gas analysis of the exhaust for different waste material, the voltage-

current characteristic at various plasma arc lengths to estimate plasma conductivity, and the surface shape of the molten slag given the pitch and roll of a ship.

[1]Supported by ONR and NSWC.
[2]B. Sartwell, (Chemistry Division NRL); J. Apruzese, (Plasma Physics Division NRL); S. Peterson, D. Counts, (Geo-Centers Inc.),and Q. Han (U. Minn.)

SESSION H2A: PLASMA AND SURFACE CHEMISTRY IN SEMICONDUCTOR PROCESSING
Thursday morning, 24 October 1996; Auditorium at 10:30; M. Surendra, IBM Watson, presiding

Invited Paper

10:30
H2A 1 A Study of Plasma-Surface Interactions during ECR Plasma Etching of S i in Cl_2.
KOUICHI ONO, *Mitsubishi Electric Corp., Advanced Technology R&D Center, Amag asaki 661, Japan*

A mechanistic study of ECR plasma etching processes for Si in Cl_2 (0.2-10 mTorr) has been made through in situ diagnostics of reactant and product species during processing, to unravel the reaction mechanisms characteristic of low-pressure, high-density plasma etching environments. The fluxes and energies of ions and neutrals onto the substrate were specified primarily by LIF and electrical measurements with Langmuir probes and a retarding grid analyzer. These diagnostics, in combination with etch rate measurements, indicated that at low pressures <1 mTorr, the Si etch rate is limited by the supply of neutrals onto the surface, where the flux of Cl_2 molecules cannot account for the etch yields obtained; the chlorine needed to form reaction products is provided by the incoming Cl_2^+ ions as well as neutral reactants of Cl_2 and Cl, but the Cl-coverage on the surface is expected to be still lower than unity. Moreover, the reaction products were monitored both in the gas phase and on the substrate surface by FTIR absorption spectroscopy, where $SiCl_4$ was the only IR-absorbing etch product species detected in the gas phase, and in contrast, unsaturated $SiCl_x$ (x=1-3) as well as $SiCl_4$ were observed on the surface. Absolute calibration showed that at low pressures <1 mTorr, the concentrations of $SiCl_4$ in the discharge during etching are comparable to the feedstock Cl_2 gas densities. A broad absorption feature due to silicon oxides was also found to occur both in the gas phase and on the surface, where oxygen came probably from erosion of the quartz microwave entrance window. Based on these observations, modeling calculations of profile evolution during etching were made as a function of ion-to-neutral flux ratio onto the substrate, including effects of etch products and oxides. A comparison of the etched profiles experimentally and numerically obtained provides an insight into plasma-surface interactions in microstructures.

Contributed Papers

11:00
H2A 2 Beam Studies of Etching Si and WSi_x with Chlorine and Oxygen GOWRI KOTA, JOHN COBURN, DAVID GRAVES, *University of California, Berkeley, CA* Tungsten silicide (WSi_x) / poly-Si layers are commonly used as gate-electrode material in microelectronic devices. The patterning of these polycide layers is done by a variety of halogen-based dry processing etching techniques. However, there is little fundamental understanding of the etching mechanisms involved. We study the etching of WSi_x and poly-Si with Cl_2 / O_2 gas mixtures. In our experiments, a beam of Cl atoms from an inductively coupled plasma source effuses into a high vacuum chamber and impacts the sample. The etch products from the sample surface are detected with a modulated beam mass spectrometer. For the results reported here, the fraction of atomic Cl in the incident beam is estimated to be 0.7. In the presence of 1 keV Ar^+ ion bombardment, etch rate for WSi_x with atomic chlorine is about six-times that with molecular chlorine. The Si etch rate is enhanced by only a factor of two with atomic chlorine. Therefore, the etch selectivity of WSi_x over Si increases in the presence of chlorine atoms. The etch rate dependence of WSi_x and Si for various chlorine to oxygen composition ratios is also reported.

11:15
H2A 3 On the Origin of the Notching Effect in Uniform High Density Plasmas GYEONG S. HWANG, KONSTANTINOS P. GIAPIS, *Caltech, Pasadena, CA* We present a Monte Carlo simulation of profile evolution during the overetch step of polysilicon-on-insulator structures, which considers explicitly a) electric field effects during the charging transient, b) etching reactions of energetic ions impinging on the poly-Si, and c) forward inelastic scattering effects. The simulation predicts that local sidewall etching (notching) will occur as a result of ion trajectory bending caused by a combination of positive charging of the trench bottom and negative charging of the sidewall foot. The latter is particularly significant at the outermost poly-Si line of a grating-type structure, which receives more electrons at the side facing the open area. The electrostatics of the problem requires electron redistribution in the poly-Si and accumulation near the poly-Si/SiO_2 boundary at the inner sidewall surface. The excess negative charge there re-accelerates ions to energies sufficient for reaction. Forward scattering of reactive particles, which occurs at large incident angles, is essential in determining the shape of the notch profile. The model explains why notching occurs near the poly-Si/SiO_2 inter-

face and predicts precisely the topography evolution during overetching. Furthermore, the model delineates the effects of plasma parameters and the open area between grating structures on the notching depth and shape, in agreement with experimental observations.

11:30

H2A 4 Microwave spectroscopic measurements of intermediate products in ECR silicon oxide deposition plasmas R. CLAUDE WOODS, EDWARD AUGUSTYNIAK, KOK HENG CHEW, J. LEON SHOHET, *ERC for Plasma-Aided Manufacturing, University of Wisconsin, Madison, WI 53706* Microwave spectroscopy in the 75-110 GHz range was applied to measure densities of 20 molecules in O_2+TEOS (tetraethoxysilane) and $O_2+SiH_4/SiF_4/CF_4$ silicon oxide deposition plasmas created in a 2.45 GHz electron cyclotron resonance (ECR) reactor. In the O_2+TEOS system, sequential oxidation products of the ethoxy fragments from TEOS were observed: C_2H_5OH, CH_3CHO, CH_2CO, CH_3OH, H_2CO, and HCOOH. In fuorinated silane-based plasmas neutral CH_xF_{4-x}, OCF_2,FHCO, CF_2, SiH_xF_{4-x}, and SiF_2, as well as the SiF^+ ion, were monitored. The SiF^+ density increased with plasma power, while concentrations of the neutral molecules decreased with power. It appears that the dissociation of molecular species is very extensive at the higher power used in industrial microelectronics applications. This work was supported by the NSF under Grant No. EEC-8721545.

11:45

H2A 5 GaAs Surface Chemistry and Surface Damage in a Cl_2/Ar High Density Plasma Etching Process C.R. EDDY, JR., O.J. GLEMBOCKI, D. LEONHARDT, V.A. SHAMAMIAN, R.T. HOLM, J.E. BUTLER, *U.S. Naval Research Laboratory* S.W. PANG, *University of Michigan* High density plasma etching of III-V compound semiconductors is critically important to the development of advanced optoelectronic and high frequency devices. Unfortunately, the surface chemistry of these processes is not well understood. In an effort to monitor surface processes and their dependence on process conditions in a realistic etching environment, we have applied optical emission and mass spectroscopic techniques for the study of GaAs etching in a Cl_2/Ar chemistry. Etch product chlorides were monitored, together with optical measurement of the surface temperature by diffuse reflectance spectroscopy, as pressure (neutral flux), microwave power (ion flux) and rf bias of the substrate (ion energy) were varied. Observations from the spectroscopic techniques were correlated with ex situ surface damage assessments by photoreflectance spectroscopy. As a result, insights are made into regions of process conditions that are well suited to anisotropic, low damage etching.

Invited Paper

12:00

H2A 6 Plasma Processing for Flat Panel Displays: Mechanisms for Polysilicon Passivation in Hydrogen Plasmas.

AMY E. WENDT, *Dept. of Electrical and Computer Engineering and ERC for Plasma-Aided Manufacturing, University of Wisconsin, Madison, WI 53705*

Although fabrication of liquid crystal-based flat panel displays has much in common with integrated circuit processing on large diameter silicon wafers, it also presents some new challenges. Fabrication of flat panel displays involves plasma processing for sputter deposition, plasma-enhanced chemical vapor deposition (PECVD), etching and for displays using polycrystalline silicon, hydrogen passivation. This presentation will include an overview of plasma processing issues for flat panel displays, in addition to a more in-depth discussion of the particular problem of polysilicon passivation. Plasma immersion has been proposed as a technique for introduction of hydrogen into the polysilicon film to passivate defects, as is necessary to achieve required thin film transistor (TFT) performance for AMLCD flat panel display circuitry. It has been demonstrated that high rates of hydrogen passivation can be obtained by using electron cyclotron resonance (ECR) discharges, with optimal process rates at well below 1 mTorr H_2 pressure. This presentation addresses mechanisms governing observed rates and implications for production scale processes. In-line mass spectrometer measurements at the substrate location in H_2 ECR discharges support the hypothesis that the process rate is correlated with the flux of atomic (H and H^+) as opposed to diatomic hydrogen species to the substrate. Measurements of both neutral and ion fluxes to the substrate surface, to be presented, show that the flux of atomic species relative to that of H_2 and H_2^+ increases with decreasing discharge pressure over the range 0.1-1 mTorr. In combination with Langmuir probe measurements of plasma potential, electron density and electron temperature, these results yield both ion composition and total flux as well as an estimate of ion energy for each operating condition. These results point to both ion energy and the flux of H^+ as likely factors influencing process rates. Finally, we examine the possible benefits of 1) applying a substrate bias voltage to increase ion bombardment energy and 2) O_2 addition to the discharge. Based on these results, prospects for process transfer to planar rf inductive discharges will be discussed. *Contributions of R. Bassett, E. Cielaszyk, K. H. R. Kirmse, D. Smith and T. J. King, and support through NSF Grant #ECD8721545 are gratefully acknowledged.

➢ ➢ ➢ ➢ ➢ ➢ ➢ ➢ ➢ ➢ ➢ ➢ ➢

SESSION H2B: DISCHARGE MODELS
Thursday morning, 24 October 1996
Lecture Hall at 10:30
W.N.G. Hitchon, Univ. of Wisconsin, presiding

10:30
H2B 1 Electron Energy Degradation in Rare Gases. M. DILLON, *Argonne National Lab, Argonne, IL* M. KIMURA, *Yamaguchi University* The one dimensional Boltzmann equation was solved for the degradation of high energy electrons in rare gases. An iterative integration method was employed in which the continuous slowing down approximation replaces the energy loss integral in the collision term. The results are compared with those obtained from an exact integration. This work extends an earlier study employing a steady state formulation [1].

[1]K. Kowari Phys. Rev. A 4, 2500(1989)

10:45
H2B 2 Argon Metastables at High Degrees of Ionization R.F. FERNSLER, M. LAMPE, W.M. MANHEIMER, D. LEONHARDT, C.R. EDDY, V.A. SHAMAMIAN, J.E. BUTLER, *Naval Research Laboratory* The metastable density in plasma discharges in argon and other noble gases is often high, because of the long lifetime of the metastables and the absence of low-lying excited states. Collisions of the second kind then control the discharge, and the simplicity of using noble gases is lost. However, electron excitation to higher-lying resonance states destroys metastables and caps their population, as long as the radiation is not trapped. In this work a simple model is presented to show that the metastable density is a strong function of electron temperature but a weak function of electron density, and that it is generally less that 0.1% of the ground-state density. The electron density can therefore considerably exceed the metastable density, which suggest that metastables become unimportant at high degrees of ionization, contrary to conventional wisdom. Measurements taken in an ECR argon plasma support the analysis. Work supported by the Office of Naval Research

11:00
H2B 3 Dust Transport in a Strongly Coupled Plasma* HELEN H. HWANG, MARK J. KUSHNER, *University of Illinois, Urbana, IL 61801* Particulate contamination in plasma processing reactors is a continuing problem in the microelectronics industry. When particle densities get large (100s to 1000s cm^{-3}), particularly in trapping locations, particle-particle Coulomb interactions become important. Under conditions where the particle kinetic energy is small due to damping by fluid drag, particles may condense to form strongly coupled Coulomb fluids or solids. We will present results from a computer simulation for dust transport in reactive ion etching discharges which includes Coulomb particle-particle interactions. The model is an extension of the existing Dust Transport Simulation (DTS) that integrates particle trajectories based on electrical and mechanical forces. The Coulomb interactions are included on a particle-particle basis using a cutoff distance based on the linearized Debye length. We will demonstrate Coulomb condensation of particles in trapping locations, particle ejection from filled traps, and phase changes (solid to liquid) due to impingment of energetic particles. *Work supported by SRC, NSF, SNLA/Sematech and the U of Wisconsin ERC.

11:15
H2B 4 A two dimensional modeling of capacitively coupled plasma reactor N. NAKANO, T. MAKABE, *Keio University, Yokohama* We have developed a two dimensional modeling based on the relaxation continuum (RCT) model for capacitively coupled plasma(CCP) reactor. Present 2D-model is one of the powerful tool to understand and design dry processes using a nonequilibrium plasma. 2D-t profile of net excitation rate and number densities of charged particles are shown in Ar 0.1-1.0Torr at 13.56MHz, with or without selfbias. These results are compared with tomographic imagings using optical emission spectroscopy [1]. A 2D-ion flux distribution provides an important information for the surface uniformity in plasma processings. The degree of non-uniformity of the ion flux changes with increasing the sustaining voltage. Under almost the minimum sustaining condition of 30V at 0.5Torr, the ion flux has no peak in the radial direction, because of a weak field E_r. With increasing the voltage, the radial peak of ion flux appears inside of the electrode edge. At 150V, the axial field component E_z is much higher than the E_r even near the rf electrode edge, and the uniformity of the ion flux is recovered again. At the 0.1Torr, the radial peak is weakened due to a wide sheath in front of the drive electrode.

[1]T. Kitajima, M. Izawa, R. Hashido, N. Nakano and T. Makabe, Appl Phys. Lett., (accepted)

11:30
H2B 5 Three-dimensional DSMC Simulations of the GEC Reference Cell Reactor MARC RIEFFEL, STEPHEN TAYLOR, *Scalable Concurrent Programming Laboratory, Caltech, Pasadena, CA* SADASIVAN SHANKAR, *Intel Corporation* This paper presents several simulations of the Gaseous Electronics Conference (GEC) Reference Cell Reactor. A novel simulation technique, using a scalable parallel implementation of the Direct Simulation Monte Carlo (DSMC) method, is used to simulate electrons, ions, and neutrals as they flow through the reactor. Complex gas-phase chemical processes are modeled, including electron-impact dissociation and electron excitation. The simulations are fully three-dimensional, using the complete geometry of the reactor. Several cases are considered, using different pressures, flowrates, and injection configurations. Results demonstrate that changing the injection configuration can have significant effects on the uniformity of gases above the wafer.

11:45
H2B 6 PIC Simulations of Pulsed-power O_2 Discharges* VENKATESH P. GOPINATH, *U. C. Berkeley, Berkeley, CA* VAHID VAHEDI, *Lam Research Corporation, Fremont, CA* Pulsed-power discharges are attracting much attention due to their ability to control processing performance by changing pulse period and duty ratio, in addition to the conventional control parameters such as gas pressure, input power and flow rate. It has been proposed that negative ions can be extracted from the plasma during the power off time of the cycle and can enhance the etch rate and reduce device damage. Because the negative ions can leave the discharge only when the sheath collapses, one can study the afterglow of a discharge to investigate the time it takes for the negative ions to arrive at the wall, and the decay of the electron energy distribution function. Hence we simulate the afterglow of an O_2 discharge using PDP1, a 1D3V PIC-MCC (Particle in Cell-Monte Carlo Collisions) code. The behavior of electron temperature, charged particle densities and plasma potential during the off time will be observed. We will determine the sheath collapse time and the time it takes to extract negative ions. The results of the PIC

simulations will be compared with a volume averaged global model of a pulsed power O_2 discharge.

*This work was supported in part by ONR under grant FD-N00014-90-J-1198

12:00

H2B 7 High-Resolution, Adaptive Simulation of Inductively Coupled Plasma Reactors MILO R. DORR, PHILLIP COLELLA, *Lawrence Berkeley National Laboratory, Center for Computational Sciences and Engineering, One Cyclotron Road, MS:50D-141, Berkeley CA 94720* DANIEL D. WAKE, *Lawrence Livermore National Laboratory, University of California at Davis, P.O. Box 808, L-416, Livermore, CA 94551* A significant challenge arising in the use of fluid codes for the study of inductively coupled plasma (ICP) reactors is that the use of a grid spacing appropriate for sheath regions throughout the plasma would be prohibitively expensive while using a coarse grid spacing within a sheath region would miss much of its behavior. This problem has previously been addressed by utilizing analytic sheath boundary conditions or various types of hybrid methods. However, a number of complications arise concerning the appropriate location of the bulk/sheath boundary, unphysical behavior of the state variables at the transition, and communication between the bulk and sheath models. In this talk, we present a new computational technique for the modeling of ICP reactors that addresses these issues. A multi-component fluid model is discretized and solved by combining high-resolution finite-difference methods with an adaptive mesh refinement (AMR) strategy. By employing different grid resolutions in the bulk and sheath regions in a single integrated model, one can eliminate many of the aforementioned difficulties. We will discuss the model, the AMR technique and software implementation. Numerical results will be presented.

12:15

H2B 8 Modeling of atmospheric pressure discharges M. MEYYAPPAN, T.R. GOVINDAN, *Scientific Research Associates, Glastonbury, CT* PETER VENTZEK, *Hokkaido University* Recently atmospheric pressure glow discharges have been developed as commercial plasma sources for material processing applications. Potential applications include wafer thinning, plasma ashing etc. in the fabrication of flat panel displays. In developing these sources, several techniques have been used to stabilize the plasma which is important and used to be a problem preventing the use in processing. A model for atmospheric pressure Rf discharges has been developed. The approach consists of a fluid model for electrons and ions in an inert gas mixture. Rate constants from a Boltzmann solver are used for inelastic processes. This model is iterated with a two dimensional gas flow and heat transfer analysis to predict gas density variations and heat dissipation. Results are presented for a 2 mm electrode gap at various driving voltages in terms of plasma density, current-voltage predictions, power coupling mechanisms and gas flow related issues.

SESSION H3A: DISCHARGE EXPERIMENTS
Thursday afternoon, 24 October 1996
Auditorium at 13:30
N. Sr. J. Braithwaite, Open Univ. Oxford, presiding

13:30

H3A 1 Formation of Methanol and Dimethyl Ether in Dielectric Barrier Disch arges ULRICH KOGELSCHATZ, *ABB Corporate Research, 5405 Baden, Switzerland* The generation of liquid fuels like methanol (MeOH) and dimethyl ether (DME) from the greenhouse gases (GHG) methane and carbon dioxide has recently attracted growing attention. Investigations of this kind are part of efforts to reduce GHG emissions to the atmosphere. For our investigations we used a tubular dielectric barrier discharge reactor with an annular discharge gap of 1 mm width and a cylindrical quartz dielectric of 2.5 mm thickness. It was operated in methane-oxygen mixtures at pressures between 1 and 4 bar. The discharge was operated at a frequency of about 18 kHz. The power density could be raised up to 20 kW/m^2 of electrode area by increasing the applied voltage. Up to 1.3% MeOH and .4% DME were measured after a single passage through a discharge gap of 310 mm length by GC and GC/MS detection. These values were obtained at 2 bar, substantially lower values were measured at 1 or 4 bar operating pressure. At high specific energies >8 eV per molecule of feed gas the MeOH concentration decreased and methyl formate appeared in the product stream.

13:45

H3A 2 Hollow Electrode Discharge Triodes K.H. SCHOENBACH, F.E. PETERKIN, *present address: NSWC Dahlgren, VA* T. TESSNOW, *Physical Electronics Research Institute, Old Dominion University, Norfolk, VA* W.C NUNNALLY, . *Dept. Electrical Engineering, University of Missouri, Columbia, MO* The current through a direct current micro-hollow electrode (electrode hole diameter: 0.7 mm) discharge in argon was shown to be controllable by means of a third, external electrode placed close to the cathode opening. By increasing the potential of the positively biased control electrode from zero to 30 V the discharge current could be linearly reduced from 5 μA to 0.75 μA, at a discharge voltage of 300 V. The current-voltage characteristic of the micro-hollow electrode discharge was found to have a positive slope, allowing parallel discharge operation without ballast. By drilling holes through a metal-plated, dielectric film, an array of hollow electrode discharges could be generated. It was shown that each discharge responds individually to variations in the potential of the corresponding external control electrode. The simplicity of the electrode configuration and the possibility of linear, electrical control of the individual discharge currents offers the possibility to use these triode arrays in addressable flat panel displays (patent pending).

14:00

H3A 3 Hydrogen fractional dissociation in H_2/He mixture discharges B. N. GANGULY, P. BLETZINGER, R. NAGPAL, *Wright Laboratory, WPAFB, OH* The fractional dissociation efficiency of H_2 in $He-H_2$ and H_2-N_2-He gas mixture discharges has been measured by two-photon laser induced fluorescence in the downstream region of a helical resonator plasma source operating in the inductive mode. The measurements were performed with 0.5 Torr up to 3 Torr total gas pressure, and $40-60$ Watt input power. For lower pressure discharge conditions where $50-60\%$ of total input power goes to H_2 dissociation, the increasing He dilution leads to a decrease in H atom density nearly proportional to the H_2 partial pressure. For higher pressure discharges the fractional H_2 dissociation efficiency increased with increase in He dilution. The measurements are consistent with the calculated direct electron impact dissociation rates of H_2 for $He-H_2$ gas mixture discharges operating from $30-120$ Td. This is in contrast to H_2-N_2-He gas mixture discharges, where heavy particle energy transfer processes from the N_2 vibronic states have to be invoked to explain the observed dissociation efficiency.

14:15

H3A 4 Measurements of $N_2(A)$ Metastable State Density in a Nitrogen Glow Discharge J.SEBASTIAN ODDONE, JUAN A. CURIAL, TONY J. COSCHIGNANO, KENNETH A. HARDY, J.W. SHELDON, *Physics Department, Florida International University* Measurements of the rate of effusion of metastable $N_2(A)$ molecules from a slit in the anode of a low pressure, low voltage, hot cathode discharge are reported. The effusing metastables are collimated into a beam from which charged particles are electrostatically removed. The beam is chopped near the anode source and detected by counting pulses initiated by metastable ejection of Auger electrons in a channeltron. This arrangement allows time-of-flight (TOF) analysis of the beam. The metastable yield as a function of discharge pressure, temperature, current, voltage and axial magnetic field are reported. The temperature is determined by fitting the TOF spectra to the function expected from a Maxwellian distribution of $N_2(A)$ in the discharge. The yield is compared with a kinetic model of $N_2(A)$ production following the work of Cernogora *et al.* [1] [2]

[1]G. Cernogora, L. Hochard, M. Touisau and C. Matos Ferreira, J. Phys. B. At. Mol. Phys. 14, 2977 (1981).

[2]Supported by grants from NASA (NAG 5-2583) and the AFSOR(F49620-93-1-015DEF).

14:30

H3A 5 Optical Pumping of a He RF Discharge M. A. HUMPHREY, *Western Michigan University* B. G. BIRDSEY, *University of Nebraska-Lincoln* K. W. TRANTHAM, *The Australian National University, Canberra, Australia* H. BATELAAN, T. J. GAY, *University of Nebraska-Lincoln* A helium RF discharge has been investigated as a source of polarized electrons. By optical pumping with distributed Bragg reflector (DBR) diode lasers, metastable 2^3S_1 He atoms have been spin oriented, and a measure of the metastable polarization has been made. Since the predominant ionization channels in the discharge favor production of spin-polarized electrons from the metastable atoms, a beam of polarized electrons can be extracted. [1] In previous measurements with a DC discharge, we have measured between 6% and 7% electron polarization in an extracted current of 200 microamps. [2] We will present results on the polarization of the He atoms as a function of various discharge and pump laser parameters. This work is supported by NSF grant PHY-9504350.

[1]M. V. McCusker, P.R.A. 5, 177 (1972)

[2]R. J. VanDiver, Ph.D. Thesis, Univ. of Missouri-Rolla (1994, unpublished)

SESSION H3B: MODELS OF GLOW DISCHARGES AND POSITIVE COLUMNS
Thursday afternoon, 24 October 1996
Lecture Hall at 13:30
Graeme Lister, presiding

13:30

H3B 1 3D Modeling of a dc glow discharge in argon, and comparison with experiment ANNEMIE BOGAERTS, RENAAT GIJBELS, *University of Antwerp, Dept. of Chemistry, Belgium* In order to achieve a better understanding of the glow discharge, 3D models have been developed for different plasma species, and combined to obtain an overal picture of the glow discharge. The fast electrons are treated with a Monte Carlo model in the entire discharge. The slow electrons and the argon ions are considered in a fluid model in the entire discharge. Moreover, the argon ions, together with the fast argon atoms which are created by charge transfer and elastic collisions from the argon ions, are described with a Monte Carlo model in the cathode dark space only. The argon metastable atoms are handled with a fluid model in the entire discharge. The thermalization process of the sputtered cathode atoms is described with a Monte Carlo model. The further diffusion and the creation of cathode ions, are handled in a fluid model. Finally, the behavior of these cathode ions in the cathode dark space is treated with a Monte Carlo model. Typical results of the models are the densities and fluxes of the different plasma species, the electric field and potential distributions throughout the discharge, the energy distribution and information about collision processes of the plasma species. The modeling results have been compared with results of laser induced fluorescence measurements, and very good agreement is reached.

13:45

H3B 2 3-D PIC-MCC Simulation of DC Glow Discharge VLADIMIR SERIKOV, KENICHI NANBU, *Institute of Fluid Science, Tohoku University, Sendai 980-77, Japan* Particle-in-Cell Monte Carlo Collision (PIC-MCC) algorithm is developed to clarify the 3-D structure of a parallel-plate DC glow discharge. The case study is then fulfilled, in which the discharge in argon under a low pressure (=42 mTorr) is simulated as taking place between 6 cm diameter powered and grounded circular electrodes separated by 4 cm in a grounded conducting rectangular chamber. Motion of ions and electrons is calculated in a self-consistent electric field, which is obtained from Poisson's equation by the FFT algorithm at each time-step for electrons. The model of collision processes in argon encompasses ionization, excitation and elastic collisions between electrons and atoms, as well as charge exchange and elastic collisions between ions and atoms. Spatial distributions of the electric field and discharge macroparameters are calculated. The oscillations of the discharge parameters have been revealed as taking place with the frequency close to the plasma frequency.

14:00

H3B 3 Determination of the Self–Consistent Space Charge Potential Using the Nonlocal Approach ERIC J. BENNETT, WILLIAM F. BAILEY, *Air Force Institute of Technology, Wright–Patterson AFB, OH* In the positive column of a DC glow discharge, the electron distribution function (EDF) is determined by the axial electric field and, in part, by the transverse space charge potential. Conversely, the form of this potential depends upon the EDF. A theory has been developed which extends the nonlocal approach [1] by coupling the solution of the Boltzmann equation with solutions of Poisson's equation and balance equations for both electrons and ions, enabling a self–consistent solution for the discharge operating point and transverse potential. Comparisons with the traditional local theory of Schottky revealed mean energy differences of over 60 percent and potential profiles that deviate significantly from those found in the local theory. The spatial distribution of the excitation and ionization rates reflected the influence of the potential, becoming highly centralized. Comparisons with experimental results in neon showed reasonable agreement for both the wall potential and operating point and confirm the failure of the local theory under these conditions.

[1]Bernstein, I. B. and T. Holstein. "Electron Energy Distributions in Stationary Discharges," Physical Review, 94:1475-1482 (June 1954).

14:15

H3B 4 Numerical Simulations of Glow Discharge between Two dissimilar electrodes in a Body Fitted Coordinate System WEI "IVY" QIN, IRA M. COHEN, P. S. AYYASWAMY, *University of Pennsylvania* In this paper, heat transfer to the electrodes, current growth and potential drop between the electrodes have been calculated by a complete numerical simulation of the discharge between a cylindrical wire and a planar wand electrode with a body fitted coordinate system. The body fitted coordinate system was generated by solving a set of elliptic equations. The simulation includes investigation of the discharge development and ionization growth from the initial electrostatic field between the electrodes. In the computations, the conservation equations for ions and electrons, Poisson's equation for the self-consistent electric field, and the energy conservation equation for electrons have been solved until the steady state is reached; the voltage between the two electrodes is adjusted after each time step depending on the current flow in the gap. Results for current growth, potential drop in the gap as well as heat transfer to the wire are presented for two different current levels. The heat transfer to the electrode as well as the charge particle densities were found to be proportional to the current level. The temperature of the electrons in the gap during the discharge does not vary significantly with current. The numerical results compare favorably with those of experiments.

14:30

H3B 5 Fluid Analysis of the DC Positive Column with Nonzero Ion Temperature. JOHN INGOLD, *One Bratenahl Place #610, Bratenahl, OH 44108* Fluid analysis of the transition from free to ambipolar diffusion in the DC positive column is revisited.[1] Using Gear's BDF method, constant temperature fluid equations, including Poisson's equation, are solved numerically for zero ion temperature, then for nonzero ion temperature by "jumping over" the apparent singularity which occurs at the position where radial ion velocity is equal to the isothermal ion sound speed. Comparison shows that the zero ion temperature approximation predicts the correct electron impact ionization frequency over the entire range of central electron density from the ambipolar diffusion limit to the free electron diffusion limit. Numerical solutions for electron, ion densities $n_{e,p}(r)$, and space charge potential $V(r)$, are presented for model atoms similar to neon and argon without ionization of excited levels using transport coefficients determined as functions of E_z/N by 0-D Boltzmann analysis,[2] with gas density N ranging from $1-100\times10^{14}$ cm^{-3}, gas temperature of 300 K, tube radius of 1 cm, and tube current of 10 mA. Results are compared with results from various simulations reported in adjoining abstracts.

[1]W. P. Allis and D. J. Rose, Phys. Rev. **93**, 84 (1954); J. H. Ingold, Phys. Fluids **15**, 75 (1972).
[2]0-D Boltzmann transport coefficients for argon provided by U. Kortshagen; those for neon by Kinema Software's ELENDIF.

14:45

H3B 6 Benchmark Monte Carlo simulations of positive column discharges J. E. LAWLER, *Physics Department, University of Wisconsin, Madison, WI 53706* U. KORTSHAGEN**, *Physics Department, University of Wisconsin, Madison, WI 53706* G. J. PARKER, *Lawrence Livermore National Lab* A null-collision Monte Carlo algorithm is being used to simulate electron transport in positive column discharges. The use of a piecewise harmonic radial potential makes the electron motion completely analytic and makes the Monte Carlo code very efficient. The Monte Carlo code is partially self-consistent in that the axial electric field and sheath potential are adjusted to satisfy ionization balance constraints. The detailed radial potential is either imported from a fully self-consistent simulation or is assumed. These results serve as a benchmark for comparison to results from other models based on the nonlocal and the local field approximations, and the Convected Scheme. Identical cross sections and boundary conditions are used in the various simulations which are reported in adjoining abstracts. The primary goal of the project is to define the accuracy limits and range of applicability of various approximations in positive column simulations. Accurate radial dependencies are of particular interest. [1]

[1]Supported by the NSF.

15:00

H3B 7 On the treatment of wall losses of energetic electrons in nonlocal Boltzmann calculations U. KORTSHAGEN, *Univ. of Minnesota–Minneapolis, Mech. Eng.* J. E. LAWLER, *Univ. of Wisconsin–Madison* G. J. PARKER, *Lawrence Livermore National Laboratory* The nonlocal approximation to the solution of the Boltzmann equation in low pressure discharges applies strictly only to the electrons which are confined in the plasma volume by the space charge electric field. The free electrons which have a sufficiently high total energy to overcome the space charge potential barrier in front of the walls and which can therefore be lost from the plasma to the walls are not consistently addressed by the nonlocal model. We compare nonlocal calculations for the electron distribution function in a positive column plasma with and without inclusion of the wall losses in different approximations to results of a Monte Carlo benchmark method. The importance of a correct treatment of the wall losses of free electrons is demonstrated. Also the impact of the wall losses on the isotropy of the electron distribution function is discussed.

15:15

H3B 8 New Convected Scheme simulations of positive column discharges G. J. PARKER, *Lawrence Livermore National Laboratory* U. KORTSHAGEN, J. E. LAWLER*, *Univ. of Wisconsin–Madison* The Convected Scheme (CS) provides a solution of the Boltzmann equation by using a phase-space computational mesh on which particle densities are iterated in time by use of Green's functions or "propagators'U. A new propagator to describe the collisionless radial motion in a piecewise harmonic radial potential is presented and discussed. In contrast to previous propagators, this one exhibits no cumulative errors due from either the finite size of the computational mesh or the time step used. In the absence of collisions, the propagator is exact at all time scales to within the limit of the spatial resolution specified. The new CS is used to calculate electron transport in positive column discharges over a range of neutral pressures. The axial electric field and sheath potential are adjusted to insure that ionization and radial loss constraints are met. Results are compared to Monte Carlo and other simulations which are reported in adjoining abstracts. *Supported by the N.S.F.

Author Index

A

Abraham, Ion C. **M1A 3**
Abraham-Shrauner, Barbara **MPB 5**, MPB 6
Abramzon, N. TUPB 13
Adams, Nigel G. **M3B 2**, MPC 10, WPB 4
Alexandrovich, Benjamin MPA 1, MPA 17
Ali, M.A. MPC 1
Aliev, Y.M. **TU1A 4**
Allen, Mark M2A 2
Alvarez, I. TUPB 2, WPB 5
Alves, L.L. WPA 1
Al-Wazzan, R. WPC 2
Amorim, J. WPA 9
Anderle, Mariano M1A 2
Anderson, Cheryl MPB 7
Anderson, Harold **M2A 1**, MPA 7, MPA 8
Anderson, Heidi M. WPB 3
Anderson, L.W. W2B 1, W2B 2, WPA 7, WPA 8
Ang, L.K. TUPA 22
Angus, John **W1B 3**
Anschütz, Franz-Burkhard **TUPC 10**
Antonio Algatti, Mauricio WPA 12
Aragon, B.P. H1A 8
Arai, Hiroyoshi TUPA 2
Arnold, John **M1A 1**
Arnott, Dina WPA 2
Arnush, D. **TUPA 10**
Arriaga, C.A. TUPB 2
Ash, Robert L. WPD 2
Ashida, Sumio TU3A 6
Augustyniak, Edward H2A 4, **M3B 4**, TUPA 15
Avila, Carlos **W2B 7**
Awakowicz, Peter MPC 4, TUPC 10
Ayyaswamy, P.S. H3B 4

B

Babcock, Lucia MPC 10, WPB 4
Badakhshan,, Ali **WPA 18**
Bailey, William F. H3B 3
Baravian, G. WPA 9
Barnes, Michael S. TU3A 2
Barnes, Paul **TU1B 5**
Bartschat, Klaus **M1B 1**
Basner, R. M3A 1, MPC 2
Basurto, E. WPB 5
Batelaan, H. H3A 5, W2B 4
Becker, K. **M3A 1**, **MPC 2**, MPC 5, TUPB 13
Bell, B. WPD 4
Bell, Gary MPA 8
Benck, Eric C. MPA 2, **WPC 1**
Benjamin, R.D. WPA 25
Bennett, Eric J. **H3B 3**
Bernecki, Thomas **M2B 4**
Bica de Moraes, Mario **H1A 4**, **WPA 17**
Birdsey, B.G. H3A 5, **W2B 4**
Bletzinger, P. H3A 3
Boesten, L. M3A 5, WPB 11
Boesten, Ludwig **WPB 10**
Boeuf, J.P. TU3B 2
Boffard, John B. W2B 1, **W2B 2**, W2B 3
Bogaerts, Annemie **H3B 1**
Bonham, R.A. TUPB 15
Booske, J.H. MPD 13
Booske, John WPA 2
Booth, Jean-Paul **WPA 15**
Booth, J.P. **M2A 7**, **WPA 22**
Borthwick, I.S. MPD 8
Boswell, R.W. H1A 7, M3B 5, **MPB 10**, TU1A 2, TU1A 5, TUPA 4, WPA 22
Bowden, M.D. **H1A 6**, **M2A 6**, MPA 3, **TUPA 3**, WPA 4, **WPA 6**
Braithwaite, N.St J. WPA 22
Braithwaite, N.St.J. MPD 1
Brake, Mary L. TUPA 11
Branch, Michael W3A 3
Bretagne, J. WPB 6, WPB 7
Breun, Robert A. M1A 3, W2A 5
Brooke, G. WPA 11
Brooks, C.B. **TUPA 7**
Brunger, M.J. **W2B 8**, W2B 9
Buckman, S.J. **W2B 9**
Buddemeier, U. **TU1A 7**, **WPA 19**, **WPC 4**
Buie, M.J. **WPA 13**
Bukowski, J. TUPC 8
Butler, J.E. H2A 5, H2B 2, M2A 4
Butler, Jeffery **MPC 10**

C

Campbell, L. W2B 8
Campbell, Robert B. **MPA 13**, TU3B 4, TUPC 1, TUPC 2
Carter, Chris MPA 16
CartwrightJ, D.C W2B 8
Chabert, P. H1A 1, M2A 7
Chabert, Pascal WPA 15
Chaker, M. TUPA 12, TUPA 13
Champion, R.L. WPB 7
Champion, Roy L. M3B 3, W1A 4
Chang, Chong H. **M2B 3**
Chang, Jen-Shih **H1B 2**, H1B 4
Chang, J.S. **WPD 1**
Charles, C. **M3B 5**, MPB 10
Charrada, Kamel TUPB 8
Chen, F.F. **TU1A 3**, TUPA 10
Chen, Wenjing **MPB 6**
Chen, Zhifan **MPC 7**
Cherigier, L. WPA 24
Cherrington, B.E. WPC 12
Cheung, P. WPA 18
Chew, Kok Heng H2A 4, M3B 4, **TUPA 15**
Childs, M.A. **TUPA 21**
Chilton, J.Ethan **W2B 3**, W2B 5
Choi, Seung J MPB 3
Choi, S.J. **TU3A 3**
Choi, Y.W. M2A 6
Christophorou, L.G. **M3A 4**
Christophorou, Loucas G. TUPB 3, **TUPB 10**
Chuc, Kien TU3A 4
Chung, Sunggi W2B 5
Cisneros, C. TUPB 2, WPB 5
Coburn, John H2A 2
Cocito, G. **MPD 10**
Cognolato, L. MPD 10
Cohen, Ira M. H3B 4
Cohen, W.E. TUPA 22
Colella, Phillip H2B 7
Collett, W.L. **WPD 4**
Collins, George J. WPA 14
Collison, Wenli Z. **TU3A 2**
Colombo, V. MPD 10
Conrad, John W2A 5
Conway, G.D. MPB 10, **TUPA 4**
Cooper, J.C. **WPB 2**
Coschignano, Tony J. H3A 4
Cronrath, W. H1A 6
Cuneo, M.E. MPD 2
Cunge, G. M2A 7, WPA 22
Cunge, Gilles WPA 15
Curial, Juan A. H3A 4
Curry, J.J. **WPB 3**
Curtiss, Larry **W1B 2**
Czarnetzki, U. **WPA 24**

D

Da Cruz, Nilson H1A 4
Date, H. TUPC 8, W3A 4, W3B 4
Datskos, Panos **TUPB 7**
Daulton, T.L. **W1B 5**
Davies, Paul B. WPA 10

Davis, C.A. **H1A 7**, MPB 10
Davis, Steven M2A 2
de Hoog, F.J. MPA 4
de Urquijo, J. **TUPB 2**, **WPB 5**
Deebel, M. MPD 11
Degeling, A.W. **TU1A 2**
Den Hartog, E.A. WPB 3
Den, Shoji TUPA 18
Derbyshire, J.M. **TUPB 12**
Derouard, J. M2A 7, TUPA 17
Deutsch, H. M3A 1
Dhali, Shirshak **WPD 5**
Dillon, M. **H2B 1**, M3A 5
Dillon, Michael WPB 10
Dobbyn, Kieran **WPA 21**
Döbele, H.F. WPA 23, WPA 24
Domínguez, I. TUPB 2, WPB 5
Dorr, Milo R. **H2B 7**
Doughty, C. **W2A 3**
Durandet, A. H1A 7, MPB 10
Durrant, Steven H1A 4, WPA 17

E

Eddy, C.R. H2B 2, M2A 4
Eddy Jr., C.R. **H2A 5**
Eiji Kayama, Milton WPA 12
Eisner, E. WPA 5
ElHabachi, Ahmed TU3B 5
Ellingboe, Albert R. **MPA 15**, **TU1A 1**, **WPA 25**
Engemann, J. MPD 17
England, Jeff L WPA 18
Evans, J.D. TU1A 3

F

Falconer, Ian MPA 16
Fan, Wai Y. **WPA 10**
Felfli, Z. **MPC 12**
Fernsler, R.F. **H2B 2**
Ferreira, C.M. WPA 1
Fetherston, Paul W2A 5
Filuk, A.B. **MPD 2**
Fincke, Jim R. **M2B 2**
Fleddermann, C.B. **WPD 3**
Foest, R. MPC 2
Fons, John T. **W2B 5**
Forrister, Ray MPA 7
Frost, Robert M. **MPC 4**
Fujii, Toshiaki **TUPA 24**
Fujimoto, Milton Massumi WPB 13

G

Gahl, J.M. WPD 3
Gallagher, Alan TUPA 21
Ganguly, B.N. **H3A 3**
Garofalo, A. WPA 5
Gates, Amelia WPC 1
Gay, T.J. H3A 5, W2B 4
Gehrke, Mark F. W2B 2
Geohegan, David **W3B 3**
Getty, Ward D. TUPA 11
Giapis, Konstantinos P. H2A 3, **MPB 7**
Gibson, N.D. **MPD 3**, WPB 2
Gierling, Joachim **WPC 6**
Gijbels, Renaat H3B 1
Gilgenbach, R.M. TUPA 22, **W3B 2**
Girshick, Steven L. **M2B 1**
Giuliani, John L. **H1B 5**
Glembocki, O.J. H2A 5
Godoy de Santana, Regiane WPA 12
Godyak, Valery MPA 1, MPA 17, **MPA 18**, **W3A 8**
Golde, Michael F. MPC 9
Gonzalez, Patrick F. **WPA 14**
Goodyear, Alec **MPD 1**
Gopinath, Venkatesh P. **H2B 6**, TU3A 6
Gordon, M.H. H1A 3
Gordon, Michael MPB 7
Goree, J. TUPA 20
Goree, J. H1A 5
Gortchakov, Serguei **MPD 6**
Goto, T. WPA 20
Goto, Toshio **M1A 6**, MPA 10, TUPA 1, TUPA 2, TUPA 8, TUPA 16, TUPA 24
Gougousi, Theodosia **MPC 9**
Gousset, G. H1A 1, WPB 6, WPB 7
Govindan, T.R. H2B 8
Goyette, A.N. **WPA 7**, WPA 8
Graham, W.G. WPC 2
Grapperhaus, Michael J. **W2A 4**, W3A 2
Graves, David H2A 2, W1A 5
Graves, D.B. **TUPC 8**
Green, K.M. TUPA 9
Green, M.A. W2B 8
Gruen, Dieter **W1B 1**
Guarnieri, C.Richard M1A 2

H

Haaland, Peter D. MPC 13
Hamada, R. **TUPB 9**, WPB 12
Hamilton, T.W. H1A 8
Hanawa, Hiroji TU3A 4
Hanley, Luke **W1A 2**
Harb, T. **TUPB 14**
Hardy, K.A. W2B 7
Hardy, Kenneth A. H3A 4
Harms, M. WPA 19, WPC 4
Harper, Mike MPA 6
Hattori, Shuzo TUPA 24
Hayashi, Hisataka **M1A 4**
Hayashi, T. MPD 7, WPA 20
Hayashi, Yuzo TUPA 18
Hayaud, C. WPA 9
Hayden, D.B. **TUPA 9**
Hayden, Douglas B. MPA 9
Hebner, Gregory A. **M2A 3**
Helmer, Bryan **W1A 5**
Helmsen, John J. **MPB 9**
Hernandez, Gessler W2B 7
Hershkowitz, Noah MPA 6, TUPA 14, WPC 3
Hing, M. **WPA 11**
Hiramatsu, Mineo TUPA 1, TUPA 23, TUPA 24
Hirose, S. WPA 20
Hiskes, J.R. **MPB 11**
Hitchon, W.N.G. TUPC 4
Hoekstra, Robert MPB 3
Hoffman, Dan MPA 8
Holland, Murray **M3B 1**
Holm, R.T. H2A 5
Hopkins, M.B. TUPA 3, WPC 12
Hopkins, Michael **MPA 11**, WPA 21
Hori, Masaru M1A 6, MPA 10, TUPA 1, TUPA 2, TUPA 8, **TUPA 16**, TUPA 24
Hori, T. **MPA 3**, TUPA 3
Hubert, J. WPA 1
Humphrey, M.A. **H3A 5**
Huo, Winifred M. **TUPB 4**
Hwang, Gyeong S. **H2A 3**, MPB 7
Hwang, Helen H. **H2B 3**
Hwang, W. MPC 1

I

Iga, Ione WPB 13
Ikeda, Masanobu **MPA 10**
Imaeda, Kouichi **TUPA 23**
Ingold, John **H3B 5**
Ishii, J. TUPA 9
Itikawa, Y. WPB 11
Ito, Haruhiko MPA 10
Ito, Masafumi MPA 10, TUPA 1, **TUPA 8**, TUPA 16
Ito, Tairo H1B 4
Itoh, H. **MPD 7**
Itoh, M. WPA 4

Ivers, T.H. WPA 5
Iyanagi, K. W3A 6

J
Jamal, S. WPD 1
James, Brian MPA 16
James, Geoffrey **M1B 2**
Jelenković, B.M. MPB 12
Jenkins, Maura WPA 2
Jhonston, M.E. W2B 4
Jiang, X. TU1A 3
Jiao, Charles Q. **MPC 13**
Johnsen, Rainer MPC 9, MPC 11
Joyce, Glenn **TU3A 5**
Juliano, Daniel R. **MPA 9**
Juliano, D.R. TUPA 9

K
Kadota, K. M1A 5
Kaganovich, I.D. TU1A 4, TU1A 7, **TUPC 7**, WPC 4
Kajiwara, T. WPA 3
Kalashnikov, E.V. **MPD 14**
Kamal, Husain **WPC 3**
Kasperski, Grzegorz MPC 8
Kawai, Y. M1A 5
Kedzierski, W. **MPC 3**, TUPB 12, TUPB 14
Keiter, E.R. TUPC 4
Kelkar, U.M. **H1A 3**
Keller, John H. **W3A 1**
Kessler, William **M2A 2**
Ketsdever, Andrew D. TUPC 5
Kettlitz, Manfred **WPB 1**
Khachan, Joseph **MPA 16**
Khatchatrian, David **TUPC 12**
Khromov, N.A. **WPA 16**
Kim, K.B. W1B 4
Kim, Y.-K. **MPC 1**
Kim, Yong-Ki **M1B 4**
Kimura, M. H2B 1, M3A 5, TUPB 9, WPB 11, **WPB 12**
Kindel, Eckhard **MPD 5**, WPB 1
Kitamori, K. W3A 4, W3B 4
Kleber, J. WPC 12
Kogelschatz, Ulrich **H3A 1**
Kolobov, Vladimir W3A 8
Kombargi, R. WPA 5
Komuro, Shuji TUPA 18
Kono, A. **WPA 20**
Kortshagen, U. H3B 6, **H3B 7**, H3B 8, MPD 3, TU1A 7, WPC 4
Korzec, D. **MPD 17**
Kota, Gowri **H2A 2**
Kovaleski, S.D. **TUPA 22**
Krishnan, Anantha MPA 14
Kroesen, G.M.W. MPA 4
Kroin, Teodosio WPB 13
Kudryavtsev , A.A. WPA 16
Kudryavtsev, A.A. TUPC 3
Kurunczi, P. **MPC 5**
Kushner, Mark J. H1B 3, H2B 3, MPB 1, MPB 3, MPB 4, TU1B 5, W2A 4, **W3A 2**, W3A 7, WPA 2

L
Lagus, Mark E. W2B 1, W2B 2
Lampe, M. H2B 2
Lampe, Martin TU3A 5
Langan, John **W2A 2**
Lantsman, A. TUPA 9
Lash, J.S. TUPA 22
Lau, Y.Y. TUPA 22
Lawler, J.E. **H3B 6**, H3B 7, H3B 8, MPD 3, MPD 9, WPA 7, WPA 8, WPB 2, WPB 3
Lazaryuk, S.N. WPA 16
LeClair, L.R. TUPB 14
Lee, H.B. W1B 4
Lee, J.W. W1B 4
Lee, K.W. W1B 4
Lee, Mu-Tao **WPB 13**
Lee, Y.K. W1B 4, **W1B 4**
Leonhardt, D. H2A 5, H2B 2, **M2A 4**
Leprince, P. H1A 1
Li, Jing WPD 5
Li, M. TUPC 8
Lieberman, Michael **TU3A 6**
Lin, Chun C. **TU2A 1**, W2B 1, W2B 2, W2B 3, W2B 5
Lister, Graeme **TU1B 1**
Liu, H. MPD 13
Loewenhardt, Peter K. **TU3A 4**
Loffhagen, Detlef MPD 5, MPD 6, **TUPC 6**
Loureiro, J. **TUPA 5**
Lykke, Keith R. H1A 2, TU1B 4

M
Ma, Diana X. TU3A 4
Maeda, M. WPA 3
Mahajan, S.M. WPD 4
Mahony, C.M.O. **WPC 2**
Makabe, T. H2B 4, M2A 5, **W3A 6**
Malik, Shamim **W2A 5**
Manheimer, W.M. H2B 2, TU3A 5
Margot, J. TUPA 12, TUPA 13, WPA 1
Martus, K. MPC 5
Masai, T. **WPB 11**
Masters, M.F. MPD 11
Matsuda, Y. WPA 7, WPA 8
Mauel, M.E. WPA 5
Maurer, D. WPA 5
McConkey, J.W. MPC 3, TUPB 12, TUPB 14
McCorkle, Dennis **TUPB 1**, TUPB 6
McGrath, Robert T. TU3B 4, TUPC 1, TUPC 2
Mechlińska-Drewko, Jadwiga **MPC 6**
Meeks, Ellen **W2A 1**
Mehlhorn, T.A. MPD 2
Menningen, K.L. MPD 12
Mentel, Juergen WPC 10
Merry, Walter TUPA 7
Meyer, Peter **WPC 7**
Meyyappan, M. **H2B 8**, **MPB 8**
Mi, L. **TUPB 15**
Miers, R.E. MPD 11
Minton, Timothy MPB 7
Miyata, Koji **TUPA 2**
Miyazaki, K. WPA 3
Mojarrabi, B. W2B 8
Moore, Teresa MPB 7
Morikawa, Takitaro TUPA 18
Możejko, Paweł **MPC 8**
Msezane, and Alfred Z. MPC 7
Msezane, A.Z. MPC 12
Mullman, K.L. **MPD 9**
Munukutla, S.S. WPD 4
Muraoka, K. H1A 6, M2A 6, MPA 3, TUPA 3, **TUPA 19**, **WPA 3**, WPA 4, WPA 6
Murata, Kazuya TUPA 8
Murnick, D.E. MPD 4
Mutoh, Harunobu TUPA 18

N
Nadle, D. WPA 5
Nagpal, R. H3A 3
Nagpal, Rajesh MPC 13
Nakahata, T. TUPA 6
Nakamura, Masayuki TUPA 16
Nakamura, S. TUPA 19
Nakano, N. **H2B 4**, M2A 5, W3A 6
Nakano, Toshiki **TU3A 1**
Nanbu, Kenichi H3B 2
Navratil, G.A. WPA 5
Nawata, Masahito TUPA 23, TUPA 24
Neuilly, F. M2A 7
Ni, Tom Q. TU3A 2
Niemöller, N. WPA 23
Norimoto, K. MPD 7
Novog, D.R. WPD 1
Nozawa, Ryouichi TUPA 8, TUPA 16
Nunnally, W.C H3A 2

O
Oddone, J.Sebastian **H3A 4**
Oh, Jae J. **TUPC 11**
Ohtake, Hiroto TU3A 1
Okada, T. WPA 3
O'Keeffe, Patrick **TUPA 18**
Okigawa, A. **M2A 5**, W3A 6
Olthoff, James K. MPA 5, TUPB 10
Olthoff, J.K. M3A 4, WPB 6, WPB 7, WPB 8
O'Morain, C. TUPA 3
O'Morain, Ciaran WPA 21
Ono, K. TUPA 6
Ono, Kouichi **H2A 1**
Orel, Ann E. **M3A 3**
Orlando, Thomas M. **TU1B 2**
Overzet, Lawrence MPD 16
Overzet, L.J. **WPC 12**
Ozima, M. W1B 5

P
Panciatichi, C. MPD 10
Pang, S.W. H2A 5
Parish, John **WPB 9**
Park, K.C. W1B 4
Parker, Gergory W3A 3
Parker, G.J. H3B 6, H3B 7, **H3B 8**, **TU3B 3**, **TUPC 4**
Paterson, A.M. **MPD 8**
Pautonier, S. MPB 10
Peck, J.R. **WPA 8**
Peko, B.L. WPB 7
Peko, Brian L. **M3B 3**
Peres, I. **WPA 1**
Perry, A.J. MPB 10, TUPA 4
Peterkin, F.E. H3A 2
Peterson, J.R. W2B 7
Petrović, Z.Lj. MPB 12
Petrović, Zoran MPC 6
Phelps, A.V. **WPC 11**
Piech, Garrett A. **W2B 1**, W2B 2
Piejak, Robert **MPA 1**, **MPA 17**, MPA 18
Pieper, J.B. H1A 5
Pinnaduwage, Lal TUPB 1, **TUPB 6**, TUPB 7
Pinto Mota, Rogério **WPA 12**
Pitchford, L.C. TU3B 2
Pointon, T.D. MPD 2
Popović, S. WPA 11
Punset, C. **TU3B 2**

Q
Qian, X.Y. MPA 12
Qin, Wei "Ivy" **H3B 4**
Quick, Anthony **TUPA 14**
Quinn, R.A. **H1A 5**

R
Rabalais, J.Wayne **W1A 1**
Radovanov, Svetlana **MPA 7**, **MPA 8**
Raizer, Yuri **W3B 1**
Rangel, Elidiane WPA 17
Rao, M.V.V.S. M3A 4, TUPB 10, **WPB 6**, WPB 7, **WPB 8**
Rasmussen, Dave MPA 8
Rauf, Shahid **MPB 4**, **W3A 7**
Resta, Victoria MPA 8
Rhodes, Charles TUPC 12
Rieffel, Marc **H2B 5**
Riemann, Karl-Ulrich WPC 7
Riemann, Karl–Ulrich WPC 6
Riley, Merle MPB 3, **WPC 8**, **WPC 9**
Rintamaki, J.I. TUPA 22
Roberts, James R. MPA 2
Roberts, Jim WPC 1
Roe, L.A. H1A 3
Roepcke, Juergen WPA 10
Romanenko, V.A. **TUPC 3**, WPA 16
Rousseau, A. **H1A 1**
Roznerski, Władysław MPC 6
Rudd, M.E. MPC 1
Ruzic, David N. MPA 9, **W1A 3**
Ruzic, D.N. TUPA 9

S
Sá, P.A. TUPA 5
Sadeghi, N. H1A 6, M2A 7, **MPA 4**, TUPA 17, WPA 22
Sakai, M. MPD 9
Sakai, Y. W3A 4, W3B 4
Sakoda, T. TUPA 19, **WPA 4**
Salzman, Phillip TU3A 4
Samsonov, D. **TUPA 20**
Samukawa, Seiji TU3A 1
Sarfaty, Moshe **MPA 6**, TUPA 14
Sasaki, K. **M1A 5**
Sato, A.H. **MPA 12**
Sato, Arthur TU3A 4
Sato, H. M3A 5, TUPB 9, WPB 12
Savina, Michael R. **TU1B 4**
Schein, Jochen **WPC 10**
Schimke, Conrad MPD 5, WPB 1
Schlüter, H. TU1A 4, WPA 19
Schmidt, M. M3A 1, MPC 2
Schoenbach, Karl H. **TU3B 5**
Schoenbach, K.H. **H3A 2**
Schöpp, Heinz WPB 1
Schulz-von der Gathen, V. **WPA 23**, WPA 24
Schumann, Michael WPC 10
Schwabedissen, Axel **MPA 2**
Schwarzenbach, W. TUPA 17
Schweigert, V.A. TUPC 7
Seibert, Ch. MPD 17
Sekine, Makoto M1A 4
Serikov, Vladimir **H3B 2**
Shamamian, V.A. H2A 5, H2B 2, M2A 4
Shankar, Sadasivan H2B 5
Shannon, Steve S. TUPA 11
Shaw, Denis WPA 14
Sheldon, J.W. H3A 4, W2B 7
Shi, Z. TUPB 5
Shi, Zhong **WPD 2**
Shin, Jai K. **MPB 1**
Shohet, J.L. MPD 13
Shohet, J.Leon H2A 4, M3B 4, TUPA 15
Shohet, Leon WPA 2
Shon, J.W. **MPB 2**, TU3A 3
Siegel, R. **TUPB 13**
Skrzypkowski, Miroslaw P. **MPC 11**
Slinker, Steve TU3A 5
Smith, Brian **MPD 16**
Smith, H.B. **TU1A 5**
Smith, Preston C. W1A 3
Snodgrass, Thomas **WPA 2**
Snyder, H.R. WPD 3
Sobolewski, Mark **TU1A 6**, **WPC 5**
Solodky, S.A. TUPC 3
Song, Y.B. TUPA 19
Sonnenfroh, David M2A 2
Spence, David **H1A 2**
Speth, R.R. **MPD 13**
Spindler, H.L. TUPA 22
Sridharan, Kumar W2A 5
Stampa, A. WPA 23
Steffens, Kristen L. **MPD 15**
Stewart, R.S. MPD 8
Stojanović, V.D. **MPB 12**
St-Onge, L. **TUPA 12**, **TUPA 13**
Su, M. WPA 5
Sueoka, O. TUPB 9, WPB 12
Sugai, Hideo **M3A 2**
Suganuma, Shinji TUPA 1
Suleymanov, I.A. TUPC 3
Sultan, G. **WPA 9**
Surendra, Maheswaran **M1A 2**
Suvarov, V **W2B 6**
Suzuki, Motoyuki **W3B 4**
Szmytkowski, Czesław MPC 8

Author Index

T

Tadokoro, M. M2A 5
Tagashira, H. W3A 4, W3B 4
Tagawa, H. WPA 6
Taguchi, S. M2A 6
Takeda, Hirohisa TUPA 16
Takekawa, M. WPB 11
Tanaka, H. **M3A 5**, WPB 11
Tanaka, Hiroshi WPB 10
Tarnovsky, R. M3A 1
Taylor, E. WPA 5
Taylor, Stephen H2B 5
Terrell, M. MPD 11
Tessnow, T. H3A 2
Tessnow, Thomas TU3B 5
Teubner, P.J.O. W2B 6, W2B 8
Thompson, P WPA 18
Thoreson, E. **MPD 11**
Tishchenko, Nicholas W3A 3
Todorov, Valentin TU3A 4
Todorov, V.N. MPA 12
Tokonami, S. WPA 6
Tolk, Norman **TU1B 3**
Trajmar, Sandor **M1B 3**
Trantham, K.W. H3A 5
Tsendin, L.D. WPC 4
Tserepi, A. **TUPA 17**
Tucek, John C. **W1A 4**
Tuda, M. **TUPA 6**
Turkot Jr., Robert B. W1A 3
Turner, M.M. **TUPC 9**
Tuszewski, Michel **W3A 5**
Tynan, G. TU1A 3

U

Uchida, T. WPA 4
Uchino, K. H1A 6, MPA 3, TUPA 3, TUPA 19, WPA 3, WPA 4
Ulrich, A. MPD 4
Urashima, kuniko **H1B 4**

V

Šimko, T. WPB 6, **WPB 7**
Vahedi, Vahid H2B 6
Valentini, Hans-Burkhard TUPC 10
Van Brunt, Richard J. MPA 5
Van Brunt, R.J. **H1B 1**, TUPB 11, WPB 6, WPB 7, WPB 8
van de Grift, M. MPA 4
Veerasingam, Ramana **MPB 3, TU3B 4, TUPC 1, TUPC 2**
Vender, D. MPA 4, TU1A 5
Vender, Vender MPA 11
Ventzek, Peter L.G. H2B 8, W3A 4, W3B 4
Ventzek, P.L.G. WPA 13
Vesey, R.A. MPD 2
Vijaya Sankar, M.K. **WPA 5**
Vitello, P. MPB 2
Vitello, Peter **W3A 3**
Vušković, L. TUPB 5, WPA 11

W

Wadsworth, Dean C. **TUPC 5**
Wake, Daniel D. H2B 7
Wang, Y. TUPB 5
Wang, Yicheng M3A 4, **MPA 5, TUPB 3, TUPB 11**, WPB 7
Weaver, David P. TUPC 5
Weber, Larry **TU3B 1**
Wei, H. **TUPB 5**
Weiss, C.A. TUPA 9
Welch, D. MPD 2
Welter, M.D. **MPD 12**
Wendt, Amy E. **H2A 6**
Wickliffe, M.E. WPB 3
Wieser, J. **MPD 4**
Williams, Ted MPC 10, **WPB 4**
Wilson, Aaron R. **TUPA 11**
Winkler, Rolf MPD 6, TUPC 6
Woods, R.C. MPA 6
Woods, R.Claude **H2A 4**, M1A 3, M3B 4, TUPA 15
Woodworth, J.R. **H1A 8**
Wu, Hanming MPA 14

X

Xiao, Q. WPA 5
Xu, Xudong "Peter" **H1B 3**

Y

Yamada, Naoki **W3A 4**
Yamamoto, Yasuo **TUPA 1**
Yanagishita, K. TUPA 19
Yaney, Perry WPB 9
Yi, K. WPC 12
Yi, Whikun MPB 1
Yin, Gerald Z. TU3A 4
Yokoi, Tsuneki TUPA 24
Yu, Ben **MPA 14**
Yzumi Honda, Roberto WPA 12

Z

Zachariah, Michael R. MPD 15
Zazo, A. MPD 10
Zhang, Hong-Mei MPA 8
Zissis, Georges **TUPB 8**

NOTES

1996

JANUARY

S	M	T	W	T	F	S
	1	2	3	4	5	6
7	8	9	10	11	12	13
14	15	16	17	18	19	20
21	22	23	24	25	26	27
28	29	30	31			

FEBRUARY

S	M	T	W	T	F	S
				1	2	3
4	5	6	7	8	9	10
11	12	13	14	15	16	17
18	19	20	21	22	23	24
25	26	27	28	29		

MARCH

S	M	T	W	T	F	S
					1	2
3	4	5	6	7	8	9
10	11	12	13	14	15	16
17	18	19	20	21	22	23
24	25	26	27	28	29	30
31						

APRIL

S	M	T	W	T	F	S
	1	2	3	4	5	6
7	8	9	10	11	12	13
14	15	16	17	18	19	20
21	22	23	24	25	26	27
28	29	30				

MAY

S	M	T	W	T	F	S
			1	2	3	4
5	6	7	8	9	10	11
12	13	14	15	16	17	18
19	20	21	22	23	24	25
26	27	28	29	30	31	

JUNE

S	M	T	W	T	F	S
						1
2	3	4	5	6	7	8
9	10	11	12	13	14	15
16	17	18	19	20	21	22
23	24	25	26	27	28	29
30						

JULY

S	M	T	W	T	F	S
	1	2	3	4	5	6
7	8	9	10	11	12	13
14	15	16	17	18	19	20
21	22	23	24	25	26	27
28	29	30	31			

AUGUST

S	M	T	W	T	F	S
				1	2	3
4	5	6	7	8	9	10
11	12	13	14	15	16	17
18	19	20	21	22	23	24
25	26	27	28	29	30	31

SEPTEMBER

S	M	T	W	T	F	S
1	2	3	4	5	6	7
8	9	10	11	12	13	14
15	16	17	18	19	20	21
22	23	24	25	26	27	28
29	30					

OCTOBER

S	M	T	W	T	F	S
		1	2	3	4	5
6	7	8	9	10	11	12
13	14	15	16	17	18	19
20	21	22	23	24	25	26
27	28	29	30	31		

NOVEMBER

S	M	T	W	T	F	S
					1	2
3	4	5	6	7	8	9
10	11	12	13	14	15	16
17	18	19	20	21	22	23
24	25	26	27	28	29	30

DECEMBER

S	M	T	W	T	F	S
1	2	3	4	5	6	7
8	9	10	11	12	13	14
15	16	17	18	19	20	21
22	23	24	25	26	27	28
29	30	31				

1997

JANUARY

S	M	T	W	T	F	S
			1	2	3	4
5	6	7	8	9	10	11
12	13	14	15	16	17	18
19	20	21	22	23	24	25
26	27	28	29	30	31	

FEBRUARY

S	M	T	W	T	F	S
						1
2	3	4	5	6	7	8
9	10	11	12	13	14	15
16	17	18	19	20	21	22
23	24	25	26	27	28	

MARCH

S	M	T	W	T	F	S
						1
2	3	4	5	6	7	8
9	10	11	12	13	14	15
16	17	18	19	20	21	22
23	24	25	26	27	28	29
30	31					

APRIL

S	M	T	W	T	F	S
		1	2	3	4	5
6	7	8	9	10	11	12
13	14	15	16	17	18	19
20	21	22	23	24	25	26
27	28	29	30			

MAY

S	M	T	W	T	F	S
				1	2	3
4	5	6	7	8	9	10
11	12	13	14	15	16	17
18	19	20	21	22	23	24
25	26	27	28	29	30	31

JUNE

S	M	T	W	T	F	S
1	2	3	4	5	6	7
8	9	10	11	12	13	14
15	16	17	18	19	20	21
22	23	24	25	26	27	28
29	30					

JULY

S	M	T	W	T	F	S
		1	2	3	4	5
6	7	8	9	10	11	12
13	14	15	16	17	18	19
20	21	22	23	24	25	26
27	28	29	30	31		

AUGUST

S	M	T	W	T	F	S
					1	2
3	4	5	6	7	8	9
10	11	12	13	14	15	16
17	18	19	20	21	22	23
24	25	26	27	28	29	30

SEPTEMBER

S	M	T	W	T	F	S
	1	2	3	4	5	6
7	8	9	10	11	12	13
14	15	16	17	18	19	20
21	22	23	24	25	26	27
28	29	30				

OCTOBER

S	M	T	W	T	F	S
			1	2	3	4
5	6	7	8	9	10	11
12	13	14	15	16	17	18
19	20	21	22	23	24	25
26	27	28	29	30	31	

NOVEMBER

S	M	T	W	T	F	S
						1
2	3	4	5	6	7	8
9	10	11	12	13	14	15
16	17	18	19	20	21	22
23	24	25	26	27	28	29

DECEMBER

S	M	T	W	T	F	S
	1	2	3	4	5	6
7	8	9	10	11	12	13
14	15	16	17	18	19	20
21	22	23	24	25	26	27
28	29	30	31			

1998

JANUARY

S	M	T	W	T	F	S
				1	2	3
4	5	6	7	8	9	10
11	12	13	14	15	16	17
18	19	20	21	22	23	24
25	26	27	28	29	30	31

FEBRUARY

S	M	T	W	T	F	S
1	2	3	4	5	6	7
8	9	10	11	12	13	14
15	16	17	18	19	20	21
22	23	24	25	26	27	28

MARCH

S	M	T	W	T	F	S
1	2	3	4	5	6	7
8	9	10	11	12	13	14
15	16	17	18	19	20	21
22	23	24	25	26	27	28
29	30	31				

APRIL

S	M	T	W	T	F	S
			1	2	3	4
5	6	7	8	9	10	11
12	13	14	15	16	17	18
19	20	21	22	23	24	25
26	27	28	29	30		

MAY

S	M	T	W	T	F	S
					1	2
3	4	5	6	7	8	9
10	11	12	13	14	15	16
17	18	19	20	21	22	23
24	25	26	27	28	29	30
31						

JUNE

S	M	T	W	T	F	S
	1	2	3	4	5	6
7	8	9	10	11	12	13
14	15	16	17	18	19	20
21	22	23	24	25	26	27
28	29	30				

JULY

S	M	T	W	T	F	S
			1	2	3	4
5	6	7	8	9	10	11
12	13	14	15	16	17	18
19	20	21	22	23	24	25
26	27	28	29	30	31	

AUGUST

S	M	T	W	T	F	S
						1
2	3	4	5	6	7	8
9	10	11	12	13	14	15
16	17	18	19	20	21	22
23	24	25	26	27	28	29
30	31					

SEPTEMBER

S	M	T	W	T	F	S
		1	2	3	4	5
6	7	8	9	10	11	12
13	14	15	16	17	18	19
20	21	22	23	24	25	26
27	28	29	30			

OCTOBER

S	M	T	W	T	F	S
				1	2	3
4	5	6	7	8	9	10
11	12	13	14	15	16	17
18	19	20	21	22	23	24
25	26	27	28	29	30	31

NOVEMBER

S	M	T	W	T	F	S
1	2	3	4	5	6	7
8	9	10	11	12	13	14
15	16	17	18	19	20	21
22	23	24	25	26	27	28
29	30					

DECEMBER

S	M	T	W	T	F	S
		1	2	3	4	5
6	7	8	9	10	11	12
13	14	15	16	17	18	19
20	21	22	23	24	25	26
27	28	29	30	31		

1999

JANUARY

S	M	T	W	T	F	S
					1	2
3	4	5	6	7	8	9
10	11	12	13	14	15	16
17	18	19	20	21	22	23
24	25	26	27	28	29	30
31						

FEBRUARY

S	M	T	W	T	F	S
	1	2	3	4	5	6
7	8	9	10	11	12	13
14	15	16	17	18	19	20
21	22	23	24	26	26	27
28						

MARCH

S	M	T	W	T	F	S
	1	2	3	4	5	6
7	8	9	10	11	12	13
14	15	16	17	18	19	20
21	22	23	24	25	26	27
28	29	30	31			

APRIL

S	M	T	W	T	F	S
				1	2	3
4	5	6	7	8	9	10
11	12	13	14	15	16	17
18	19	20	21	22	23	24
25	26	27	28	29	30	

MAY

S	M	T	W	T	F	S
						1
2	3	4	5	6	7	8
9	10	11	12	13	14	15
16	17	18	19	20	21	22
23	24	25	26	27	28	29
30	31					

JUNE

S	M	T	W	T	F	S
		1	2	3	4	5
6	7	8	9	10	11	12
13	14	15	16	17	18	19
20	21	22	23	24	25	26
27	28	29	30			

JULY

S	M	T	W	T	F	S
				1	2	3
4	5	6	7	8	9	10
11	12	13	14	15	16	17
18	29	20	21	22	23	24
25	26	27	28	29	30	31

AUGUST

S	M	T	W	T	F	S
1	2	3	4	5	6	7
8	9	10	11	12	13	14
15	16	17	18	19	20	21
22	23	24	25	26	27	28
29	30	31				

SEPTEMBER

S	M	T	W	T	F	S
			1	2	3	4
5	6	7	8	9	10	11
12	13	14	15	16	17	18
19	20	21	22	23	24	25
26	27	28	29	30		

OCTOBER

S	M	T	W	T	F	S
					1	2
3	4	5	6	7	8	9
10	11	12	13	14	15	16
17	18	19	20	21	22	23
24	25	26	27	28	29	30
31						

NOVEMBER

S	M	T	W	T	F	S
	1	2	3	4	5	6
7	8	9	10	11	12	13
14	15	16	17	18	19	20
21	22	23	24	25	26	27
28	29	30				

DECEMBER

S	M	T	W	T	F	S
			1	2	3	4
5	6	7	8	9	10	11
12	13	14	15	16	17	18
19	20	21	22	23	24	25
26	27	28	29	30	31	

2000

JANUARY

S	M	T	W	T	F	S
						1
2	3	4	5	6	7	8
9	10	11	12	13	14	15
16	17	18	19	20	21	22
23	24	25	26	27	28	29
30	31					

FEBRUARY

S	M	T	W	T	F	S
		1	2	3	4	5
6	7	8	9	10	11	12
13	14	15	16	17	18	19
20	21	22	23	24	25	26
27	28	29				

MARCH

S	M	T	W	T	F	S
			1	2	3	4
5	6	7	8	9	10	11
12	13	14	15	16	17	18
19	20	21	22	23	24	25
26	27	28	29	30	31	

APRIL

S	M	T	W	T	F	S
						1
2	3	4	5	6	7	8
9	10	11	12	13	14	15
16	17	18	19	20	21	22
23	24	25	26	27	28	29
30						

MAY

S	M	T	W	T	F	S
	1	2	3	4	5	6
7	8	9	10	11	12	13
14	15	16	17	18	19	20
21	22	23	24	25	26	27
28	29	30	31			

JUNE

S	M	T	W	T	F	S
				1	2	3
4	5	6	7	8	9	10
11	12	13	14	15	16	17
18	19	20	21	22	23	24
25	26	27	28	29	30	

JULY

S	M	T	W	T	F	S
						1
2	3	4	5	6	7	8
9	10	11	12	13	14	15
16	17	18	19	20	21	22
23	24	25	26	27	28	29
30	31					

AUGUST

S	M	T	W	T	F	S
		1	2	3	4	5
6	7	8	9	10	11	12
13	14	15	16	17	18	19
20	21	22	23	24	25	26
27	28	29	30	31		

SEPTEMBER

S	M	T	W	T	F	S
					1	2
3	4	5	6	7	8	9
10	11	12	13	14	15	16
17	18	19	20	21	22	23
24	25	26	27	28	29	30

OCTOBER

S	M	T	W	T	F	S
1	2	3	4	5	6	7
8	9	10	11	12	13	14
15	16	17	18	19	20	21
22	23	24	25	26	27	28
29	30	31				

NOVEMBER

S	M	T	W	T	F	S
			1	2	3	4
5	6	7	8	9	10	11
12	13	14	15	16	17	18
19	20	21	22	23	24	25
26	27	28	29	30		

DECEMBER

S	M	T	W	T	F	S
					1	2
3	4	5	6	7	8	9
10	11	12	13	14	15	16
17	18	19	20	21	22	23
24	25	26	27	28	29	30
31						

GASEOUS ELECTRONICS CONFERENCE

Oct. 20 — Oct. 24

Monday, October 21		Tuesday, October 22		Wednesday, October 23		Thursday, October 24	
M1A. 8:00 - 10:00 Dielectric Plasma Etching **Chair:** Mike Hartig, Motorola AUDITORIUM	**M1B. 8:00 - 10:00** Advances in Electron Scattering Techniques **Chair:** M. Inokuti, ANL LECTURE HALL	**Tu1A. 8:00 - 10:00** Electromagnetic Coupling Effects in Discharges **Chair:** Rusty Jewett, Lam Research Corp. AUDITORIUM	**Tu1B. 8:00 - 10:00** Radiation Transport and Photon Processes **Chair:** Russ Huebner, ANL LECTURE HALL	**W1A. 8:00 - 10:00** Ion - Surface Interactions **Chair:** Wally Calaway, ANL AUDITORIUM	**W1B. 8:00 - 10:00** Diamond and Diamond - Like Deposition **Chair:** Ben Yu, CFD Research LECTURE HALL	**H1A. 8:00 - 10:00** Phenomena in Glow Discharge Plasmas **Chair:** Uwe Kortshager, Univ. of Minnesota AUDITORIUM	**H1B. 8:00 - 10:00** Environmental Applications **Chair:** S. Dhali, Southern Illinois Univ. LECTURE HALL
Break							
M2A. 10:30 - 12:30 Laser and Optical Diagnostics for Analysis and Control **Chair:** Tom Ni, Lam Research Corp. AUDITORIUM	**M2B. 10:30 - 12:30** Plasma Sprays **Chair:** C. B. Fleddermann, Univ. of New Mexico LECTURE HALL	**Tu2A. 10:30 - 11:30** William P. Allis Prize Lecture 11:30 - 12:00 Business Meeting **Chair:** Wilmer Anderson, Univ. of Wisconsin AUDITORIUM		**W2A. 10:30 - 12:30** Plasma and Surface Chemistry in Materials Processing **Chair:** Kostas Giapis, CIT AUDITORIUM	**W2B. 10:30 - 12:30** Electron Scattering **Chair:** Russell Bonham, IIT LECTURE HALL	**H2A. 10:30 - 12:30** Plasma and Surface Chemistry in Semi-conductor Processing **Chair:** M. Surendra, IBM Watson AUDITORIUM	**H2B. 10:30 - 12:30** Discharge Models **Chair:** W. N. G. Hitchon, U. of Wisconsin LECTURE HALL
Lunch							
M3A. 13:30 - 15:30 Critical Electron Scattering Processes **Chair:** Steve Buckman, Australian National U. AUDITORIUM	**M3B. 13:30 - 15:30** Heavy Particle Collisions and Effects **Chair:** Dick Van Brunt, NIST LECTURE HALL	**Tu3A. 13:30 - 15:30** Modeling and Diagnostics in High Density Plasmas **Chair:** P. Lowenhardt, Univ. of Wisconsin AUDITORIUM	**Tu3B. 13:30 - 15:30** Plasmas in Displays **Chair:** Robert McGrath, Applied Materials LECTURE HALL	**W3A. 13:30 - 15:30** Inductive Coupling and Heating in Low Pressure Plasmas **Chair:** Greg Hebner, SNL AUDITORIUM	**W3B. 13:30 - 15:30** Laser Discharges and Ablation **Chair:** Ken Stabler, SRI LECTURE HALL	**H3A. 13:30 - 15:30** Discharge Experiments **Chair:** N. Braithwaite, Open Univ. Oxford AUDITORIUM	**H3B. 13:30 - 15:30** Models of Glow Discharges and Positive Columns **Chair:** Graeme Lister LECTURE HALL
Break							
MP. 15:45 - 17:30 POSTER SESSION MPA - Inductively Coupled Plasmas MPB - Discharge Modeling MPC - Electron Interactions I MPD - Discharge Experiments **Chair:** Dave Spence, ANL ALCOVE A, ALCOVE B		**TuP. 15:45 - 17:30 POSTER SESSION** TuPA - ECR and Microwave Discharges Ablation and Dusty Plasmas TuPB - Electron Interactions II TuPC - Discharge Theory and Simulation **Chair:** Kieth Lykke, ANL ALCOVE A, ALCOVE B		**WP. 15:45 - 17:30 POSTER SESSION** WPA - Discharge Phenomena WPB - Heavy Particle and Electron Interactions WPC - Sheaths and Electrode Effects WPD - Environmental Applications **Chair:** Steve Pratt, ANL ALCOVE A, ALCOVE B			
		Social Hour 18:00 - 19:00 Banquet 19:00 - 21:00 Hyatt Regency